



^b
UNIVERSITÄT
BERN

Graduate School for Cellular and Biomedical Sciences
University of Bern

Modelling HIV Drug Resistance in Southern Africa

PhD Thesis submitted by

Anthony Willy Hauser

from **Allschwil, BL**

for the degree of

PhD in Biomedical Sciences

Supervisor

Prof. Dr. Matthias Egger

Institute of Social and Preventive Medicine
Faculty of Medicine of the University of Bern

Co-advisor

Prof. Dr. Roger Kouyos

Division of Infectious Diseases and Hospital Epidemiology
University Hospital Zurich

Accepted by the Faculty of Medicine, the Faculty of Science and the Vetsuisse
Faculty of the University of Bern at the request of the Graduate School for
Cellular and Biomedical Sciences

Bern, Dean of the Faculty of Medicine

Bern, Dean of the Faculty of Science

Bern, Dean of the Vetsuisse Faculty Bern

Contents

| | |
|---|------------|
| Abstract | vii |
| 1 Introduction | 1 |
| 2 Systematic review and Bayesian evidence synthesis of acquired NNRTI/NRTI drug resistance | 17 |
| 3 Modelling NNRTI drug resistance in South Africa | 33 |
| 4 Impact of DTG introduction on NNRTI resistance | 51 |
| 5 HIV drug resistance in Sub-Saharan Africa: public healths questions and the role of mathematical modelling | 65 |
| 6 Discussion | 73 |
| 7 Additional work | 85 |
| 7.1 Estimation of SARS-CoV-2 age specific mortality | 87 |
| List of abbreviations | 103 |
| Bibliography | 105 |
| Annexes | 115 |
| Annex A: S1 File of Chapter 2 | 117 |
| Annex B: S2 File of Chapter 2 | 123 |
| Annex C: S1 File of Chapter 3 | 137 |
| Annex D: S1 Text of Chapter 4 | 155 |
| Curriculum vitae & list of publications | 177 |
| Acknowledgements | 181 |

Declaration of originality

183

Abstract

Southern Africa is the region most affected by HIV globally. In South Africa, for example, the prevalence of HIV reaches 17% among adults. In the early 2000s, the roll-out of antiretroviral therapy (ART), a non-nucleoside reverse transcriptase inhibitor (NNRTI) and two nucleoside reverse transcriptase inhibitors (NRTIs), had a dramatic impact on decreasing mortality related to acquired immunodeficiency syndrome (AIDS). However, the recent emergence of resistance to NNRTI threatens the long-term efficacy of such regimen. As a response, a new ART first-line regimen is introduced in several countries of Southern Africa, where the NNRTI drug is replaced by an integrase strand transfer inhibitor (InSTI) drug, called dolutegravir (DTG). DTG has a high genetic barrier to resistance, is highly effective, well tolerated and affordable in resource-limited settings. In this thesis, I develop mathematical models aimed at characterizing different aspects of the dynamics of HIV drug resistance in Southern Africa.

In Chapter 1, I give a brief timeline of the HIV-epidemic in Southern Africa. I then introduce basic concepts on HIV, ART, and HIV drug resistance. I present the different strategies that have been implemented in Southern Africa to fight HIV. Finally, I discuss the increasing role that mathematical models play to gain insight on the HIV-epidemic.

In Chapter 2, I run a systematic review and meta-analysis estimating the prevalence of NRTI/NNRTI drug resistance mutations among adults failing a first-line NNRTI-based regimen in Southern Africa. I develop a Bayesian hierarchical model that synthesizes evidence from the collected studies. The model estimates high levels of K65 and M184 mutations after 2 years of regimen including emtricitabine or lamivudine (FTC/3TC) and tenofovir (TDF), the two NRTI backbones that are now commonly associated in first-line regimen. The K65 and M184 mutations confer high levels of resistance to FTC/3TC and TDF, respectively. Therefore, it suggests that between 43% and 55% of people failing a NNRTI-based regimen, will switch to DTG-based regimen with substantially compromised NRTI backbones, if they are not optimized. These results show the importance of monitoring DTG-response in this population, as they have higher risk of DTG-failure, where resistance could develop.

In Chapter 3, I develop a compartmental model, the MARISA model, which captures both the general HIV-epidemic and the dynamic of NNRTI drug resistance in South Africa. Data from several sources, including cohort data on thousands of people living with HIV (PLWH), are used to calibrate the model. The MARISA model also assesses the impact of counterfactual scenarios reflecting alternative countrywide policies during 2005-2016, considering either increasing ART coverage, improving management of treatment failure, broadening ART eligibility, or implementing drug resistance testing before ART initiation. I identify key drivers of the NNRTI resistance epidemic: large-scale ART roll-out and insufficient monitoring of first-line treatment failure. The results also suggest that no simple measure

could have prevented the rise of NNRTI resistance in the South African context, where NNRTIs have been rapidly rolled out.

In Chapter 4, I adapt the MARISA model to assess the impact of different strategies of DTG introduction on the level of NNRTI resistance in South Africa. I investigate the impact of two scenarios of the DTG-introduction: 1) DTG as a first-line ART, or 2) DTG replacing NNRTIs for all patients, including patients on NNRTI-based regimen. Due to safety concerns related to DTG during pregnancy, the model also considers scenarios where DTG is prescribed to all men and in addition to i) women beyond reproductive age, ii) women beyond reproductive age or using contraception, and iii) all women. The simulations show that, while some strategies can stabilize the level of NNRTI resistance, none of the different strategies introducing DTG leads to its elimination. To halt the increase of NNRTI resistance, DTG should become accessible to both women and people currently on NNRTI-based therapy. As some women (e.g. women at risk of pregnancy) will continue to rely on NNRTI-based ART in the future, controlling the resistance to NNRTI is key to provide them with an effective alternative to DTG.

The Chapter 5 discusses some important public-health questions regarding HIV drug resistance in sub-Saharan Africa. It stresses the central role of mathematical modelling to quantify the risk of HIV drug resistance when data is scarcely available. It also discusses the modelling idea used in Chapters 3 and 4 and shows how mathematical models can bridge the gap between the wide availability of HIV epidemiological data and the limited knowledge on HIV drug resistance in the African regions.

In Chapter 6, I summarize the main findings presented in Chapters 2-4 and discuss their implications. I also present the strengths and weaknesses of the project. Finally, I discuss the perspective of the potential emergence of resistance to DTG. The Chapter 7 presents an additional study, in which I was involved but which does not represent the core of my thesis. In this study, a mathematical model reproduces the dynamics of the SARS-CoV-2 epidemics in several regions of the world and provides estimates of the age-specific mortality related to SARS-CoV-2.

In this thesis, I use mathematical modelling to capture the emergence of NNRTI resistance in South Africa. I identify some factors that have driven the development of NNRTI resistance, such as the long time spent on a failing regimen. Due to its flexibility, the MARISA model is adapted to investigate future strategies, such as the impact of the DTG-introduction on the levels of NNRTI resistance. This shows that processes such as the acquisition and the spread of HIV drug resistance can be reproduced at the population-level using mathematical models calibrated with clinical resistance data. As South Africa is currently introducing DTG-based regimen, such modelling approach can be implemented to investigate the future risk of emergence of DTG resistance. However, even if mathematical models could help to bridge the gaps between clinical and real-world resource-limited settings, more real-world data is needed to understand the actual risk of DTG resistance development in the context of a countrywide implementation of DTG. The meta-analysis in Chapter 2 adds to the body of evidence, as it highlights the potential threat on the long-term efficacy of DTG posed by the switch of patients with elevated viral load. Close follow-up and resistance monitoring of these patients are therefore key to ensure an early detection of DTG resistance and prevent it from spreading through the population.

Chapter 1

Introduction

1.1 Origins and transmission of the human immunodeficiency virus (HIV)

The two types of the human immunodeficiency viruses (HIV-1 and HIV-2) have evolved from simian immunodeficiency viruses (SIV), which are retroviruses causing infections in several species of African non-human primates [1–3]. The transfer of SIV from monkeys to humans occurred through multiple zoonosis events [4], probably in Cameroon [5, 6]. The first verified case of HIV has been retrospectively identified from a blood sample collected in 1959 in Kinshasa, in the Democratic Republic of the Congo (DRC), which is considered as the epicenter of HIV-1 pandemic [7]. The virus is assumed to have then spread to the rest of DRC, and across all sub-Saharan Africa. HIV is transmitted from person to person by three major routes: by sexual contact, through blood (e.g. using contaminated needles) or from mother to infant [8]. HIV-1 is more virulent and transmissible than HIV-2, which is largely confined to West Africa.

South Africa identified its first case of HIV in 1982. The number of annual new infections rapidly increased, attaining 550,000 new infections in 2001 (Fig 1.1) [9]. The implementation of prevention strategies in the 1980s and 1990s, such as the provision of condoms and "safe-sex" education programs, contributed to reduce the number of new infections [10]. Despite that, the HIV prevalence outreached 20% in the end of the 1990s. During these years, the mortality related to acquired immunodeficiency syndrome (AIDS) was still increasing, attaining 290,000 deaths in 2006. Delivery of the first HIV treatments, called antiretroviral (ARV) drugs, in South Africa started in 2001 but only concerned a few HIV-infected individuals with advanced disease. In 2004, South Africa launched its first national antiretroviral treatment (ART) programme, which rapidly helped to reduce the HIV-related mortality. During its first years, the programme focused on individuals with advanced disease, before gradually expanding its eligibility. In 2019, 5.2 millions of people have access to ART in South Africa, representing 70% of the people living with HIV (PLWH) [9].

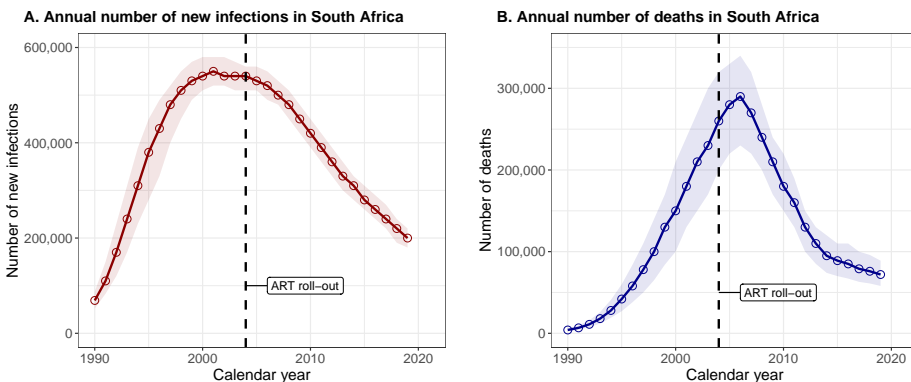


Fig 1.1: UNAIDS estimates of: A. the annual number of new infections in South Africa, B. the annual number of AIDS-related deaths in South Africa. Source: Plots produced with data from <https://aidsinfo.unaids.org/>

1.2 Biology of HIV

1.2.1 HIV replication

HIV mainly infects T helper cells, a type of T cells that plays a vital role in the immune system. These cells, also called CD4+ T cells, modulate the adaptive immune response. As a retrovirus, HIV has a positive single-stranded RNA genome, located inside a capsid. This capsid also contains several enzymes essential for HIV replication, namely the integrase, the reverse transcriptase, and the protease. The process of producing new HIV virions occurs in several stages. First, the virus attaches to a CD4 receptor, located on the surface of the target cell. The HIV envelope then fuses with the cell membrane and the HIV capsid enters the cytoplasm. Reverse transcription is then initiated, whereby the HIV RNA is converted into DNA. The integrase then attaches itself to the end of the viral DNA, forming a complex that enters the nucleus, where the replication machinery of the cell lies. The integrase mediates the integration of the viral DNA into the host genome, where it is now termed as provirus. HIV generally remains dormant and the cell is described as "latently infected". When the proviral DNA is transcribed by the cellular machinery, viral RNA is produced, which is then exported into the cytoplasm. There, the viral RNA is translated and the viral proteins, together with untranslated full-length HIV-1 genomic RNA, assemble at the cell membrane, where they bud off. Infected cells eventually die due to various cell death mechanisms. The new HIV virion will mature, whereby the viral protease cleaves the polyproteins, and eventually form an infectious virion (Fig 1.2).

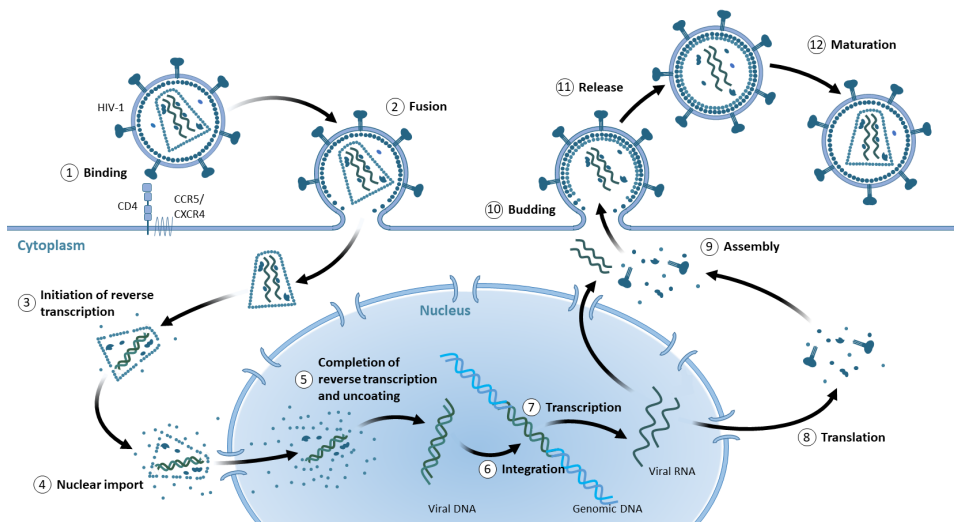


Fig 1.2: The different stages of HIV replication. Source: Figure created by Tom Loosli.

1.2.2 HIV diversity

HIV-1 is characterized by a high genetic diversity and is classified into groups, subtypes and sub-subtypes. HIV-1 is split in four groups: M (major), O (outlier), N (non-M, non-O) and P, originating from four independent transmission events to the human population. Group M is the predominant circulating HIV-1 group and has been divided into subtypes, denoted with letters, and sub-subtypes, denoted with numbers: A1, A2, A3, A4, B, C, D, F1, F2, G, H, J, and

K. The different subtypes are the results of the high rates of mutation, recombination and replication of HIV-1. First, the reverse transcriptase has a relatively high error rate and lacks proofreading activity, i.e. it cannot correct mutations originating from random transcription error. This leads to a high mutation rate of approximately $3.4 \cdot 10^{-5}$ per base pair per replication cycle [11, 12]. Since the HIV genome has 10^4 base pairs and 10^{10} virions are produced per day, this results in a high within-host diversity, with billions of viral variants. Even if natural selection subsequently limits the number of variants, this explains the high within-host diversity that is usually observed. HIV-1 recombination, which occurs when a cell is infected with two different strains of the virus, can lead to further diversity [13].

1.2.3 The course of HIV disease

Two measures are usually used to characterize the infection stage in a HIV-infected person: the CD4 counts and the viral load (VL). The VL measures the number of HIV RNA copies in a millilitre of blood. The CD4 counts are used to measure the immunity response towards HIV, by estimating the number of CD4+ T cells per microlitre of blood. Even if these two measures are different characterizations of the disease, their trajectories over time are closely related (Fig 1.3). Acute infection refers to the first weeks after infection and is characterized by a rapid spread of the virus and a drop in CD4 counts. Within a few weeks, the viral load already reaches high values, over a million copies per millilitre. The timepoint when the viral load reaches a detectable level is called seroconversion. As HIV directly attacks the CD4+ T cells, the CD4 counts quickly decrease. This activates the immune system, which leads to a partial recovery of the CD4+ T cells. As the immune system fights the infection, the viral load quickly decreases to reach a low level. However, if treatment is not provided to prevent the replication of the virus, the viral load gradually rises. The period following the acute phase is referred to as the latency (or chronic) period and usually lasts several years. At that time, the CD4 counts progressively diminish, weakening the immune system, reducing its capability to fight the HIV infection. Once the CD4 count is below 200 cells/ μ l, the risk of developing common infections such as tuberculosis (TB) or other opportunistic infections (OI) increases dramatically. This period is accompanied with symptoms such as rapid weight loss, recurring fever or extreme tiredness. We refer to these late symptoms of infection as acquired immunodeficiency syndrome (AIDS). Deaths among HIV-infected individuals usually occur at this stage.

The role of HIV treatment is to prevent the replication of the virus in order to keep the number of CD4 cells sufficiently high to limit the risk of opportunistic infection. HIV treatment is usually initiated during the chronic phase, characterized by reduced CD4 counts and high VL. When HIV treatment is correctly functioning, the viral load drops quickly and the CD4 counts rise slowly. The VL is used to monitor treatment and a low value indicates that treatment manages to suppress the virus. Below 50 copies/ml, the viral load is undetectable and it is assumed that the infected individuals cannot transmit the virus. While this threshold is used in Europe to define viral suppression, sub-Saharan countries usually use a higher threshold ranging between 200 and 1000 copies/ml [14].

1.3 HIV treatment

1.3.1 The five types of antiretroviral medications

Antiretroviral drugs are used to control HIV infection and achieve viral suppression by preventing the replication of the virus. There are five main classes of ART drugs, taking action

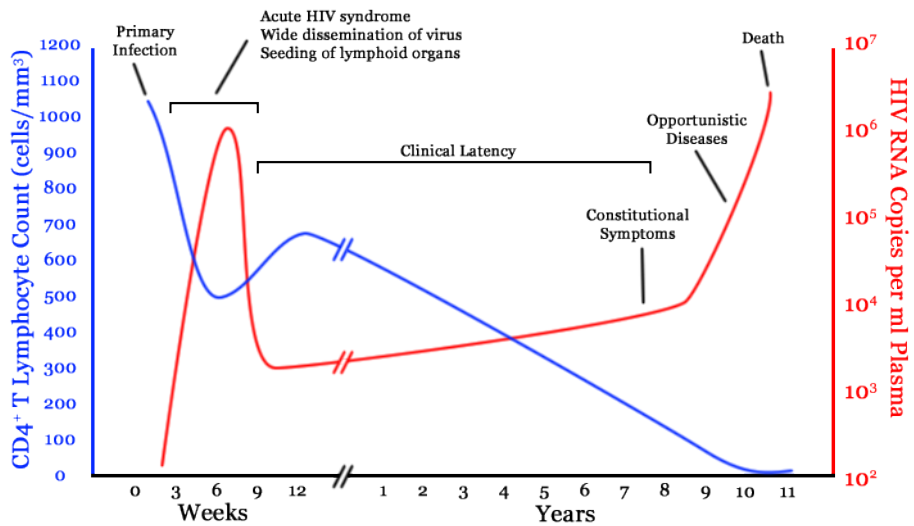


Fig 1.3: Evolution of the CD4 counts (blue) and the HIV viral load (red) over time since infection.

Source: <https://i-base.info/ttfa/section-2/14-how-cd4-and-viral-load-are-related/>

at different stages of the replication of the virus: nucleos(t)ide reverse transcriptase inhibitor (NRTI), non-nucleoside reverse transcriptase inhibitor (NNRTI), protease inhibitor (PI), integrase strand transfer inhibitor (InSTI) and entry inhibitor [15]. Aside from entry inhibitor drugs, which are rarely used, the four other classes of ART drugs inhibit three enzymes that are essential to replicate the virus: the reverse transcriptase (NRTI and NNRTI), the protease (PI) and the integrase (InSTI). The NRTI drugs, by disrupting the reverse transcription of the viral RNA genome, interrupt the generation of viral DNA, and thus, prevent the replication of HIV within the body. The NNRTI drugs directly bind to the reverse transcriptase, which blocks the reverse transcription process, inhibiting the generation of viral DNA. The PI drugs stop the activity of the protease, which is normally used to cleave the polyproteins into the functional individual proteins. As this occurs after the HIV replication stage, the PI drugs do not prevent the virus from replicating but make it unable to mature and to infect new cells. Finally, the InSTI drugs prevent the virus from inserting itself into the human DNA, by blocking the integrase. Figure 1.4 summarizes the modes of action of the different ART classes.

1.3.2 Timeline of ART discoveries

The first ARV, zidovudine, a NRTI drug, appeared in the end of the 1980s and was first used as a monotherapy in patients with advanced disease [16]. The use of zidovudine in patients with low CD4 counts decreased the short-term mortality risk. However, no consensus existed at that time as to whether patients with high CD4 counts should also be treated. The discovery of NNRTI and PI drugs in the early 1990s was a key milestone in the fight against HIV, as it provides HIV treatment alternatives to the toxic zidovudine. At this time, the field also understood the need of ART drug combination in order to achieve sustainable viral suppression and limit the risk of emergence of drug resistance. First, zidovudine was combined with another NRTI drug, which improved the efficacy compared to zidovudine alone. For instance, several controlled trials showed that combining zidovudine with

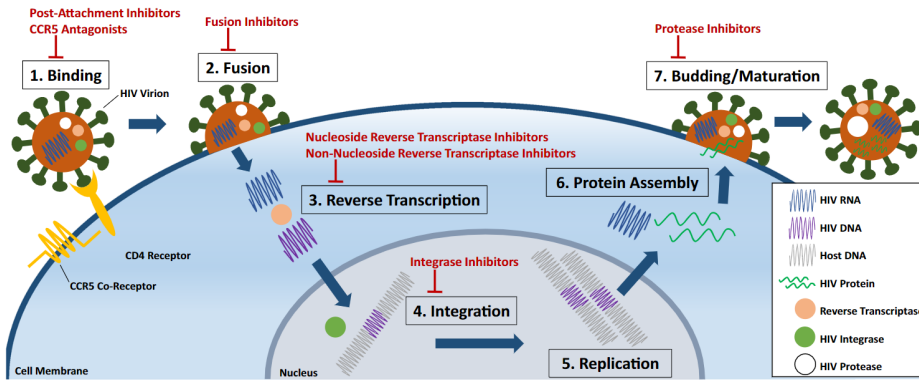


Fig 1.4: Mode of action of the different ART classes throughout the replication of HIV. Source: <https://link.springer.com/article/10.1007/s11481-019-09880-z>

lamivudine – a NRTI drug introduced in 1995 – led to a stronger decrease in viral load and increase in CD4 counts compared to the zidovudine monotherapy. However, most benefits were only observed over a short period and HIV mortality rates remained high [17]. At the end of the 1990s, two studies demonstrated the higher long-term efficacy of triple therapies, which combined two NRTIs with either a NNRTI or a PI drug [18, 19]. Unlike NRTI dual therapy, such triple therapy maintained immunologic function and viral suppression even after several years of ART. This led to the construction of regimens that comprised three or more ARV drugs in order to achieve sustained virologic suppression. The introduction of triple therapy outside the selected patient groups included in clinical trials were also shown to reduce both mortality and disease progression [20]. However, the high number of tablets and complicated dosing schedule that such regimens require resulted in problems of adherence to treatment. Combining several drugs in a single tablet helped to increase drug adherence by providing simplified treatment options. Such co-formulations first combined the two NRTI drugs, such as zidovudine and lamivudine in 1997 or tenofovir and emtricitabine in 2004. The first triple combination containing two NRTIs and a NNRTI drug in a single tablet, called Atripla, was approved in 2006. Since then, the use of two NRTI drugs, often called NRTI backbones, with one core agent, NNRTI, PI or InSTI, has become the norm.

1.3.3 ART in South Africa

While triple therapy was available in developed countries since 1996, its high price prevented its use in resource-limited settings such as sub-Saharan Africa. A growing international movement fought against the high cost of treatment in the early 2000s and managed to considerably reduce the price of ART in Africa [21]. As a result, South Africa could launch its public sector ART programme in 2004. In view of the high number of people that were diagnosed HIV-positive, it was clear that South Africa would have lacked qualified health personnel who could ensure the same personalized follow-up as in developed countries. A simplified treatment paradigm was required, in which the majority of clinical tasks could be ensured by lower health cadres. In particular, fixed-dose combination ART was developed, together with standardized guidelines. In South Africa, the first-line regimen consisted of a NNRTI drug combined with two NRTI drugs. Patients failing first-line regimen were recommended to switch to second-line regimen, where PI replaced NNRTI. In the first years

following ART scale-up in South Africa, only people with low CD4 counts (below 200 cells/ μ l) or with comorbidities were eligible for ART. With the development of treatments with less side effects, it was then suggested that people with higher CD4 counts could also benefit from early ART initiation. In fact, an early initiation of ART could reduce both mortality and HIV transmission [22, 23]. Based on these findings, the World Health Organization (WHO) first recommended to expand the ART eligibility criteria at CD4 counts below 500 cells/ μ l in 2013 [24]. Following WHO's recommendation, South Africa gradually expanded its ART eligibility criteria throughout the years. In 2016, WHO launched the "Treat-All" policy, which recommends a rapid ART initiation after diagnosis for all PLWH, irrespective of their CD4 counts [25], and this strategy was immediately implemented by South Africa [26]. As a consequence of the increasing use of NNRTI-based first-line regimen in South Africa, resistance to NNRTI drugs emerged, threatening the efficacy of such regimens. In 2020, as a response to the increasing level of resistance to NNRTI, South Africa introduced dolutegravir (DTG), an INSTI drug, in combination with two NRTI backbones as the new first-line regimen [27]. In view of the low price and the high genetic barrier to resistance of DTG regimens, South Africa also decided to transition people currently on NNRTI-based regimens to DTG-based regimens.

1.4 HIV drug resistance

1.4.1 Biological mechanisms

As previously mentioned, HIV is a highly diverse virus: regions of the world show different HIV subtypes. This diversity between infected individuals of different regions of the world results from the interplay of recombination events, a high turn-over and the high error rate of reverse transcriptase combined with the absence of proofreading mechanism. The HIV genome contains nine genes encoding the proteins that are essential for the maturation and the replication of the virus. We call mutation, when a nucleotide in the viral genome is altered, e.g. by a random error made by the reverse transcriptase. Due to the error-prone nature of reverse transcriptase, the large size of the HIV virus and the high replication rates of HIV, such errors often occur. Most of the time, these mutations are deleterious, i.e. decrease the fitness and replication capacity of the virus compared with the wild-type virus (i.e. the variant without any mutation). Due to natural selection, the variants of the virus with deleterious mutations go rapidly extinct. This nevertheless creates many HIV variants, leading to a high within-host diversity. However, in the absence of antiretroviral drug pressure, the wild-type variant remains the dominant strain.

Antiretroviral drugs are developed to prevent the replication of the wild-type virus. However, some mutations in the virus can considerably decrease its susceptibility to an antiretroviral agent [28]. These resistance mutations are located in the gene coding for the different viral enzymes, such as the reverse transcriptase, the integrase or the protease. The presence of these mutations causes some change in the conformation of the enzymes, which hinders or even prevents the antiretroviral agent from achieving its task. For instance, a single mutation, the K103N, already induces a conformational change of the reverse transcriptase, which blocks the binding of some NNRTI drugs [29]. An antiretroviral agent will therefore confer a selective advantage to the variants that are resistant to it. Under the drug selective pressure of ART, the resistant variants are thus more likely to predominate than the susceptible variants.

1.4.2 Acquisition and transmission of resistance

Acquisition of HIV drug resistance mutations to an antiretroviral regimen usually occurs during treatment failure, as the ongoing viral replication increases the number of HIV genome copies and therefore the probability of the emergence of a resistant strain due to random mutations. The number of drug resistance mutations needed to confer resistance to an antiretroviral agent largely depends on the antiretroviral class. This number is often referred to as the genetic barrier to resistance. It is defined as the “threshold above which ART drug resistance develops, or the ease to which resistance develops” [30]. Regimens containing a first-generation NNRTI drug (i.e., efavirenz or nevirapine) are considered to have a low genetic barrier to resistance, as a single mutation is sufficient to render the virus resistant. Other regimens, e.g. those containing either PI or InSTI drugs, have a higher barrier to resistance, as the virus requires the accumulation of several successive mutations to acquire resistance. The drug resistance mutations develop at different rates from the time of treatment failure, which also depend on the regimen used, as each ARV drug selects for specific drug resistance mutations.

Individuals on ART with ongoing viral replication might potentially infect other individuals. If they have previously acquired resistance, they might therefore transmit these resistances. As drug pressure is usually not exerted for several years after the infection, the selective advantage of resistance is lost, which might cause the reversion of the resistant strains to the wild-type variant. The rates of reversion differ across the resistance mutations and can be very low [31, 32]. For instance, the K103N mutation persists on average 10 years before reverting to the wild-type virus, thus conferring resistance to NNRTI several years after infection. Reversion of resistance also occurs in ART-experienced individuals in case of prolonged treatment interruption.

1.4.3 The role of ART combination

The combination of antiretroviral drugs substantially reduces the risk of emergence of drug resistant variants for two reasons [33]. First, as the employed drugs have multiple modes of action, several specific mutations are required to occur concurrently to acquire resistance to all the drugs combined in the regimen. In addition, it is highly unlikely that the resistant variants present before treatment initiation are able to resist to the different drugs. Second, combining drugs of different classes increases the chance of viral suppression, and thus, prevents the generation of new resistance variants of the virus. Similarly, if there is a too low concentration of ARV drugs in the cells, the drug selective pressure is not sufficient to select for new resistant strains. In this case, the wild-type virus remains the dominating variant. Therefore, the risk of development and selection of drug resistance mutations is closely related to the activity of the antiretroviral agent. The risk of emergence of drug resistance is the highest when ART is present at a sufficient level to exert a drug selective pressure, but not at a high enough level that would prevent resistant variants from replicating.

Although higher drug concentration favors viral suppression and diminishes the risk of resistance emergence, it is often accompanied with unwanted side effects caused by the toxicity of ART drugs. These side effects differ across ART drugs but generally includes fatigue, headache, insomnia or nausea. In addition, they can be associated with poor adherence to ART [34]. Therefore, optimizing drug dosing is key to guarantee long-term efficacy of ART-regimen (Fig 1.5).

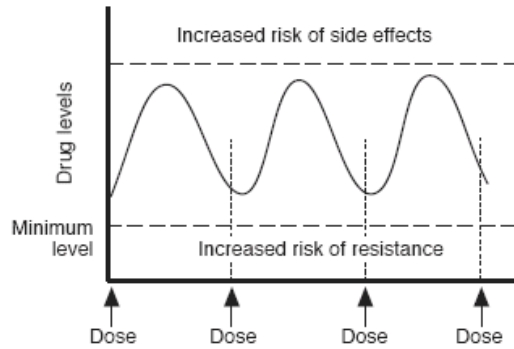


Fig 1.5: Drug activity over time. Source: <https://i-base.info/resistance-taking-drugs-on-time-and-missed-doses/>

1.4.4 ART adherence and the risk of developing resistance

Adherence to ART plays an important role in the emergence of drug resistance, as it influences the ART drug concentration. Suboptimal adherence reduces drug activity, potentially leading to treatment failure and acquisition of drug resistance mutations. Adherence to ART has been shown to be a major predictor of achieving HIV suppression and of minimizing the emergence of drug resistance [29]. Even if bell-shaped curves are often used to represent the relationship between the level of adherence and the risk of resistance, the impact of adherence on the development of resistance is more complex in practice and differs across the antiretroviral drug classes [35]. For example, clinical studies have reported a high risk of resistance even with very low levels of adherence to NNRTI, while much higher levels of adherence to PI is required for resistance to emerge (Fig 1.6) [36]. These differences are partly driven by the different half-lives (i.e. the time for a drug to lose half of its original concentration) between the antiretroviral drug classes. Due to the higher half-life of NNRTI compared with NRTI, poor adherence to NNRTI-based ART or ART interruption of several days leads to a prolonged NNRTI monotherapy, which favors the emergence of NNRTI resistance. Unlike NNRTI, PI drugs have relatively short half-lives, preventing prolonged low-dose exposure to PI that would lead to the development of resistance.

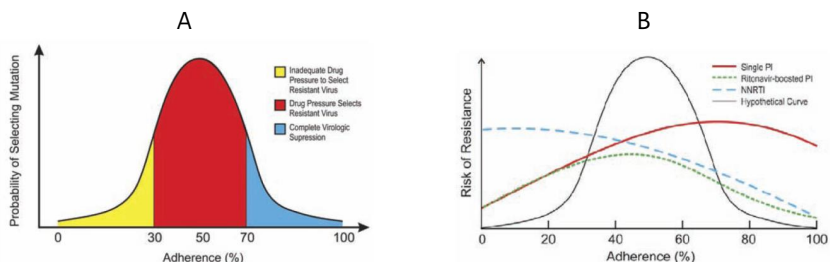


Fig 1.6: Relationship between adherence and the risk of developing resistance, represented schematically (Panel A) and observed in practice (Panel B). Source: <https://www.ncbi.nlm.nih.gov/pmc/articles/PMC5072419/> [35]

1.4.5 Impact of resistance on ART efficacy

The level of resistance conferred by a resistance mutation is measured by in-vitro studies, which determine the decrease in ARV susceptibility caused by the mutation. To assess the actual impact of resistance on the efficacy of ART regimen, the presence of baseline resistances in ART-initiators is retrospectively determined and suppression rates between patients with and without resistance are compared. Wittkop and colleagues show that the presence of high-level resistance increases the risk of failure after 12 months from less than 5% to almost 25%, corresponding to an adjusted hazard ratio of 3.13 [37]. Even if the presence of resistance prior to ART initiation increases the risk of ART failure, this study stressed the fact that individuals starting ART with high resistance level keep a good chance of viral suppression. Indeed, the combination of drugs from different classes in the ART regimen, together with the residual activity of the compromised drugs, help to maintain high activity levels of ART even in the presence of resistance. Disentangling the respective effects of NNRTI and NRTI resistance on the risk of failure is however difficult, due to the limited power of such studies (as only few participants have pre-existing resistance) and to the fact that occurrence of NNRTI and NRTI resistances are associated.

1.4.6 Monitoring resistance

The prevalence of transmitted drug resistance (TDR) is used as an indicator of the transmission potential of a resistance to a specific antiretroviral agent or class. This prevalence is usually measured among newly diagnosed individuals who intend to initiate ART. The term "pretreatment drug resistance" (PDR) is sometimes preferred over TDR, as some individuals might have undisclosed past-exposure to ARV drugs, which could have driven previous development of resistance. In these patients, it is therefore impossible to know whether resistances have been acquired or transmitted. Levels of NRTI and NNRTI PDR are usually reported in South Africa, as they inform about the proportion of ART-initiators who have reduced susceptibility to first-line NNRTI-based ART.

The prevalence of drug resistance mutations among people failing first-line ART is another widely used measure, as it shows at which rates drug resistance mutations are acquired. It is referred to as the prevalence "acquired drug resistance" (ADR), although some resistance mutations might have been transmitted. Knowing the level of ADR is also key to estimate the proportion of patients that are on a non-fully working ART regimen. As second-line regimens also comprise two NRTI backbones, the prevalence of NRTI ADR is an important indicator of the proportion of patients that will switch to second-line regimen with pre-existing NRTI resistance.

The 2017 *WHO HIV drug resistance report* warns about the increasing levels of NNRTI PDR in Southern Africa [38]. From less than 1% at the beginning of ART scale-up in 2004, this level reached 10% in 2017, which threatens the long-term efficacy of NNRTI-based regimens (Fig 1.7). As stated by the WHO, reaching this 10% threshold calls for a change of the first-line regimen. Unlike NNRTI, the level of NRTI PDR remained at a low level in Southern Africa, below 5%. The WHO also reported high levels of ADR to both NRTI and NNRTI, thus showing rapid development of NNRTI and NRTI resistance during failure. The contrast between high level of NRTI ADR and low level of NRTI PDR indicates that NRTI resistance is rarely transmitted. As second-line regimens also comprise two NRTI backbones, the high level of NRTI ADR raises concerns on a potentially reduced efficacy of second-line regimen due to pre-existing NRTI resistances.

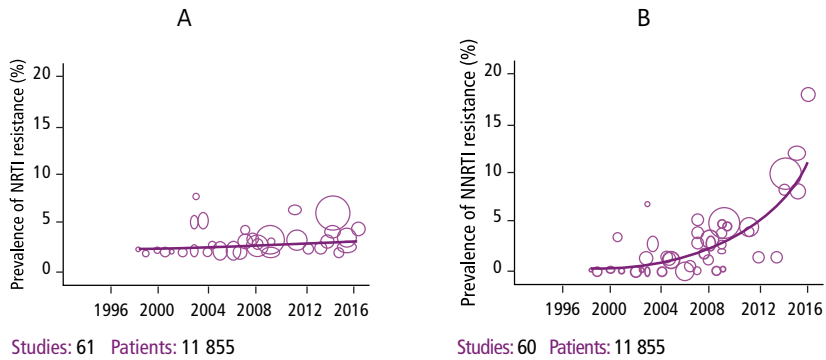


Fig 1.7: Prevalence of PDR to NRTI (panel A) and NNRTI (panel B) measured in studies from Southern Africa. Source: WHO HIV Drug Resistance Report 2017 [38]

1.5 HIV strategies in South Africa

In this section, I present the different HIV interventions that South Africa has implemented in addition to the ART roll-out. Their implications in terms of HIV drug resistance are also discussed.

1.5.1 Fast-Track strategy

In 2014, UNAIDS communicated its goal of ending the AIDS epidemic as a public health threat by 2030. The Fast-Track strategy aims to achieve this goal, by stepping up HIV response in low and middle-income countries [39]. This strategy gathers several targets for prevention and treatment that needed to be reached by 2020. The "90-90-90" target states that in 2020, 90% of PLWH should be diagnosed, 90% of diagnosed individuals should be on ART and that 90% of people on ART should be virologically suppressed [40]. In South Africa, several innovations in testing strategies (e.g. community-based testing) expanded HIV testing coverage and helped achieve the first 90 target. WHO estimates that 92% of PLWH know their status in 2020 [9]. Despite the national scale-up of ART and the expansion of ART-eligibility criteria, only 75% of the HIV-diagnosed people are on ART. Several challenges regarding the retention in care, such as drug toxicity or risk of loss to follow-up, undermined the progress towards achieving the second 90 target. Finally, 92% of people on ART are estimated to have achieved viral suppression. The recent emergence of NNRTI resistance is nevertheless threatening the long-term achievement of this target.

1.5.2 Treatment as prevention (TasP)

Treatment as Prevention (TasP) is a concept that promotes the use of ART to reduce the risk of HIV transmission. By starting ART at an earlier stage, HIV-positive individuals increase their chance of viral suppression and reduce the time during which they are infectious. The public-health policy that reflects this concept is called universal test-and-treat (UTT), which offers counselling and testing to an entire population, followed by immediate ART initiation for all PLWH. The UTT approach is sometimes referred to as the "Treat-All" policy, as it recommends expanding ART for all HIV-positive people, abandoning the policies restricting ART to individuals with low CD4 counts. Four randomized population-based trials have

1 evaluated the UTT approach in Southern Africa. Two of them showed a reduction of 20% and 31% in HIV-incidence due to UTT implementation, while the two other studies did not find significant differences between the control arm(s) and the arm implementing UTT [41–44]. In addition, some concerns were raised on the risk of emergence of drug resistance caused by the UTT implementation [45]. The implementation of UTT implies a rapid increase of the number of patients on ART, all potentially at risk of acquiring and transmitting HIV drug resistance. As patients starting ART with high CD4 might have lower adherence and lower retention in care [46], this could favor the development of HIV drug resistance [47]. However, as showed by a South African cohort study [48], the higher viral suppression achieved by individuals initiating ART early reduces the risk of development of resistance.

1.5.3 Introduction of Dolutegravir

As a response to the increasing levels of NNRTI TDR in Southern Africa, WHO recommended the use of DTG as an alternative option for first-line regimen from 2016 [25]. DTG has many advantages. It has a higher barrier to resistance and is well tolerated [49]. DTG also has a higher potency, i.e. lower concentration of the drug is needed to prevent the replication of HIV. Due to the low dosage required, DTG can be combined with its two NRTI backbones into a single tablet. The generic fixed-dose combination includes tenofovir, lamivudine and dolutegravir (TLD). Finally, thanks to a pricing agreement between the manufacturer and several low- and middle-income countries including South Africa, TLD costs 75 dollars per person per year [50]. In view of all these advantages, not only will DTG-based regimen be used as first-line regimen in South Africa, but also to transition patients currently on NNRTI-based first-line regimen to DTG-based regimen.

Launched in 2020 in South Africa, the implementation of DTG-based regimen was initially delayed by safety concerns on the use of DTG among pregnant women. Preliminary results of the Tsepamo study in Botswana in 2018 showed a higher risk of neural tube defect (NTD) among infants born of women using DTG than when using other ART ($4/426=0.94\%$ vs $14/11,300=0.12\%$ respectively) [51]. An update from the Tsepamo study in 2020 showed a lower estimated risk of NTD in women using DTG at conception ($2/1,908=0.1\%$), suggesting that the higher preliminary estimates of NTD risks were mainly due to the low sample size [52]. This early safety signal has nevertheless influenced the implementation of guidelines regarding the use of DTG. South Africa recommends the use of NNRTI rather than DTG in women wanting to conceive and in women initiating ART within the first six weeks of pregnancy [27].

Some uncertainty also subsists on how to transition to DTG-based regimen. Both suppressed patients on NNRTI-based regimen and patients failing NNRTI-based regimen are supposed to transition to DTG. Discussions have been raised about patients switching to DTG with unsuppressed VL, as they are at higher risk of DTG-failure. Because of the ongoing virus replication, resistances are more likely to develop in these individuals. In addition, these patients might start DTG with preexisting NRTI resistance accumulated during NNRTI failure. This is of particular concern as the presence of NRTI resistance among patients switching to DTG could leave them on a functional DTG-monotherapy. In the absence of drug resistance testing, South Africa recommends to replace tenofovir, usually present in the NNRTI-based drug, by stavudine when starting DTG-based regimen, in order to have at least one working NRTI [27]. The higher toxicity of stavudine compared with tenofovir might however be a barrier to the wide use of such optimized regimen.

1.5.4 Resistance testing

Genotype resistance testing at diagnosis establishes the resistance profile of an individual initiating ART. Some countries recommend it in order to guide the selection of initial ART and optimize viral suppression. As suggested by a modelling study [53], baseline resistance testing is not cost-effective, as it only brings clinical benefit to a small fraction of ART-initiators. Resistance testing can also be performed in individuals failing ART to identify the development of potential resistance to ART and assess whether a switch to other ART combinations is needed. However, due to its high cost, low and middle-income countries do not systematically test for resistance.

1.5.5 PrEP, PEP and PMTCT, and their contribution to HIV drug resistance

Pre-exposure prophylaxis (PrEP), post-exposure prophylaxis (PEP) and prevention of mother-to-child transmission (PMTCT) are three different interventions involving antiretroviral agents used to prevent the transmission of HIV. PrEP provides ART to HIV-negative individuals to protect them from contracting HIV. PrEP usually contains two NRTI agents (tenofovir and emtricitabine). South Africa has been implementing it since 2016, but only in some clinics across the country. PrEP users can only develop resistance if they are on PrEP after having been infected, making PrEP an unlikely contributor of resistance. PEP is used as a short-term treatment for individuals having been exposed to HIV. It aims to reduce the risk of HIV infection after a risky behavior. PEP regimen contains two NRTI backbones generally combined with an InSTI drug. Due to its marginal use and its low duration, PEP is not considered as a driver of resistance in South Africa. Finally, PMTCT has been widely used since 2004 in South Africa to decrease mother-to-child transmission of HIV. It usually comprises a single NRTI drugs such as zidovudine, given to pregnant HIV-positive women. More recently, South Africa implemented the "Option B" PMTCT regimen, which consists of three ART drugs. PMTCT considerably reduced perinatal HIV transmission risk. However, PMTCT failure might result in the emergence of HIV drug resistance in the infants, either directly transmitted by the mother or acquired due to the selective pressure of PMTCT drugs. Poppe and colleagues have reported a higher prevalence of drug resistance in children exposed to PMTCT [54]. As HIV is essentially transmitted through sexual contact in South Africa, PMTCT is not considered to have played a major role yet in the spread of HIV resistance.

1.6 Mathematical modelling

1.6.1 History

Infectious diseases have played an important role in human history. The first mathematical model used in epidemiology is the work of Daniel Bernoulli on the effect of inoculation against smallpox in the 18th century [55, 56]. Breakthrough on the transmission of disease helped epidemiologist to make assumptions about the means of spreading infections. The first models representing the dynamic of an infectious disease over time were developed in the early 1900s. Kermack and McKendrick in three articles published between 1927 and 1933 set the theoretical basis of the compartmental model used in infectious disease modelling [57–59].

Such compartmental models divide a population in different groups (or compartments) according to some characteristics such as the exposure to a disease. For instance, the SIR model splits the population in three groups representing the number of susceptible (S),

infected (I) and recovered (R) individuals. It is represented mathematically by a system of differential equations, where each equation determines how many people enter and leave a given compartment as time passes. A compartmental model makes two main assumptions [60]. First, it assumes the homogeneity of the population, i.e. that all individuals behave the same manner. Second, it relies on the law of mass action, which states that the number of new infections in a given period is proportional to the product of the number of susceptible and infected individuals [61]. These two assumptions imply a homogeneous mixing of the population, which has been the source of many criticisms. The heterogeneity between individuals can be taken into account by stratifying the compartmental model by some characteristics driving this heterogeneity. For instance, when modelling sexually transmitted diseases, we usually differentiate the population across age groups and sex to model differences in transmission between these groups. Despite this assumption of homogeneous mixing, compartmental models are still widely used, as they have been proved to be robust and predictive [61, 62]. As they are based on simple differential equations, compartmental models can be solved by basic numerical approximation methods. The simplicity of such models also allows to produce closed-form formula of important epidemiological indicators.

These last decades, a new class of models – the agent-based models (ABMs) - has emerged, spurred by the recent advances in computer performance that allow to simulate more complex models [63]. ABMs reject the homogeneous-mixing assumption and simulate the dynamic of an infectious disease at an individual level. Their higher flexibility is used to model more complex behaviours, such as the dynamic of an infectious disease in a given network. However, ABMs have several limitations. First, their too high complexity can lead to unexpected results that are often difficult to interpret. Second, even if their simulation time has considerably decreased in the recent years, their complexity often hampers the calibration of a large number of parameters.

The comparison between compartmental models and ABMs highlights a recurrent challenge when modelling infectious disease dynamics: the trade-off between complexity and realism. Too simple models often fail to accurately reproduce the dynamic of an infectious disease, while calibrating complex models requires precise data that are often unavailable. Following Occam's razor, a principle stating that complexity should never be chosen without necessity, we should thus reject a more complex model as soon as the limited data resource prevents the model from identifying its parameters.

1.6.2 Modelling HIV epidemic in South Africa

Mathematical models have been widely used to describe the HIV epidemic in South Africa [64]. The first model representing the dynamic of the HIV epidemic in South Africa, the so-called Actuarial Society of South Africa (ASSA) model, was developed in the early 1990s [65]. It provided estimates on several HIV-indicators such as the total number of new infections or the number of AIDS-related deaths. The complexity of such models has evolved together with the accumulation of data. The ASSA models were superseded by the Thembisa model, a demographic projection model on which UNAIDS estimates are based [66]. In addition to providing estimates on key HIV-indicators, some mathematical models were also developed to assess the impact of different HIV interventions. Johnson and colleagues quantified the number of AIDS-related deaths and HIV-infections averted with the national ART roll-out in South Africa [67]. Finally, some mathematical models were also built for the purpose of predicting the evolution of the epidemic under different scenarios. In 2009, Granich and colleagues investigated the future impact of universal testing coupled with

immediate ART start for adults and found that this strategy could eventually eliminate HIV [68]. Such predictions inevitably contains high uncertainty, especially on the long-term efficacy of newly implemented ART regimen. The recent increase of NNRTI resistance has questioned the long-term sustainability of NNRTI-based regimen and has thus belied many model projections. This highlighted the need of considering the risk of emergence of HIV drug resistance when modelling the long-term effectiveness of HIV interventions.

Recent modelling works have integrated the effect of drug resistance on treatment outcome in different ways. The HIV Synthesis model, developed by Philips and colleagues, capture the effect of every drug resistance mutation relative to the different ARV classes [53]. Such agent-based models have the advantage to be able to represent complex mechanisms, such as the acquisition of specific drug resistance mutations. However, such models often make assumptions on the rate of acquiring and transmitting drug resistance mutations that are difficult to verify. Simpler compartmental models have also been used to capture the dynamic of HIV drug resistance in sub-Saharan Africa [69, 70]. To limit the number of compartments, these models either have a dichotomized representation of HIV drug resistance (i.e. with two layers representing the presence/absence of resistance) or only represent some specific resistance mutations (e.g. the K65R and M184V for NRTI drugs).

1.6.3 Data availability

Several sources of data cover different aspects of the HIV epidemic. First, general HIV-indicators (e.g. number of new-infections, ART-coverage, mortality) inform about the progresses done over time in the fight against AIDS. Second, epidemiological data have been longitudinally collected from several observational cohorts in South Africa. The International epidemiological Databases to Evaluate AIDS in sub-Saharan Africa (IeDEA-SA) collaboration gathers individual cohort data on treatment response on thousands of patients [71].

Third, randomized clinical trials (RCTs) give high-quality information on HIV drug resistance parameters, such as the risk of acquiring resistance mutations to the different ART drugs. However, the particular characteristics of the patients included in RCTs limit the applicability of such data. Their strict inclusion criteria often select patients with high levels of adherence and the monitoring frequency is considerably higher than in real-world settings. The particular settings of RCTs thus prevent them from observing development of HIV drug resistance as it would have occurred in real-world settings. To overcome this issue, resistance data collected from cohorts studies (e.g. studies that test for resistance a group of individuals failing ART-regimen) can be used instead. However, the majority of these cohorts are located in North America or Europe. In view of the many differences between South Africa and North America or Europe (e.g. HIV subtype, quality of care, regimens used), their results cannot be directly extrapolated to resource-limited settings.

The scarcity of data on resistance in South Africa is thus a major challenge to predict the impact of HIV drug resistance in such settings. Mathematical models can overcome this issue by integrating knowledge from different levels of evidence. They could therefore bridge the gap between good epidemiological data and scarce resistance data from resource-limited settings [72].

1.7 Aims and outline of the thesis

The overall aim of this project is to explore the past and future dynamics of HIV drug resistance in Southern Africa, using mathematical models.

In Chapter 2, I assess the prevalences of acquired drug resistance mutations against first-line regimens in Southern Africa. To do so, I perform a systematic review, searching studies that report the proportion of single NRTI/NNRTI resistance mutations among adults failing first-line regimens in this region. I then develop a hierarchical Bayesian model to synthesize evidence from the collected studies.

In Chapter 3, I reproduce the past dynamics of the general HIV-epidemic and NNRTI resistance among adults in South Africa, using a compartmental model. Epidemiological cohort data are used together with clinical data on resistance to calibrate the model. Observed levels of TDR and ADR in South Africa are compared with model outputs to validate the calibration procedure. I then run several counterfactual scenarios to identify some factors that have driven the spread of NNRTI resistance in South Africa.

In Chapter 4, I explore the potential impact of the introduction of DTG-based regimen on the future dynamic of NNRTI resistance in South Africa. To do so, I adapt the compartmental model developed in Chapter 3. I investigate several prospective scenarios representing different strategies of DTG introduction and various levels of DTG uptake among women.

The Chapter 5 discusses the future issues that HIV drug resistance raises and explain how real-world data and mathematical models could be combined to provide some answers.

In Chapter 6, I provide a summary of the main findings and discuss their implications. I then describe the current state of knowledge about the future risk of resistance to DTG and discuss how mathematical models could be used to fill the knowledge gaps.

In Chapter 7, I present an additional work, in which I was involved but which does not form the core of my PhD project. In this work, a mathematical model was developed to estimate the SARS-CoV-2 mortality in different regions. This project emerged at the very beginning of the SARS-CoV-2 epidemic as an attempt to address our earlier inability to provide reliable age-specific estimates on SARS-CoV-2 mortality.

Chapter 2

Acquired HIV drug resistance mutations on first-line anti-retroviral therapy in Southern Africa: Systematic review and Bayesian evidence synthesis

Anthony Hauser¹
Fardo Goldstein¹
Martina L. Reichmuth¹
Roger D. Kouyos^{2,3}
Nicola Low³
Gilles Wandeler^{1,4}
Matthias Egger^{1,5,6}
Julien Riou¹

¹ Institute of Social and Preventive Medicine, University of Bern, Bern, Switzerland

² Division of Infectious Diseases and Hospital Epidemiology, University Hospital Zurich, University of Zurich, Zurich, Switzerland

³ Institute of Medical Virology, University of Zurich, Zurich, Switzerland

⁴ Department of Infectious Diseases, Bern University Hospital, University of Bern, Bern, Switzerland

⁵ Centre for Infectious Disease Epidemiology and Research, University of Cape Town, South Africa

⁶ Population Health Sciences, Bristol Medical School, University of Bristol, Bristol, United Kingdom

This article is in preparation.

Contribution: I coordinated and participated in the screening and extraction of evidence. I performed the analysis, made the figures and wrote the first draft of the manuscript and integrated co-authors' comments.

2.1 Abstract

Background: In Southern Africa, first-line antiretroviral therapy (ART) consisted of one non-nucleoside reverse transcriptase inhibitor (NNRTI) and two nucleoside reverse transcriptase inhibitors (NRTI) but is now being replaced by dolutegravir (DTG)-based ART. We estimated the prevalence of NRTI and NNRTI drug resistance mutations (DRMs) in patients failing NNRTI-based ART using Bayesian evidence synthesis.

Methods: We searched seven databases from inception to May 2019 to identify studies reporting DRMs among adults living with HIV (PLWH) who experienced virological failure on first-line NNRTI-based ART in Southern Africa. We used a hierarchical meta-regression model to synthesize the emergence of NRTI- and NNRTI-DRMs across different ART regimens, accounting for ART duration and study characteristics. We estimated the prevalences of nine NRTI and seven NNRTI DRMs after two years of ART.

Results: We included 17 study populations, including 2,432 PLWH with genotyping information from South Africa (13 studies), Mozambique (1), Botswana (1), Lesotho (1), and Zambia (1). In patients failing first-line ART, emtricitabine and lamivudine were strongly associated with the M184V/I mutation (risk >70% after two years). With tenofovir disoproxil fumarate, the prevalence of the K65R mutation was estimated at 55.2% at two years. On efavirenz, K103 was the most prevalent NNRTI resistance mutation (59.8%) followed by V106 (44.6%).

Interpretation: In patients failing first-line ART in Southern Africa, the prevalence of NRTI/NNRTI DRM is high. Many patients failing an NNRTI-based regimen may switch to a DTG-based regimen with compromised NRTIs, which could impair the long-term efficacy of DTG-based ART in Southern Africa.

2.2 Introduction

In 2014, UNAIDS communicated its goal of ending the AIDS epidemic as a public health threat by 2030 [39]. The strategy to achieve this objective involved stepping up testing and anti-retroviral therapy (ART) in low and middle-income countries (LMIC). In the last two decades, first-line ART implemented in most LMIC consisted of a non-nucleoside reverse-transcriptase inhibitor (NNRTI) combined with two nucleos(t)ide reverse transcriptase inhibitors (NRTI). For many NNRTIs, a single mutation will lead to drug resistance; for example, the K103N mutation [73]. Pre-treatment drug resistance (PDR) to NNRTIs has exceeded the WHO threshold of 10% in Southern Africa [38]. Several countries in the region are therefore transitioning from the NNRTI based first-line triple therapy towards an integrase-strand-transfer-inhibitor (InSTI) based first-line triple therapy. WHO recommends TLD, a fixed-dose combination of tenofovir, lamivudine and dolutegravir (DTG) [25].

People living with HIV (PLWH) on NNRTI-based ART should also transition to DTG-based therapy. Among them, those with unsuppressed viral load are likely to have acquired resistance to NNRTIs or NRTIs. As NRTI-resistance reduces the activity of the NRTI backbone of DTG-based regimens, PLWH switching with pre-existing NRTI resistance are at higher risk of DTG-failure and of developing DTG-resistance. A cross-sectional survey in South Africa showed that 83% of patients failing NNRTI-based treatment had the M184V/I mutation, and over half the patients developed K65R [74]. The risk of developing drug resistance mutations (DRMs) depends on several factors, including the exact regimen used and treatment duration.

In contrast to transmitted drug resistance, only a few studies have assessed acquired drug resistance (ADR) in patients failing first-line ART in Southern Africa [38]. Most studies of ADR were performed in Europe or North America, where subtype B is most prevalent, while most HIV infections in Southern Africa are caused by subtype C [75, 76]. In-vitro studies suggest that different subtypes might lead to different rates of ADR [77–79].

We performed a systematic review and Bayesian evidence synthesis of studies reporting frequencies of drug resistance mutations in patients failing first-line ART in Southern Africa, a region heavily affected by HIV [80].

2.3 Methods

2.3.1 Literature search

We searched seven bibliographic databases, including Embase and Medline, using terms for “HIV” AND “anti-retroviral therapy” AND “drug-resistance mutations” AND “Southern Africa”. The S1 File provides details on the literature search. We performed the final search on 16 May 2019 and de-duplicated references in EndNote (version 18.0.0). We registered this review in the International Prospective Register of Systematic Reviews (PROSPERO, No. CRD42017076406) [81].

2.3.2 Inclusion criteria

We searched for studies from Southern African countries in adult (15 years or older) PLWH on NNRTI-based first-line ART who were at least three months on treatment and experienced virologic failure. The results of at least ten genotypic resistance tests covering all major single mutations listed in the Stanford HIV drug resistance database had to be reported [82]. First, FG and AH assessed articles based on their title and abstract. Second, AH and either FG or MLR assessed potentially eligible studies based on the full text. We compared the results of full-text screening and reached consensus on eligibility by discussion.

2.3.3 Data extraction

We extracted details on study populations and settings, study year and the number of patients tested for viral load and with virologic failure. We recorded the definition of failure, i.e. the viral load threshold and the number of measurements required, and the first-line ART regimen. We grouped resistance mutations by locus (for example, M184I/V). We defined year of study as the year of the analysis, the year enrolment ended, or by the “sampling date” recorded in GenBank [83]. If studies reported stratified data (for example, by country or level of urbanization), we extracted the data separately.

2.3.4 Bayesian evidence synthesis

We developed a hierarchical meta-regression model to estimate the prevalence of eight single NRTI mutations: K65N/R, M184I/V, M41L, D67N/G/E, K70E/G/R, L210W, T215F/I/N/S/Y, K219D/E/N/Q/R. Fig 2.1 and S2 File detail the model structure. The model includes a random effect to account for study-level heterogeneity (i.e. shared by all the mutations) and a random effect at the mutation level. We considered that time to acquiring a mutation was exponentially distributed, thus assuming a risk of developing a DRM constant over time.

We examined the effect of different NRTI drugs on the risk of developing a DRM. We report model estimates of the prevalences of the eight major NRTI DRMs at baseline (treatment start, corresponding to the intercept of the regression model) and after two years. We opted for weakly informative prior distributions. S2 File reports the model equations and the prior distributions.

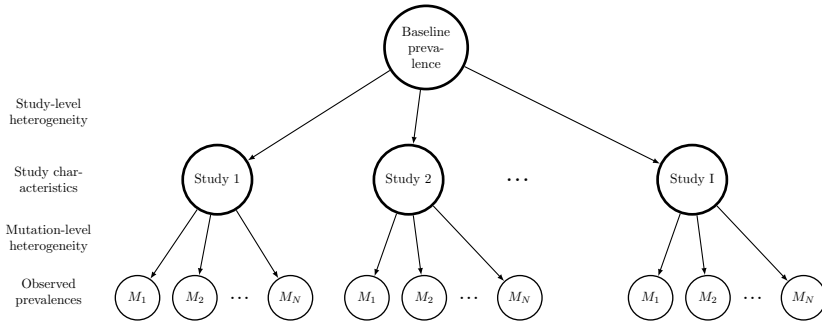


Fig 2.1: Bayesian hierarchical model adjusting for the different levels of heterogeneity.

We considered five NRTI drugs: didanosine (ddI), emtricitabine/lamivudine (FTC/3TC), tenofovir disoproxil fumarate (TDF), stavudine (d4T), and zidovudine (ZDV). As NRTI backbones mostly comprise either ddI or FTC/3TC and TDF, d4T, or ZDV, there were strong correlations between the drugs. We dealt with multicollinearity by selecting the covariates with the strongest effects first. In a sensitivity analysis, we also ran the model with all covariates (see S2 File). We imputed the time on ART in three studies [84–86] that did not report it, assuming that the missing ART durations followed a gamma distribution with mean and variance calculated from the observed ART durations. We also ran the model after discarding these three studies to assess the impact of data imputation (see S2 File).

We also estimated the prevalence of any of six thymidine-analogue mutations (TAMs), i.e. M41L, D67E/G/N, K70E/G/R, L210W, T215F/I/N/S/Y, or K219Q/E. As only a few studies reported the prevalence of any TAM, we adopted a method that estimated the correlation between the six TAMs (using results from the nine studies reporting the prevalence of the single TAMs and the prevalence of any TAM), assuming a multivariate Bernoulli distribution. We used this estimate to calculate the prevalence of any TAM (see S2 File). Finally, we applied the same model to estimate the prevalence of seven NNRTI mutations (K101E/H/P/Q, K103N/R/S, V106A/I/M, V108I, Y181C/I/V, Y188C/H/L, G190A/E/R/S) as for the NRTI DRMs. Estimates of the prevalence of DRMs are given after two years of efavirenz (EFV)- or nevirapine (NVP)-based regimens. The baseline prevalence of NNRTI DRMs was not reported because EFV and NVP select for the same NNRTI DRMs, which in turn prevents the model from providing reliable estimates.

All Analyses were performed in a Bayesian framework using the *rstan* package in R. All code and data are available from <https://github.com/anthonyhauser/ADR-meta-analysis>.

2.3.5 Risk of bias

Two of us (AH, ME) independently assessed study designs to gauge the representativeness of the patients for whom HIV genotypes were available. We calculated the percentage among patients with virologic failure who had HIV genotypes. We considered studies at high risk of

selection bias if i) genotyping rates were low (<50% of patients with failure were successfully genotyped); ii) there were relevant differences between the characteristics of genotyped and non-genotyped patient groups or iii) there was no clearly defined source population for patients to be genotyped. In a sensitivity analysis, we removed studies fulfilling one or more of these criteria and reran the analyses to examine the effect these studies had on the results.

2.4 Results

2.4.1 Selection and characteristics of studies

Our initial search produced 7,579 articles; 3247 were duplicates (Fig 2.2). We further excluded 4,138 papers based on title and abstract. We read the full texts of the remaining 194 articles. Of these, 16 studies were eligible, with 17 unique study populations and 2,432 individuals with genotyping information from South Africa (13 studies), Botswana (1), Lesotho (1), Mozambique (1), and Zambia (1) [14, 74, 84–97]. Most study populations were from urban settings.

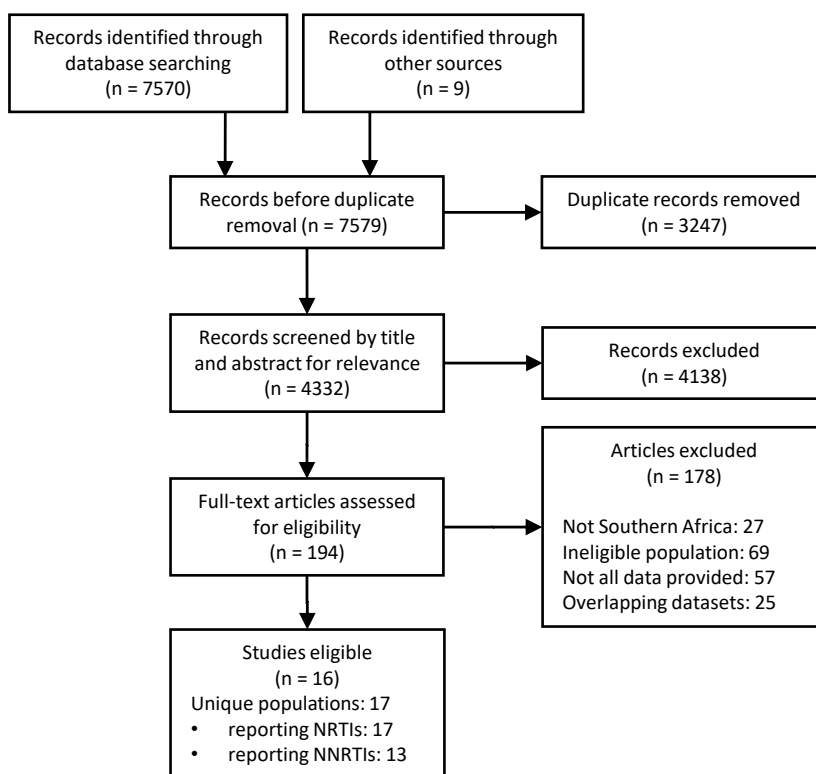


Fig 2.2: PRISMA flow-chart of inclusion of studies and populations in the systematic review.

Table 2.1 summarizes the study samples, the numbers of patients included, and their characteristics. Most studies defined virologic failure as a viral load >1000 copies/ml, either as a single measurement or confirmed by a second measure, as recommended by the WHO [25]. The most commonly used NRTI combinations were FTC/3TC with TDF (38% of patients), d4T

(38%), or ZDV (19%). These NRTI drugs were mostly combined with EFV (74%) or NVP (26%). Of 3,592 patients with virological failure, 68% (2,432) had HIV genotype data available. In most study populations (11/17, 57.9%), the percentage of patients with virologic failure with information on the HIV genotype was above 90%. Three large studies are responsible for the gap between the numbers of PLWH with virological failure and the number with genotype data. A national survey in South Africa [74] included 1,033 patients but obtained genotypes only for 788 (76.3%), and three other studies in South Africa [93, 95, 96], where only a subsample of the patients failing first-line ART had genotyping of HIV performed. Table 2.2 provides a detailed description of each study population.

Table 2.1: Characteristics of the 17 study populations included in the systematic review.

| | Patients |
|--|--------------------------|
| Total No. of patients with virologic failure | 3592 |
| No. of patients with genotype data | 2432 (67.7%) |
| Median (range) number of patients with virological failure | 103 (31-950) |
| Median (range) number of patients with HIV genotype | 68 (19-788) |
| Median (range) percent patients with HIV genotype among patients with virologic failure | 92% (10-100%) |
| | Study populations |
| Definition of virologic failure (copies/mL) | |
| Confirmed >1000 | 6 |
| Single value >1000 | 6 |
| Value >5000 | 3 |
| Single value >400 | 1 |
| Confirmed >80 | 1 |
| Median (range) study year | 2012 (2004-2014) |
| Most common first-line regimen | |
| d4T + 3TC + EFV | 6 |
| TDF + 3TC + EFV | 2 |
| ZDV + 3TC + NVP | 2 |
| ZDV + 3TC + EFV | 3 |
| Other | 4 |
| Median (range) time on ART (months) | 27.5 (5-49.2) |
| Country | |
| Botswana | 1 |
| Lesotho | 1 |
| Mozambique | 1 |
| South Africa | 13 |
| Zambia | 1 |
| Urbanization | |
| Urban | 8 |
| Rural | 5 |
| Both | 4 |

Table 2.2: Characteristics of 17 study populations included in the systematic review and meta-analysis.

| No. | Publication | Study population | Setting | Urban/ rural | Study period | No. of patients (% female) | | | Definition of VL | Most common first-line regimen (%) | Use of NNRTI and NRTI reported | At high risk of bias | |
|-----|----------------------------|--|---|-----------------|--------------|---------------------------------|-------------|---------------------------|-----------------------------|------------------------------------|--------------------------------|-------------------------|-----|
| | | | | | | No. tested for VL at least once | No with VF* | No. with genotype number# | Threshold (cps/ml) | No. of measures | | | |
| 1 | Barth et al. 2012 [93] | Cohort of patients on first-line ART \geq 2 years | Ndlwv Medical Centre, Elandsdoorn, South Africa | Rural | n.r. | 562 (72%) | 47 | 19 | > 1000 | Repeated measure | d4T+3TC+EFV (58%) | NRTI: yes NNRTI: yes | Yes |
| 2 | Brehm et al. 2012 [94] | Patients participating in CIPRA-SA trial [98] of nurse versus physician led care (NCT00080522) | Primary care clinics in Masiphumelele, Cape Town and Soweto, Johannesburg, South Africa | Urban | 2007 | 812 (71%) | 63 | 63 | > 1000 after 24 weeks | Single measure | d4T+3TC+EFV (65%) | NRTI: yes NNRTI: yes | No |
| 3 | El-Khatib et al. 2010 [84] | Cross-sectional study of patients on first-line ART \geq 12 months | Outpatient clinics at Chris Hani Baragwanath Hospital, Soweto, South Africa | Urban | 2008 | 883 (75%) | 102 | 94 | > 400 | Single measure | d4T+3TC (100%) | NRTI: yes NNRTI: no | No |
| 4 | Hoffmann et al. 2009 [95] | Cohort of HIV-positive miners on first-line ART | Multi-site workplace HIV program in mining regions, South Africa | Both | 2007 | 3727 (7%) | 676 | 68 | > 1000 | Mostly repeated measure | ZDV+3TC+EFV (95%) | NRTI: yes NNRTI: yes | Yes |
| 5 | Hoffmann et al. 2013 [96] | Cohort of patients on first-line ART switching to TDF | Multisite workplace and community HIV program, South Africa | Both | 2011 | 1682 (50%) | 270 | 40 | > 1000 with prior RNA < 400 | Repeated measure | TDF+3TC+EFV/INVP (100%) | NRTI: yes NNRTI: no | Yes |

| | | | | | | | | | | | | | |
|----|---------------------------|--|---|-------|------|-----------|-----------|-----------|-----------------------|------------------|------------------------|-------------------------|-----|
| 6 | Hunt et al. 2017 [97] | Cross-sectional study of patients on first-line ART \geq 12 months | 15 ART-providing primary healthcare facilities in KwaZulu-Natal, South Africa | Rural | 2017 | 1299 | 123 | 123 | > 1000 | Single | TDF+3TC (85%) | NRTI: yes NNRTI: no | No |
| 7 | Labhardt et al. 2016 [14] | Cohort of patients on first-line ART \geq 6 months | Ten nurse-led clinics in rural Lesotho | Rural | 2014 | 1563 | 80 | 74 | > 80 | Repeated measure | ZDV/TDF+3TC+EFV (65%) | NRTI: yes NNRTI: yes | No |
| 8 | Marconi et al. 2008 [87] | Cross-sectional study of patients on first-line ART \geq 6 months | Outpatient clinic in Durban and Mariannhill, South Africa | Both | 2006 | n.r. | 124 | 115 (52%) | > 1000 | Single measure | d4T+3TC+EFV (49%) | NRTI: yes NNRTI: yes | No |
| 9 | Novitsky et al. 2007 [88] | Participants in one arm of Tshelo trial [99, 100] (NCT00197613) | Princess Marina Hospital, Gabarone, Botswana | Urban | 2004 | 108 (69%) | 31 | 23 | > 5000 after 16 weeks | Repeated measure | ZDV+ddI+EFV/NVP (100%) | NRTI: yes NNRTI: no | No |
| 10 | Rossouw et al. 2017 [89] | Cohort of patients on first-line ART \geq 6 months | Tshwane District Hospital in Pretoria, South Africa | Urban | 2012 | n.r. | 103 (73%) | 102 | > 1000 | Repeated measure | ZDV+3TC+EFV (23%) | NRTI: yes NNRTI: yes | No |
| 11 | Rossouw et al. 2017 [89] | Cohort of patients on first-line ART \geq 6 months | Clinic in Hlabisa subdistrict, KwaZulu-Natal, South Africa | Rural | 2013 | n.r. | 492 (72%) | 492 | > 1000 | Repeated measure | d4T+3TC+EFV (44%) | NRTI: yes NNRTI: yes | No |
| 12 | Ruperez et al. 2015 [85] | Cross-sectional study of patients on first-line ART \geq 1 year. | District Hospital in Manhica, Mozambique | Rural | 2013 | 332 (70%) | 81 | 61 | > 1000 | Single measure | ZDV+3TC+NVP (90%) | NRTI: yes NNRTI: yes | No |
| 13 | Seu et al. 2015 [90] | Patients referred after failing first-line ART after \geq 6 months | University Teaching Hospital, Lusaka, Zambia | Urban | 2012 | n.r. | 68 (54%) | 68 (54%) | > 1000 | Single measure | ZDV+3TC+NVP (38%) | NRTI: yes NNRTI: yes | Yes |

| | | | | | | | | | | | | | |
|----|--------------------------|--|--|-------|------|------|----------|-----------|-----------------------|--|---------------------------|-------------------------|----|
| 14 | Singh et al. 2011 [91] | Patients failing first-line ART after ≥ 6 months | McCord Hospital, Durban, South Africa | Urban | 2009 | n.r. | 45 (65%) | 43 | >5000 | Single measure | d4T+3TC+EFV (51%) | NRTI: yes NNRTI: yes | No |
| 15 | Steege et al. 2017 [74] | National survey of patients failing first-line ART after ≥ 6 months | 91 healthcare facilities in 9 provinces in South Africa | Both | 2014 | n.r. | 1033 | 788 (65%) | > 1000 | Repeated measure | TDF+3TC (52%) + EFV (82%) | NRTI: yes NNRTI: yes | No |
| 16 | Sunpath et al. 2012 [92] | Cross-sectional study of patients on TDF-containing first-line ART >5 months | McCord Hospital, Durban, South Africa | Urban | 2011 | 585 | 35 (46%) | 33 | > 1000 | Single measure | TDF+3TC+EFV (89%) | NRTI: yes NNRTI: yes | No |
| 17 | Wallis et al. 2010 [86] | Patients with virologic failure on first-line regimens | Charlotte Maxele Academic Hospital and Helen Joseph Hospital, Johannesburg, South Africa | Urban | 2007 | n.r. | 226 | 226 | >5000 or >1000, resp. | Repeated measure and single measure, resp. | d4T+3TC+EFV (65%) | NRTI: yes NNRTI: yes | No |

ART, antiretroviral therapy; VL, viral load; VF, virologic failure; n.r.: not reported; d4T, stavudine; 3TC, lamivudine; TDF, tenofovir; NVP, nevirapine; EFV, efavirenz; ACTG, AIDS Clinical Trials Group

* As defined in the corresponding study.

Reasons for lack of genotyping in patients with virologic failure: 1: >12 months between the two failure time points, no blood sample available at both time points.

2: Not applicable.

3: Unsuccessful amplification.

4: Genotyping in subsample of patients only. "Individuals with genotype results were similar in terms of sex, age, weight at cART initiation, median CD4 count at cART initiation, WHO stage, and type of NNRTI received to those viremic individuals who did not undergo genotyping (all, $p > 0.10$)." [95] 5: No stored plasma from the time of first detection of virologic failure. "Time on TDF at failure was longer for those with stored samples (261 days versus 140 days, $p < 0.001$); whereas CD4 count and HIV RNA at failure were similar between patients with and without stored serum ($p > 0.1$)." [96]

6: Not applicable.

7: Unsuccessful amplification.

8: Unsuccessful amplification; data incomplete.

9: Missed confirmatory visit, unsuccessful amplification, or technical error.

10: Subtype B.

11: Not applicable.

12: Unclear.

13: Not applicable.

14: Unsuccessful amplification.

15: "The main reason for exclusion was the inability of obtaining a PCR product ($n=151$, 14.6%). Other reasons for exclusion from the study were: volunteers <18 years of age ($n=35$, 3.4%); <6 months of ART exposure ($n=16$, 1.5%); treatment with a non-standard regimen at time of failure ($n=11$, 1.1%); inadequate completion of informed consent ($n=10$, 1.0%); poor sample integrity ($n=8$, 0.8%); <6 months of NNRTI exposure ($n=6$, 0.6%); or failure to obtain a sequence ($n=3$, 0.3%). In addition, five sequences (0.5%) were shown to be duplicate samples as per phylogenetic analysis." [74]

16: Unsuccessful amplification.

17: Not applicable.

2.4.2 Prevalence of acquired NRTI resistance mutations

Fig 2.3A shows the prevalence of the eight NRTI DRMs at baseline and after two years of either 3TC/FTC and TDF or 3TC/FTC and ZDV. The prevalence of any of six TAM mutation at baseline and after two years of ART is also displayed. Fig 2.3B-C display the prevalences of K65N/R and M184V/I, respectively, with respect to ART duration. The prevalence at baseline for NRTI DRMs was low, ranging from 0.6% to 8.5%, except for the M184V/I mutation with a baseline prevalence of 15.1% but with high uncertainty (95% credibility interval [CrI] 0.9%-29.9%). The use of FTC/3TC was associated with high-levels of the M184V/I mutation. The prevalence was 78.3% (95% CrI 64.7-90.5%) after two years on FTC/3TC combined with TDF, and 73.5% (95% CrI 57.9%-87.1%) on FTC/3TC combined with ZDV. When FTC/3TC was combined with TDF, there was a substantial increase in the K65N/R mutation: 1.5% (95% CrI 0.1%-3.2%) at baseline and 55.2% (95% CrI 34.3%-79.4%) after 2 years. The prevalence of each of the six TAM mutations after two years of FTC/3TC combined with either TDF or ZDV were moderate, ranging from 0.6% to 26%. Finally, the model showed a higher risk of developing any of the six TAMs when 3TC/TDF was combined with ZDV rather than TDF: 45.6% (95% CrI 34%-59.3%) versus 22.9% (95% CrI 16.1%-34.8%).

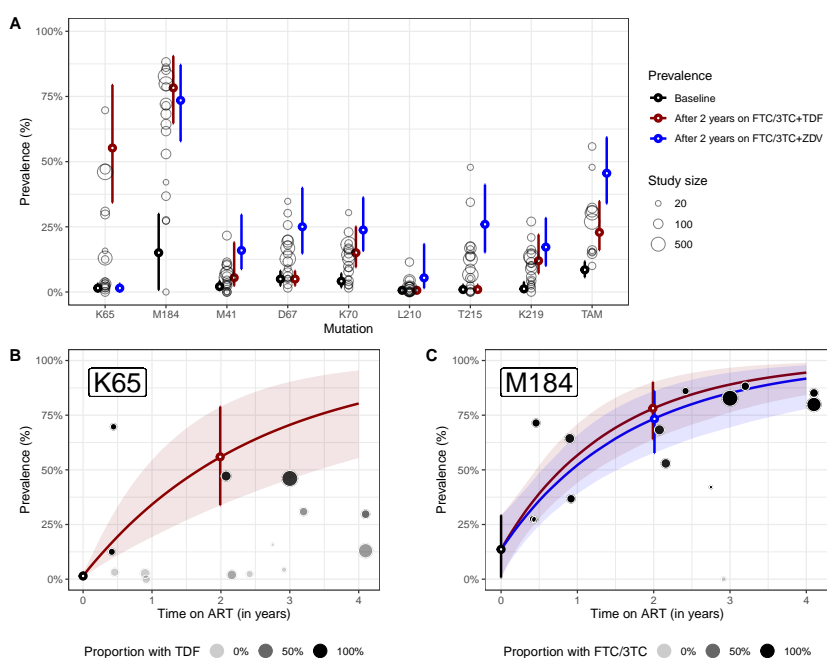


Fig 2.3: Prevalence of nine NRTI drug resistance mutations by first-line regimen. Panel A: baseline prevalence and prevalence after 2 years of treatment according to NRTI use. Panel B: Prevalence of the K65N/R mutation over time. Panel C: Prevalence of the M184V/I mutation over time. Points and vertical lines: median and 95% credibility intervals of baseline prevalence (black), prevalence after 2 years on 3TC/FTC + TDF (red) or 3TC/FTC + ZDV (blue). Shaded area: 95% credibility interval over time.

2.4.3 Prevalence of acquired NNRTI resistance mutations

Fig 2.4A shows the estimated prevalence of the seven NNRTI DRMs after two years of either EFV- or NVP-based regimens. Fig 2.4B-C display the prevalences of K103N/R/S and Y181C/I/V,

respectively, with respect to ART duration. K103N/R/S was the most frequent NNRTI DRM, with a high prevalence after two years of EFV-based (59.8%, 95% CrI 42.8-78.8%) or NVP-based regimens (39.3%, 95% CrI 22-66%). Other NNRTI DRMs with prevalence estimates over 20% included V106A/I/M, Y181C/I/V, and G190A/E/R/S. Of note, the model estimated a higher prevalence of the Y181 mutations after the use of NVP (41.9%, 95% CrI 23.5-63.1%) than with EFV (9.5%, 95% CrI 4.7-22.7%). S2 File gives the estimates of the prevalence of the NRTI/NNRTI DRMs at baseline and after 2 and 3 years of ART. The proportions of heterogeneity shared by all the mutations are displayed in Table 5 of S2 File.

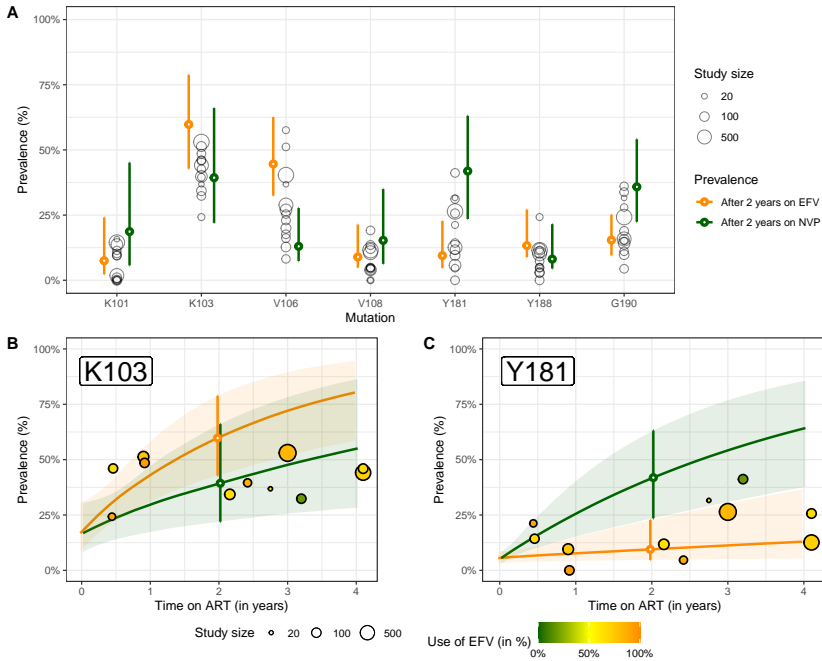


Fig 2.4: Prevalence of seven NNRTI drug resistance mutations. Panel A: Prevalences after 2 years on either EFV- or NVP-based regimen. Panel B: Prevalence of the K103N/R/S mutation over time. Panel C: Prevalence of the Y181C/I/V mutation over time. Points and vertical lines: median and 95% credibility intervals of baseline prevalence (black), prevalence after 2 years on EFV (orange) or NVP (green). Shaded area: 95% credibility interval over time.

2.4.4 Risk of bias and sensitivity analyses

We identified four studies at high risk of selection bias [90, 93, 95, 96]. Three had proportions of genotyping below 50% [93, 95, 96]. Two of these by design only genotyped a subsample of infections [95, 96]. One study [95] reported that every third patient was systematically sampled for genotyping; however, the number of infections genotyped was substantially lower (10.1% rather than the expected 33.3%, Table 2.2). Genotyping in the other study [96] depended on the availability of residual plasma. Finally, one study [90] lacked a clearly defined source population. It was based on referrals of patients with suspected first-line treatment failure at a University Teaching Hospital. Estimating the prevalence of the eight NRTI DRMs and seven NNRTI DRMs excluding the studies at high risk of bias showed that most estimates were very similar to the main analysis, but with larger uncertainty (S2 File).

Similarly, removing the studies with missing ART duration (rather than imputing it) or using all the covariates on NRTI use (rather than including a selection step) did not substantially affect the results (S2 File, Fig 4 and 5).

2.5 Discussion

This systematic review and Bayesian meta-analysis provide estimates of emerging DRMs in patients failing first-line treatment in Southern Africa. By using a hierarchical structure and adjusting for the use of different drugs, the model reliably estimates the major NRTI/NNRTI mutations while appropriately accounting for between-study heterogeneity. The most frequent acquired mutations among patients with virological failure after two years of ART were M184, K65 and K103 (prevalence 55% to 78%). Of note, K65 and M184 confer high-level resistance to 3TC/FTC and TDF, the two NRTI backbones that are usually combined in DTG-based regimens. The model also estimated that 23% to 46% of patients failing NNRTI-based regimen had at least one TAM.

The TenoRes study assessed the levels of NRTI resistance across regions of the world after the failure of NNRTI + 3TC/FTC + TDF [101]. For Southern Africa, it estimated high levels of both M184 and K65 mutations (59% and 56% respectively), in line with our study. The study found lower levels of M184 and K65 mutations in Europe (34% and 20%) or North America (42% and 22%). The authors argued that these differences in NRTI DRM levels might be driven by the higher frequency of viral load monitoring in Europe and North America. Also, in line with our study, the TenoRes study showed that Southern Africa is the only region with a similar prevalence of M184 and K65 mutations. In contrast, a higher prevalence of M184 mutations was observed in all other regions. As subtype C is most prevalent in Southern Africa, the K65 mutation might be more likely to emerge in subtype C compared with other subtypes, as found in in-vitro studies [77–79].

The high prevalence of the K65N/R and M184I/V mutations means that 43.2% (55.2%–78.3%) to 55.2% of PLWH failing first-line ART might have both, depending on the correlation between the two mutations. In its new guidelines, the South African Department of Health recommends switching patients failing a first-line regimen that includes 3TC/FTC and TDF to DTG combined with 3TC/FTC and ZDV, to have at least one fully active NRTI [27]. However, given the toxicity and side effects associated with ZDV and because there is no fixed-dose combination combining DTG and ZDV, TDF might be preferred over ZDV. In this context, our results show that nearly half of these patients will start a DTG-based regimen without a fully active NRTI. The DAWNING trial [102] showed that DTG-based ART is effective in second-line regimen provided it is combined with at least one fully active NRTI. However, it is uncertain whether a functional DTG-therapy, i.e. DTG with no fully active NRTIs, will be effective. Concerns on the efficacy of functional DTG-therapy have been raised by studies showing high failure rates with maintenance DTG-monotherapy [103]. The efficacy of functional DTG-monotherapy might be higher than DTG-monotherapy, as some NRTI activity may still exist even in case of resistance. This assumption is supported by the EARNEST study, where the presence of NRTI resistance did not impair virological response to second-line regimen [104].

Our meta-analysis also shows that TAM mutations are present at a moderate level among people failing NNRTI-based first-line regimen. Interestingly, in several studies the detection of NRTI resistance and particularly of TAMs prior to starting second-line ART was associated with better virological suppression, possibly because patients who are aware they developed

resistance may on average have better adherence [105, 106]. Clearly, the large-scale switch to DTG-based regimen should be accompanied by longitudinal, real-world studies of virologic failure and drug resistance monitoring.

We observed a high prevalence of the K103 mutation (60% after two years on EFV, 39% on NVP), conferring high resistance to both EFV and NVP. Several Southern African countries recommend adherence support in patients on failing NNRTI-based regimen to achieve viral suppression before switching to DTG. In the case where patients remain unsuppressed after six months, these patients should nevertheless switch to DTG. The high level of NNRTI-resistance harbored by these patients questions the efficacy of such a strategy. Indeed, prolonging a failing regimen might increase the risk of accumulation of NRTI DRMs, potentially impairing the efficacy of a future switch to DTG. Among the other NNRTI drug resistance mutations, Y181C/I/V is of particular concern. The estimated prevalence of this mutation was about 10% and 42% after two years of EFV and NVP, respectively, reflecting the higher impact of Y181 on NVP, as previously observed [107]. This mutation also confers resistance to the newer generation of NNRTIs, such as etravirine and rilpivirine.

Most previous reviews of HIV drug resistance focused on transmitted drug resistance, rather than resistance that was likely acquired during ART [108]. Previous reviews on ADR tended to focus on failure rates, CD4-positive lymphocyte counts, and the prevalence of drug resistance mutations overall [109, 110], or a subset of mutations [38, 101, 111]. Our study provides estimates of all relevant ADR mutations according to the drugs used, for the whole region of Southern Africa, the region with the highest burden of HIV. To our knowledge, this is the first meta-analysis of this literature that uses a hierarchical structure and estimates the DRMs simultaneously to identify the study effect that is shared across the DRMs.

Our review has several limitations. Many of the included studies were based on patients attending one or few outpatient clinics. We carefully assessed the likely representativeness of the patients undergoing HIV genotyping. Still, even if results reflect the situation in these clinics, they may not be representative of all patients who fail first-line ART in the region. Indeed, the between-study heterogeneity was large, and decision-makers should consider the studies most relevant to their settings, as well as the regional data. Many factors may have introduced heterogeneity, including differences between patient populations, their levels of adherence, the first-line regimen used, and the time spent on a failing regimen. The hierarchical structure of the model adjusted for regimen and time spent on a failing regimen, but some heterogeneity remains. Of note, in our sensitivity analyses, the likely risk of selection bias did not appear to influence estimates. Finally, we attempted to assess pre-treatment NRTI mutations, but the wide credibility intervals illustrate the difficulty to disentangle pre-treatment from acquired drug NNRTI resistance.

Although we searched for studies from all over Southern Africa, the majority of data included in our analysis were from South Africa. South Africa is one of few countries in the regions that have implemented routine viral load monitoring in patients on ART, and routine viral load monitoring is associated with a reduced probability of drug resistance [111]. Therefore, the overrepresentation of South Africa studies in our meta-analysis might underestimate the frequencies of the different DRMs in the rest of Southern Africa.

In conclusion, our analysis demonstrates that in Southern Africa, many patients failing first-line ART have DRMs, with important implications for the likely future transmission of drug resistance, the choice of second-line regimen, and the large-scale transition to DTG-based first-line ART. These implications are particularly pertinent to settings where

routine viral load and drug resistance testing is not routinely available [112].

2.6 Acknowledgements

We are grateful to Doris Kopp and Beatrice Minder for their support in searching and evaluating the literature.

2.7 Supporting information

S1 File. Literature search. Criteria and results of the literature search by bibliographic database.

S2 File. Supplementary material. Section 1: Model description. Section 2: Parameter estimates. Section 3: Sensitivity analysis.

Chapter 3

Bridging the gap between HIV epidemiology and antiretroviral resistance evolution: Modelling the spread of resistance in South Africa.

Anthony Hauser¹
Katharina Kusejko²
Leigh F. Johnson³
Gilles Wandeler^{1,4}
Julien Riou¹
Fardo Goldstein¹
Matthias Egger^{1,3,5}
Roger D. Kouyos^{2,6}

¹ Institute of Social and Preventive Medicine, University of Bern, Bern, Switzerland

² Division of Infectious Diseases and Hospital Epidemiology, University Hospital Zurich, University of Zurich, Zurich, Switzerland

³ Centre for Infectious Disease Epidemiology and Research, University of Cape Town, South Africa

⁴ Department of Infectious Diseases, Bern University Hospital, University of Bern, Bern, Switzerland

⁵ Population Health Sciences, Bristol Medical School, University of Bristol, Bristol, United Kingdom

⁶ Institute of Medical Virology, University of Zurich, Zurich, Switzerland

This article is published in ***PLOS Computational Biology***: Bridging the gap between HIV epidemiology and antiretroviral resistance evolution: Modelling the spread of resistance in South Africa (2019) DOI: 10.1371/journal.pcbi.1007083.

Contribution: I contributed to the study design, performed the analysis, made the figures, wrote the first draft of the manuscript and integrated co-authors' comments.

3.1 Abstract

The scale-up of antiretroviral therapy (ART) in South Africa substantially reduced AIDS-related deaths and new HIV infections. However, its success is threatened by the emergence of resistance to non-nucleoside reverse-transcriptase inhibitors (NNRTI). The MARISA (Modelling Antiretroviral drug Resistance In South Africa) model presented here aims at investigating the time trends and factors driving NNRTI resistance in South Africa. MARISA is a compartmental model that includes the key aspects of the local HIV epidemic: continuum of care, disease progression, and gender. The dynamics of NNRTI resistance emergence and transmission are then added to this framework. Model parameters are informed using data from HIV cohorts participating in the International epidemiology Databases to Evaluate AIDS (IeDEA) and literature estimates, or fitted to UNAIDS estimates. Using this novel approach of triangulating clinical and resistance data from various sources, MARISA reproduces the time trends of HIV in South Africa in 2005-2016, with a decrease in new infections, undiagnosed individuals, and AIDS-related deaths. MARISA captures the dynamics of the spread of NNRTI resistance: high levels of acquired drug resistance (ADR, in 83% of first-line treatment failures in 2016), and increasing transmitted drug resistance (TDR, in 8.1% of ART initiators in 2016). Simulation of counter-factual scenarios reflecting alternative public health policies shows that increasing treatment coverage would have resulted in fewer new infections and deaths, at the cost of higher TDR (11.6% in 2016 for doubling the treatment rate). Conversely, improving switching to second-line treatment would have led to lower TDR (6.5% in 2016 for doubling the switching rate) and fewer new infections and deaths. Implementing drug resistance testing would have had little impact. The rapid ART scale-up and inadequate switching to second-line treatment were the key drivers of the spread of NNRTI resistance in South Africa. However, even though some interventions could have substantially reduced the level of NNRTI resistance, no policy including NNRTI-based first line regimens could have prevented this spread. Thus, by combining epidemiological data on HIV in South Africa with biological data on resistance evolution, our modelling approach identified key factors driving NNRTI resistance, highlighting the need of alternative first-line regimens.

3.2 Author summary

Resistance to non-nucleoside reverse transcriptase inhibitors (NNRTI) threatens the long-term success of antiretroviral therapy (ART) roll-out in South Africa. We developed a compartmental model integrating the local HIV epidemiology with biological mechanisms of drug resistance. A first dimension of the model accounts for the continuum of care: infection, diagnosis, first-line treatment with suppression or failure, and second-line treatment. Other dimensions include: disease progression (CD4 counts), gender, and acquisition and transmission of NNRTI resistance. Whenever possible, we informed the parameters using the data available from local cohorts. Other parameters were informed using literature or UNAIDS estimates. The model captured the rise of NNRTI resistance during the period. We assessed the impact of counter-factual scenarios reflecting alternative countrywide policies during the period 2005 to 2016, considering either increasing ART coverage, improving management of treatment failure, broadening ART eligibility, or implementing drug resistance testing before ART initiation. We identified key drivers of the NNRTI resistance epidemic: large-scale ART roll-out and insufficient monitoring of first-line treatment failure. The model also suggested that no policy including NNRTI-based first line regimen could have prevented the spread of NNRTI resistance.

3.3 Introduction

Since ART has been introduced in Southern Africa in 2004, ART coverage has continuously increased. In 2016, 55% of individuals living with HIV were receiving ART in the region, the great majority being treated with a standard first-line regimen consisting of two nucleoside reverse transcriptase inhibitors (NRTI) and one non-nucleoside reverse transcriptase inhibitor (NNRTI) [113]. The scale-up of ART led to a substantial reduction in mortality but the emergence of drug resistance could jeopardize its long-term success [67]. Of particular concern are NNRTIs, as this class has a relatively low genetic barrier to resistance [114]. As documented by the World Health Organization (WHO), the level of pretreatment NNRTI resistance has rapidly increased and reached the 10% threshold in the Southern Africa region in 2015 [38]. According to WHO, this threshold should trigger considerations on changing the first-line regimen. By contrast, resistance to NRTIs, though relevant at the individual level, is only rarely transmitted [38].

In South Africa, adult HIV deaths have decreased from 220,000 in 2006 to 99,000 in 2014 [67]. In 2016, an estimated 63% of HIV positive people were on ART in South Africa [113]. While initially only people with CD4 counts lower than 200 cells/ μ L were eligible to start ART, South Africa adopted the "Treat-All" policy in 2017, which recommends ART for all HIV-positive people regardless of their CD4 counts [115]. The goal is to reach 90% of diagnosed people on ART in 2020, in line with the 90-90-90 targets of UNAIDS [116]. While the HIV epidemic in South Africa has been well described and extensively modelled [67, 117, 118], relatively little work has been done on drug resistance [53, 119]. The rapid increase in ART coverage might fuel further increase in drug resistance as more and more people become exposed to the drug, but the impact of the scaling up of ART on the development of NNRTI resistance is not well defined at present. Another key question is whether a better management of treatment failure would have mitigated NNRTI resistance.

While understanding the drivers of antiretroviral resistance is crucial for public health, representative, longitudinal data on drug resistance are scarce, compared to the large amount of cohort data available on the clinical and public health epidemiology of HIV. Moreover, quantifying the spread of resistance is challenging because it involves both epidemiological (transmission, cascade of care, disease progression) and evolutionary processes (emergence and selection of resistance mutations) [120–122], with the parameters governing the latter typically unknown [122].

We aimed to capture the dynamics of NNRTI resistance in South Africa during 2005-2016 and to quantify the impact that different policy changes would have had on the rise of drug resistance. To this end we developed MARISA (Modelling Antiretroviral drug Resistance In South Africa), a mathematical model integrating the specificities of HIV epidemiology in the country with the evolutionary epidemiology of drug resistance. MARISA is a compartmental, deterministic model whose structure reflects gender-specific dynamics of continuum of care and disease progression, as well as acquisition and transmission of HIV NNRTI resistance. We calibrated the model using data from the International epidemiology Databases to Evaluate AIDS in Southern Africa (IeDEA-SA, www.iedea-sa.org, [71]), literature estimates and HIV key outcomes provided by UNAIDS [113]. The acquisition and transmission of NNRTI drug resistance was integrated within the general dynamics of the HIV epidemic in the country and parametrized with estimates derived from other cohorts. This allowed the estimation of the yearly levels of acquired and transmitted drug resistance (ADR and TDR, respectively). We then assessed the impact of counter-factual scenarios reflecting alternative countrywide

public health policies, including policies of increasing ART coverage, improving management of treatment failure, broadening ART indications, or implementing drug resistance testing before initiation.

3.4 Method

3.4.1 Model structure

MARISA is a mechanistic, compartmental model. The first dimension of the model accounts for the whole continuum of care: infection of susceptible individuals, diagnosis, first-line treatment including NNRTI with subsequent suppression or failure, and second-line treatment including protease inhibitors (PI) with subsequent suppression or failure (8 classes). We then consider three additional dimensions: disease progression as characterized by CD4+ T cell counts (4 classes); NNRTI resistance status (2 classes); and gender (2 classes). This leads to a total of 128 compartments. The first two dimensions describe the different care stages and their interaction with HIV progression. The third dimension is key to capture the acquisition of NNRTI resistance by individuals with first-line treatment failure (with rate σ_{res}), the transmission of resistant strains of HIV to susceptible individuals, and the reversion of HIV resistance mutations when no more drug pressure is exerted (with rate σ_{rev}). We assume that individuals infected with the NNRTI resistant virus have higher failure and lower viral suppression rates (hazard ratio α and α^{-1} , respectively). As one mutation (e.g. the K103N mutation) alone confers high-level resistance to NNRTI drugs [123], only one layer is used to represent NNRTI resistance. The fourth dimension reflects differences observed between women and men, with diagnosis and treatment rates being higher for women than for men [66, 124]. This dimension is also involved in modelling HIV transmission among adults (≥ 15 years old).

Movement between compartments is determined by different rates, some of which change over time to reflect modifications in treatment policies or in behavior. Adults living in South Africa who are not infected are represented by the susceptible compartment ($Susc$), as shown in Fig 3.1. The I compartments represent undiagnosed HIV-positive individuals. The force of infection considers three transmission routes among adults: a man can either be infected by a woman ("heterosexual" or HET transmission) or, less commonly, by a man ("men having sex with men" or MSM transmission), while a woman can only be infected by a man. HET and MSM populations are only implicitly modelled: we assume a density-dependent transmission that accounts for different risk behaviors according to knowledge of HIV status (monthly number of unprotected sexual contacts β_u and β_d for undiagnosed and diagnosed HIV-infected individuals, respectively) and the expected proportion of HET and MSM among men. Inflow of infected children reaching the age of 15 is also taken into account by using estimates from the Thembisa model and published literature (See Section 1.5 in S1 File) [66, 67, 125, 126]. Infected individuals become diagnosed at a rate $\gamma_{I \rightarrow D}(t)$ that is allowed to vary over time, by CD4 count and by gender. Once diagnosed (compartment D), individuals will start treatment at a rate $\gamma_{D \rightarrow T_1}(t)$ that also varies over time, reflecting the successive changes in ART guidelines. This rate also depends on the CD4 count, as individuals with lower counts will initiate treatment at higher rates (see Section 1.3 in S1 File).

First-line ART initiation is represented by the T_1 compartment, which characterizes individuals who have been on ART for three months or less. After this period, they can either suppress viral replication (S_1) or fail treatment (F_1). These two compartments reflect the use of viral load monitoring in South Africa to identify patients failing first-line treatment that should

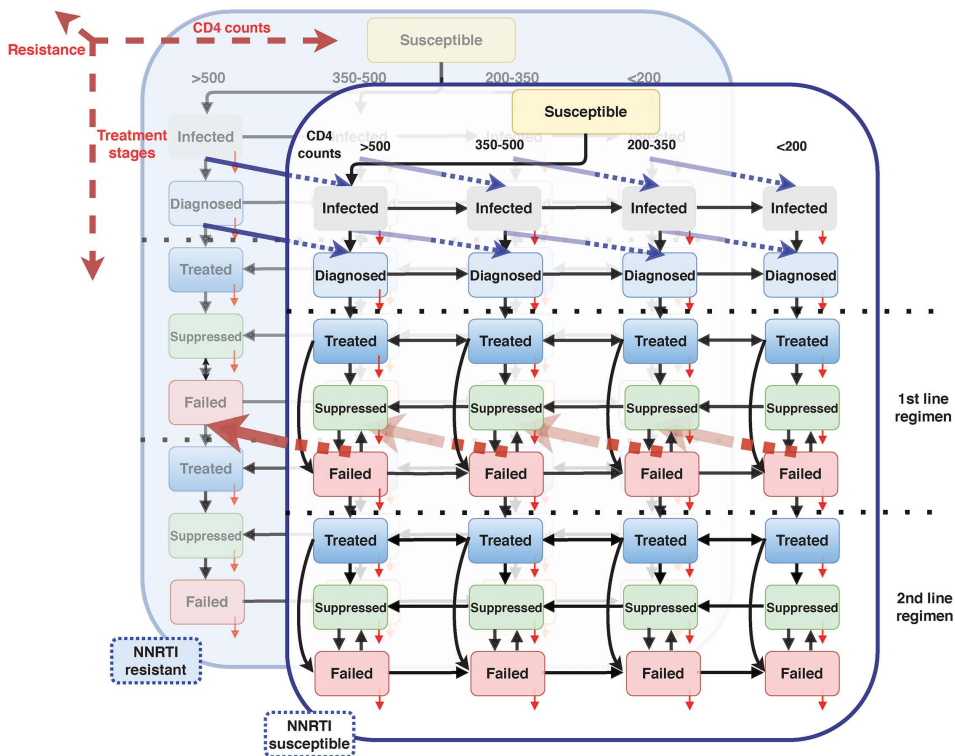


Fig 3.1: Compartmental model. Three of the four dimensions are represented: 1) care stages (vertically), 2) disease progression (horizontally, stratified in 4 CD4 counts strata), 3) NNRTI resistance (represented by the two overlapped layers). For sake of clarity, arrows representing treatment interruption are not displayed. Red arrows represent acquisition of NNRTI resistance, while blue arrows represent reversion to wild-type HIV-strain.

switch to second-line regimen. We assume that virally suppressed individuals cannot transmit the virus. When failing first-line treatment, individuals are switched to second-line treatment (compartment T_2) at rate $\gamma_{F_1 \rightarrow T_2}$. Care and disease progression on second line treatment are modelled identically to first-line therapy. Mortality at each stage differs according to disease progression and care stage. In addition, the mortality rates for patients with CD4 counts below 200 cells/ μl are time-dependent, due to the highly variable mortality risk in this class [127]. Overall, the model contains 137 different rates. The total population of each gender follows the WHO estimates for South Africa, and initial conditions in each compartment reflect UNAIDS estimates for 2005. Further details on the MARISA model are available in Sections 1 and 2 in S1 File.

3.4.2 Parameter values and calibration procedure

We parameterized and calibrated the model in two successive steps. First, some parameters were given fixed values using external sources. Literature estimates were used for parameters related to NNRTI resistance (σ_{res} , σ_{rev} , and α), for transmission probabilities per sexual contact, for the proportion of MSM and for the mortality risks (relatively to

3 suppressed individuals with more than 500 CD4/ μ L). Similarly, values were defined for the time-dependent diagnosis rates (differentiating between testing asymptomatic individuals, symptomatic individuals and pregnant women, and relatively to the treatment rate in 2005) and treatment rates (relatively to the treatment rate for an eligible individual with less than 200 CD4/ μ L in 2005). We used estimates from studies conducted in South Africa whenever available. For parameters related to disease progression (movements between CD4 strata) and to the continuum of care after starting first-line treatment (rates of suppression, treatment failure, switching to second line, and treatment interruption), we used data from five leDEA cohorts in South Africa (Aurum Institute, Hlabisa, Khayelitsha, Kheth'Impilo and Tygerberg) that provided longitudinal information for 54,016 HIV-infected adults [71]. The majority of them were female (62%). All patients started a first-line regimen and 3905 (7.2%) received a second-line regimen. Viral load measurements were used to identify the occurrence of suppression or treatment failure in treated individuals (using a threshold of 1000 copies/mL). Because of low monitoring frequency, the number of available measurements per patient was limited and some intermediate steps in disease or care progression were missing. We thus adapted methods from survival analysis in order to reconstruct patients' care histories (see Section 3.1 in S1 File). See Table 3.1 for more details about parameters.

During the second phase, the 7 remaining unknown parameters were estimated by fitting the model to estimates from the Thembisa model for the period 2005 to 2015: annual numbers of new HIV infections, number of undiagnosed individuals, annual number of AIDS-related deaths and ART coverage (Table 3.2 and Fig 3.2). The Thembisa model is a compartmental model providing UNAIDS with estimates on the South African HIV epidemic. Inference relied upon a maximum likelihood approach, assuming Poisson-distributed errors. We thus obtained point estimates for the monthly numbers of unprotected sexual contacts β_u and β_d , for the base diagnosis rate in 2005 and its increase between 2005 and 2016, for the treatment rate in 2005, for a scale parameter modelling the decrease in the proportion of individuals with CD4 <50 cells/ μ L (only used for mortality estimates), and for the mortality rate of suppressed individuals with more than 500 CD4/ μ L (see Table 3.1). Further details are available in the Section 3 in S1 File.

3.4.3 Simulations and counterfactual scenarios

The model was simulated from 2005 to 2016 using the specified parameter values and a monthly time step. Several outcomes were computed from the output, including the proportions of NNRTI ADR (proportion of individuals in F_1 compartments with NNRTI resistance, see Eq. 15 in S1 File) and of NNRTI TDR (proportion of individuals coming from I to D compartments with NNRTI resistance). When not specified otherwise, NNRTI TDR is measured in newly diagnosed patients (D) (see Eq. 16 in S1 File). Alternatively, we determine the proportion of NNRTI resistance in newly infected patients, newly diagnosed patients or in ART initiators. In this latter case, as it comprises drug-experienced people, we used the term pre-treatment drug resistance (PDR), rather than TDR.

Four counterfactual scenarios were examined with the model. The first counterfactual scenario assessed the impact of treatment initiation ($\gamma_{D \rightarrow T_1}$) increased by factors 2, 3 or 5. The second counterfactual scenario investigated the impact of an earlier switch to second-line regimen ($\gamma_{F_1 \rightarrow T_2}$) when failing the first-line regimen, by factors 2, 5 or 10. The third and fourth scenario examined the impact of different testing and treatment policies. In the third scenario, the "Treat-All" policy, i.e. initiating first-line treatment of diagnosed individuals

Table 3.1: Parameters used in the model. leDEA cohort data were used to estimate clinical progression rates. Parameters that could not be estimated with these data were collected from literature. Finally, time-varying parameters were estimated by fitting the MARISA model to estimates from Thembisa model.

| Parameters | Definition | Reference |
|---|--|------------|
| Parameters obtained from literature (see Table 4 in S1 File) | | |
| <i>Resistance parameters</i> | | |
| σ_{res} | Rate of acquiring NNRTI resistance when failing 1 st -line treatment | [128] |
| σ_{rev} | Reversion rate when no more NNRTI-drug pressure | [31] |
| α | Positive impact of NNRTI resistance on treatment failure | [37] |
| <i>HIV-transmission parameters</i> | | |
| | Probabilities of HIV infection across gender | [129] |
| | MSM prevalence | [130] |
| <i>Mortality parameters</i> | | |
| | Relative mortality risks across CD4 strata and care treatment status | [127, 131] |
| <i>Diagnosis and treatment rates</i> | | |
| $\gamma_{I \rightarrow D}(t)$ | Diagnosis rates according to gender and CD4 strata | [66] |
| $\gamma_{D \rightarrow T_1}(t)$ | Treatment rates according to CD4 strata | [66] |
| Parameters estimated of leDEA cohort data by survival analysis (see Tables 2 and 3 in S1 File) | | |
| <i>Parameters related to disease progression</i> | | [71] |
| | Transition rates between CD4 strata | |
| <i>Parameters related to continuum of care</i> | | |
| $\gamma_{T_1 \rightarrow S_1}, \gamma_{F_1 \rightarrow S_1},$ $\gamma_{T_2 \rightarrow S_2}, \gamma_{F_2 \rightarrow S_2}$ | Suppression rates for first- and second-line treatment | |
| $\gamma_{T_1 \rightarrow F_1}, \gamma_{S_1 \rightarrow F_1},$ $\gamma_{T_2 \rightarrow F_2}, \gamma_{S_2 \rightarrow F_2}$ | Failure rates for first- and second-line treatment | |
| $\gamma_{F_1 \rightarrow T_2}$ | Switching rate from first- to second-line treatment | |
| $\gamma_{T_1 \rightarrow D}, \gamma_{S_1 \rightarrow D}, \gamma_{F_1 \rightarrow D},$ $\gamma_{T_2 \rightarrow D}, \gamma_{S_2 \rightarrow D}, \gamma_{F_2 \rightarrow D}$ | Treatment interruption rates | |
| Parameters estimated by fitting MARISA to Thembisa model data (see Table 5 in S1 File) | | |
| β_u, β_d | Monthly numbers of unprotected sexual contacts for undiagnosed and diagnosed people respectively | [66, 113]) |
| $\gamma_{I \rightarrow D}(2005),$ $\gamma_{I \rightarrow D}(2016) / \gamma_{I \rightarrow D}(2005)$ | Base diagnosis rate in 2005 and its increase between 2005 and 2016 | |
| $\gamma_{D \rightarrow T_1}(2005)$ | Treatment rate in 2005 | |
| q | Scale parameter modelling the decrease in the proportion of individuals with CD4<50 cells/ μ L | |
| $\mu_{S_1/S_2}^{i=1}$ | Mortality rate of suppressed individuals with >500 CD4/ μ L. | |

Table 3.2: Outcomes and data sources used to calibrate the model and to compare the resistance related outcomes of the model. The six outcomes are displayed in Fig 3.2. See Section 3.2 in S1 File for more details.

| Outcome | Definition | Source | Reference |
|--|---|--|-----------|
| Data used during the fitting procedure | | | |
| <i>New infections</i> | Number of newly HIV-infected adults per year | Thembisa model | [66] |
| <i>Undiagnosed people</i> | Number of undiagnosed HIV-infected adults | Thembisa model | [66] |
| <i>AIDS-related deaths</i> | Number of AIDS-related deaths per year (for adults) | Thembisa model | [66] |
| <i>Treatment coverage</i> | Percentage of HIV-infected adults that are treated | UNAIDS data | [113] |
| Resistance estimates from cross-sectional studies | | | |
| <i>Level of NNRTI ADR</i> | Percentage of people failing first-line treatment that are resistant to NNRTI | 2 cross-sectional studies done in 2010 and 2014 in South Africa | [74,128] |
| <i>Level of NNRTI TDR</i> | Percentage of treatment-naïve people that are resistant to NNRTI | Data from a systematic review on the prevalence of PDR in South Africa, among other low and middle income countries. | [132] |

regardless of CD4 counts, was implemented at a hypothetical earlier point in time (moved forward by 1.5, 3 or 6 years). The fourth scenario implemented drug resistance testing and immediate second-line treatment of individuals harboring a resistant strain at baseline.

3.4.4 Sensitivity analysis

We performed a multivariate sensitivity analysis in order to quantify the impact of uncertainty on the values of 1) four parameters related to NNRTI resistance (σ_{res} , σ_{rev} , α and the rates of treatment interruption) and 2) three parameters related to HIV transmission (percentage of MSM, probability of male-to-male infection per sexual contact, and ratio between HIV prevalence in MSM and HET). Multivariate uncertainty within specified ranges was introduced using Latin hypercube sampling [133]. Each model estimate is reported with a 100% sensitivity range. Further details are available in Section 4.2 in S1 File.

3.5 Results

3.5.1 Model outcomes

The model reproduces the main time trends of the HIV epidemic in South Africa 2005-2016 (Fig 3.2A-D). There is a clear increase in ART coverage since 2005, attaining 48% of infected individuals in 2015, and a significant drop in the number of undiagnosed individuals, as a result of the increasing number of HIV tests performed annually. In 2015, the model estimated that 0.79 million of the 6.9 million infected individuals (11.4%) were not yet diagnosed. The number of yearly newly-infected individuals decreased from over 400,000 individuals in 2006 to about 300,000 in 2016. The decrease in risk behavior due to testing among HIV-positive individuals is estimated at 46% ($\beta_d/\beta_u=0.54$), in line with a behavioral study conducted in

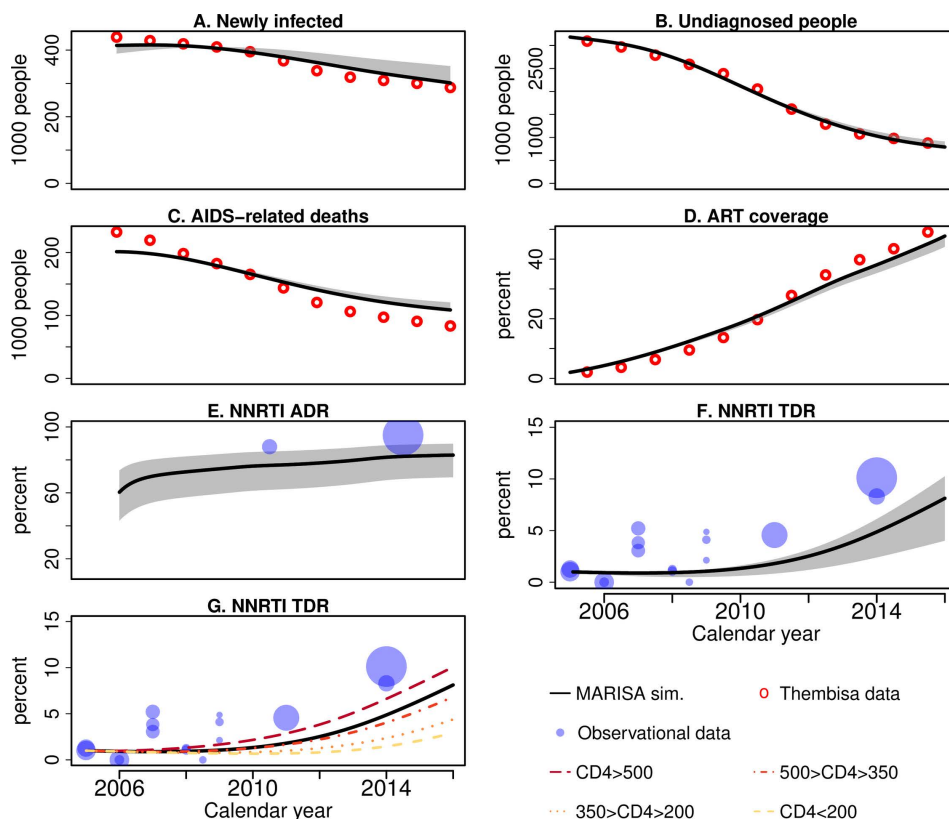


Fig 3.2: Best fit of the model. The plots A, B, C and D correspond to the four outcomes used during the fitting procedure: A) the number of newly infected per year, B) the total number of undiagnosed individuals at each year, C) the number of AIDS-related deaths per year and D) the percentage of infected individuals that are on ART. NNRTI ADR and TDR levels are displayed in E and, F and G respectively, and are not used to fit the model. Lines correspond to model output and circles to Thembisa estimates (in red) or to results from cross-sectional studies (in blue, see Table 6 in S1 File). Grey shades correspond to 100% sensitivity ranges. See Table 3.2 for more details.

South Africa in 2013 [134]. Finally, HIV-related deaths dropped from over 200,000 in 2006 to 109,000 in 2016.

The MARISA model also captures the dynamics of NNRTI ADR and TDR, showing very high levels of ADR (Fig 3.2E) and increasing levels of TDR (Fig 3.2F) in South Africa after 2004. The model estimates that 73% of the individuals failing the first-line regimen had ADR to NNRTI in 2008, with a slight yet steady increase in the following years, surpassing 83% in 2016. Moreover, the model estimated that 13.8% of these individuals were already resistant at the time of failure. NNRTI TDR among newly diagnosed individuals increased from 0.9% to 8.1% during the period. Interestingly, the model indicates substantial variation in TDR levels over the four CD4 strata, ranging from 2.9% for newly diagnosed individuals with less than 200 CD4/ μ L to 10.0% for those with more than 500 CD4/ μ L in 2016. For newly infected individuals, the NNRTI TDR level reaches 15.0% in 2016. We also observe a high PDR prevalence among

individuals initiating first-line ART (6.5% in 2016). Finally, the model estimated that 16.9% of ADR cases in 2016 were related to TDR (see Eq 17, in S1 File).

3.5.2 Counterfactual scenarios

In the first scenario, increasing the treatment rate by a factor 2, 3 or 5 during the whole period would have led to a substantial reduction of the number of annual deaths, but would have had little effect on the number of newly-infected or the number of undiagnosed individuals (Fig 3.3). The decrease in new infections due to increased treatment rates is modest for two reasons: 1) the low proportion of HIV-infected individuals who are ART eligible (only 28% of HIV-infected individuals are diagnosed in 2005) and 2) the decrease in the number of deaths of infectious individuals when increasing ART coverage (67,000 deaths of infectious individuals prevented per year in 2005-2012 under the 5-fold increase scenario). As expected, increasing treatment rates would not have impacted NNRTI ADR levels. On the other hand, by increasing the number of individuals at risk of acquiring NNRTI resistance, it would have led to a considerable increase of NNRTI TDR levels, surpassing 15.0% in 2016 in the 5-fold increase scenario.

In the second scenario, increasing the rate of switching to second-line treatment in case of first-line treatment failure (i.e. dividing the time spent in treatment failure) by factors 2, 5 or 10 would not have influenced the four key HIV outcomes (Fig 3.4). However, the model predicts a substantial decrease in the levels of both NNRTI ADR and TDR (to 51.5% and 3.1%, respectively), for the 10-fold increase scenario compared to 83% and 8.1%, respectively, for the baseline model in 2016.

Moving the "Treat-All" policy forward in time by 1.5, 3 or 6 years in the third scenario, would have hardly reduced mortality, as it targets individuals with high CD4 counts. On the other hand, removing infectious individuals with high CD4 counts, who are most likely to achieve viral suppression, would have led to a decrease in the number of new infections (256,000 for the 6-year-early implementation scenario instead of 302,000 in the baseline model in 2016). Increasing ART coverage might, however, increase the spread of resistance as NNRTI TDR increased to 10.3% in this scenario.

Finally, in the fourth scenario, drug resistance testing, by directly starting individuals with NNRTI resistance on second-line regimens, would have slightly improved viral suppression among resistant individuals (59.3% instead of 56.9% in the baseline model) and also reduced the transmission of resistance (14.4% instead of 15% resistant among newly infected in 2016). The relative impact of each counterfactual scenario on the number of new infections, AIDS-related deaths and the numbers of both new NNRTI TDR and ADR cases in 2016, as well as their relative percentages is shown in Table 3.3.

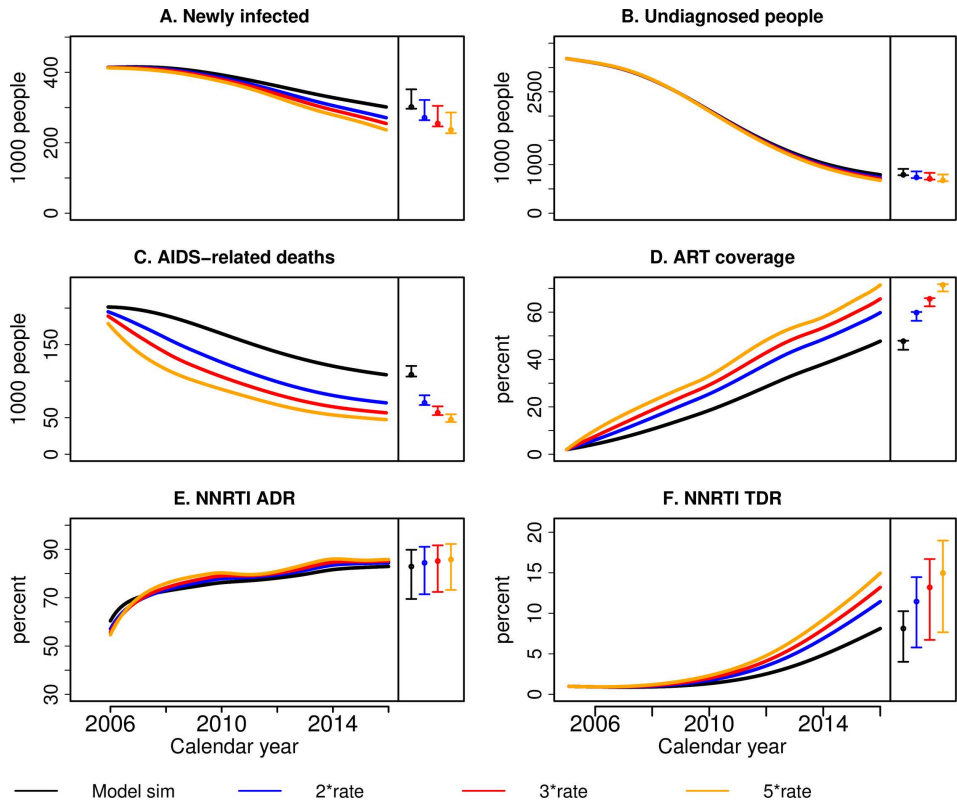


Fig 3.3: Counterfactual scenario that investigates the impact of increased treatment rate. Simulations of the MARISA model from 2005 to 2016 under the scenarios where the treatment rate is increased by 2, 3 and 5, represented respectively by the blue, red and yellow curves. Simulations of the baseline model are represented in black. The following HIV outcomes are displayed: A) the number of newly infected per year, B) the total number of undiagnosed individuals at each year, C) the number of AIDS-related deaths per year and D) the percentage of infected individuals that are on ART, E) level NNRTI ADR and F) level of NNRTI TDR. Different colours correspond to different rates of starting treatment, where the rates are expressed as multiple of the rate in the standard model. The coloured circles and vertical lines at the right of each sub-figure correspond to the point estimates and 100% sensitivity ranges in 2016, respectively.

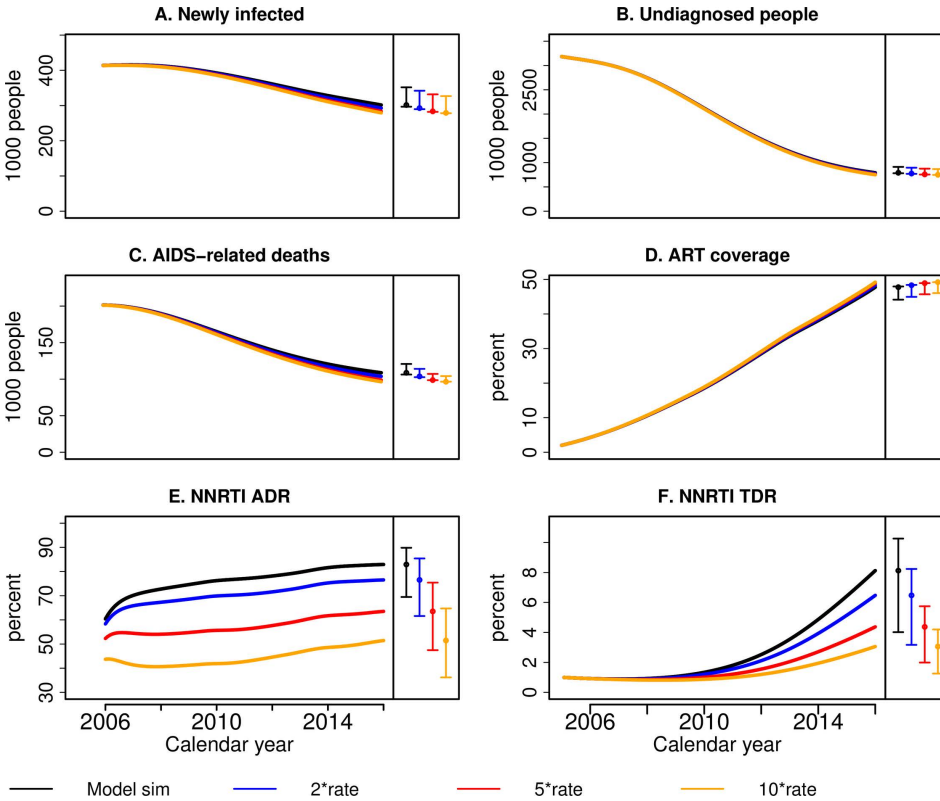


Fig 3.4: Counterfactual scenario that investigates the impact of increased switching rate to second line regimen. Simulations of MARISA model from 2005 to 2016 under the scenarios where the switching rate to second-line regimen $\gamma_{F_1 \rightarrow T_2}$ is increased by factor 2, 5 and 10, represented by the blue, red and yellow curves. In the baseline simulations represented by the black curves, a switching rate $\gamma_{F_1 \rightarrow T_2}$ of $1/2.9 \text{ years}^{-1}$ is assumed for individuals with $\text{CD4} < 200 \text{ copies}/\mu\text{l}$. The following HIV outcomes are displayed: A) the number of newly infected per year, B) the total number of undiagnosed individuals at each year, C) the number of AIDS-related deaths per year and D) the percentage of infected individuals that are on ART, E) level NNRTI ADR and F) level of NNRTI TDR. Different colours correspond to different rates of starting treatment, where the rates are expressed as multiple of the rate in the standard model.

Table 3.3: Impact of counterfactual scenarios on six outcomes: Yearly death, new infections, TDR level, ADR level, number of TDR cases, number of ADR cases, all in 2016. For each of the 6 outcomes and each of the 10 counterfactual scenarios, the absolute difference between the given scenario and baseline model, as well as the 100% sensitivity range (100% SR) are calculated.

| | Scenario 1: increasing treat. rate | | | Scenario 2: increasing switching rate | | | Scenario 3: earlier Treat-All | | | Scenario 4: DR testing |
|------------------|---------------------------------------|---------------|---------------|--|-----------------|-----------------|----------------------------------|---------------|---------------|---------------------------|
| | 2 · γ | 3 · γ | 5 · γ | 2 · γ | 5 · γ | 10 · γ | 1.5y | 3y | 6y | |
| Death | -38.5 | -52.0 | -61.4 | -5.0 | -10.0 | -12.2 | 0.0 | -1.3 | -8.1 | -1.1 |
| Sens. range | (-41.2,-38.1) | (-56.4,-51.6) | (-67.3,-60.9) | (-6.7,-3.6) | (-13.6,-7.6) | (-16.7,-9.5) | (-0.0,0.0) | (-1.3,-1.0) | (-8.5,-7.1) | (-2.9,-0.5) |
| New inf. | -30.5 | -47.0 | -65.0 | -8.8 | -18.0 | -22.4 | -5.2 | -20.5 | -45.8 | -2.1 |
| Sens. range | (-34.3,-27.0) | (-53.2,-41.9) | (-73.9,-58.6) | (-11.3,-5.5) | (-22.5,-12.1) | (-27.6,-15.7) | (-5.9,-5.1) | (-22.7,-19.8) | (-49.7,-43.4) | (-4.7,-0.9) |
| TDR level | 3.3% | 5.1% | 6.8% | -1.7% | -3.8% | -5.1% | 0.1% | 0.6% | 2.1% | -0.3% |
| Sens. range | (1.8%,4.2%) | (2.7%,6.4%) | (3.6%,8.8%) | (-2.0%,-0.8%) | (-4.5%,-2.0%) | (-6.1%,-2.7%) | (0.1%,0.1%) | (0.4%,0.8%) | (1.1%,2.6%) | (-0.7%,-0.1%) |
| ADR level | 1.5% | 2.2% | 2.9% | -6.4% | -19.4% | -31.5% | -0.7% | 0.7% | 2.2% | -1.4% |
| Sens. range | (1.0%,2.9%) | (1.4%,4.3%) | (1.8%,5.7%) | (-8.8%,-4.4%) | (-24.3%,-14.3%) | (-36.5%,-25.0%) | (-1.1%,-0.4%) | (0.6%,0.9%) | (1.6%,3.1%) | (-3.9%,-0.8%) |
| TDR cases | 12.3 | 17.3 | 21.2 | -9.6 | -20.9 | -27.7 | 0.6 | 3.2 | 6.0 | -2.0 |
| Sens. range | (8.6,16.9) | (11.8,24.4) | (14.2,30.9) | (-12.0,-6.2) | (-25.4,-14.4) | (-33.3,-19.3) | (0.3,0.9) | (2.2,4.3) | (4.3,8.3) | (-4.5,-0.8) |
| ADR cases | 31.8 | 40.5 | 47.3 | -14.3 | -44.7 | -74.8 | 19.4 | 27.1 | 7.7 | -0.1 |
| Sens. range | (29.3,39.0) | (37.7,50.2) | (43.9,58.3) | (-19.0,-10.3) | (-54.0,-34.5) | (-83.1,-62.0) | (14.8,23.0) | (25.1,28.1) | (6.1,11.4) | (-0.3,-0.0) |

3.5.3 Sensitivity analysis

Sensitivity analyses showed that uncertainty in the values of four resistance-related parameters (σ_{res} , σ_{rev} , α and the rates of treatment interruption) and of three parameters related to HIV transmission (percentage of MSM, probability of male-to-male infection per sexual contact, and ratio between HIV prevalence in MSM and HET) did not modify substantially the main outcomes of the MARISA model (Fig 3.2).

3.6 Discussion

In this comprehensive modelling study, we show that the MARISA model captured the dynamics of the HIV epidemic in South Africa over the years 2005-2016. More importantly, it reproduced the emergence of NNRTI resistance, following the roll-out of ART in 2004. The four counterfactual scenarios provided insights into the drivers of NNRTI resistance. They highlighted the close association between the magnitude of ART roll-out and the extent of NNRTI drug resistance. The results also suggest that a better management of first-line treatment failure, improving identification of treatment failure and switching to second-line treatment, might have reduced AIDS-related mortality and new HIV infections, while offering a better control of NNRTI resistance. However, our results also show that while some policies result in substantial reductions in NNRTI TDR, no measure could have stopped its increase. Even with optimal monitoring and management, NNRTI resistance would have rapidly spread in South Africa, suggesting that NNRTI resistance is inevitable if NNRTI-based regimens are used for first-line therapy.

The MARISA model fit was good regarding all four key outcomes of the HIV epidemic in South Africa produced by Thembisa/UNAIDS for the period of study: new infections, number of undiagnosed individuals, AIDS-related deaths and ART coverage [66, 113]. The estimates related to the "90-90-90" target provided by our model are also in line with those from UNAIDS. The proportion of HIV-infected individuals knowing their HIV status was estimated at 88% and 86% in 2015 by our model and UNAIDS, respectively. The second "90" was slightly underestimated by the MARISA model: the proportion of individuals with diagnosed HIV infection receiving ART was estimated at 52% in 2015, compared to estimates of 56% and 60% from Thembisa and UNAIDS, respectively. Finally, the proportion of individuals receiving ART achieving viral suppression was estimated at 79%, compared to 78% by UNAIDS [113].

NNRTI ADR and TDR levels estimated by the MARISA model were comparable, though slightly lower, to estimates from six cross-sectional studies conducted during this period [74, 128, 135–137]. Of note, these observational data were not used for model calibration and the resistance-specific processes of the MARISA model were partly informed using published estimates from other settings (in particular the rate of reversion to a drug-susceptible strain [31] and the positive association between drug resistance and treatment failure [37]), since no data for South Africa were available. Beyond sampling variability in the estimates from the cross-sectional studies, the discrepancy in ADR and TDR estimates between MARISA and the cross-sectional studies could be explained by several factors: a higher proportion of individuals with previous exposure to ART in the studied samples (e.g. through prevention of mother-to-child transmission, not included in the MARISA model), selection bias in the cross-sectional studies (e.g. regarding gender, age, socio-economic features or time since infection), publication bias by which lower measurements of ADR and TDR are less likely to be published, or possibly a misspecification of some parameters of the MARISA model due to geographical differences.

Note that TDR and ADR reflect different populations and processes. ADR is measured in people failing therapy, while TDR is measured in newly diagnosed individuals. The term ADR is somewhat imprecise since we measure it as the proportion of all drug resistant infections among individuals failing treatment and some of these individuals acquired the resistance already by infection. It reflects, however, the terminology used in resource limited settings, where baseline resistance tests are not routinely performed. Our simulations showed that the vast majority of these ADR cases were indeed acquired after treatment failure: in 2016, only 16.9% of ADR cases resulted from treatment failing in individuals already infected with a resistant virus, while the remaining resulted from the selection of resistance mutations in individuals failing on therapy with an initially sensitive virus (see Eq.17 in S1 File). This pattern also explains the relatively weak increase over time (from a high initial level) that is observed for ADR (Fig 3.2E).

Interestingly, MARISA revealed heterogeneity in NNRTI TDR levels across CD4 strata, with higher levels of NNRTI TDR associated with higher CD4 counts. This can be explained by the fact that individuals with high CD4 counts are more likely to have been recently infected, and thus exposed to a higher risk of NNRTI TDR as the prevalence of NNRTI resistance increases with time. Other studies have indeed observed a higher NNRTI TDR level among acutely than chronically HIV-infected patients [138]. Given that untreated patients with low CD4 counts might have been infected for a longer time, another explanation could be the increased probability of reversion from a drug-resistant to a wild-type strain in these patients.

The counterfactual scenarios identified two main drivers of the emergence and spread of NNRTI resistance: the magnitude of the ART roll-out and low frequency of monitoring of first-line treatment failure. The first scenario underlined the inherent risks of resistance emergence induced by a rapid and generalized ART scale-up. This observation is supported by findings of Hamers et al. [139] that the level of NNRTI TDR is associated with time since ART roll out in sub-Saharan Africa. According to the first scenario, policies focused on increasing ART coverage would have allowed a better control of the HIV epidemic, reducing both mortality and new infections. However, such policies would have likely resulted in even higher levels of NNRTI TDR during 2005-2016, leaving doubt about the long-term sustainability of this approach. As seen in the second counterfactual scenario, an earlier treatment switch for individuals failing NNRTI-based treatment would not have prevented resistance from emerging. In this context, the high NNRTI-mutation rate (after on average 6 months in the presence of treatment failure) makes the emergence of NNRTI resistance almost inevitable. For instance, we observe an emergence of TDR (3.3% in 2016) and a substantial level of ADR (50% in 2016), even when assuming that from 2005 an optimal management of treatment failure complying with the South African Department of Health 2016 guidelines [140] was in place. The guidelines recommend a VL measure every six months and an immediate switch to second-line ART after failure of two months of adherence counselling (corresponding to an average time before switching of $1/\gamma_{F_1 \rightarrow T_2} = 5$ months). Still, policies focused on improving first-line treatment failure identification and early switching to second-line treatment would have likely led to better control of both the HIV epidemic (with fewer AIDS-related deaths and new infections) and the extent of NNRTI resistance in South Africa. An earlier implementation of the "Treat-All" policy in the third scenario would have modestly decreased mortality, as it extends ART to individuals with high CD4 counts. However, the simulations emphasized the risk of increased levels of NNRTI TDR following implementation of this policy, in a similar way to policies simply increasing ART coverage. Finally, the fourth scenario showed the limited impact on HIV outcomes of

implementing drug resistance testing at baseline. Immediate PI-based treatment in patients with TDR only slightly diminished NNRTI TDR prevalence. This small effect may be explained by the limited number of patients affected by the policy (i.e. newly-infected individuals carrying a resistant strain and initiating ART), whose contribution to the transmission of resistance was relatively small (TDR accounts for only 16.9% of ADR cases). We acknowledge that assuming the same failure rates in the counterfactual scenario for patients on a PI-based first-line regimen as for patients on a PI-based second-line regimen may lead to under estimation of the effect of baseline resistance monitoring, because rates of failure in patients on first-line PI-based regimen are probably lower.

3 The model has several limitations. First, as the estimates from the Thembisa model were used to fit MARISA, findings produced by MARISA partly rely on the accuracy of Thembisa model. Second, it does not take into account NRTI mutations, which could also affect the success of first-line treatment. However, as transmission of NRTI mutations remains at a low level, their impact on the overall effectiveness of first-line regimens is limited [38]. Third, adherence is not modelled explicitly in the model, as it is not systematically assessed in the leDEA cohorts. Nevertheless, adherence is implicitly included in MARISA, as estimates of suppression and failure rates rely on a large cohort of individuals with different levels of adherence. Moreover, modelling of HIV transmission was based on simplified assumptions: the model only distinguished male from female transmission and attributed two different transmission rates according to awareness of HIV-status. The probability of HIV-infection per sexual act was assumed to be identical for all unsuppressed individuals. The heterogeneity in sexual behavior within genders was only approximated, and MARISA does not account for interactions between resistance status and sexual behavior. However, in view of the good fit to the number of new infections, there is no need for introducing a more complex representation of HIV transmission dynamics. Finally, the model does not simulate prevention of mother-to-child transmission, which could be an important source of NNRTI resistance. Overall, there is a trade-off between these potential additional layers of complexity and the limited knowledge about specific mechanisms. We argue that the ability of the MARISA model to capture the dynamics of NNRTI resistance with parameters fixed to known values from external data supports the validity of these simplifications. As it stands, the model does not make any unverifiable assumptions, and the sensitivity analyses showed that conclusions were robust, despite uncertainty in the main parameters related to resistance and transmission. Furthermore, the relatively simple representation of NNRTI resistance emergence and transmission makes the model easily interpretable.

MARISA can be adapted to address other questions on HIV drug resistance by adding further layers of complexity. The imminent roll-out of Dolutegravir (DTG), and has been presented as a response to the NNRTI resistance epidemic [115]. In South Africa, DTG in combination with two NRTI-class drugs will progressively replace NNRTI as the first-line regimen for men, but there is uncertainty as to whether it should be recommended for women of reproductive age due to safety issues [141]. DTG will also be prescribed to patients failing NNRTI-based regimens. As NRTI resistance mutations might already have occurred in these patients, this could affect the future success of the DTG-based regimen [142, 143]. From this basis, MARISA can be extended in order to evaluate the potential impact of introducing DTG-based regimens, either for men and women or for men only. While the overall structure of the model in terms of care and disease progression will stay unchanged, the resistance dimension can be expanded by adding key NRTI resistance mutations (e.g. K65R and M184V). We could also stratify the model by age group in order to represent the difference in drug prescription (NNRTI or DTG) in

women according to age. MARISA could thus be used to predict the spread of NRTI- and NNRTI resistance mutations according to the different strategies of DTG roll-out and their impact on the overall success of HIV-epidemic.

To conclude, we propose MARISA, a mechanistic model aimed at providing insight into the NNRTI resistance epidemic in South Africa in 2005-2016. Integrating information from several sources, including local cohorts of HIV-infected individuals, the model captured the essence of NNRTI resistance emergence in South Africa. Counter-factual scenarios identified key drivers of the NNRTI resistance epidemic at the policy level: a rapid, large-scale ART roll-out and an insufficient monitoring of first-line treatment failure. The model also showed that the rapid rate of acquisition and slow rate of reversion of NNRTI drug resistance mutations make it difficult to prevent their spread if NNRTI-based treatments are used as a first-line regimen, and it indicated the limited effect of drug resistance testing. Understanding future challenges in HIV drug resistance such as the introduction of DTG, its effect on the epidemic, the possibility of DTG resistance, and the impact of NRTI mutations on DTG based regimens will require the modelling of a more complex and uncertain mutational landscape. MARISA, with its backbone of a simple yet adequate epidemiological model will provide a suitable foundation to address this challenge.

3.7 Supporting information

S1 File. Detailed description of the MARISA model. Detailed description of the MARISA model and the computational methods used to calibrate and then run it.

Chapter 4

Impact of Scaling up Dolutegravir on Antiretroviral Resistance in South Africa: a modeling study.

Anthony Hauser¹
Katharina Kusejko²
Leigh F. Johnson³
Huldrych F. Günthard^{2,4}
Julien Riou¹
Gilles Wandeler^{1,5}
Matthias Egger^{1,3,6}
Roger D. Kouyos^{2,4}

¹ Institute of Social and Preventive Medicine, University of Bern, Bern, Switzerland

² Division of Infectious Diseases and Hospital Epidemiology, University Hospital Zurich, University of Zurich, Zurich, Switzerland

³ Centre for Infectious Disease Epidemiology and Research, University of Cape Town, South Africa

⁴ Institute of Medical Virology, University of Zurich, Zurich, Switzerland

⁵ Department of Infectious Diseases, Bern University Hospital, University of Bern, Bern, Switzerland ⁶ Population Health Sciences, Bristol Medical School, University of Bristol, Bristol, United Kingdom

This article is published in ***PLOS Medicine***: Impact of Scaling up Dolutegravir on Antiretroviral Resistance in South Africa: a modeling study. (2020) DOI: 10.1371/journal.pmed.1003397.

Contribution: I contributed to the study design, performed the analysis, made the figures and wrote the first draft of the manuscript and integrated co-authors' comments.

4.1 Abstract

Background: Rising resistance of HIV-1 to non-nucleoside reverse transcriptase inhibitors (NNRTIs) threatens the success of the global scale-up of antiretroviral therapy (ART). The switch to WHO-recommended dolutegravir (DTG)-based regimens could reduce this threat due to DTG's high genetic barrier to resistance. We used mathematical modelling to predict the impact of the scale-up of DTG-based ART on NNRTI pre-treatment drug resistance (PDR) in South Africa, 2020-2040.

Methods and Findings: We adapted the MARISA (Modelling Antiretroviral drug Resistance In South Africa) model, an epidemiological model of the transmission of NNRTI resistance in South Africa. We modelled the introduction of DTG in 2020 under two scenarios: DTG as first-line regimen for ART-initiators, or DTG for all patients, including patients on suppressive NNRTI-based ART. Due to safety concerns related to DTG during pregnancy, we assessed the impact of prescribing DTG to all men and in addition to i) women beyond reproductive age, ii) women beyond reproductive age or using contraception, and iii) all women. The model projections show that, compared to the continuation of NNRTI-based ART, introducing DTG would lead to a reduction in NNRTI pre-treatment drug resistance (PDR) in all scenarios if ART initiators are started on a DTG-based regimen and those on NNRTI-based regimens are rapidly switched to DTG. NNRTI PDR would continue to increase if DTG-based ART was restricted to men. When given to all men and women, DTG-based ART could reduce the level of NNRTI PDR from 52.4% (without DTG) to 10.4% (with universal DTG) in 2040. If only men and women beyond reproductive age or on contraception are started on or switched to DTG-based ART, NNRTI PDR would reach 25.9% in 2040. Limitations include substantial uncertainty due to the long-term predictions and the current scarcity of knowledge about DTG efficacy in South Africa.

Conclusions: Our model shows the potential benefit of scaling up DTG-based regimens for halting the rise of NNRTI resistance. Starting or switching all men and women to DTG would lead to a sustained decline in resistance levels whereas using DTG-based ART in all men, or in men and women beyond childbearing age, would only slow down the increase in levels of NNRTI PDR.

4.2 Author summary

Why was this study done?

- The scale-up of antiretroviral therapy in resource-limited settings has achieved an unprecedented reduction in HIV-related morbidity and mortality.
- The success of antiretroviral therapy is however threatened by increasing levels of resistance to antiretroviral drugs of the non-nucleoside reverse transcriptase inhibitors (NNRTI) class.
- Replacing NNRTIs by dolutegravir may curb the spread of resistance but it is unclear how effective this switch will be and which patient groups should be switched from NNRTI to dolutegravir.
- It has been debated whether Dolutegravir should be given to women, because of a potential risk of birth defects, and to patients already on an NNRTI based therapy.

What did the researchers do and find?

- Using a mathematical model simulating the HIV epidemic in South Africa, we find that scaling up dolutegravir-based antiretroviral therapy can halt the increase of NNRTI resistance.
- This predicted effect of dolutegravir depends crucially on including both women and people already on NNRTI-based ART among patients to whom dolutegravir will be prescribed.
- Restricting dolutegravir to men or to patients initiating antiretroviral therapy would substantially reduce its potential to curb resistance at the population level, as in this case it could merely slow down but not halt the spread of NNRTI resistance.
- Patients still relying on NNRTI-based therapy would in this case face increased risk of resistance and therapy failure.

What do these findings mean?

- Our model highlights the potential of dolutegravir scale up to curb NNRTI resistance.
- In order to halt the increase in NNRTI resistance, dolutegravir should become accessible to both women and people currently on NNRTI-based therapy.

4.3 Introduction

The rollout of antiretroviral therapy (ART) in South Africa is estimated to have prevented 0.73 million HIV infections between 2004 and 2013 as well as 1.72 million deaths between 2000 and 2014 [67, 144]. However, the spread of non-nucleoside reverse transcriptase inhibitor (NNRTI) resistant viruses is threatening this success [145]. An estimated 16% of AIDS-related deaths and 8% of ART costs will be attributable to HIV drug resistance up to 2030 in the sub-Saharan African countries that reached HIV pretreatment drug resistance (PDR) levels above 10% in 2016 [53].

In Southern Africa, dolutegravir (DTG), an integrase inhibitor drug, is being introduced on a large scale as part of fixed-dose combinations of Tenofovir, Lamivudine, and Dolutegravir (TLD) [146]. With a high genetic barrier to resistance, DTG has the potential to curb the spread of antiretroviral resistance, as it is highly effective, well tolerated and affordable in resource-limited settings [114, 147–149]. Mathematical models explored the effectiveness and cost-effectiveness of prescribing DTG to all ART initiators [150]. These models found that the introduction of DTG was cost-saving and reduced HIV mortality in people living with HIV who initiate ART [150].

The introduction of DTG has been complicated by the increased risk of neural tube defects (NTD) in women living with HIV using DTG at the time of conception [151] and other potential side effects such as weight gain [149, 152]. Concerns surrounding NTD risk have delayed the rollout of DTG and, in some settings, led to recommending DTG-based regimens only for men and women who are not at risk of pregnancy [153, 154]. For South Africa, a mathematical modelling study showed that DTG-based first-line ART for all women of child-bearing potential would prevent more deaths among women and more sexual HIV transmissions than either NNRTI-based ART for women of child-bearing potential or women

without contraception, but increase pediatric deaths [155]. In its 2019 guidelines, the WHO recommends DTG in combination with nucleoside reverse-transcriptase inhibitors (NRTIs) for first-line ART, with the proviso that "women should be provided with information about benefits and risks to make an informed choice regarding the use of DTG" [156].

It is likely that in many settings, people living with HIV on NNRTI-based first-line ART will be switched to DTG-based ART; however, the rate of the transition will vary between countries and settings. For second-line ART, WHO recommends DTG-based ART in people living with HIV for whom an NNRTI-based first-line regimen has failed [156]. Again, the rate of switching to DTG-based second-line ART will vary, influenced by concerns about the development of DTG resistance in patients who switch with pre-existing resistance to NRTIs [157]. Taken together, it is likely that for the foreseeable future a considerable fraction of people living with HIV, and particularly women, may continue to rely on NNRTI-based ART regimens, even in the case when guidelines recommend DTG. In this context, NNRTI resistance will likely remain an important issue during and after the rollout of DTG.

We adapted the MARISA model (Modelling Antiretroviral drug Resistance In South Africa) [158] to predict the impact of different scenarios regarding the scale-up of DTG-based ART on NNRTI pre-treatment drug resistance ("NNRTI resistance" in the remaining of this article) in South Africa for 2020 to 2040.

4.4 Materials and methods

4.4.1 Extended MARISA model

Described in detail elsewhere [158], MARISA is a deterministic compartmental model of both the general HIV epidemic and the NNRTI resistance epidemic in South Africa. It consists of four dimensions representing (1) care stages (see Fig 4.1); (2) disease progression according to the CD4 cell counts; (3) sex; and (4) NNRTI resistance. Care stages distinguish between infected, diagnosed and treated individuals (either with NNRTI- or protease inhibitor (PI)-based regimen), with subsequent treatment-specific suppression (*Supp* compartment in Fig 4.1) or failure (*Fail* compartment). *Treat init.* compartments represent individuals treated for less than 3 months.

We simulated the adapted model from 2005 to 2040 assuming the rollout of DTG-based ART started in 2020 under different scenarios (see below). We further assumed that all men and a proportion p_1 of women are eligible for DTG, this proportion varied between scenarios. Before 2020, an NNRTI is used in first-line ART and PIs in second-line regimens. As first line regimen, DTG is prescribed from 2020 on either to ART initiators (i.e., eligible, ART-naive people living with HIV) or for switching to DTG-based first-line ART (i.e., people on NNRTI and eligible for DTG). We assumed that patients failing DTG are switched to a PI-based regimen. For DTG-ineligible women, the cascade of care remains unchanged after 2020 (Fig 4.1).

4.4.2 Calibration and extension of the MARISA model

We previously calibrated the MARISA model by combining different sources of data. Rates either related to treatment response (NNRTI- or PI-based regimen) or disease progression (characterized by CD4 counts) were estimated using clinical data from five cohorts in South Africa (Aurum Institute, Hlabisa, Kheth'Impilo, Rahima Moosa and Tygerberg) that participate in the leDEA collaboration [71]. These cohorts provided longitudinal information

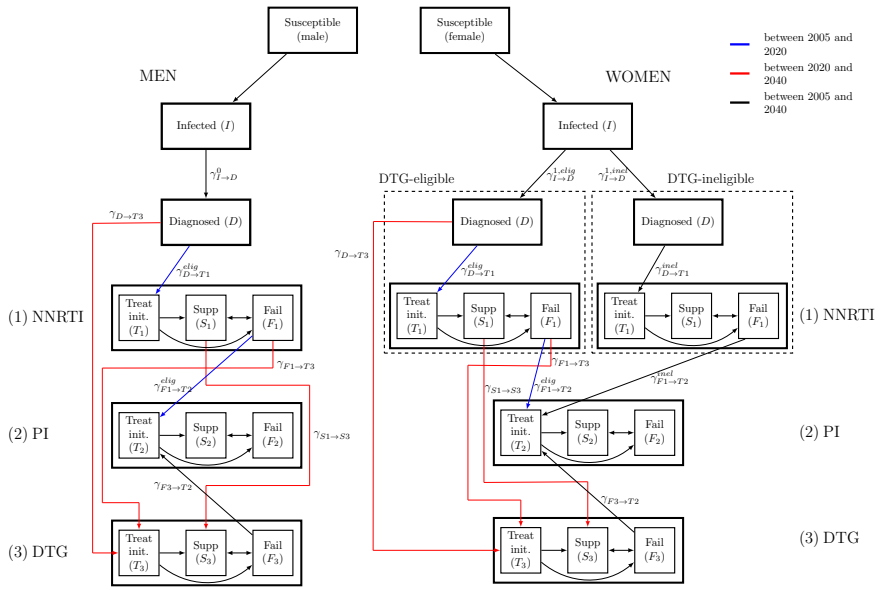


Fig 4.1: The adapted MARISA model. The model differentiates DTC-eligible from DTC-ineligible women. The model structure related to the cascade of care is shown.

for 30,317 HIV-infected adults. Other parameters were either estimated from the literature (e.g. resistance-related parameters) or fitted to estimates from the Thembeisa model (e.g. diagnosis rates and treatment initiation rates). Thembeisa is a demographic projection model on which the official UNAIDS estimates for South Africa are based [66]. More details about the calibration procedure can be found in [158] and in the supplementary materials (S1 Text, Section 1.1).

We added and modified parameters in order to model the introduction of DTG. We assumed that the DTG initiation rate $\gamma_{D \rightarrow T_3}(t)$ is the same as the NNRTI initiation rate $\gamma_{D \rightarrow T_1}(t)$ from 2020. Both NNRTI and DTG initiation rates increase until 2022, as a consequence of the Treat-All policy that was implemented in 2017. From 2022 onwards, they are assumed to remain constant (S1 Text, Section 2.2). Finally, we fixed switching rates from NNRTI- to DTG-based regimens for both eligible suppressed (see “Scenarios”) and all failing individuals ($\gamma_{S_1 \rightarrow S_3}(t)$ and $\gamma_{F_1 \rightarrow T_3}(t)$ respectively) to 1 year^{-1} . We assumed that suppressed individuals would stay suppressed when switching, while failing individuals would start DTG in the *Treat init.* compartment (see Fig 4.1). The main parameters are summarized in Table 4.1.

In the adapted MARISA model, we also added a fifth NRTI resistance dimension to model the impact of NRTI resistance on DTG-efficacy. NRTI resistance is defined as having resistance to both tenofovir (TDF) and lamivudine/emtricitabine (3TC/FTC), the two backbones that are usually combined with DTG (see S1 Text, Section 2.5) [27]. We assumed that NRTI resistance is acquired when failing NNRTI-based regimen. In view of the low levels of NRTI PDR that are observed in Africa and its rapid reversion to wild-type, we assumed as an approximation that it cannot be transmitted. We investigated different impacts of NRTI resistance on DTG-based regimen and different DTG-efficacies. For this aim, we re-calibrated the model so that it reflects different odds ratios (ORs) of DTG-failure

Table 4.1: Main parameters used in the extended MARISA model.

| Rate | Description | Source/Definition |
|--|--|---|
| Rates estimated in the previous MARISA model [158] | | |
| $\gamma_{I \rightarrow D}^{k,elig/inel}, \gamma_{D \rightarrow T_1}^{k,elig}$ | Diagnosis rate, treatment initiation rate to NNRTI | Calibrated by fitting MARISA to Thembisa model (see [158]) from 2005 to 2016 (see S1 Text Section 2.2) |
| $\gamma_{T_1 \rightarrow S_1}, \gamma_{T_1 \rightarrow F_1}, \gamma_{F_1 \rightarrow S_1}, \gamma_{S_1 \rightarrow F_1}$ | NNRTI suppression and failure rates | Estimated with individual epidemiological data from leDEA-SA [71] (see S1 Text Table B) |
| $\gamma_{T_2 \rightarrow S_2}, \gamma_{T_2 \rightarrow F_2}, \gamma_{F_2 \rightarrow S_2}, \gamma_{S_2 \rightarrow F_2}$ | PI suppression and failure rates | Estimated with data from leDEA-SA [71] (see S1 Text Table B) |
| $\gamma_{F_1 \rightarrow T_2}^{k,elig/inel}$ | Rate of switching from NNRTI to PI (before 2020) | Estimated with data from leDEA-SA and then adjusted (see S1 Text Section 2.2) |
| Added rates | | |
| $\gamma_{T_3 \rightarrow S_3}, \gamma_{T_3 \rightarrow F_3}, \gamma_{F_3 \rightarrow S_3}, \gamma_{S_3 \rightarrow F_3}$ | DTG suppression and failure rates | Calibrated with data from NAMSAL study [152] (see S1 Text Section 2.5) |
| $\gamma_{D \rightarrow T_3}(t) (t \geq 2020)$ | DTG initiation rate (from 2020) | Same DTG initiation rate as for NNRTI (for DTG-inel. people) $\gamma_{D \rightarrow T_3} := \gamma_{D \rightarrow T_1}^{inel}$ |
| $\gamma_{I \rightarrow D}^{k,elig}(t), \gamma_{I \rightarrow D}^{k,inel}(t), (t \geq 2020)$ | Diagnosis rate from 2020 (distribution across DTG-eligibility classes) | $\gamma_{I \rightarrow D}^{1,elig}(t) = p_1 \cdot \gamma_{I \rightarrow D}^1(2020)$ and $\gamma_{I \rightarrow D}^{1,inel}(t) = (1 - p_1) \cdot \gamma_{I \rightarrow D}^1(2020)$, for $t \geq 2020$ (see S1 Text Section 2.2) |
| $\gamma_{F_1 \rightarrow T_2}^{elig/inel}(t), (t \geq 2020)$ | Rate of switching from NNRTI to PI (DTG-inel.) | $\gamma_{F_1 \rightarrow T_2}^{inel}(t) = \gamma_{F_1 \rightarrow T_2}, \gamma_{F_1 \rightarrow T_2}^{elig}(t) = 0$, for $t \geq 2020$ (see S1 Text Section 2.2) |
| $\gamma_{F_3 \rightarrow T_2}(t), (t \geq 2020)$ | Rate of switching from DTG to PI | $\gamma_{F_3 \rightarrow T_2}(t) := \gamma_{F_1 \rightarrow T_2}^{inel}(t), t \geq 2020$ |
| $\gamma_{S_1 \rightarrow S_3}(t), (t \geq 2020)$ | Switching rate from NNRTI to DTG (maintenance therapy) | $\gamma_{S_1 \rightarrow S_3}^k(t) := 1 \text{ year}^{-1}, t \geq 2020$ |
| $\gamma_{F_1 \rightarrow T_3}(t), (t \geq 2020)$ | Switching rate from NNRTI to DTG (switch therapy) | $\gamma_{F_1 \rightarrow T_3}(t) = 1 \text{ year}^{-1}, t \geq 2020$ |

between NRTI-resistant and NRTI-susceptible individuals (OR=1, OR=2, OR=5). In the main analysis, we assumed that DTG-efficacy was similar to the one observed in the New Antiretroviral and Monitoring Strategies in HIV-infected Adults in Low-income countries (NAMSAL) study [152], corresponding to an OR of failure between NNRTI and DTG of 1.02, after adjusting for the different baseline characteristics of the two groups (see S1 Text, Section 2.5). Other DTG efficacy corresponding to an OR of 2 and 5 were investigated in an additional analysis (see S1 Text, Section 5.3). All code and manuscript are available from <https://github.com/anthonyhauser/MARISA2>. This study was approved by the Ethics Committee of the Canton of Bern, Switzerland.

4.4.3 Scenarios

The model investigated the impact of the introduction of DTG-based regimens on the level of NNRTI resistance in diagnosed individuals (i.e. NNRTI PDR) under 2 main scenarios, with 4 variations for each of the two scenarios. We also examined the scenario where DTG-based ART is not introduced. There were thus 9 scenarios in total. The two main scenarios were:

1. DTG is only used in first-line regimen of ART-initiators and, as second-line, in patients failing NNRTI-based ART,
2. DTG is used as initial first-line regimens (for ART-initiators), with all patients on NNRTI-based regimens being switched to a DTG-based regimen.

For the second scenario, we varied the impacts of NRTI resistance on DTG-based regimen, by either assuming an OR of DTG-failure between NRTI-resistant and NRTI-susceptible individuals of 1 (i.e. no impact) or of 2. Each scenario also investigated four different DTG eligibility levels p_1 for women. The population eligible for DTG in each scenario was:

- a) only men (100% men, 0% women)
- b) men and women beyond reproductive age (100% of men, 17.5% of women)
- c) men and women beyond reproductive age or using contraception (100% of men, 63% of women)
- d) all men and women (100% of men, 100% of women)

The percentages of women eligible for DTG in b) and c) were determined by analyzing cohort data from leDEA, which show that 17.5% adult women on ART are 50 or older [71], and estimates on the use of contraception from the World Bank [159](see S1 Text, Section 3.1). Throughout the rest of the paper, scenarios (b) and (c) will be referred as "men and women beyond childbearing age" and "men and women not at risk of pregnancy", respectively. Of note, to model scenario 1., we set $\gamma_{S_1 \rightarrow S_3}(t) = 0$ and $\gamma_{F_1 \rightarrow T_3}(t) = \gamma_{F_1 \rightarrow T_2}^{inel}(t)$ (as opposed to scenario 2., where $\gamma_{S_1 \rightarrow S_3}(t) = \gamma_{F_1 \rightarrow T_3}(t) = 1 \text{ year}^{-1}$). We thus assumed that in all scenarios DTG will be used in second-line regimens for people failing NNRTI-based first-line ART.

4.4.4 Additional analyses

We predicted the impact of different levels of DTG introduction on the level of NNRTI failure. We considered the scenario where DTG was prescribed to ART initiators and those on

NNRTI-based first-line ART were switched to a DTG-based regimen, with the four different levels of women accessing DTG-based ART (see "Scenarios"). However, we assumed that 99% of women were eligible for DTG in scenario d) (instead of 100%), in order to estimate NNRTI failure when only a very small fraction of women rely on it. For each of these scenarios, we predicted the percentage of individuals failing an NNRTI-based regimen in 2035 after different durations on ART (1 or 2 years). For each of the scenarios, we ran the model from 2005 up to 2035 and retained the numbers of people starting NNRTI-based first-line ART (by CD4 groups, NNRTI resistance and sex) in 2035. We then ran the model for the compartments related to NNRTI-treatment, using the previously saved starting values. This way, we could predict the levels of NNRTI-failure in patients starting NNRTI in 2035 after 1 or 2 years of ART.

We assessed the impact of different switching rates from NNRTI- to DTG-based regimens, fixed to 1 year^{-1} for both suppressed and failing individuals. We varied both rates $\gamma_{S_1 \rightarrow S_3}(t)$ and $\gamma_{F_1 \rightarrow T_3}(t)$ within a range corresponding to a time to switch of between 0.5 and 10 years after start of ART. For each analysis, the percentage of women who are DTG-eligible varied from 0% to 100%.

4.4.5 Sensitivity analyses

The values of eight parameters were varied in the sensitivity analysis: three transmission-related parameters (percentage of men who have sex with men (MSM), probability of male-to-male infection per sexual contact, and HIV prevalence ratio between MSM and heterosexuals), four resistance-related parameters (resistance rates, reversion to wild-type rate and the effect of NNRTI resistance on NNRTI efficacy) and one parameter related to treatment (efficacy of DTG-based treatment). Multivariate uncertainty within specified ranges was assessed using Latin hypercube sampling [160]. Each model estimate is reported with a 95% sensitivity range. Further details are available in S1 Text, Section 3.2. and Fig C and D. In addition, we also investigated the impact on NNRTI PDR of 1) lower treatment-initiation rates than suggested by the Treat-All policy (as suggested by [161]), 2) treatment interruption, 3) higher efficacy of DTG and different impacts of NNRTI resistance on DTG (S1 Text, Section 5).

4.5 Results

4.5.1 Use of NNRTIs and levels of resistance

The percentages of patients treated with DTG and NNRTI for each of the 9 scenarios are shown in Fig 4.2. The predicted evolution of levels of NNRTI PDR up to 2040 across 13 scenarios is shown in Fig 4.3. The model predicts that while NNRTI PDR would increase substantially under continued NNRTI-based ART, the introduction of DTG-based ART can halt this increase, if in addition to starting new patients on a DTG-based regimen the patients on NNRTI-based regimens are switched to DTG-based first-line ART. Specifically, under the scenario of continued NNRTI-based ART as standard first-line therapy, NNRTI PDR would increase to 29.8% (95% sensitivity range: 7.4%-39.4%) by 2030 and 52.4% (21.1%-63.4%) by 2040 (Fig 4.3A). At the other end of the spectrum, initiating all new ART patients on DTG-based ART and rapidly switching all patients currently on NNRTI-based ART to DTG-based regimens, independently of their sex, would stabilize NNRTI PDR at a moderate level, with a prevalence of 8.4% (2%-11.8%) by 2030 and 10.4% (4.4%-13.8%) by 2040 (Fig 4.3B). When assuming an impact of NNRTI resistance on DTG-failure (Fig 4.3C), we found slightly higher levels of NNRTI PDR: 9.7% (2.4%-13%) in 2030 and 13.2% (5.6%-16.9%) in 2040, but a similar impact of the

different scenarios of DTG introduction. Using DTG only in first-line regimens of patients initiating ART is not sufficient to curb the increase of NNRTI PDR, even when given to all men and women (Fig 4.3A).

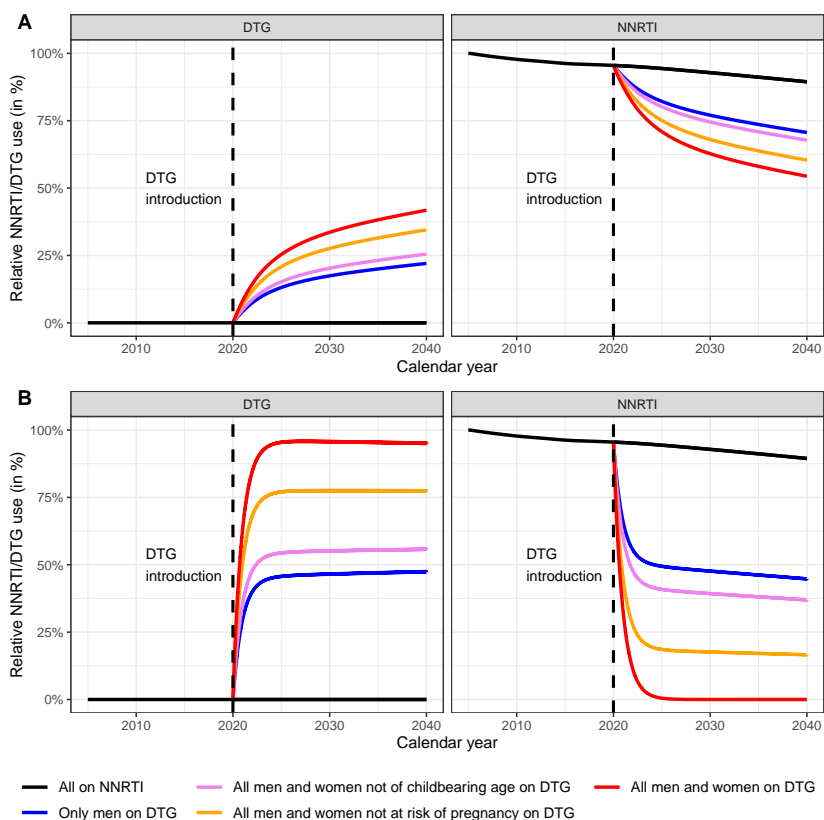


Fig 4.2: Predicted use of NNRTI- and DTG-based regimens. Percentages of patients treated with NNRTI- and DTG-based regimens (left and right panels, respectively) are shown. Panels A represent the scenarios where DTG is used in patients initiating ART, while in panels B patients are also switched to DTG-based first line ART.

If restricted to men, DTG-based ART will not curb the increase in NNRTI PDR: the prevalence of resistance is predicted to increase over the entire study period, reaching values of close to 40% by 2040 (Fig 4.3B). The situation is similar under the scenario of initiating or switching men and women beyond childbearing age (17.5% of women in the leDEA cohorts). However, the model estimates that the increase in the prevalence of NNRTI PDR is substantially slowed down if women beyond the age of reproduction or on contraception (63% of women) also initiate a DTG-based regimen or switch to DTG. Under this scenario the prevalence of NNRTI PDR is predicted to reach 25.9% (8.5%-37%) in 2040 and 13.3% (3%-18.7%) in 2030, if DTG is given to both ART-initiators and individuals already on NNRTI-based ART (Fig 4.3). Again, slightly higher NNRTI PDR levels are observed when including the impact of NRTI resistance on DTG-efficacy: 27% (9.3%-37.9%) in 2040 and 14.2% (3.4%-19.3%) in 2030.

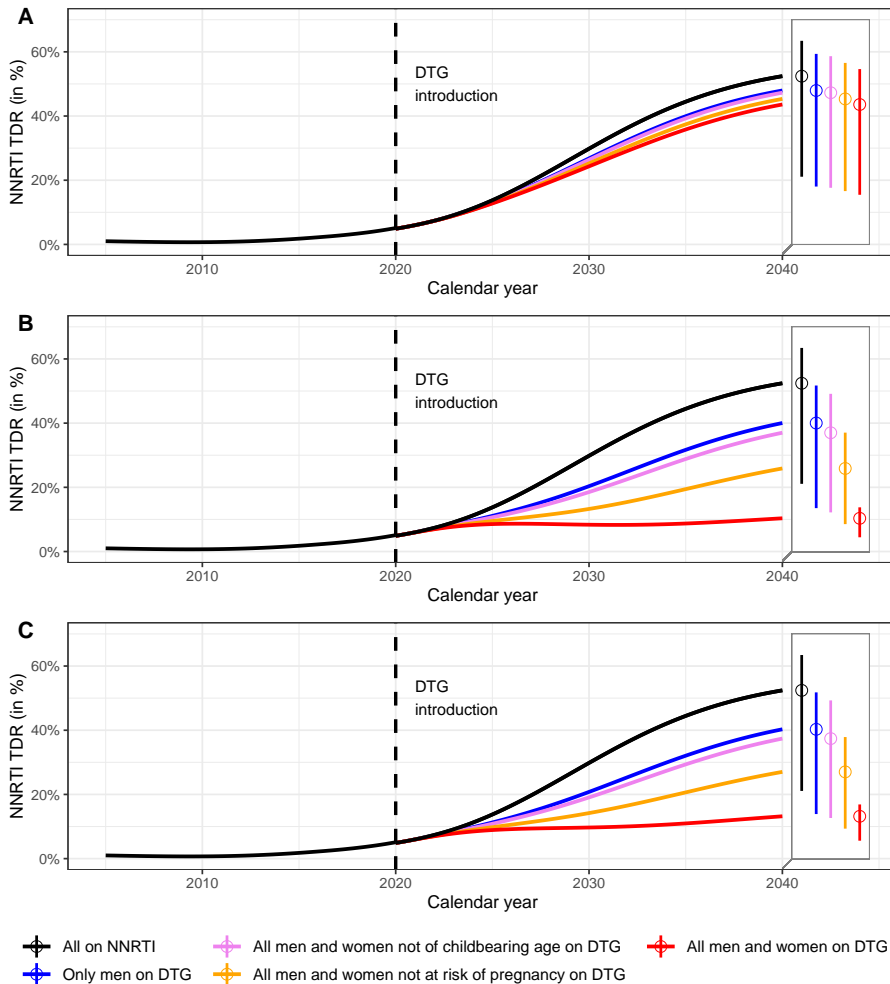


Fig 4.3: Predicted levels of NNRTI pre-treatment drug resistance in South Africa (PDR) 2005-2040. Dolutegravir is introduced in 2020 under three scenarios: DTG as first-line regimen for ART-initiators (panel A), DTG for all patients (panel B) or DTG for all patients, assuming an impact of NRTI resistance on DTG-efficacy (panel C), and with different eligibility criteria for women (colors). The baseline model shows the situation without the introduction of DTG (black line). The two boxes on the right of each panel represent the levels of NNRTI PDR in 2040 and their 95% sensitivity ranges.

4.5.2 Impact of switching rates

We calculated levels of NNRTI PDR for 2035 for different average switching delays and percentages of women eligible for DTG-based ART, however without considering the effect of NRTI-resistance. We considered the effect of a modified switching rate both in suppressed individuals (Fig 4.4A) and in individuals on a failing regimen (Fig 4.4B). The predicted levels of NNRTI PDR range from 8.4% to 33.1%. The results indicate potential benefits of both strategies to reduce NNRTI resistance. However, as shown by the greater variation in the prevalence of NNRTI PDR in the vertical than horizontal direction in Fig 4.4, allowing a

higher proportion of women access to DTG-based ART has a greater impact than increasing switching rates.

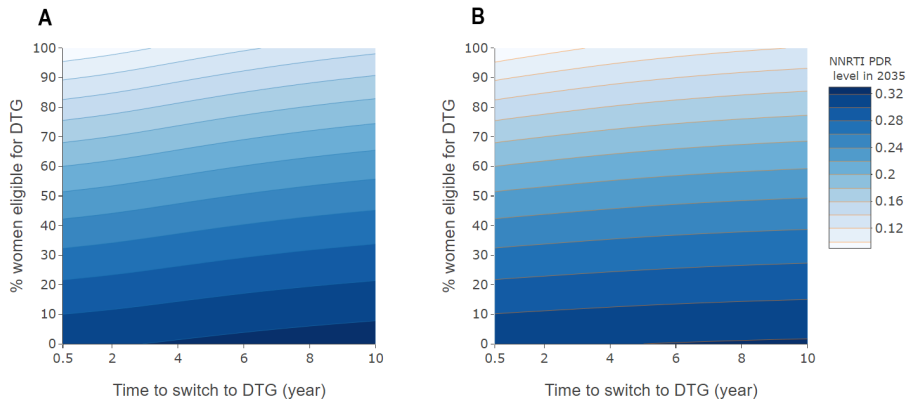


Fig 4.4: Level of NNRTI pre-treatment drug resistance in 2035, by rate of switching to DTG-based ART and percent women eligible for DTG-based ART. Panel A relates to patients on first-line ART with suppressed HIV-1 replication, and panel B to individuals failing NNRTI-based ART. The average time to switching (i.e. the inverse of the switching rate) varies from 0.5 to 10 years for individuals with viral suppression (panel A) or failure (panel B).

4.5.3 Impact of DTG-eligibility on the rate of NNRTI failure

As expected from their effect on NNRTI resistance, the different scenarios of the rollout of DTG-based ART also influence the virological failure under NNRTI-based ART. Fig 4.5 shows the predicted proportion of NNRTI-failure after 1 and 2 years among DTG-ineligible women according to different scenarios of DTG-introduction. In the absence of DTG introduction, we observe a high level of failure in women starting NNRTI in 2035, reaching 18.2% after 2 years of ART. If all men are started on or switched to DTG, it would help diminish the level of failure by 2 years to 14.3% in 2035, and to 14.5% when including the impact of NRTI resistance. This percentage decreases to 13.1% , when including all women not at risk of pregnancy (13.4% when including NRTI resistance), and to 12.3% (12.7% when including NRTI resistance) if all men and 99% of women are included. Finally, we find that the increase of virological failure in DTG-ineligible women who still rely on NNRTI can be stopped by the introduction of DTG (see S1 Text Fig E).

4.6 Discussion

We adapted the epidemiological MARISA model to examine the impact of the scale-up of DTG-based ART on NNRTI pre-treatment drug resistance in South Africa. Overall, our findings suggest that if a large fraction of women is excluded from receiving DTG-based ART, they will not only receive a potentially inferior NNRTI-based regimen but will also face increasing rates of resistance to this regimen due to the population level effects of continued NNRTI use. In contrast, the spread of NNRTI resistance can be slowed down if DTG-based ART is made accessible both to women at low risk of pregnancy and to people currently on a NNRTI-based first-line regimen, thereby indirectly protecting those still requiring a

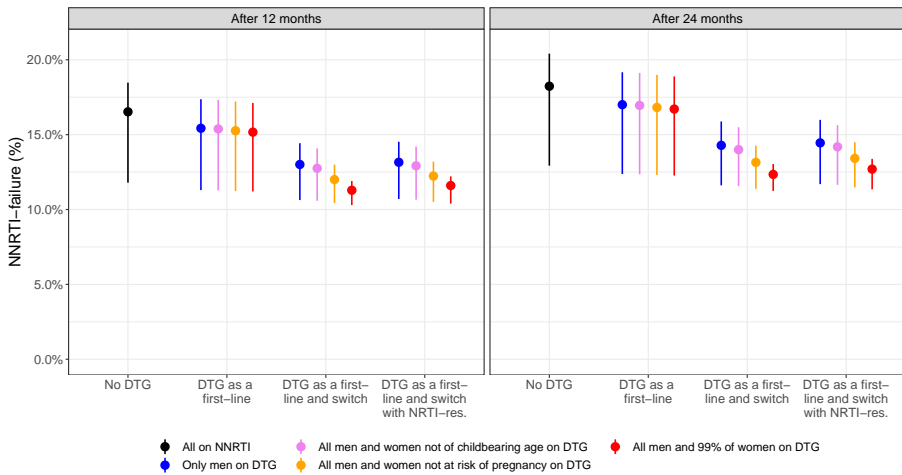


Fig 4.5: Predicted percentage of women failing NNRTI-based ART after one and two years of ART in 2035, depending on the scenario of the rollout of DTG-based ART. Note that the scenario in which DTG is given to all men and 99% of women (in red) replaces the scenario in which DTG was given to all men and women (see "Additional analyses"). Failure is given after 1 and 2 years of ART.

NNRTI-based treatment. Model simulations emphasize the importance of starting on or switching a maximum number of women to DTG-based ART: increasing use of DTG-based regimens was the strategy with the greatest potential to curb the spread of NNRTI resistance. The latter strategy will also lower the risk of virologic failure in women who have to rely on NNRTI-based ART in the future. Finally, it is interesting to observe that, even when using DTG for all patients, NNRTI PDR is not expected to decrease but rather to remain approximately stable at a moderate level, due to the very slow reversion of NNRTI resistance that allows subsequent transmission of NNRTI resistance (in line with [162]).

While some countries, such as South Africa, first considered limiting access to DTG to men, menopausal women, and women using long-term family planning as a potential policy, the new WHO guidelines state that women should not in principle be excluded from DTG-based ART, even women who are at risk of pregnancy or desire to get pregnant. WHO recommends a woman-centered approach where women should be provided with information about benefits and risks to make an informed choice [49, 156]. It is unclear what proportion of women will effectively receive DTG-based ART, as it depends on individual women's decisions. In this context, model simulations are essential in order to assess the impact of the different options proposed and different levels of DTG uptake. A strength of our model is that it deals with the two most significant sources of uncertainty associated with the introduction of DTG, namely DTG uptake in women and the delay in switching people currently on NNRTI regimens. Despite the uncertainty concerning the uptake of DTG in women, it is likely that a proportion of women will continue to rely on NNRTI-based ART. Therefore, even with the rollout of DTG, NNRTI resistance will continue to be relevant for these women. Compared with other modelling work that assessed risks and benefits of DTG introduction (e.g. [155]), our model focused on its indirect, population-level impact on NNRTI resistance. Rather than assigning a level of NNRTI resistance that is fixed over time, HIV care and disease stages (as in

[155]), our model considered the dynamic development of NNRTI resistance under relevant scenarios.

Our model also has several limitations. First, real-world data on the efficacy of DTG, especially in resource-limited settings are scarce. Therefore, we conservatively assumed that DTG has a similar efficacy as observed in the NAMSAL study [152]. Higher DTG efficacies as well as different impacts of NRTI resistance on DTG-failure are investigated in supplementary analyses (see S1 Text, Section 5.3). Second, predictions of levels of NNRTI resistance over the next twenty years are naturally uncertain, as reflected by the wide sensitivity ranges in Fig 4.3. However, despite the uncertainty, it is clear that the different strategies of rolling out DTG-based ART influenced the levels of NNRTI resistance. Finally, the MARISA model includes some simplifying assumptions, e.g. we did not model prevention of mother to child transmission (PMTCT), or treatment interruption. However, relaxing some of these assumptions did not drastically change our conclusion (see S1 Text, Section 5).

Another limitation of this study is the fact that the MARISA model does not take into account resistance to DTG and uses a simplified representation of NRTI resistance. In the context of the introduction of DTG-based ART, modelling of NRTI resistance is particularly relevant as individuals starting on DTG as a functional monotherapy due to resistance to both NRTI backbones - tenofovir and lamivudine - experience higher risk of treatment failure [103]. As they are considerably less frequently transmitted [38] and revert back quickly [31, 32], NRTI resistances might primarily be an issue for ART-experienced individuals and more specifically, in patients failing NNRTI-based regimens, who often exhibit high levels of NRTI resistance [74]. These patients who are on non-suppressive NNRTI-based regimens are expected to switch to DTG, either after identification of treatment failure, following the new WHO guidelines, or blindly [157]. In the context of modelling the DTG rollout, this consideration has two important implications. First, patients currently failing NNRTI-based regimens are expected to have higher DTG failure rates, mainly due to previously acquired NRTI resistance. Second, due to ongoing viral replication and due to pre-existing NRTI resistance, they are at higher risk of accumulating resistance, which may also lead to the emergence of DTG resistance. So far, data on emergence of DTG resistance is primarily available from patients in whom treatment failure was detected relatively early, which may not be the case in African settings [149]. Therefore, to understand risk inherent in the emergence of DTG resistance, adapting the MARISA model by extending its resistance dimension to DTG resistance will be necessary.

4.7 Conclusion

In conclusion, our study indicates that giving access to DTG-based ART to all women not at risk of pregnancy could limit the increase of NNRTI PDR, but even if all women receive DTG-based ART the level of NNRTI PDR will remain above 10% in South Africa. Our model highlights the importance of a rapid switch of patients currently on NNRTI-based to DTG-based ART in order to limit the increase in NNRTI PDR. Women who remain on NNRTI-based ART will indirectly benefit from a high level of DTG uptake due to a reduced risk of virologic failure.

4.8 Acknowledgements

Computations were conducted on UBELIX (<http://www.id.unibe.ch/hpc>), the high performance computing cluster at the University of Bern, Switzerland.

4.9 Supporting information

S1 Text. Supplementary Material. Section 1: description of the adapted MARISA model. Section 2: description of model parameters. Section 3: Model simulation, Section 4: Model equations. Section 5: Additional results and sensitivity analyses.

Chapter 5

HIV drug resistance in sub-Saharan Africa: public health questions and the potential role of real-world data and mathematical modelling

Renee de Waal¹
Richard Lessells²
Anthony Hauser³
Roger Kouyos^{4,5}
Mary-Ann Davies¹
Matthias Egger^{2,6,7}
Gilles Wandeler⁸

¹ Centre for Infectious Disease Epidemiology and Research, School of Public Health and Family Medicine, University of Cape Town, Cape Town, South Africa

² KwaZulu-Natal Research Innovation and Sequencing Platform, Department of Laboratory Medicine & Medical Sciences, University of KwaZulu-Natal, Durban, South Africa

³ Institute of Social and Preventive Medicine, University of Bern, Bern, Switzerland

⁴ Division of Infectious Diseases and Hospital Epidemiology, University Hospital Zurich, University of Zurich, Zurich, Switzerland

⁵ Institute of Medical Virology, University of Zurich, Zurich, Switzerland

⁶ Centre for Infectious Disease Epidemiology and Research, University of Cape Town, South Africa

⁷ Population Health Sciences, Bristol Medical School, University of Bristol, Bristol, United Kingdom

⁸ Department of Infectious Diseases, Bern University Hospital, University of Bern, Bern, Switzerland

This article is published in *Journal of Virus Eradication*: HIV drug resistance in sub-Saharan Africa: public health questions and the potential role of real-world data and mathematical modelling (2018) DOI: 10.1016/s2055-6640(20)30347-2.

Contribution: I contributed to the writing of the section on the current knowledge gaps and the role of mathematical modelling. I also reviewed papers on modelling HIV drug resistance to produce the Box 1.

5.1 Abstract

The prevalence of pretreatment resistance to non-nucleoside reverse transcriptase inhibitors (NNRTIs) is >10% in many low-income countries. As a consequence, several sub-Saharan African countries have implemented, or are considering the introduction of, non-NNRTI-based first-line antiretroviral therapy (ART) for treatment-naïve and treatment-experienced patients. This is occurring at a time when ART programmes are expanding, in response to the World Health Organization guidelines, which recommend ART initiation regardless of CD4 cell count. Both those developments raise important questions regarding their potential impact on HIV drug resistance and the impact of HIV drug resistance on clinical outcomes. Those issues are particularly relevant to sub-Saharan Africa, where standardised ART regimens are used and where viral load monitoring and resistance testing are often not done routinely. It is therefore essential to forecast the impact of the implementation of universal ART, and the introduction of drugs such as dolutegravir to first-line regimens, on HIV drug resistance in order to inform future policies and to help ensure sustainable positive long-term outcomes. We discuss important public health considerations regarding HIV drug resistance, and describe how mathematical modelling, combined with real-world data from the four African Regions of the International epidemiology Databases to Evaluate AIDS consortium, could provide an early warning system for HIV drug resistance in sub-Saharan Africa.

5.2 Introduction

The widespread emergence and transmission of HIV drug resistance (HIVDR) has impaired the success of the currently recommended first-line antiretroviral therapy (ART) regimens including efavirenz in sub-Saharan Africa (SSA). The prevalence of pretreatment non-nucleoside reverse transcriptase inhibitor (NNRTI) resistance ranges from 8% in Cameroon to 15% in Uganda [38]. As many countries in the region consider shifting to dolutegravir-containing regimens, surveillance and monitoring of HIVDR will be key to ensuring the durability of this new drug. The introduction of universal test-and-treat policies [163] will increase the number of individuals on ART from 20 million in mid-2017 to approximately 30 million by 2020. This rapid expansion of ART programmes might impact the occurrence of HIVDR, particularly in under-resourced health systems with little capacity for virological monitoring. In this viewpoint article we discuss important public health considerations regarding HIVDR in SSA, namely the potential impact of universal test-and-treat policies on HIVDR, and the potential implications of HIVDR on the effectiveness of dolutegravir-based ART. We also identify gaps in current knowledge, and describe how we could address current and future challenges in the field using real-world data from the International epidemiology Databases to Evaluate AIDS (IeDEA), a large consortium of HIV cohorts, and mathematical modelling.

5.3 Universal test-and-treat policies and the emergence of HIV drug resistance in sub-Saharan Africa

Randomised controlled trials have shown the benefits of early ART initiation in terms of individual patient outcomes and reduction in HIV transmission rates [164, 165]. However, there are concerns that early ART initiation may increase the prevalence of antiretroviral drug resistance due to compromised adherence, as patients who feel healthy might be less likely

to be fully adherent [166]. Data regarding the impact of early ART on adherence and the development of HIVDR are limited and inconsistent. In a prospective study of 473 patients from Uganda, those who initiated ART with a CD4 cell count ≥ 250 cells/ μ L were twice as likely to have treatment interruptions of >72 hours in the first 90 days of ART, as assessed by electronic pill bottles. As a consequence, they were nearly three times as likely to have HIV viral load >400 copies/mL at 120 days than those with CD4 count <250 cells/ μ L [167]. However, a study of 900 patients from South Africa found that CD4 count at ART initiation was not associated with adherence $<95\%$ in the first 12 months on ART (assessed by visual analogue scale and pill count) [44]. In terms of the impact of early ART initiation on HIVDR, in a cohort study from Europe, patients who initiated ART immediately (within three months of having a CD4 count and viral load measured while AIDS-free), were slightly more likely to develop drug resistance within seven years than those who initiated ART at CD4 <500 , or <350 cells/ μ L [47]. In contrast, in the HPTN052 trial, which showed decreased HIV transmission between sero-discordant couples with ART initiation at a CD4 cell count of 350–550 versus <250 cells/ μ L, the risk of drug resistance was higher in the delayed versus early ART initiation arm [168].

These differences in the effect of timing of ART initiation on the development of HIVDR might be explained by differences in adherence: patients in clinical trials are generally more closely monitored, and may be more motivated to take treatment than those in routine care. Although the evidence that early ART initiation in itself influences the emergence of HIVDR is not compelling, there is reason to believe that the continued expansion of ART programmes might result in increased rates of HIVDR through suboptimal adherence and suboptimal retention in care in the context of resource-limited health systems. Along with HIVDR surveys, adherence monitoring and interventions to improve adherence should be studied in more depth in these settings.

5.4 Potential implications of HIV drug resistance on the success of dolutegravir-based antiretroviral therapy in sub-Saharan Africa

In many African countries, the prevalence of pretreatment NNRTI resistance mutations is $>10\%$, the World Health Organization's threshold for countries to consider implementing non-NNRTI-based first-line ART [38, 169]. As a consequence, many SSA countries have either started or are considering implementation of dolutegravir-based first-line ART, although recent concerns regarding its safety in early pregnancy may limit its use in women of child-bearing age [151]. It is anticipated that dolutegravir will be used in both ART-naïve and ART-experienced patients; the latter will switch from their current NNRTI-based first-line regimens. This raises concerns regarding its use in settings where resistance testing is not standard of care, and where even viral load monitoring may not be performed routinely.

Dolutegravir has a high genetic barrier to resistance and development of resistance mutations has not been shown in clinical trials of treatment-naïve patients initiating dolutegravir-containing ART without pretreatment drug resistance [170, 171]. In ART-naïve patients, dolutegravir was superior to efavirenz and to ritonavir-boosted darunavir in terms of virological outcomes, and much of that superior efficacy was due to dolutegravir's better tolerability [170, 171]. However, in a study of dual therapy with dolutegravir and lamivudine in the US, three out of 120 patients had virological failure at 24 weeks, and one patient

developed resistance mutations to both drugs (M184V and R263R/K) [172]. This patient was thought to be poorly adherent to ART as his plasma dolutegravir concentrations were below the limit of quantification on at least one occasion.

In treatment-experienced patients receiving dolutegravir, development of HIVDR is also uncommon, but has been reported in patients on dolutegravir monotherapy. In the DOMONO trial, ART-experienced patients who were virologically suppressed were randomly allocated to switch to dolutegravir monotherapy immediately or at 24 weeks [143]. Eight of 95 participants experienced virological failure and three developed integrase resistance mutations at 48 weeks. In another clinical trial from Spain, two of 31 patients who were randomly allocated to be switched to dolutegravir monotherapy developed integrase resistance [142]. The authors of both studies concluded that dolutegravir should not be used as monotherapy. Of note, ART-experienced patients in the studies described above were virologically suppressed at baseline, and patients with previously documented HIVDR were excluded. Routine viral load monitoring is not carried out in many SSA countries, so it is likely that many patients will switch to dolutegravir-based ART when they are not virologically suppressed. The DAWNING study, a multicentre trial that randomly allocated patients whose first-line ART was failing to receive dolutegravir-based or protease inhibitor-based ART provides some reassurance regarding the use of dolutegravir in patients who are not virologically suppressed [173]. Importantly, all patients had to have at least one active nucleoside/nucleotide reverse transcriptase inhibitor (NRTI) predicted by resistance testing. Dolutegravir-based ART was superior to protease inhibitor-based ART, and no patients in the dolutegravir arm developed resistance mutations.

In summary, based on the available evidence, dolutegravir seems to be highly effective, both in ART-naïve and ART-experienced patients, provided that it is combined with a functional NRTI backbone. The TenoRes collaboration, which comprises data from clinical trials and observational studies, reported a prevalence of tenofovir resistance of 57% (370/654), and a prevalence of M184V/I mutation of 61% (401/654) in patients whose first-line ART regimens including tenofovir were failing [101]. Even though the high prevalence of NRTI resistance in patients with failing first-line ART in SSA may have important implications for the use of dolutegravir in settings without viral load monitoring, the long-term clinical significance of NRTI resistance in patients starting dolutegravir is not yet known. Interestingly, HIV-suppressed, treatment-experienced individuals with the M184V mutation switching to a dolutegravir/lamivudine dual therapy do not seem to have an increased risk of virological failure [174]. This finding is supported by results from *in vitro* studies, which showed that the presence of either of the NRTI resistance mutations M184I/V or K65R prevented the development of resistance to dolutegravir [175].

5.5 Gaps in current knowledge: the place for using leDEA cohort data and mathematical modelling to predict and monitor HIV drug resistance in sub-Saharan Africa

While treatment guidelines and drug prescribing policy are usually based on results from randomised controlled trials, such studies often give little insight into the real-world effectiveness of the interventions evaluated. Clinical trials usually have strict inclusion and exclusion criteria, provide close follow-up and monitoring of patients, and adherence is usually better than in routine care. Observational cohorts are often able to provide

generalisable data from many more patients in settings that reflect real-world use of interventions. However, in terms of predicting how HIVDR will affect the success of universal test-and-treat policies and the introduction of new drugs to first-line ART regimens in SSA, both clinical trials and observational cohorts have limitations. The vast majority of studies published to date were conducted in North America or Europe, in clinical settings that differ substantially from SSA. Although we can be confident that dolutegravir-based first-line triple therapy will lead to favourable virological outcomes in SSA, data on its use among patients whose NNRTI-based first-line therapy was failing are insufficient to date.

The scarcity of HIVDR surveillance data in resource-limited settings, together with the fact that those data are usually not linked with observational cohorts, presents challenges for assessing and predicting the transmission of HIVDR. Mathematical models offer a unique opportunity to bridge this gap [176] by combining observational data on rates of HIV diagnosis, treatment, and virological response with cross-sectional HIVDR surveillance data from local settings. Mathematical models have been used to address several key questions regarding HIVDR in various populations, and they are increasingly being used to inform policy [163, 169, 176]. Box 1 and Table 5.1 briefly discuss several examples.

The African regional cohorts of the IeDEA consortium provide the ideal platform to explore many of the outstanding research questions highlighted in this article, as they comprise large cohorts of patients on ART from 23 countries across West, Central, East, and Southern Africa [183]. The Consortium collects routine clinical data of patients managed largely in primary healthcare settings, and has a strong capacity for data management and analysis, with a long track record of research that influences policy. Few cohorts measure or collect HIVDR data, but many have the infrastructure to collect them, provided dedicated funding is available.

We have also recently developed a deterministic compartmental mathematical model that comprises three layers: treatment stage (e.g. diagnosis, treatment, viral suppression or failure); disease progression (represented by CD4 count strata); and the presence/absence of HIVDR (in process for future publication). Disease progression at each treatment stage, as well as the transition from one treatment stage to another, are estimated from observational data from the IeDEA Southern Africa cohorts and UNAIDS data. The model has the potential to address key questions regarding HIVDR in Southern Africa. Specifically, we aim to describe time trends and drivers of HIVDR, and to estimate how the spread of resistance is affected by alternative interventions. For example, we could assess the impact of enhanced laboratory monitoring (i.e. viral load and resistance testing) on the development of acquired drug resistance under universal test-and-treat conditions. Furthermore, we aim to assess to what extent changes in ART guidelines (e.g. dolutegravir-based first-line ART), can curb the transmission of resistance and improve clinical outcomes. As described above, a key question in this context is the potential impact of NRTI resistance on the effectiveness of dolutegravir-based ART. Finally, we hope to predict the potential development and spread of resistance to dolutegravir. The main difficulty of making such a prediction is the lack of long-term data regarding the impact of dolutegravir resistance on clinical outcomes. Nevertheless, we believe that, by integrating the accumulating clinical data or by making reasonable assumptions on such parameters based on comparable processes or settings [184], mathematical models will be helpful in providing risk assessments, and identifying key knowledge gaps that should be addressed by clinical, epidemiological, and laboratory studies.

Box 1: HIV drug resistance mathematical models

The HIV Synthesis Model, developed by Phillips et al, captures resistance to the different antiretroviral classes and its effect on treatment outcome [53, 150, 177]. More specifically, it models HIVDR in terms of the presence or absence of every mutation specific to the antiretrovirals in use. Agent-based models such as the HIV Synthesis Model have the advantage of being able to represent complex processes, like the process of acquiring resistance mutations. However, the drawback of using such models is that many assumptions are made but may not be verifiable. This can be avoided by using simpler models, such as compartmental models. Abbas et al [69], Nichols et al [178], and Supervie et al [179] have developed deterministic compartmental models to model HIV drug resistance and calibrated them with data from South Africa, Zambia and Botswana, respectively. These three models capture resistance in a simpler way than the HIV Synthesis Model. The South African Transmission Model [69] has only two layers (absence/presence of resistance) to model resistance, while the HIV-transmission models developed by Nichols et al [70] and Supervie et al [179] represent the main resistance mutations (K65R and M184V mutations for nucleoside reverse transcriptase inhibitors) (Table 5.1).

Table 5.1: Examples of how mathematical models have been used to address key HIV drug resistance questions.

| Model | HIV drug resistance questions |
|---|--|
| HIV Synthesis Model: individual-based model calibrated with sub-Saharan African data | <ul style="list-style-type: none"> · Assessing the impact of viral load monitoring on HIVDR [180] · Predicting the impact of HIVDR on mortality [53, 181] · Assessing the effectiveness and cost-effectiveness of interventions such as dolutegravir-based ART in settings with a relatively high prevalence of HIVDR [53, 177] |
| Deterministic compartmental model calibrated with Ugandan and Kenyan data | <ul style="list-style-type: none"> · Assessing the impact of increasing second-line ART coverage; and earlier ART initiation on HIVDR |
| South African Transmission Model: compartmental model calibrated to replicate the South African HIV-1 epidemic | <ul style="list-style-type: none"> · Assessing the impact of PrEP on HIVDR [69] |
| Macha HIV Transmission model: deterministic compartmental model calibrated with Zambian data | <ul style="list-style-type: none"> · Assessing the impact of PrEP [178] on HIVDR |
| PrEP Intervention Transmission model: compartmental model integrating PrEP and ART and calibrated with data from Botswana | <ul style="list-style-type: none"> · Assessing the impact of PrEP on HIVDR [179] |
| PrEP intervention model: compartmental model representing the MSM population in San Francisco | <ul style="list-style-type: none"> · Assessing the impact of PrEP on HIVDR [182] |

5.6 Conclusion

Universal test-and-treat policies and the introduction of new drugs such as dolutegravir to first-line ART regimens have the potential to improve patient outcomes and reduce the transmission of HIV in SSA. However, it is important to monitor their implementation, and to forecast their effect on the development of HIVDR. The African regional cohorts of the IeDEA global consortium represent an ideal platform to provide data regarding the real-world effectiveness of novel ART strategies and mathematical models have the potential to help predict the emergence of HIVDR in SSA. Such research is essential to ensure positive long-term outcomes, and to inform future programmatic and policy changes, tailored to local settings.

Chapter 6

Discussion

6.1 Summary of the findings

In Chapter 2, I conducted a systematic review and Bayesian meta-analysis in order to assess the prevalences of NNRTI/NRTI resistance mutations among adults failing NNRTI-based first-line regimen in Southern Africa. Rather than opting for the commonly used approach that analyzes each outcome separately, I developed a hierarchical model in order to identify the study-level heterogeneity. The model estimated high level of K65 (55%) and M184 (78%) mutations after two years of TDF and 3TC/FTC, the two currently used NRTI backbones. These results suggest that around half (43%-55%) of the people failing the first-line regimen are resistant to their two NRTI backbones, as K65 and M184 confer high resistance to TDF and 3TC/FTC, respectively. The model also estimated high level of resistance to some NNRTI resistance mutations, such as the K103 mutation (39% after two years on NVP, 60% after two year on EFV), conferring high resistance to both EFV and NVP. Finally, the high prevalence of the Y181 mutation estimated after two years of NVP is of some concern, as not only does it confer resistance to both EFV and NVP, but also to newer NNRTI drugs.

In Chapter 3, I developed the MARISA model, a mathematical model that reproduces both the general HIV-epidemic and the dynamic of NNRTI resistance in South Africa from 2005 to 2016. It showed that models whose resistance-related parameters were informed from general clinical data are able to provide reliable population-scale estimates on resistance. Indeed, the model captured the high level of NNRTI ADR and increasing level of NNRTI TDR observed from surveillance studies in South Africa. By running counterfactual scenarios, the model identified two main factors driving the emergence of NNRTI resistance in South Africa: the magnitude of the ART roll-out and the low switching rate to second-line regimen during first-line ART failure. Increasing access to ART, either by increasing the treatment rate or by an earlier implementation of the Treat-All strategy, reduces HIV-related mortality and new infections. However, such strategies also result in higher level of NNRTI TDR. An earlier switch to second-line would have reduced both levels of ADR and TDR. However, due to the rapid development of NNRTI resistance during ART failure and the low reversion rates of NNRTI resistance in untreated patients, it would have hardly prevented NNRTI resistance from emerging.

In Chapter 4, I extended the MARISA model to model the impact of the introduction of DTG on the level of NNRTI resistance. The impact of different strategies of DTG implementation were assessed, such as the use of DTG only as first-line or both as a first-line and switch regimen. Different proportions of DTG-eligible women were also considered in order to reflect the hesitancy of using DTG due to safety issues in pregnant women that were preliminary reported. The model shows that, while DTG can halt the increase of NNRTI resistance, none of the strategies implementing DTG are able to eliminate NNRTI resistance. However, we observed that the effect of DTG crucially depends on including both women and people currently on NNRTI-based ART among people to whom DTG should be prescribed. Rapidly transitioning patients currently receiving NNRTI, especially those with active viremia, also reduces the level of NNRTI resistance. By reducing the level of NNRTI TDR, a wide introduction of DTG will also decrease the future risk of NNRTI-failure among ART-naïve individuals. Nevertheless, we observe that none of the strategies is able to reduce the level of NNRTI TDR below 10%.

Finally, the Chapter 5 presented a publication to which I have contributed as a co-author, which discussed the role of mathematical models in synthesizing evidence on HIV drug resistance. It emphasized the importance of monitoring the implementation of DTG in

sub-Saharan Africa to forecast their effect on the development of HIV drug resistance. Mathematical models can help combine different levels of evidence in order to predict the emergence of HIV drug resistance in sub-Saharan Africa

6.2 Implications

6.2.1 Transitioning to DTG

The results shown in Chapter 2 have important implications regarding the transition of patients currently on NNRTI to DTG in South Africa. In its guidelines, the National Health Department recommends different DTG-switching strategies based on the viral load [27]. Suppressed individuals, defined as a viral load below 50 cells/ml here, should be immediately transitioned to DTG, given the informed consent of the patients. Individuals with active viremia should undergo a thorough assessment of the cause of the elevated VL, including adherence support and repeated VL test after three months. Patients with suppressed viral load at that time can transition to DTG, while the other continue adherence support for another three months. After this period, both suppressed and unsuppressed patients are recommended to switch to DTG. In this context, adherence support aims at reducing the proportion of individuals switching with elevated VL in order to limit the risk of subsequent DTG-failure and development of resistance.

As indicated in Chapter 2, between 43% and 55% of patients failing the recommended NNRTI-based first-line are resistant to the two NRTI backbones that accompany DTG. In fact, if we assume that adherence support will be consistently provided to all unsuppressed patients, this percentage might be even higher. Indeed, adherence support favours the suppression of patients whose failure is due to adherence issues uniquely, and not due to resistance. Therefore, while adherence support will reduce the number of individuals failing NNRTI-based regimens, it might increase the proportion of unsuppressed patients with NRTI resistance. To prevent this latter group of patients to start DTG-based regimen without any working NRTI drug, an optimized backbone regimen could be used instead of the recommended 3TC and TDF combination. For instance, guidelines recommend replacing TDF by ZDV to increase susceptibility to NRTI backbones. However, the higher NRTI-susceptibility provided by such strategy should be balanced with the higher toxicity of ZDV.

The low frequency of VL testing in practice also questions the feasibility of using optimized backbones. Optimizing NRTI backbones presupposes that every patient is tested for viral load before switching to DTG in order to identify the patients who need to change their NRTI backbones due to resistance. In view of the high proportion of patients currently on NNRTI-based regimens [185], it is questionable whether this condition can be fulfilled in practice. Therefore, some patients currently on NNRTI might be switched to DTG blindly, i.e. without viral load testing [157]. In this context, the strategy of optimizing NRTI backbones is questionable, as the patients who would benefit from it, i.e. the patients with unsuppressed VL, could not be identified anymore.

6.2.2 Bridging the gap between clinical and epidemiological data

Mathematical models are useful to predict the impact of public-health measures at the population-level as they aggregate evidence from different sources. However, the validity of such models is often questioned, as there are several differences between real-world settings and the clinical settings, in which these data are collected [72]. In addition, mathematical

models often make strong assumptions. In Chapter 3, I showed that the MARISA model captured the population dynamic of NNRTI drug resistance, as it leads to realistic estimates of the levels of ADR and TDR. This validates the approach of using clinical data to calibrate the resistance layer of the model.

In the context of the introduction of DTG in sub-Saharan Africa, similar models could be used to predict the potential risk of emergence of DTG resistance. Several clinical trials have assessed the risk of development of DTG resistance. However, as the implementation of DTG first-line regimen has just started, surveillance data on the risk of acquiring and transmitting DTG resistance are not yet available. In this context, an adapted version of the MARISA could bridge the gap between the large availability of epidemiological data and the limited clinical evidence regarding DTG resistance in order to model the introduction of DTG in real-world settings. This issue is discussed in more details in Section 6.4 of this chapter.

6.2.3 Emergence of resistance in the South African context

Identifying the drivers of NNRTI resistance is important in order to prevent the future emergence of resistance to newer drug classes, such as DTG. In Chapter 3, the long time on a failing NNRTI-based regimen has been identified as one of the drivers of NNRTI resistance. This long duration reflects the challenges that are associated with a rapid national-wide ART roll-out [186]. First, the frequency of viral load testing is often lower in practice than the frequency recommended in the guidelines, which delays the identification of virological failure [112, 187]. Second, the high cost of PI-based regimens has limited its access as a second-line regimen in South Africa and considerably prolonged the time from recognition of first-line failure to second-line switch [185, 188]. Moreover, to avoid switching patients whose treatment failure is uniquely due to low adherence, adherence counselling has also been proposed [27]. This led to prolonged time on failing regimens, increasing the risk of developing resistance and of transmitting it. As shown by the MARISA model, even a considerable increase of the switching rate to values that reflect the national recommendation would not have prevented NNRTI resistance from emerging. This suggests that in the South African context, where the access of first-line ART has quickly increased, no simple measure could have prevented the emergence of NNRTI resistance.

6.2.4 Control of the NNRTI resistance level with the introduction of DTG

While the emergence NNRTI resistance might have been difficult to prevent, the current implementation of DTG-based regimen offers the opportunity to control it. Halting the current increase in NNRTI resistance is essential to sustain high suppression level among people who will continue to rely on NNRTI despite the introduction of DTG. In its new consolidated guidelines, the South African Health Department recommends the use of NNRTI-based regimen for pregnant women up to six weeks of gestation or women wanting to conceive in the near future [27]. However, the ultimate decisions belongs to the patients, who will choose between NNRTI- and DTG-based regimen based on the risks and benefits of both options. In Chapter 4, different scenarios of DTG-introduction model the uncertainty on the proportion of women who will take DTG-regimen. In view of the many advantages of DTG, we can fairly assume that all men and women not at risk of pregnancy will follow the guidelines' recommendation, i.e. opting for DTG. In this perspective, the results suggest that NNRTI resistance could be stabilized somewhere around 20%, depending on the proportion of women opting for DTG among the ones who are at risk of pregnancy. Preventing the rise of

NNRTI resistance is important in order to leave a sustainable alternative to patients who will refuse DTG.

The fact that even the strategy where all men and women are started with or transitioned to DTG does not lead to the elimination of NNRTI resistance highlights its rather irreversible nature. As shown by its very slow reversion to wild-type, the low fitness cost of NNRTI resistance mutations allows them to persist for several years without drug selective pressure [31, 32].

6.3 Strengths and limitations

6.3.1 Strengths

The MARISA model collected evidence of different levels and from different sources in order to reproduce the mechanisms of drug resistance development and transmission at the scale of a country. It combined epidemiological cohort data about more than 30,000 HIV-infected individuals on ART, together with national HIV indicators and clinical data on HIV drug resistance. This approach was validated by comparing the levels of TDR and ADR estimated by the model with the ones observed in surveillance data. This approach offers perspective to model the population-scale emergence of resistance when it has only been clinically observed in a limited number of patients (e.g. DTG resistance).

The relative simplicity of the MARISA model can also be considered as a strength, as more complex models often force us to make unverifiable assumptions. I also tried to provide an exhaustive description of the different versions of the MARISA model and the assumptions that were involved in the supplementary material of the published papers (see "Annexes") for the sake of transparency. To ensure reproducibility of the adapted MARISA model (Chapter 4), the model code is publicly available (see <https://github.com/anthonyhauser>). Moreover, I arranged the model code in a flexible way, to make it able to integrate additional layers of complexity (e.g. resistance layers), without changing its structure.

Mathematical models often involve high levels of uncertainty, which should be transparently represented. Throughout my project, two different methods were used to capture and represent uncertainty in order to adapt to the complexity of the model. In Chapters 3 and 4, I ran sensitivity analyses to assess the impact of the uncertainty of several parameters on the model outcomes. The parameters that involve the most uncertainty, because they are difficult either to measure (e.g. parameters related to HIV transmission) or to predict (e.g. future efficacy of DTG in South Africa), were simultaneously varied.

One of the main strengths of Chapter 2 is that, rather than applying the standard meta-analysis approach, I developed a tailor-made hierarchical model to synthesize evidence from the collected studies. In view of the simplicity of the model, I was able to apply a Bayesian framework that propagates model uncertainty. In addition, the hierarchical structure of the model disentangled the two main levels of uncertainty that could not be identified with simpler models (i.e. the study-level heterogeneity and the mutation-specific heterogeneity).

6.3.2 Limitations

In Chapter 2, the quality of the data collected from the selected studies may have limited the precision of the results. Even after adjusting for drug use and ART duration, we observed

substantial heterogeneity between the studies, caused by their different characteristics, for which the model could not adjust. In addition, the fact that not all studies reported the occurrence of DRMs at an individual level forced me to run the meta-analysis with the study-aggregated data. The absence of individual data prevents the model to systematically estimate the correlations between the DRMs and to explore how the DRMs accumulate. Using data at the study-level rather than the individual level also limits the power of the model to detect any weak effect of an ART drug on the occurrence of a DRM. In this context, making individual data available for such studies would contribute to gain key information on the accumulation of HIV drug resistance.

Some processes that might influence the dynamic of HIV drug resistance were omitted by the MARISA model (Chapters 3 and 4), as not sufficient data were available to parametrize them. The MARISA model did not model the impact of PMTCT programme on NNRTI resistance. Nevertheless, as the PMTCT programs started in 2002 in South Africa, they do not have any impact on the transmission of NNRTI resistance among adults (i.e. aged ≥ 15) before 2017 [189]. I did not include either PrEP or PEP, as their use is not systematically reported in South Africa. The transmission of HIV is also simplified in the MARISA model. Only the sexual transmission of HIV is modelled and the model did not capture the age-disparate transmission of HIV, as suggested by [190]. The implication of such findings in terms of the transmission of HIV drug resistance is unclear, making the age-stratification of the model not imperative. Adherence, which plays a central role in the risk of acquisition of HIV drug resistance was not explicitly represented by the MARISA model, as it is not systematically reported in the cohort data from leDEA-SA. Nevertheless, as leDEA-SA data includes patients with different levels of adherence, the effect of adherence on the risk of failure is already implicitly represented. Finally, the majority of parameters related to HIV disease progression and HIV continuum of care were estimated using data from leDEA-SA cohorts. As for every longitudinal study, the attrition bias might compromise the accuracy of these estimates. In particular, leDEA data might underestimate the rate of treatment interruption, as a part of the patients stopping treatment are not monitored anymore. Treatment interruption was modelled in the first version of the MARISA model, while the adapted MARISA model only investigated its effect in an additional analysis.

The parsimonious representation of HIV resistance in the MARISA model might also be seen as an oversimplification. In Chapter 3, the original MARISA model only distinguished between NNRTI-susceptible and NNRTI-resistant individuals and did not model the impact of specific NNRTI resistance mutations. This is justified by the fact that only one mutation, the K103N mutation, confers high resistance to NNRTI [82]. The original MARISA model did not include the effect of NRTI resistance on NNRTI-based regimen. Even if NRTI resistance might reduce the activity of NNRTI-based regimen, its impact on the efficacy of such regimen is more uncertain than for NNRTI resistance, making it difficult to measure in practice. Moreover, as patients with NNRTI resistance often also harbour NRTI resistance, the effect of NRTI resistance is already partially included within the effect of NNRTI resistance.

6.4 Perspective

The roll-out of NNRTI-based regimen in South Africa has considerably reduced both HIV-mortality and HIV-infections, but at the same time, lead to an uncontrolled spread of NNRTI resistance. The implementation of DTG-based regimen, from 2020 in South Africa, bring new hopes to finding a new sustainable ART regimen. In view of the contrasted

experience of the NNRTI roll-out, we should nevertheless ask ourselves whether resistance to DTG could also emerge. In this chapter, I first give the current state of knowledge on the clinical characteristics of DTG, and describe how it differs from NNRTI. I then mention some characteristics regarding DTG that are expected to be different in real-world resource-limited settings than observed in clinical trials. I then enumerate the potential knowledge gaps about the potential emergence of DTG resistance and describe how mathematical can partly overcome this issue. Finally, I show how the experience of the NNRTI roll-out might help to explore the future risk of DTG resistance in South Africa.

6.4.1 Current state of knowledge

DTG is very effective at suppressing a treated patient's viral load quickly. The SINGLE study, a RCT that compared efficacy of DTG against EFV, both combined with two NRTI drugs, among ART-naïve patients from North America, Europe, and Australia, has shown higher efficacy in the DTG group [170]. The difference in viral suppression (VL<50 copies/mL) was the most striking during the first weeks of treatment initiation but tends to decrease after 48 weeks (81% for EFV vs 88% for DTG) and 144 weeks (63% vs 71%). We observed the same patterns in two RCTs done in Africa, the NAMSAL (Cameroon) and ADVANCE (South Africa) studies [149, 152], but with different overall suppression levels (69% for EFV vs 74.5% for DTG in NAMSAL, 79% vs 85% in ADVANCE at week 48, respectively). The lower suppression levels observed in the NAMSAL study might be partially explained by its broader eligibility criteria. Some clinical trials also assessed the DTG-efficacy among ART-experienced individuals, either suppressed or with virological failure. As expected, transitioning suppressed individuals to DTG-based regimen leads to very high suppression levels. However, several RCTs showed a considerably higher risk of failure when switching ART-experienced individuals with active replication (between 29% and 36% after 48 weeks) [102, 191, 192]. Failure rates were even higher when individuals had earlier exposure to InSTI, due to the presence of pre-existing InSTI cross-resistance that undermines the success of DTG (25%-59% of VF after 24 weeks) [191, 193].

DTG has a higher genetic barrier to developing drug resistance compared to NNRTI. Unlike NNRTI, where acquiring only one mutation already confers high-level resistance, a sequential acquisition of several InSTI-mutations is required to cause a substantial decrease in DTG-susceptibility. This was first suggested by findings from in-vitro experiments, indicating that, while DTG selects for some specific mutations (e.g. mutations at positions 138 and 263), these mutations alone only confer moderate resistance to DTG [191]. In-vivo studies testing individuals failing DTG-based regimen for genotypic resistance provided higher-level evidence on the potential development of resistance. While development of DTG resistance mutation is regularly reported among InSTI-experienced individuals, the presence of DTG resistance mutations among InSTI-naïve individuals failing DTG is much rarer [191]. These case reports are nevertheless helpful to identify the mutational pathways, through which DTG resistance develops. However, due to its limited number, the impact of such groups of mutations on the efficacy of DTG-based regimen is difficult to quantify.

DTG is well tolerated. Clinical trials reported fewer side effects in individuals using DTG compared to those using NNRTI [170]. This better tolerability was associated with lower discontinuation rates and might also lead to higher adherence, limiting the risk of developing resistance.

6.4.2 Difference between clinical and real-world settings

Clinical studies have shown that DTG has low failure rates when used as first-line or maintenance therapy. Even if failures were more common among unsuppressed ART-experienced individuals, the development of high resistance level to DTG was almost exclusively limited to individuals with previous exposure to INSTI, a drug class that was barely available in South Africa before the implementation of DTG. These clinical findings suggest that the risk of emergence of DTG resistance in South Africa is limited. However, some differences between the real-world resource-limited settings and settings, from which data are collected (i.e. from clinical trials or from cohorts in rich-resource settings) might increase this risk when implemented nationally.

First, adherence in the real-world settings might be lower than the one observed in clinical trials. The high adherence levels usually observed in RCTs are not representative to the overall treated population and are often a result of strict inclusion criteria and close follow-up. In consequence, RCTs might often underestimate the proportion of DTG-failures. For example, the NAMSAL study, which applied eligibility criteria that were wider and thus closer to real-world settings than the other RCTs, observed higher DTG-failure rate. Even if some differences in the study characteristics might also have driven the higher failure rate in NAMSAL, this suggests that the efficacy of DTG-based regimen when implemented at a national scale for all PLWH might be lower than previously observed in RCTs.

Second, the frequency of virological failure monitoring is lower in practice than in RCTs where patients receive a closer follow-up. The national guidelines currently recommend testing for viral load at ART initiation, after 6 months, 1 year and then every year. In practice, the frequency of viral load test is considerably lower [112]. This might prevent the rapid identification of DTG-failure and thus prolongs the time spent on a failing DTG-regimen, which favors the development of resistance.

Third, pre-existing NRTI resistance in patients switching from NNRTI to DTG might increase the risk of DTG-failure. In Chapter 2, the results from the meta-analysis suggested that, among failing individuals, half of them will switch to a functional DTG-monotherapy, in the case where NRTI backbones are not optimized. In this context, the failure rate among unsuppressed individuals switching to DTG might be higher than the ones found in RCTs (estimated at around 30% after 1 year), potentially driving the emergence of DTG resistance.

6.4.3 Knowledge gaps on DTG resistance

In the previous section, I enumerated several factors that could drive the emergence DTG resistance in practice. However, due to limited availability of data, it is unclear to what extent these factors will affect rates of DTG-failure and risk of developing DTG resistance.

Although the level of adherence in real-world settings is expected to be lower than observed in RCTs, ART adherence is difficult to measure in practice. Several devices have been developed to measure adherence among patients, but there is currently no gold-standard methods accurately measuring ART adherence [194]. Due to its high potency, DTG might have a higher "forgiveness" regarding lower adherence, allowing patients to regularly miss ART doses without undermining their chance of viral suppression. However, the relationship between DTG adherence level and the risk of failure is not well known. Our limited understanding on how real-world level of adherence might affect the development of DTG resistance is a major obstacle to determining the risk of DTG resistance emergence in South Africa.

DTG-failures in RCTs have been observed in a limited number of patients and only a few of them have developed resistance to DTG [191]. This restricts our ability to identify the different DTG resistance mutations and to precisely estimate the rate at which they develop, as well as the pathways along which they accumulate. Similar limitations applies for estimating the impact of the DTG resistance mutations on the efficacy of DTG-based regimen, as this requires information on a high number of patients. Therefore, in-vitro studies are often used in order to estimate these values, but the validity of such approaches is sometimes questionable. Finally, information on the transmission of DTG resistance is scarce [195].

Some uncertainty also subsists about the actual impact of pre-existing NRTI resistance on the efficacy of DTG-based regimen. In the case where NRTI resistance would annihilate any activity of the NRTI drugs, the efficacy of DTG in patients with two compromised NRTIs would be similar to the efficacy of a DTG-monotherapy. As indicated by Wandeler and colleagues who compared the efficacy of transitioning suppressed individuals to DTG with and without NRTI, the absence of any NRTI drug activity substantially increases the risk of failure (8.9% in DTG-monotherapy vs 0.7% in DTG combined with a working NRTI after 48 weeks) [103]. However, accumulating evidence shows that the presence of NRTI resistance may only have a limited impact on the risk of failure, suggesting a residual activity of the NRTI backbones even in case of resistance. The EARNEST study found that even high level of NRTI resistance did not impair virological response to PI-based second-line ART [104]. An observational study from European HIV cohorts also found similar failure rates in suppressed individuals switching to DTG, whether or not they harbored the M184 mutation [196]. However, I did not find an observational study that investigated the effect of NRTI resistance on the efficacy of a DTG-based regimen, in patients who switch after virological failure. More clinical evidence is therefore needed to assess the long-term efficacy of DTG alongside a compromised NRTI backbone [197].

6.4.4 The role of mathematical models

The scarcity of observational data on DTG resistance in resource-limited settings limits our current understanding of the risk of DTG resistance in South Africa. The implication of findings from clinical trials and from cohorts in resource-rich settings should be interpreted with caution due to the afore-mentioned differences with resource-limited settings. In this context, mathematical models offer the opportunity to bridge these knowledge gaps by integrating evidence of different levels. Specifically, in order to model the risk of DTG resistance in South Africa, we would need to inform the model about the following parameters: the overall DTG-efficacy, the rates at which DTG resistance develops, the reversion rate of DTG resistance (i.e. the time before resistant strains revert to wild-type in the absence of drug selective pressure) and the impact of DTG resistance on the efficacy of DTG-based regimens. The model could be developed in a similar way as in Chapter 3, with a DTG resistance dimension primarily informed by clinical studies. However, the current scarcity of data on DTG resistance would require making more assumptions, especially on how findings from clinical studies (e.g. RCTs and in-vitro studies) translate into real-world parameters. In this context, looking at the past NNRTI experience in South Africa is insightful, as it allows to assess whether prior clinical evidence could predict the spread of HIV drug resistance at a population level.

6.4.5 Comparison between DTG and NNRTI roll-outs

At the time of NNRTI roll-out in South Africa (from 2004), estimates on the efficacy of NNRTI-based regimen were available from several randomized trials that either compared

NNRTI with PI or compared different combinations of NNRTI and NRTI drugs [198–201]. These early studies already showed high levels of failure, with 20% - 50% of patients having a VL above 50 copies/ml after 48 weeks, depending on the drug combination. The efficacy of NNRTI was nevertheless comparable, if not superior, to the unboosted PI drugs that were available at that time [198]. However, the low barrier to resistance of NNRTI, compared with PI drugs, was already widely acknowledged, as well as the fact that resistance developed quickly after failure [202]. A randomized trial estimated that half of the patients with VL > 400 copies/ml after 48 weeks had NNRTI resistance [201]. Higher incidence of adverse events were also found in patients treated with NNRTI, leading to treatment discontinuation [203]. In this context, some studies also shared concerns about the particular risk of developing NNRTI resistance when adherence is low or treatment is discontinued. The higher half-lives of NNRTI, compared with NRTI, estimated from in-vivo studies [36], warned about the risk of prolonged NNRTI-monotherapy, potentially leading to NNRTI resistance, in case of ART discontinuation or poor adherence. Finally, several events of transmission of NNRTI resistance were also documented [204].

Therefore, at the time of NNRTI roll-out in South Africa, there were already clear indications of potential risk of developing and transmitting NNRTI resistance. These early findings highlighted the need of creating proper health care infrastructure to monitor treatment response and develop strategies to control the spread of NNRTI resistance. As setting up such infrastructure in South Africa would have taken years, some proposed to postpone the roll-out of NNRTI-based regimens [205–207]. However, withholding the NNRTI drug class during this period would have been highly unethical, as South Africa faced at that time an urgent need to supply ART in order to reduce HIV mortality [208]. In this context, South Africa decided to implement NNRTI roll-out, despite clear risks of emergence of NNRTI resistance and in the absence of a clear strategy and of infrastructures to control it.

In Section 6.4.2, I enumerated some differences between clinical and real-world settings that could make the emergence of drug resistance more likely in practice than observed in clinical trials. In the case of NNRTI, clinical findings showing high failure rates and a low resistance barrier already provided some strong indications that the emergence of NNRTI resistance in the South African context would occur. The situation is different for the roll-out of DTG-based regimens. On the one hand, clinical trials and cohort studies from resource-rich settings found high suppression rates and rare cases of acquisition of DTG resistance. In terms of infrastructure, South Africa is also better prepared, which is essential to ensure sustained monitoring of treatment failure. National guidelines have also integrated adherence support of patients, which should limit the risk of developing DTG resistance.

On the other hand, a particular feature of the implementation of DTG, compared with NNRTI, could drive the emergence of DTG resistance. Unlike the roll-out of NNRTI, where the overwhelming majority of patients were ART-naïve, a substantial fraction of people will start DTG with previous ART exposure and therefore, with pre-existing NRTI resistance. This mainly concerns patients failing first-line NNRTI-based regimen, as almost half of them will switch to DTG with heavily compromised NRTI backbones. While pre-existing NRTI resistance might affect the efficacy of DTG, it is currently difficult to predict its actual impact due to the scarcity of data. This nevertheless suggests that emergence, if it occurs, might be driven by individuals switching to DTG with unsuppressed VL. Close monitoring of this specific group of patients is thus key to control the potential emergence of DTG resistance.

Long duration on a failing regimen can drive the emergence of resistance, jeopardizing its long-term efficacy. This was shown for NNRTI in Chapter 3, but the same conclusions could

also apply to DTG resistance. Quite paradoxically, a too rapid switch from DTG-regimen could also threaten the sustainability of DTG-regimen, as it limits the spectrum of ART alternative for these patients. Most patients failing DTG-regimen will probably do so because of poor adherence rather than resistance. Therefore, a direct switch to PI-based regimen may be a waste of resource for all the individuals switching without DTG resistance. In this context, the focus should rather be on promoting adherence among these patients. Not only will adherence support limit the development of resistance, but it will also avoid unnecessary switch. As suggested by Maartens and colleagues [209], resistance testing, if it becomes more affordable, could also be implemented to identify the patients that are failing DTG-regimen because of resistance.

6.5 Conclusion

In this thesis, I use mathematical modelling to capture the emergence of NNRTI resistance in South Africa. I identify some factors that have driven the development of NNRTI resistance, such as the long time spent on a failing regimen. Due to its flexibility, the MARISA model is adapted to investigate future strategies, such as the impact of the DTG-introduction on the levels of NNRTI resistance. This shows that processes such as the acquisition and the spread of HIV drug resistance can be reproduced at the population-level using mathematical models calibrated with clinical resistance data. As South Africa is currently introducing DTG-based regimen, such modelling approach can be implemented to investigate the future risk of emergence of DTG resistance. However, even if mathematical models could help to bridge the gaps between clinical and real-world resource-limited settings, more real-world data is needed to understand the actual risk of DTG resistance development in the context of a countrywide implementation of DTG. The meta-analysis in Chapter 2 adds to the body of evidence, as it highlights the potential threat on the long-term efficacy of DTG posed by the switch of patients with elevated viral load. Close follow-up and resistance monitoring of these patients is therefore key to ensure an early detection of DTG resistance and prevent it from spreading through the population.

Chapter 7

Additional work

Chapter 7.1 is a publication that was not initially planned to be part of my PhD project. The sudden and unexpected SARS-CoV-2 outbreak offered unique opportunities to exploit the ability of mathematical to synthesize evidence when data are scarcely available. At the early stage of the SARS-CoV-2 epidemic, there was high uncertainty on the mortality associated with SARS-CoV-2 and the case fatality rate - the number of deaths divided by the number of reported cases - was often reported. However, this indicator has two important biases: 1) it only counts reported infections, and 2) it does not take into account the deaths that will occur afterwards. The aim of the project was thus to develop an age-stratified compartmental model to provide age-specific mortality estimates corrected for these two biases.

Chapter 7.1

Estimation of SARS-CoV-2 mortality during the early stages of an epidemic: a modeling study in Hubei, China, and six regions in Europe

Anthony Hauser¹
Michel J. Counotte¹
Charles C. Margossian²
Garyfallos Konstantinoudis³
Nicola Low¹
Christian L. Althaus¹
Julien Riou^{1,4}

¹ Institute of Social and Preventive Medicine, University of Bern, Bern, Switzerland

² Department of Statistics, Columbia University, New York, NY

³ MRC Centre for Environment and Health, Department of Epidemiology and Biostatistics, School of Public Health, Imperial College London, London, UK

⁴ Division of infectious diseases, Federal Office of Public Health, Bern, Switzerland

This article is published in ***PLOS Medicine***: Estimation of SARS-CoV-2 mortality during the early stages of an epidemic: A modeling study in Hubei, China, and six regions in Europe. (2020)
DOI: [10.1371/journal.pmed.1003189](https://doi.org/10.1371/journal.pmed.1003189).

Contribution: I contributed to the study design and, together with Julien Riou, we performed the analysis, made the figures and wrote the first draft of the manuscript and integrated co-authors' comments.

7.1.1 Abstract

Background. As of 16 May 2020, more than 4.5 million cases and more than 300,000 deaths from disease caused by severe acute respiratory syndrome coronavirus 2 (SARS-CoV-2) have been reported. Reliable estimates of mortality from SARS-CoV-2 infection are essential to understand clinical prognosis, plan health care capacity and for epidemic forecasting. The case fatality ratio (CFR), calculated from total numbers of reported cases and reported deaths, is the most commonly reported metric, but can be a misleading measure of overall mortality. The objectives of this study were to: 1) simulate the transmission dynamics of SARS-CoV-2 using publicly available surveillance data; 2) infer estimates of SARS-CoV-2 mortality adjusted for biases and examine the CFR, the symptomatic case fatality ratio (sCFR) and the infection fatality ratio (IFR) in different geographic locations.

Method and Findings. We developed an age-stratified susceptible-exposed-infected-removed (SEIR) compartmental model describing the dynamics of transmission and mortality during the SARS-CoV-2 epidemic. Our model accounts for two biases: preferential ascertainment of severe cases and right-censoring of mortality. We fitted the transmission model to surveillance data from Hubei province, China and applied the same model to six regions in Europe: Austria, Bavaria (Germany), Baden-Württemberg (Germany), Lombardy (Italy), Spain and Switzerland. In Hubei, the baseline estimates were: CFR 2.4% (95% credible interval [CrI]: 2.1-2.8%), sCFR 3.7% (3.2-4.2%) and IFR 2.9% (2.4-3.5%). Estimated measures of mortality changed over time. Across the six locations in Europe estimates of CFR varied widely. Estimates of sCFR and IFR, adjusted for bias, were more similar to each other but still showed some degree of heterogeneity. Estimates of IFR ranged from 0.5% (95% CrI 0.4-0.6%) in Switzerland to 1.4% (1.1-1.6%) in Lombardy, Italy. In all locations, mortality increased with age. Among 80+ year olds, estimates of the IFR suggest that the proportion of all those infected with SARS-CoV-2 who will die ranges from 20% (95% CrI: 16-26%) in Switzerland to 34% (95% CrI: 28-40%) in Spain. A limitation of the model is that count data by date of onset are required and these are not available in all countries.

Conclusions. We propose a comprehensive solution to the estimation of SARS-Cov-2 mortality from surveillance data during outbreaks. The CFR is not a good predictor of overall mortality from SARS-CoV-2 and should not be used for evaluation of policy or comparison across settings. Geographic differences in IFR suggest that a single IFR should not be applied to all settings to estimate the total size of the SARS-CoV-2 epidemic in different countries. The sCFR and IFR, adjusted for right-censoring and preferential ascertainment of severe cases, are measures that can be used to improve and monitor clinical and public health strategies to reduce the deaths from SARS-CoV-2 infection.

7.1.2 Author summary

Why was this study done?

- Reliable estimates of measures of mortality from severe acute respiratory syndrome coronavirus 2 (SARS-CoV-2) infection are needed to understand clinical prognosis, plan health care capacity and for epidemic forecasting.
- The case fatality ratio (CFR), the number of reported deaths divided by the number of reported cases at a specific time point, is the most commonly used metric, but is a biased measure of mortality from SARS-CoV-2 infection.

- The symptomatic case fatality ratio (sCFR) and overall infection fatality ratio (IFR) are alternative measures of mortality with clinical and public health relevance, which should be investigated further in different geographic locations.

What did the researchers do and find?

- We developed a mathematical model that describes infection transmission and death during a SARS-CoV-2 epidemic. The model takes into account the delay between infection and death and preferential ascertainment of disease in people with severe symptoms, both of which affect the assessment of mortality.
- We applied the model to data from Hubei province in China, which was the first place affected by SARS-CoV-2, and to six locations in Europe: Austria, Bavaria (Germany), Baden-Württemberg (Germany), Lombardy (Italy), Spain and Switzerland, to estimate the CFR, the sCFR and the IFR.
- Estimates of sCFR and IFR, adjusted for bias, were similar to each other and varied less geographically than the CFR. IFR was lowest in Switzerland (0.5%) and highest in Hubei province (2.9%). The IFR increased with age; among 80+ year olds, estimates ranged from 20% in Switzerland to 34% in Spain.

What do these findings mean?

- The CFR does not predict overall mortality from SARS-CoV-2 infection well and should not be used for the evaluation of policy or for making comparisons between geographic locations.
- There are geographic differences in the IFR of SARS-CoV-2, which could result from differences in factors including emergency preparedness and response, and health service capacity.
- SARS-CoV-2 infection results in substantial mortality. Further studies should investigate ways to reduce death from SARS-CoV-2 in older people and to understand the causes of the differences between countries.

7.1.3 Introduction

The pandemic of severe acute respiratory syndrome coronavirus 2 (SARS-CoV-2) infection has resulted in more than 4.5 million confirmed cases and more than 300,000 deaths from coronavirus disease 2019 (COVID-19), as of 16 May, 2020 [210]. The infection emerged in late 2019 as a cluster of cases of pneumonia of unknown origin in Wuhan, Hubei province [211, 212]. China had reported 84,038 cases and 4,637 deaths by 16 May, 2020, with no new deaths since early April. The largest outbreaks are now in the United States of America and Western Europe. The transmission characteristics of SARS-CoV-2 appear to be similar to those of the 1918 pandemic influenza strain [213], but, at this early stage of the pandemic, the full spectrum and distribution of disease severity and of mortality are uncertain. Reliable estimates of measures of mortality are needed to understand clinical prognosis, plan health care capacity and for epidemic forecasting.

The case fatality ratio (CFR), the number of reported deaths divided by the number of reported cases at a specific time point, is the most commonly used metric because most countries

collect this information [211, 214]. However, the CFR can be misleading if used to assess the overall risk of death from an infection because of two opposing biases [215, 216]. First, because of the delay of several weeks between symptom onset and death, the number of confirmed and reported deaths at a certain time point does not consider the total number of deaths that will occur among already infected individuals (right-censoring). Second, surveillance-based case reports underestimate the total number of SARS-CoV-2-infected patients, because testing focuses on individuals with symptoms of COVID-19 and, among symptomatic cases, on patients with more severe manifestations (preferential ascertainment). In addition, the World Health Organization does not distinguish between SARS-CoV-2 infection and COVID-19 and defines a confirmed case as a person with laboratory confirmation of infection, irrespective of signs and symptoms. The number of cases detected and reported therefore depends on the extent and strategy of testing for SARS-CoV-2, especially amongst people without severe symptoms. Precisely defined measures could be more useful for describing SARS-CoV-2 mortality than the CFR [215]. The symptomatic case fatality ratio (sCFR) is the proportion of infected individuals showing symptoms who die over the course of their SARS-CoV-2 infection and is clinically relevant to assessment of prognosis and healthcare requirements. The infection fatality ratio (IFR) is the proportion of all people with SARS-CoV-2 infection who will eventually die from the disease, and is a central indicator for public health evaluation of the overall impact of an epidemic in a given population.

Estimates of the sCFR and IFR can be obtained from prospective longitudinal studies of representative samples of individuals with SARS-CoV-2 infection but such studies cannot provide the information needed for clinical and public health decision-making in real time. The objectives of this study were to: 1) simulate the dynamics of transmission and mortality of SARS-CoV-2 using publicly available surveillance data; and 2) provide overall and age-stratified estimates of sCFR and IFR for SARS-CoV-2, adjusted for right-censoring and preferential ascertainment, in different geographic locations.

7.1.4 Methods

We developed an age-stratified susceptible-exposed-infected-removed (SEIR) compartmental model that describes the dynamics of SARS-CoV-2 transmission and mortality. We fitted the model to surveillance data from Hubei province (China) and six geographic locations in Europe: Austria, Bavaria (Germany), Baden-Württemberg (Germany), Lombardy (Italy), Spain and Switzerland. There is no written prospective protocol for the study. The analysis has been developed specifically for the research question, and adapted in response to peer review comments. Main changes include assuming pre- and asymptomatic transmissions and running additional sensitivity analyses. In the revised version, the analysis also includes additional regions, for which data had been made available. All code including the different versions of the model and manuscript are available from https://github.com/jriou/covid_adjusted_cfr. This study is reported as per the TRIPOD guideline (S2 Text).

7.1.4.1 Setting and data, Hubei province, China

The first known case of SARS-CoV-2 infection was traced back to December 1st, 2019 in Wuhan, the main city of Hubei province, China [212]. The first reported death was on 11 January 2020. Human-to-human transmission of SARS-CoV-2 led to exponential growth of the reported incidence of cases (Fig 7.1.1A). On 20 January 2020, Chinese authorities

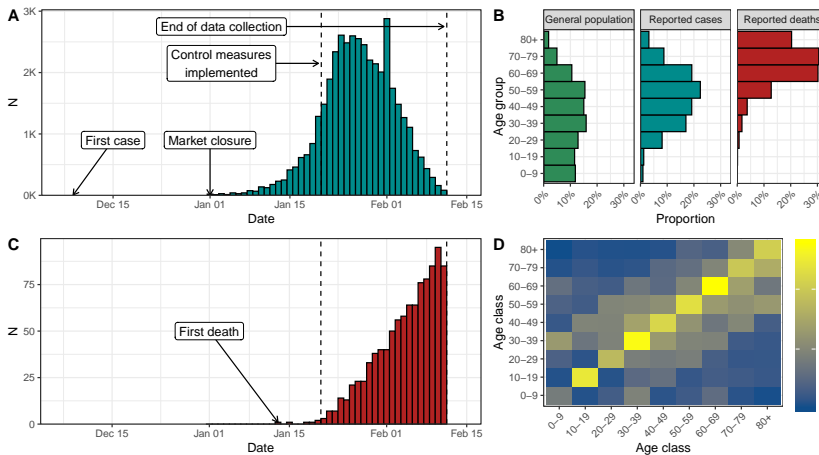


Fig 7.1.1: (A) Reported number of confirmed cases of SARS-CoV-2 infection by date of symptom onset in Hubei, China until 11 February 2020. (B) Age distribution of the Chinese population and of the reported cases and deaths in Hubei, China. (C) Reported number of deaths associated with SARS-CoV-2 infection in Hubei, China until 11 February 2020. (D) Age-specific contact matrix from a 2018 survey conducted in Shanghai, China [218] applied to Hubei province.

implemented extensive control measures in Hubei: early identification and isolation of clinical cases, tracing and quarantining of contacts, temperature checks before accessing public areas, extension of the lunar new year holiday period, and extreme social distancing, including cancellation of mass gatherings [217]. Three days later, a cordon sanitaire was imposed, with strict traffic restrictions. From 27 January, the daily incidence of cases, by date of symptom onset, started to plateau, then decreased.

The Chinese Center for Disease Control and Prevention (China CDC) reported the number of cases by date of symptom onset, and the age distribution of cases and deaths up 11 February 2020 in China (Fig 7.1.1B) [219]. We extracted these data, together with the age distribution of the Chinese population. Deaths counts were obtained from a repository aggregating data from Chinese public data sources [220]. We used data about the daily number of potentially infectious contacts by age group in Shanghai [218]. We assumed that all data sources were applicable to the population of Hubei. As of 11 February, after which information about date of symptom onset was no longer available, there were 41,092 cases and 979 deaths, resulting in a CFR of 2.4%.

7.1.4.2 Setting and data, six geographic locations in Europe

The first cases of SARS-CoV-2 infection in Europe were reported at the end of January 2020. Italy was the first country with a large epidemic, after a cluster of cases, followed shortly by the first deaths, emerged in Lombardy at the end of February. As of 16 May 2020, Europe is the continent having reported the highest number of cases and deaths (more than 1,800,000 confirmed cases and 160,000 deaths) [210].

We selected European countries that reported the daily number of cases of confirmed SARS-CoV-2 infection by date of symptoms onset. In countries where this information was available at a regional level, we selected worst-affected regions. We extracted data about

the number of confirmed cases by symptom onset, the daily number of deaths, and the distribution of cases and deaths across age groups for each of six locations: Austria, Bavaria (Germany), Baden-Württemberg (Germany), Lombardy (Italy), Spain and Switzerland.

For Austria, we obtained all required data from published reports from 11 March to 14 April [221]. On 14 April, there were 14,151 reported cases and 399 deaths (CFR 2.8%). For Germany, we used published data from 3 March to 16 April [222]. Age distributions, available at the country level only, were applied to both regions. On 16 April, there were 31,196 cases (62% with date of onset) and 802 deaths in Baden-Württemberg (CFR 2.6%) and 36,538 cases (56% with date of onset) and 1,049 deaths in Bavaria (CFR 2.9%). For Lombardy, we collected published data from 11 February to 25 April [223, 224]. Age distributions at the national level were applied to Lombardy. On 25 April, there were 74,346 cases (77% with date of onset) and 13,263 deaths (CFR 17.8%). For Spain, we used published data from 2 March to 16 April [225]. On 16 April, 178,031 cases (79% with date of onset) and 19,478 deaths were reported (CFR 10.9%). For Switzerland, we used individual-level data from 2 March to 23 April aggregated by day of onset or day of death [226]. On 23 April, there were 33,228 cases (11% with date of onset) and 1,302 deaths (CFR 3.9%). Further details about the data are available in S1 Text, section 1.

7.1.4.3 Age-structured model of SARS-CoV-2 transmission and mortality

We used an age-stratified susceptible-exposed-infected-removed (SEIR) compartmental model that distinguished between incubating, pre-symptomatic, asymptomatic and symptomatic infections. We stratified the population into nine 10-year groups (0-9 up to 80+ years) for all locations except Austria where the age groups were 0-4, 5-14, up to 75+ years. We assumed that susceptibility to SARS-CoV-2 and the risk of acquisition per contact is identical for each age group and that transmission is possible during pre-symptomatic and asymptomatic infections. We used age-specific contact matrices to model contact patterns according to age group (contact matrix derived by Zhang et al. for Hubei [218], and the POLYMOD contact matrix for the six European locations [227]). We modelled the decrease in SARS-CoV-2 transmission due to control measures using a logistic function for the transmission rate.

In the model, after an average incubation period of 5.0 days [228], 81% (95%CrI: 71-89) of infected people develop symptoms of any severity and the rest remain asymptomatic [229, 230]. The estimated proportion of symptomatic infections was derived from outbreak investigations included in a systematic review and is implemented as a beta distribution to propagate uncertainty. Studies that have estimated the proportion of asymptomatics have not provided conclusive evidence of an age trend, so we assumed it to be constant [231]. We assumed reduced infectiousness during the period of 2.3 days preceding symptom onset (pre-symptomatic compartment) and also among asymptomatic individuals [228].

The model was used to compute the number of symptomatic SARS-CoV-2 infections by day of symptom onset in each age group. We applied an age-specific ascertainment proportion to the number of symptomatic infections to estimate the number of reported cases of SARS-CoV-2 infections by date of symptom onset. To identify the parameters, we assumed that 100% of infections in the oldest age group (80+ years old, 75+ years old in Austria) were reported. We assumed that mortality only occurred in symptomatic people, and that the time from symptom onset to death followed a log-normal distribution with mean 20.2 days and standard deviation 11.6 [232]. This allowed us to account for the deaths occurring after

the date of data collection.

Separately for Hubei and the six European locations, we simultaneously fitted our model to the data sets described above (Fig 7.1.1): (1) the number of confirmed cases by day of symptom onset, (2) the number of deaths by day of occurrence, (3) the age distribution of all confirmed cases and (4) the age distribution of all reported deaths. We assumed a negative binomial distribution for data (1) and (2), and a multinomial distribution for data (3) and (4). All parameters were estimated from data except for the incubation period, the generation time, the contribution of presymptomatics to transmission, the presymptomatic duration, and the time from symptom onset to death.

The fitted model was used to produce estimates (median posterior distributions with 95% credible intervals, CrI) of the total number of symptomatic and pre-/a-symptomatic infections (adjusted for preferential ascertainment) and of the total number of deaths (adjusted for right-censoring). These were then transformed into adjusted estimates of sCFR and IFR. Besides parameter values and model structure, these estimates rely on the following additional assumptions:

1. The severity of symptoms differs by age group and influences the probability of reporting;
2. All deaths due to SARS-CoV-2 infection have been identified and reported;
3. The susceptibility to SARS-CoV-2 infection is identical across age groups;
4. The average standard of care is stable for the period of interest and the next two months, during which a proportion of the infected people will eventually die;
5. The ascertainment probability by age is constant over the periods considered.

Further details about the method are available in S1 Text, section 2.

7.1.4.4 Sensitivity analysis

From 12 February 2020, the Chinese authorities changed their criteria for reporting cases, increasing the total by more than 25,000. Reported numbers of deaths increased on 16 April, when Wuhan city reported an additional 1,290 deaths. We ran a sensitivity analysis with corrected numbers of cases and deaths in Hubei province. We also examined the impact of assuming a 50% lower susceptibility in 0-19 years old, and of a lower ascertainment among 80+ year olds (from 90% to 10%, compared with a fixed proportion of 100% in the main analysis). We also re-fitted the model at different dates of data collection (every 5 days from 12 January to 11 February) to examine the effect of the accumulation of data over time. Additional sensitivity analyses are presented in S1 Text, section 6.

We implemented the model in a Bayesian framework using Stan [233]. All code and data are available from https://github.com/jriou/covid_adjusted_cfr.

7.1.5 Results

Our model accurately describes the dynamics of transmission and mortality by age group during the SARS-CoV-2 epidemic in Hubei from 1 January to 11 February 2020 (Fig 7.1.2). The

model predicts that control measures implemented from 20 January reduced SARS-CoV-2 transmissibility by 92% (95%CrI: 87-100), with a steep diminution in case incidence 4.3 (95%CrI: 3.2-5.4) days after 20 January. Assuming 100% of cases aged 80 and older were initially reported, we estimate that a total of 83,300 individuals (95%CrI: 73,000-98,600) were infected in Hubei between 1 January and 11 February 2020. Of these, the number of symptomatic cases is estimated at 67,000 (95%CrI: 60,500-73,600), 1.6 times (95%CrI: 1.5-1.8) more than the 41,092 reported cases during that period. Accounting for the later correction in the number of reported cases, the total number of infections increases to 138,000 (95%CrI: 120,000-162,000). The proportion of ascertained cases by age group increased from less than 9% (95%CrI: 8-10) under 20 years old to 93% (95%CrI: 88-98) in the age group 70-79 (the ascertainment proportion was assumed to be 100% in the age group 80+, Fig 7.1.3A).

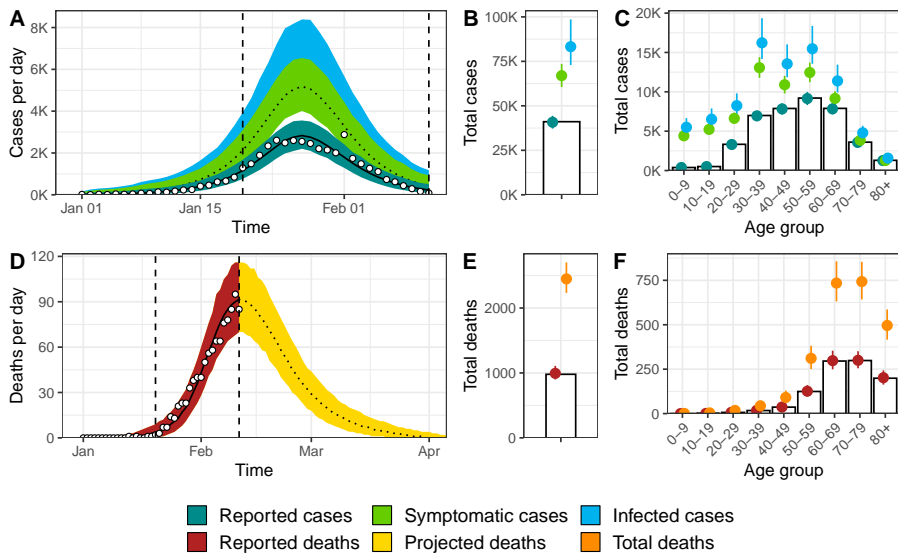


Fig 7.1.2: Model fit for Hubei, China of (A) incident cases of SARS-CoV-2 infection by date of symptom onset, (B) total cases, (C) age distribution of cases, (D) incidence of deaths, (E) total number of deaths among individuals infected until 11 February 2020 and (F) age distribution of deaths. White circles and bars represent data. Lines and shaded areas or points and ranges show the posterior median and 95% credible intervals for six types of model output: reported cases, symptomatic cases, overall cases (i.e. symptomatic and asymptomatic cases), reported deaths until 11 February 2020, projected deaths after 11 February 2020 and overall deaths.

The model predicts a total of 2,450 deaths (95%CrI: 2,230-2,700) among all people infected until 11 February in Hubei (compared with 979 deaths at this point without adjusting for right-censoring). This results in an estimated IFR of 2.9% (95%CrI: 2.4-3.5, Table 7.1.1). Assuming the later correction of deaths was evenly distributed by date of symptom onset and age group, the total number of deaths increases to 3,430 (95%CrI: 3,120-3,760). When using the corrected numbers of cases and deaths, we derived an IFR of 2.5% (95%CrI: 2.1-2.9).

The estimated sCFR, more relevant to the clinical setting, was 3.7% (95%CrI: 3.2-4.2) in the baseline analysis and 3.1% (95%CrI: 2.7-3.6) after correction of the increase number of reported cases and deaths. The estimated sCFR increased with age (S1 Text, section 5): under 20 years of age, below 1 in 1,000; 20-49 years, between 3 and 8 per 1,000; 50-59 years, 2.5%

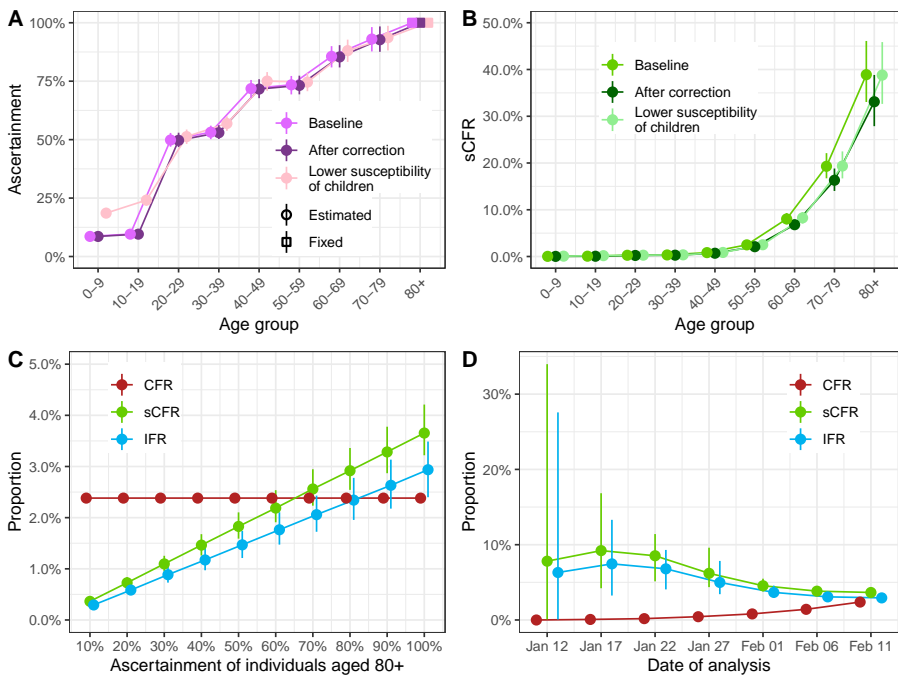


Fig 7.1.3: (A) Estimated proportion of cases ascertained by age group in Hubei, China (baseline, after the later correction of the number of reported cases and deaths, and assuming 50% lower susceptibility of children aged 0-19). (B) Estimated case symptomatic fatality ratio by age group in Hubei, China. (C) Impact of varying the fixed proportion of cases ascertained among individuals aged 80 and older from 10% to 100% on the mortality estimates. (D) Mortality estimates at different dates of reporting (every 5 days from January 12 to February 11).

(95%CrI: 2.0-3.0); 60-69 years, 8.0% (95%CrI: 6.9-9.3); 70-79 years, 19.3% (95%CrI: 16.7-22.1); 80 years and older, 39.0% (95%CrI: 33.1-46.1).

In sensitivity analyses, the correction of the number of reported cases (+65%) and deaths (+40%) by the local authorities in Hubei did not influence the ascertainment proportion (Fig 7.1.3A) but led to a proportional decrease of the sCFR and IFR estimates by 15%, as expected from the correction applied ($1.40/1.65 = 0.85$, Fig 7.1.3B and Table 7.1.1). Second, lowering the susceptibility of individuals aged 0-19 years by 50% did not affect the ascertainment proportion or the sCFR in other age groups (Fig 7.1.3A and B). The decrease in the denominator led to a proportional increase of total sCFR and IFR. Third, relaxing the assumption of complete reporting of cases among individuals aged 80 years and older resulted in a proportional decrease of the sCFR and IFR (Fig 7.1.3C). Fourth, patterns in the observed mortality changed as the epidemic progressed (Fig 7.1.3D). The CFR increased as delayed deaths were reported. The sensitivity analysis suggests that our proposed approach overestimates the sCFR and IFR when applied before the peak of incidence (around 27 January) and stabilizes afterwards. Additional sensitivity analyses examining how the contribution of pre-symptomatic transmission, the susceptibility of children and several other choices in model structure and parameter values did not impact the results (S1 Text, section 6).

Table 7.1.1: Model estimates of total infections of SARS-CoV-2 infection, attack rate, total deaths, case fatality ratio (CFR), symptomatic case fatality ratio (sCFR) and infection fatality ratio (IFR) by location until the limit date.

| Location (limit date) | Estimated total infections | Estimated attack rate | Estimated total deaths | CFR | sCFR | IFR |
|--|------------------------------------|-----------------------|------------------------|-------|----------------|----------------|
| Hubei, China (11 February) | | | | | | |
| <i>Baseline</i> | 83,300 (73,000-98,600) | 0.1% (0.1-0.2) | 2,450 (2,230-2,700) | 2.4% | 3.7% (3.2-4.2) | 2.9% (2.4-3.5) |
| <i>After correction</i> | 138,000 (120,000-162,000) | 0.2% (0.2-0.3) | 3,430 (3,120-3,760) | 2.0% | 3.1% (2.7-3.5) | 2.5% (2.1-2.9) |
| <i>With lower susceptibility of children</i> | 74,100 (63,600-86,700) | 0.1% (0.1-0.1) | 2,440 (2,230-2,710) | 2.4% | 4.1% (3.6-4.7) | 3.3% (2.7-4.0) |
| Austria (14 April) | 69,100 (56,500-82,700) | 0.8% (0.6-0.9) | 731 (623-867) | 2.8% | 1.3% (1.1-1.6) | 1.1% (0.8-1.3) |
| Baden-Württemberg, Germany (16 April) | 212,000 (188,000-247,000) | 1.9% (1.7-2.2) | 1,580 (1,060-2,710) | 2.6% | 0.9% (0.6-1.6) | 0.7% (0.5-1.3) |
| Bavaria, Germany (16 April) | 257,000 (228,000-296,000) | 2.0% (1.7-2.3) | 1,940 (1,420-2,720) | 2.9% | 0.9% (0.7-1.3) | 0.8% (0.5-1.1) |
| Lombardy, Italy (25 April) | 1,150,000 (1,010,000-1,350,000) | 11.5% (10.1-13.4) | 15,700 (13,900-17,600) | 17.8% | 1.7% (1.5-2.0) | 1.4% (1.1-1.6) |
| Spain (16 April) | 2,650,000 (2,360,000-3,090,000) | 5.7% (5.0-6.6) | 27,800 (25,400-30,500) | 10.9% | 1.3% (1.2-1.5) | 1.0% (0.9-1.2) |
| Switzerland (23 April) | 308,000 (248,000-383,000) | 3.6% (2.9-4.5) | 1,520 (1,380-1,690) | 3.9% | 0.6% (0.5-0.8) | 0.5% (0.4-0.6) |

We applied the same model to data from six European locations with all required data: Austria, Germany (Baden-Württemberg and Bavaria), Italy (Lombardy), Spain and Switzerland. The model fit was satisfactory in all cases (S1 Text, section 3). CFR estimates differed widely between countries, while sCFR and IFR estimates were more similar to each other (Table 7.1.1 and Fig 7.1.4A). Across countries, model estimates of IFR ranged from 0.5% (95%CrI: 0.4-0.6) in Switzerland to 1.4% (95%CrI: 1.1-1.6) in Lombardy, Italy. The patterns of age-specific IFR estimates were similar across locations (Fig 7.1.4B), despite differences in the surveillance-reported age distribution of cases (Fig 7.1.4C). Some degree of variability remained between age-specific IFR estimates, especially in older age groups. Compared with Hubei province, higher proportions of cases in European locations were in older age groups, suggesting higher levels of preferential ascertainment of severe cases. This appears in the estimated patterns of the age-specific ascertainment proportion, with a generally lower ascertainment of age groups 20-79 in Europe compared to Hubei (Fig 7.1.4D). Additional results are presented in S1 Text, section 5.

7.1.6 Discussion

In this modelling study, we estimate different measures of mortality from SARS-CoV-2 infection in Hubei province, China and six geographic locations in Europe. After adjusting for right-censoring and preferential ascertainment, we estimate the IFR in Hubei to 2.9% (2.4-3.5), higher than the CFR of 2.4%. In different European settings, estimates of IFR ranged from 0.5% (95%CrI: 0.4-0.6) in Switzerland to 1.4% (95%CrI: 1.1-1.6) in Lombardy, compared with CFR of 3.9% and 17.8%, respectively. The model estimates of mortality show a strong age trend in all locations, with very high risks in people aged 80 years and older: between 20% (95%CrI: 16-26) in Switzerland and 34% (95%CrI: 28-40) in Lombardy.

7.1.6.1 Strengths and limitations

Our work has four important strengths. First, we distinguish between the crude CFR and two separate measures of mortality, sCFR and IFR. Second, we use a mechanistic model for

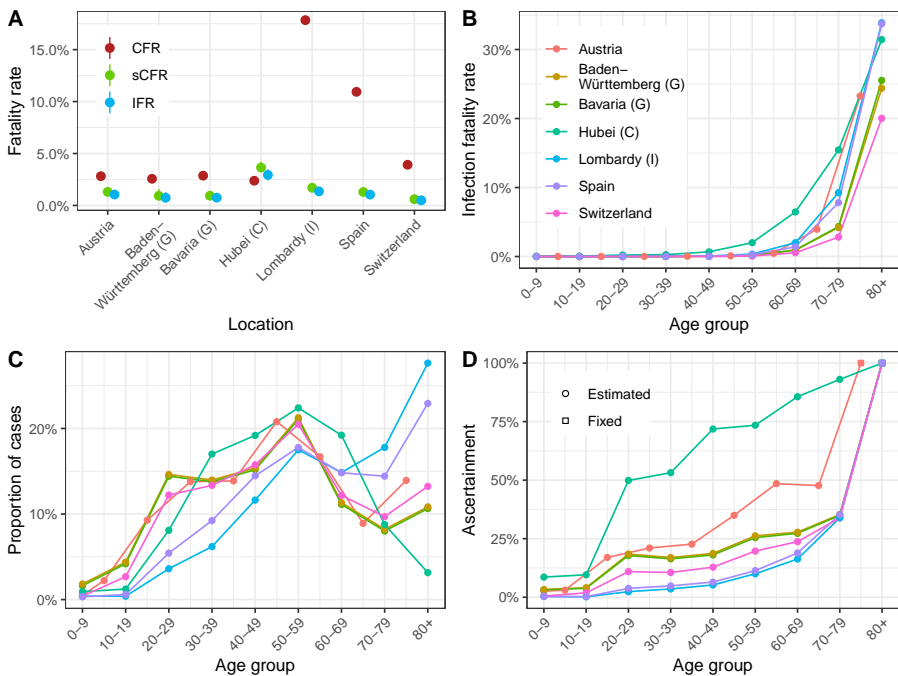


Fig 7.1.4: (A) Case fatality ratio, symptomatic case fatality ratio and infection fatality ratio estimates by geographic location. (B) Infection fatality ratio estimates by age group and location (for Austria, the estimates are adapted to the available age groups from 0-4 to 75+ years). (C) Proportion of cases ascertained by age group and location (color code as for panel B). (D) Distribution of reported cases by age group by location (color code as for panel B).

the transmission of SARS-CoV-2, and the mortality associated with SARS-CoV-2 infection which directly translates the data-generating mechanisms leading to biased observations of the number of deaths (because of right-censoring) and of cases (because of preferential ascertainment). Our model also accounts for the effect of control measures on disease transmission. We implemented the model in a Bayesian framework in order to propagate most sources of uncertainty from data and parameter values into the estimates. In Hubei, as the model captured most of the epidemic wave, the predicted number and timing of deaths could be compared with later reports of SARS-CoV-2 deaths, providing some degree of external validation (S1 Text, section 4). Third, our model is stratified by age group, which has been shown as a crucial feature for modelling emerging respiratory infections [234]. Fourth, the model uses surveillance data that can be collected routinely, and does not require individual-level data or studies in the general population.

Our study has several limitations. First, an important assumption is that all cases in symptomatic individuals aged 80 years and older were reported, as a result of more severe symptoms at older ages. We cannot confirm this, but the high risk of death from SARS-CoV-2 infection amongst the elderly was reported very early on [212], so we believe that most old people with symptoms sought care. Sensitivity analyses show that sCFR and IFR estimates decrease linearly with a lower ascertainment of infections among individuals aged 80 years and older (Fig 7.1.3C). For the IFR in Hubei province to be below 0.5%, fewer than 15% of

infections in individuals aged 80 years and older would have been ascertained by the local authorities.

Second, our model requires surveillance data about the incidence of cases of reported SARS-CoV-2 by date of symptom onset. When information on symptom onset is only available for a subset of cases, we have to assume that data are missing at random. Additionally, within a given geographic location, the model assumes a constant ascertainment proportion and a constant mortality for each age group during the period. When repeating the analysis at different stages of the epidemic in Hubei, we found that estimates obtained before the epidemic peak led to overestimation of the sCFR and IFR (Fig 7.1.3D). This finding could be the result of a decrease in mortality as the epidemic progresses, but could also be attributed to a lower ability of the model to estimate the epidemic size before epidemic peak is reached, a common problem in epidemic modelling [235].

Third, we assume that the deficit of reported cases among younger age groups is a result of preferential ascertainment, whereby younger individuals have milder symptoms and are less likely to seek care, and does not reflect a lower risk of infection in younger individuals. During the pandemic of H1N1 influenza, lower circulation in older individuals was attributed to residual immunity [236]. There is no indication of pre-existing immunity to SARS-CoV-2 in humans [217]. Lower susceptibility of younger individuals for immunological reasons seems unlikely. Different contact patterns could contribute to different attack rates by age group. We include age-specific contact patterns in the model, so our results are dependent on the contact matrix used. In a sensitivity analysis, with 50% reduced susceptibility in children, the estimates of age-specific IFR in other age groups did not change, but the lower number of total infections and led to a higher IFR.

Fourth, the proportion of SARS-CoV-2 infections that remains asymptomatic is still uncertain. To propagate this uncertainty into the results, we implemented a prior distribution informed by the findings of outbreak investigations included in a living systematic review and meta-analysis [229, 230]. Our estimate is in agreement with the findings of a statistical modelling study of an outbreak on the cruise ship “Diamond Princess”, estimating an average proportion of symptomatic infections of 82.1% (95%CrI: 79.8-84.5) [237]. Another study of 87 contacts of infected cases in Shenzhen, China, estimated that 80.4% (95%CrI: 70.9-87.4) were symptomatic [228]. Additionally, dichotomization into asymptomatic and symptomatic is a simplification; SARS-CoV-2 causes a spectrum of symptoms, likely depending on age, sex and comorbidities. Serological surveys in the general population will be needed to better characterize asymptomatic infections [238].

7.1.6.2 Comparison with other studies

Our model-based estimates have some degree of external validation from serological studies of previous exposure to SARS-CoV-2. In Geneva, Switzerland, a study reported an attack rate of 9.7% (95% confidence interval: 6.1-13.1) in the city, resulting in an IFR of 0.6%, very close to our national estimate for Switzerland [239]. Preliminary results from a national seroprevalence study in Spain, with more than 60,000 participants, found an attack rate of 5.0% (95% confidence interval: 4.7-5.4), consistent with our estimate of 5.7% (95% CrI: 5.0-6.6) [240]. A study of excess mortality in Italy estimated $17,786 \pm 269$ deaths in Lombardy, close to our credibility interval for the number of total deaths [241]. This study did not attempt to estimate the size of the epidemic, but only applied the proportion of positive tests to the population to obtain an upper limit of epidemic size, which resulted in a lower bound for the

IFR of 0.6% in Lombardy.

Model-based estimates of mortality from SARS-CoV-2 in China, adjusting for bias, vary. Our estimate for Hubei province is higher than the sCFR of 1.4% estimated in two other modelling studies [242, 243]. Differences in modelling approaches and assumptions explain the variation. Verity et al. used a similar modelling approach, but applied their findings to all of mainland China, where mortality outside Hubei province appeared lower [219]. This paper also assumed a homogeneous attack rate across age groups, rather than simulating epidemics using an age-specific contact matrix. Wu et al. used another approach, assuming that susceptibility to infection varies by age. Both Verity et al. and Wu et al. used data from individuals leaving Wuhan before lockdown was implemented to infer ascertainment, where we fixed it to 100% for the oldest age group. This resulted in comparatively lower ascertainment proportions (up to 70% for the oldest age groups in Verity et al., 2% for Wu et al.), and consequently to higher estimates of epidemic size and lower estimates of sCFR. The use of data from travellers might result in bias, especially if people who can travel are healthier than the general population.

Other studies that attempt to adjust for right-censoring of deaths give different estimates of mortality in China than in our study. A study using a competing risk model estimated mortality at 7.2% (95% confidence interval: 6.6%–8.0%) for Hubei province [244]. Using data on exported cases, another team estimated mortality of 5.3% (95% confidence interval: 3.5%, 7.5%) among confirmed cases in China [245]. Another team reported a CFR of 18% (95% credible interval: 11–81%) among cases detected in Hubei, accounting for the delay in mortality and estimated the IFR at 1.0% (95% CI: 0.5%–4%), based on data from the early epidemic in Hubei and from cases reported outside China [246]. Our estimate of mortality among all infected cases in Hubei is also higher than in an earlier version of this work (2.9% against 1.6%) [247]. We believe the newer estimate to be more reliable for two reasons. First, we implemented age-specific risks of transmission through a contact matrix, which partially explains the age patterns in reported SARS-CoV-2 infections and leads to lower estimates of the total number of infections, thus increasing mortality. Second, a higher estimated proportion of symptomatic people based on new data also led to higher estimates of mortality among all infected.

7.1.6.3 Interpretation and implications

In this study, we propose a comprehensive solution to the estimation of mortality from surveillance data during outbreaks, using two measures of mortality [215]. Adjusted for right-censoring and preferential ascertainment of severe cases, the IFR is a measure of overall mortality associated with SARS-CoV-2 infection, which can be used to assess the potential consequences of the pandemic, e.g. using theoretical estimates of final epidemic size [248]. The sCFR is a measure of mortality that is most relevant to the clinical setting, for assessment of prognosis and prioritization of health care services. Crude CFR estimates are a poor predictor of mortality from SARS-CoV-2 infection, as demonstrates for instance the comparison of CFR and IFR values in Switzerland (high CFR, lowest IFR) and Hubei (lowest CFR, highest IFR). In addition to the inherent biases, the wide variation in CFR between geographic locations is likely to reflect external factors, including policies for testing and differences in systems of surveillance and reporting more than differences in mortality. Crude CFR values should therefore not be used for evaluating policy or making comparisons across settings.

Our model-based estimates of the IFR and sCFR varied geographically (Fig 7.1.4A). The highest estimate of IFR was found in Hubei province (2.9%; 95%CrI: 2.4-3.5 in the baseline analysis). The steep increase in mortality among people aged 60 years and older, reaching very high values in people aged 80 years and older is of concern. The credibility of this estimate, and of our approach for adjusting for right-censoring, is supported by the model predictions of reported daily SARS-CoV-2-associated deaths in Hubei province after 11 February (S1 Text, section 4). The estimated IFR decreases to 2.5% (95%CrI: 2.1-2.9) when accounting for the later correction of reported cases and deaths by the local authorities, and increases to 3.3% (95%CrI: 2.7-4.0) if we consider a lower susceptibility of individuals under 20 years. We also show that applying our model at earlier stages of the epidemic would have resulted in higher estimates of sCFR and IFR, and more uncertainty (Fig 7.1.3D). However, our estimates here correspond to an average value over the considered period, and it has been shown that mortality has changed over time as a result of an improvement of the standard of care [217].

The estimated IFR in Lombardy, 1.4% (95%CrI: 1.1-1.6), was lower than in Hubei province, but higher than in five other European locations. Further research is necessary to better understand the factors associated with SARS-CoV-2 mortality. These differences highlight the importance of local factors on the outcome of SARS-CoV-2 infection, including demographic characteristics. A partial explanation for the remaining heterogeneity is the lower degree of preparedness and health service capacity in northern Italy, which in Europe was affected first by the SARS-CoV-2 epidemic. Consequently, we suggest that a single mortality estimate should not be applied to all settings to estimate the total size of the epidemic [249]. This study shows that the IFR and sCFR, adjusted for right-censoring and preferential ascertainment biases, are appropriate measures of mortality for SARS-CoV-2 infection, which can be used to improve and monitor clinical and public health strategies to reduce the deaths from SARS-CoV-2 infection.

7.1.7 Conclusions

We developed a mechanistic approach to correct the CFR for bias due to right-censoring and preferential ascertainment and provide adjusted estimates of mortality due to SARS-CoV-2 infection by age group. We applied this approach to seven different settings, showing that widely different estimates for the CFR corresponded in fact to more similar estimates of the IFR, around 3% in Hubei province, China, and ranging between 0.5 and 1.4% in six included European locations. Despite these similarities, substantial heterogeneity remains in the IFR estimates across settings, indicating the impact of local conditions on the outcome of SARS-CoV-2 infection. The steep increase in mortality among people aged 60 years and older, reaching very high values in people aged 80 years and older is of concern.

7.1.8 Acknowledgments

We warmly thank Ben Bales for his help with the implementation of the model. We also thank the Chinese Center for Disease Control and Prevention, the Austrian Bundesministerium für Soziales, Gesundheit, Pflege und Konsumentenschutz, the German Robert Koch Institute, the Italian Dipartimento della Protezione Civile and Istituto Superiore di Sanita, the Spanish Ministerio de Sanidad and the Swiss Federal Office of Public Health for collecting the data and making it publicly available. Computations were conducted on UBELIX (<http://www.id.unibe.ch/hpc>), the high performance computing cluster at the University of Bern, Switzerland.

7.1.9 Supporting information

S1 Text. Supplementary appendix. Further details about data sources, model, external validation, additional results and sensitivity analyses.

S2 Text. TRIPOD checklist. Reporting of model developing and validating according to the TRIPOD Checklist for Prediction Model Development.

List of abbreviations

| | |
|-----------------|--|
| 3TC | Lamivudine |
| ABM | Agent-based model |
| ADR | Acquired drug resistance |
| AIDS | Acquired immunodeficiency syndrome |
| ART | Antiretroviral therapy |
| ARV | Antiretroviral |
| CFR | Case fatality ratio |
| COVID-19 | Coronavirus disease 2019 |
| CrI | Credibility interval |
| d4T | Stavudine |
| ddI | Didanosine |
| DTG | Dolutegravir |
| DRM | Drug resistance mutation |
| EFV | Efavirenz |
| FTC | Emtricitabine |
| HET | Heterosexual |
| HIV | Human immunodeficiency virus |
| HIVDR | HIV drug resistance |
| IeDEA-SA | International epidemiological Databases to Evaluate AIDS in sub-Saharan Africa |
| IFR | Infection fatality ratio |
| InSTI | Integrase strand transfer inhibitor |
| LMIC | Low and middle-income countries |
| MARISA | Modelling Antiretroviral drug Resistance In South Africa |
| MSM | Men having sex with men |
| NNRTI | Non-nucleoside reverse transcriptase inhibitor |
| NRTI | Nucleos(t)ide reverse transcriptase inhibitor |

| | |
|-------------------|---|
| NVP | Nevirapine |
| NTD | Neural tube defect |
| OI | Opportunistic infection |
| OR | Odds ratio |
| PDR | Pre-treatment drug resistance |
| PEP | Post-exposure prophylaxis |
| PI | Protease inhibitor |
| PLWH | People living with HIV |
| PMTCT | Prevention of mother-to-child transmission |
| PrEP | Pre-exposure prophylaxis |
| RCT | Randomized controlled trial |
| SARS-CoV-2 | Severe acute respiratory syndrome coronavirus 2 |
| sCFR | symptomatic case fatality ratio |
| SIV | Simian immunodeficiency virus |
| SSA | sub-Saharan Africa |
| TAM | Thymidine-analogue mutation |
| TasP | Treatment as Prevention |
| TDF | Tenofovir disoproxil fumarate |
| TDR | Transmitted drug resistance |
| TLD | Tenofovir, lamivudine, dolutegravir |
| UTT | Universal Test-and-Treat |
| VF | Virological failure |
| VL | Viral load |
| WHO | World Health Organization |
| ZDV | Zidovudine |

Bibliography

- [1] Gao F, Balles E, Robertson DL, Chen Y, Rodenburg CM, Michael SF, et al. Origin of HIV-1 in the chimpanzee Pan troglodytes troglodytes. *Nature*. 1999;397(6718):436–441. doi:10.1038/17130.
- [2] Hirsch VM, Olmsted RA, Murphey-Corb M, Purcell RH, Johnson PR. An African primate lentivirus (SIVsm) closely related to HIV-2. *Nature*. 1989;339(6223):389–392. doi:10.1038/339389a0.
- [3] Williams KC, Burdo TH. HIV and SIV infection: The role of cellular restriction and immune responses in viral replication and pathogenesis; 2009. Available from: [/pmc/articles/PMC2739573/?report=abstracthttps://www.ncbi.nlm.nih.gov/pmc/articles/PMC2739573/](https://pubmed.ncbi.nlm.nih.gov/pmc/articles/PMC2739573/).
- [4] Hahn BH, Shaw GM, De Cock KM, Sharp PM. AIDS as a zoonosis: Scientific and public health implications; 2000. Available from: <https://pubmed.ncbi.nlm.nih.gov/10649986/>.
- [5] Keele BF, Van Heuverswyn F, Li Y, Bailes E, Takehisa J, Santiago ML, et al. Chimpanzee reservoirs of pandemic and nonpandemic HIV-1. *Science*. 2006;313(5786):523–526. doi:10.1126/science.1126531.
- [6] Heuverswyn FV, Li Y, Bailes E, Neel C, Lafay B, Keele BF, et al. Genetic diversity and phylogeographic clustering of SIVcpzPtt in wild chimpanzees in Cameroon. *Virology*. 2007;368(1):155–171. doi:10.1016/j.virol.2007.06.018.
- [7] Faria NR, Rambaut A, Suchard MA, Baele C, Bedford T, Ward MJ, et al. The early spread and epidemic ignition of HIV-1 in human populations. *Science*. 2014;346(6205):56–61. doi:10.1126/science.1256739.
- [8] Shaw GM, Hunter E. HIV transmission. *Cold Spring Harbor Perspectives in Medicine*. 2012;2(11). doi:10.1101/cshperspect.a006965.
- [9] UNAIDS. UNAIDS data; 2020. Available from: aidsinfo.unaids.org.
- [10] Simelela N, Venter WDF, Pillay Y, Barron P. A Political and Social History of HIV in South Africa; 2015. Available from: <https://link.springer.com/article/10.1007/s11904-015-0259-7>.
- [11] Taylor BS, Sobieszczyk ME, McCutchan FE, Hammer SM. The Challenge of HIV-1 Subtype Diversity. *New England Journal of Medicine*. 2008;358(15):1590–1602. doi:10.1056/nejmra0706737.
- [12] Maldarelli F, Kearney M, Palmer S, Stephens R, Mican J, Polis MA, et al. HIV Populations Are Large and Accumulate High Genetic Diversity in a Nonlinear Fashion. *Journal of Virology*. 2013;87(18):10313–10323. doi:10.1128/jvi.01225-12.
- [13] Santoro MM, Perno CF. HIV-1 Genetic Variability and Clinical Implications. *ISRN Microbiology*. 2013;2013:1–20. doi:10.1155/2013/481314.
- [14] Labhardt ND, Bader J, Lejone TI, Ringera I, Hobbins MA, Fritz C, et al. Should viral load thresholds be lowered? Revisiting the WHO definition for virologic failure in patients on antiretroviral therapy in resource-limited settings. *Medicine (United States)*. 2016;95(28). doi:10.1097/MD.0000000000003985.
- [15] Arts EJ, Hazuda DJ. HIV-1 antiretroviral drug therapy. *Cold Spring Harbor Perspectives in Medicine*. 2012;2(4). doi:10.1101/cshperspect.a007161.
- [16] Llibre JM, Walmsley S, Gatell JM. Backbones versus core agents in initial ART regimens: One game, two players. *Journal of Antimicrobial Chemotherapy*. 2016;71(4):856–861. doi:10.1093/jac/dkv429.
- [17] Dieterich DT. Disease management - Constructing optimal NRTI-based combinations: Past, present, and future. *MedGenMed Medscape General Medicine*. 2006;8(1):16. doi:10.1186/1758-2652-8-1-16.
- [18] Montaner JSG, Reiss P, Cooper D, Vella S, Harris M, Conway B, et al. A randomized double-blind trial comparing combinations of nevirapine, didanosine, and zidovudine for HIV-infected patients: The INCAS trial. *Journal of the American Medical Association*. 1998;279(12):930–937. doi:10.1001/jama.279.12.930.
- [19] Hammer SM, Squires KE, Hughes MD, Grimes JM, Demeter LM, Currier JS, et al. A Controlled Trial of Two Nucleoside Analogues plus Indinavir in Persons with Human Immunodeficiency Virus Infection and CD4 Cell Counts of 200 per Cubic Millimeter or Less. *New England Journal of Medicine*. 1997;337(11):725–733. doi:10.1056/nejm199709113371101.
- [20] Egger M, Hirschel B, Francioli P, Sudre P, Wirz M, Flepp M, et al. Impact of new antiretroviral combination therapies in HIV infected patients in Switzerland: Prospective multicentre study. *British Medical Journal*. 1997;315(7117):1194–1199. doi:10.1136/bmj.315.7117.1194.
- [21] Ford N, Calmy A, Mills EJ. The first decade of antiretroviral therapy in Africa; 2011. Available from: <http://globalizationandhealth.biomedcentral.com/articles/10.1186/1744-8603-7-33>.
- [22] Attia S, Egger M, Müller M, Zwahlen M, Low N. Sexual transmission of HIV according to viral load and antiretroviral therapy: Systematic review and meta-analysis. *AIDS*. 2009;23(11):1397–1404. doi:10.1097/QAD.0b013e32832b7dca.
- [23] Cohen MS, Chen YQ, McCauley M, Gamble T, Hosseinipour MC, Kumarasamy N, et al. Prevention of HIV-1 Infection with Early Antiretroviral Therapy. *New England Journal of Medicine*. 2011;365(6):493–505. doi:10.1056/nejmoa1105243.
- [24] World Health Organization (WHO). CONSOLIDATED GUIDELINES ON THE USE OF ANTIRETROVIRAL DRUGS FOR TREATING AND PREVENTING HIV INFECTION; 2013. Available from: <https://www.who.int/hiv/pub/guidelines/arv2013/download/en/>.
- [25] World Health Organization. Consolidated guidelines on the use of antiretroviral drugs for treating and preventing HIV infection; 2016. Available from: <http://www.who.int/hiv/pub/arv/arv-2016/en/>.
- [26] Department of Health: Republic of South Africa. IMPLEMENTATION OF THE UNIVERSAL TEST AND TREAT STRATEGY FOR HIV POSITIVE PATIENTS AND DIFFERENTIATED CARE FOR STABLE PATIENTS. Pretoria; 2016. Available from: <https://sahivosoc.org/Files/22816CircularUTTDecongestionCCMTDirectorate.pdf>.
- [27] Health Department Republic of South Africa. 2019 ART Clinical Guidelines for the Management of HIV in Adults, Pregnancy, Adolescents, Children, Infants and Neonates; 2020. Available from: <https://sahivosoc.org/Files/2019ARTGuideline28042020pdf.pdf>.
- [28] Liu TF, Shafer RW. Web Resources for HIV Type 1

- Genotypic-Resistance Test Interpretation; 2006. Available from: [http://www.iasusa.org/resistance\[_\]mutations/mutations\[_\]figures.pdf](http://www.iasusa.org/resistance[_]mutations/mutations[_]figures.pdf).
- [29] Zdanowicz MM. The pharmacology of HIV drug resistance; 2006. Available from: [/pmc/articles/PMC1637011/?report=abstracthttps://www.ncbi.nlm.nih.gov/pmc/articles/PMC1637011/](http://www.ncbi.nlm.nih.gov/pmc/articles/PMC1637011/?report=abstracthttps://www.ncbi.nlm.nih.gov/pmc/articles/PMC1637011/).
- [30] Lubner AD. Genetic barriers of resistance and impact on clinical response. *MedGenMed Medscape General Medicine*. 2005;7(3):69. doi:10.1186/1758-2652-7-3-69.
- [31] Yang WL, Kouyos RD, Böni J, Yerly S, Klimkait T, Aubert V, et al. Persistence of Transmitted HIV-1 Drug Resistance Mutations Associated with Fitness Costs and Viral Genetic Backgrounds. *PLOS Pathogens*. 2015;11(3):e1004722. doi:10.1371/journal.ppat.1004722.
- [32] Kühnert D, Kouyos R, Shirreff G, Pečerska J, Scherrer AU, Böni J, et al. Quantifying the fitness cost of HIV-1 drug resistance mutations through phylodynamics. *PLoS Pathogens*. 2018;14(2). doi:10.1371/journal.ppat.1006895.
- [33] Clavel F, Hance AJ. HIV Drug Resistance. *New England Journal of Medicine*. 2004;350(10):1023–1035. doi:10.1056/nejmra025195.
- [34] Neupane S, Dhungana GP, Ghimire HC. Adherence to antiretroviral treatment and associated factors among people living with HIV and AIDS in CHITWAN, Nepal. *BMC Public Health*. 2019;19(1):1–9. doi:10.1186/s12889-019-7051-3.
- [35] Nachega JB, Marconi VC, van Zyl GU, Gardner EM, Preiser W, Hong SY, et al. HIV treatment adherence, drug resistance, virologic failure: evolving concepts. *Infectious disorders drug targets*. 2011;11(2):167–74. doi:10.2174/187152611795589663.
- [36] Bangsberg DR, Moss AR, Deeks SG. Paradoxes of adherence and drug resistance to HIV antiretroviral therapy. *Journal of Antimicrobial Chemotherapy*. 2004;53(5):696–699. doi:10.1093/jac/dkh162.
- [37] Wittkop L, Günthard HF, de Wolf F, Dunn D, Cozzi-Lepri A, de Luca A, et al. Effect of transmitted drug resistance on virological and immunological response to initial combination antiretroviral therapy for HIV (EuroCoord-CHAIN joint project): A European multicohort study. *The Lancet Infectious Diseases*. 2011;11(5):363–371. doi:10.1016/S1473-3099(11)70032-9.
- [38] World Health Organization (WHO). HIV DRUG RESISTANCE REPORT 2017; 2017. Available from: <https://www.who.int/hiv/pub/drugresistance/hivdr-report-2017/en/>.
- [39] UNAIDS. Fast-Track - Ending the AIDS epidemic by 2030; 2014. Available from: [https://www.unaids.org/en/resources/documents/2014/JC2686\[_\]WAD2014report](https://www.unaids.org/en/resources/documents/2014/JC2686[_]WAD2014report).
- [40] UNAIDS. 90–90–90 - An ambitious treatment target to help end the AIDS epidemic; 2017. Available from: <https://www.unaids.org/en/resources/documents/2017/90-90-90>.
- [41] Hayes RJ, Donnell D, Floyd S, Mandla N, Bwalya J, Sabapathy K, et al. Effect of Universal Testing and Treatment on HIV Incidence — HPTN 071 (PopART). *New England Journal of Medicine*. 2019;381(3):207–218. doi:10.1056/nejmoa1814556.
- [42] Havlir DV, Balzer LB, Charlebois ED, Clark TD, Kwarisiima D, Ayieko J, et al. HIV Testing and Treatment with the Use of a Community Health Approach in Rural Africa. *New England Journal of Medicine*. 2019;381(3):219–229. doi:10.1056/nejmoa1809866.
- [43] Makhema J, Wirth KE, Pretorius Holme M, Gaolathe T, Mmalane M, Kadima E, et al. Universal Testing, Expanded Treatment, and Incidence of HIV Infection in Botswana. *New England Journal of Medicine*. 2019;381(3):230–242. doi:10.1056/nejmoa1812281.
- [44] Iwuji CC, Orne-Gliemann J, Larmarange J, Balestre E, Thiebaut R, Tanser F, et al. Universal test and treat and the HIV epidemic in rural South Africa: a phase 4, open-label, community cluster randomised trial. *The Lancet HIV*. 2018;5(3):e116–e125. doi:10.1016/S2352-3018(17)30205-9.
- [45] Hayes R, Sabapathy K, Fidler S. Universal Testing and Treatment as an HIV Prevention Strategy: Research Questions and Methods. *Current HIV Research*. 2011;9(6):429–445. doi:10.2174/157016211798038515.
- [46] Schechter M. Prioritization of antiretroviral therapy in patients with high CD4 counts, and retention in care: lessons from the START and Temprano trials. *Journal of the International AIDS Society*. 2018;21(2):e25077. doi:10.1002/jia2.25077.
- [47] Lodi S, Günthard HF, Dunn D, Garcia F, Logan R, Jose S, et al. Effect of immediate initiation of antiretroviral treatment on the risk of acquired HIV drug resistance. *AIDS*. 2018;doi:10.1097/QAD.0000000000001692.
- [48] Dorward J, Drain PK, Osman F, Sookrajh Y, Pillay M, Moodley P, et al. Short Communication: Early Antiretroviral Therapy Is Associated with Better Viral Suppression and Less HIV Drug Resistance After Implementation of Universal Treatment in South Africa. *AIDS Research and Human Retroviruses*. 2020;36(4):297–299. doi:10.1089/aid.2019.0206.
- [49] Milanga M, Rutter L. DOLUTEGRAVIR IN SOUTHERN & EASTERN AFRICA AND THE RIGHT TO CHOOSE; 2018. Available from: <https://healthgap.org/wp-content/uploads/2018/11/Policy-Brief-Dolutegravir-in-Southern-Eastern-Africa.pdf>.
- [50] Clinton Health Access Initiative. ARV market report: The state of the antiretroviral drug market in low-and middle-income countries; 2017. Available from: [https://marketbookshelf.com/wp-content/uploads/2017/11/2017-ARV-Market-Report\[_\]Final.pdf](https://marketbookshelf.com/wp-content/uploads/2017/11/2017-ARV-Market-Report[_]Final.pdf).
- [51] Zash R, Makhema J, Shapiro RL. Neural-Tube Defects with Dolutegravir Treatment from the Time of Conception. *New England Journal of Medicine*. 2018;379(10):979–981. doi:10.1056/NEJMct807653.
- [52] Zash R. Update on neural tube defects with antiretroviral exposure in the Tsepamo study, Botswana; 2020. Available from: [https://natap.org/2020/IAC/IAC\[_\]112.htm](https://natap.org/2020/IAC/IAC[_]112.htm).
- [53] Phillips AN, Stover J, Cambiano V, Nakagawa F, Jordan MR, Pillay D, et al. Impact of HIV drug resistance on HIV/AIDS-associated mortality, new infections, and antiretroviral therapy program costs in Sub-Saharan Africa. *Journal of Infectious Diseases*. 2017;215(9):1362–1365. doi:10.1093/infdis/jix089.
- [54] Poppe LK, Chunda-Liyoka C, Kwon EH, Gondwe C, West JT, Kankasa C, et al. HIV drug resistance in infants increases with changing prevention of mother-to-child transmission regimens. *AIDS*. 2017;31(13):1885–1889. doi:10.1097/QAD.0000000000001569.
- [55] Bernoulli D. Réflexions sur les avantages de l'inoculation. *Mercure de Paris*. 1760; p. 173.
- [56] Brauer F. Mathematical epidemiology: Past, present, and future; 2017. Available from: [/pmc/articles/PMC6001967/?report=abstracthttps://www.ncbi.nlm.nih.gov/pmc/articles/PMC6001967/](http://www.ncbi.nlm.nih.gov/pmc/articles/PMC6001967/?report=abstracthttps://www.ncbi.nlm.nih.gov/pmc/articles/PMC6001967/).
- [57] Kermack W, McKendrick AG. A contribution to the mathematical theory of epidemics. *Proceedings of the Royal Society of London Series A, Containing Papers of a Mathematical and Physical Character*. 1927;115(772):700–721. doi:10.1098/rspa.1927.0118.
- [58] Kermack W, McKendrick AG. Contributions to the mathematical theory of epidemics. II. —The problem

- of endemicity. *Proceedings of the Royal Society of London Series A, Containing Papers of a Mathematical and Physical Character*. 1932;138(834):55–83. doi:10.1098/rspa.1932.0171.
- [59] Kermack W, McKendrick AG. Contributions to the mathematical theory of epidemics. III.—Further studies of the problem of endemicity. *Proceedings of the Royal Society of London Series A, Containing Papers of a Mathematical and Physical Character*. 1933;141(843):94–122. doi:10.1098/rspa.1933.0106.
- [60] Bansal S, Grenfell BT, Meyers LA. When individual behaviour matters: Homogeneous and network models in epidemiology. *Journal of the Royal Society Interface*. 2007;4(16):879–891. doi:10.1098/rsif.2007.1100.
- [61] Anderson RM, May RM. *Infectious Diseases of Humans: Dynamics and Control* - Roy M. Anderson, Robert M. May. Oxford University Press; 1992.
- [62] Mollison D, Isham V, Grenfell B. Epidemics: Models and Data. *Journal of the Royal Statistical Society Series A (Statistics in Society)*. 1994;157(1):115. doi:10.2307/2983509.
- [63] Gallagher S, Eddy WF. Comparing compartment and agent-based models; 2017. Available from: http://www.stat.cmu.edu/~jsgallagher/papers/gallagher_38-17.pdf.
- [64] Geffen N, Welte A. Modelling the human immunodeficiency virus (HIV) epidemic: A review of the substance and role of models in South Africa. *Southern African Journal of HIV Medicine*. 2018;19(1):756. doi:10.4102/sajhivmed.v19i1.756.
- [65] Dorrington RE. ASSA600: an AIDS model of the third kind. *Transactions of the Actuarial Society of South Africa*. 1998;12(1):99–153.
- [66] Johnson LF, Dorrington RE. Thembisa version 4.1: A model for evaluating the impact of HIV/AIDS in South Africa; 2018. Available from: <https://www.thembisa.org/publications>.
- [67] Johnson LF, May MT, Dorrington RE, Cornell M, Boule A, Egger M, et al. Estimating the impact of antiretroviral treatment on adult mortality trends in South Africa: A mathematical modelling study. *PLOS Medicine*. 2017;14(12):e1002468. doi:10.1371/journal.pmed.1002468.
- [68] Granich RM, Gilks CF, Dye C, De Cock KM, Williams BG. Universal voluntary HIV testing with immediate antiretroviral therapy as a strategy for elimination of HIV transmission: a mathematical model. *The Lancet*. 2009;373(9657):48–57. doi:10.1016/S0140-6736(08)61697-9.
- [69] Abbas UL, Glaubius R, Mubayi A, Hood G, Mellors JW. Antiretroviral therapy and pre-exposure prophylaxis: Combined impact on HIV transmission and drug resistance in South Africa. *Journal of Infectious Diseases*. 2013;208(2):224–234. doi:10.1093/infdis/jit150.
- [70] Nichols BE, Sigaloff KC, Kityo C, Hamers RL, Baltussen R, Bertagnolio S, et al. Increasing the use of second-line therapy is a cost-effective approach to prevent the spread of drug-resistant HIV: a mathematical modelling study. *Journal of the International AIDS Society*. 2014;17(1):19164. doi:10.7448/IAS.17.1.19164.
- [71] Egger M, Ekouevi DK, Williams C, Lyamuya RE, Mukumbi H, Braitstein P, et al. Cohort Profile: The international epidemiological databases to evaluate AIDS (IeDEA) in sub-Saharan Africa. *International Journal of Epidemiology*. 2012;41(5):1256–1264. doi:10.1093/ije/dyr080.
- [72] de Waal R, Lessells R, Hauser A, Kouyos R, Davies MA, Egger M, et al. HIV drug resistance in sub-Saharan Africa: public health questions and the potential role of real-world data and mathematical modelling. *Journal of virus eradication*. 2018;4(Suppl 2):55–58. doi:10.1016/S2055-6640(20)30347-2.
- [73] Bacheleer LT, Anton ED, Kudish P, Baker D, Bunville J, Krakowski K, et al. Human immunodeficiency virus type 1 mutations selected in patients failing efavirenz combination therapy. *Antimicrobial Agents and Chemotherapy*. 2000;44(9):2475–2484. doi:10.1128/AAC.44.9.2475-2484.2000.
- [74] Steegen K, Bronze M, Papatheanasopoulos MA, van Zyl C, Goedhals D, Variava E, et al. HIV-1 antiretroviral drug resistance patterns in patients failing NNRTI-based treatment: results from a national survey in South Africa. *Journal of Antimicrobial Chemotherapy*. 2017;72(1):210–219. doi:10.1093/jac/dkw358.
- [75] Wainberg MA. HIV-1 subtype distribution and the problem of drug resistance. *AIDS (London, England)*. 2004;18 Suppl 3:S63–68.
- [76] Buonaguro L, Tornesello ML, Buonaguro FM. Human immunodeficiency virus type 1 subtype distribution in the worldwide epidemic: pathogenetic and therapeutic implications. *Journal of virology*. 2007;81(19):10209–10219. doi:10.1128/JVI.00872-07.
- [77] Coutsinos D, Invernizzi CF, Xu H, Moisi D, Oliveira M, Brenner BG, et al. Template Usage Is Responsible for the Preferential Acquisition of the K65R Reverse Transcriptase Mutation in Subtype C Variants of Human Immunodeficiency Virus Type 1. *Journal of Virology*. 2009;83(4):2029–2033. doi:10.1128/jvi.01349-08.
- [78] Invernizzi CF, Coutsinos D, Oliveira M, Moisi D, Brenner BG, Wainberg MA. Signature Nucleotide Polymorphisms at Positions 64 and 65 in Reverse Transcriptase Favor the Selection of the K65R Resistance Mutation in HIV-1 Subtype C. *The Journal of Infectious Diseases*. 2009;200(8):1202–1206. doi:10.1086/605894.
- [79] White E, Smit E, Churchill D, Collins S, Booth C, Tostevin A, et al. No Evidence That HIV-1 Subtype C Infection Compromises the Efficacy of Tenofovir-Containing Regimens: Cohort Study in the United Kingdom. *The Journal of infectious diseases*. 2016;214(9):1302–1308. doi:10.1093/infdis/jiw213.
- [80] UNAIDS. AIDSinfo. Number of people living with HIV;. Available from: <http://aidsinfo.unaids.org/>.
- [81] Booth A, Clarke M, Dooley G, Ghersi D, Moher D, Petticrew M, et al. The nuts and bolts of PROSPERO: an international prospective register of systematic reviews. *Systematic Reviews*. 2012;1(1):2. doi:10.1186/2046-4053-1-2.
- [82] Shafer RW. Rationale and Uses of a Public HIV Drug-Resistance Database. *The Journal of Infectious Diseases*. 2006;194(s1):S51–S58. doi:10.1086/505356.
- [83] Sayers EW, Cavanaugh M, Clark K, Pruitt KD, Schoch CL, Sherry ST, et al. GenBank. *Nucleic Acids Research*. 2020;(1). doi:10.1093/nar/gkaa1023.
- [84] El-Khatib Z, Ekstrom AM, Ledwaba J, Mohapi L, Laher F, Karstaedt A, et al. Viremia and drug resistance among HIV-1 patients on antiretroviral treatment: a cross-sectional study in Soweto, South Africa. *Wolters Kluwer Health | Lippincott Williams & Wilkins AIDS* Wolters Kluwer Health. 2010;24:1679–1687. doi:10.1097/QAD.0b013e32833a097b.
- [85] Rupérez M, Pou C, Maculufe S, Cedeño S, Luis L, Rodríguez J, et al. Determinants of virological failure and antiretroviral drug resistance in Mozambique. *Journal of Antimicrobial Chemotherapy*. 2015;70(9):2639–2647. doi:10.1093/jac/dkv143.
- [86] Wallis CL, Mellors JW, Venter WDF, Sanne I, Stevens W. Varied Patterns of HIV-1 Drug Resistance on Failing First-Line Antiretroviral Therapy in South Africa. *JAIDS*

- Journal of Acquired Immune Deficiency Syndromes. 2010;53(4):480–484. doi:10.1097/QAI.0b013e3181bc478b.
- [87] Marconi VC, Sunpath H, Lu Z, Gordon M, Koranteng-Apeagyei K, Hampton J, et al. Prevalence of HIV-1 Drug Resistance after Failure of a First Highly Active Antiretroviral Therapy Regimen in KwaZulu Natal, South Africa. *Clinical Infectious Diseases*. 2008;46(10):1589–1597. doi:10.1086/587109.
- [88] Novitsky V, Wester CW, DeGruttola V, Bussmann H, Gaseitsiwe S, Thomas A, et al. The Reverse Transcriptase 67N 70R 215Y Genotype Is the Predominant TAM Pathway Associated with Virologic Failure among HIV Type 1C-Infected Adults Treated with ZDV/ddI-Containing HAART in Southern Africa. *AIDS Research and Human Retroviruses*. 2007;23(7):868–878. doi:10.1089/aid.2006.0298.
- [89] Rossouw T, Nieuwoudt M, Manasa J, Malherbe G, Lessells R, Pillay S, et al. HIV drug resistance levels in adults failing first-line antiretroviral therapy in an urban and a rural setting in South Africa. *HIV Medicine*. 2017;18(2):104–114. doi:10.1111/hiv.12400.
- [90] Seu L, Mulenga LB, Siwanga M, Sikazwe I, Lambwe N, Guffey MB, et al. Characterization of HIV drug resistance mutations among patients failing first-line antiretroviral therapy from a tertiary referral center in Lusaka, Zambia. *Journal of Medical Virology*. 2015;87(7):1149–1157. doi:10.1002/jmv.24162.
- [91] Singh A, Sunpath H, Green TN, Padayachi N, Hiraman K, Lie Y, et al. Drug Resistance and Viral Tropism in HIV-1 Subtype C-Infected Patients in KwaZulu-Natal, South Africa. *JAIDS Journal of Acquired Immune Deficiency Syndromes*. 2011;58(3):233–240. doi:10.1097/QAI.0b013e318228667f.
- [92] Sunpath H, Wu B, Gordon M, Hampton J, Johnson B, Moosa MYS, et al. High rate of K65R for antiretroviral therapy-naïve patients with subtype C HIV infection failing a tenofovir-containing first-line regimen. *AIDS*. 2012;26(13):1679–1684. doi:10.1097/QAD.0b013e3182835688b.
- [93] Barth RE, Aitken SC, Tempelman H, Geelen SP, van Bussel EM, Hoepelman AI, et al. Accumulation of drug resistance and loss of therapeutic options precede commonly used criteria for treatment failure in HIV-1 subtype-C-infected patients. *Antiviral Therapy*. 2012;17(2):377–386. doi:10.3851/IMP2010.
- [94] Brehm JH, Koontz DL, Wallis CL, Shutt KA, Sanne I, Wood R, et al. Frequent Emergence of N348I in HIV-1 Subtype C Reverse Transcriptase with Failure of Initial Therapy Reduces Susceptibility to Reverse-Transcriptase Inhibitors. *Clinical Infectious Diseases*. 2012;55(5):737–745. doi:10.1093/cid/cis501.
- [95] Hoffmann CJ, Charalambos S, Sim J, Ledwaba J, Schwikard G, Chaisson RE, et al. Viremia, Resuppression, and Time to Resistance in Human Immunodeficiency Virus (HIV) Subtype C during First-Line Antiretroviral Therapy in South Africa. *Clinical Infectious Diseases*. 2009;49(12):1928–1935. doi:10.1086/648444.
- [96] Hoffmann CJ, Ledwaba J, Li JF, Johnston V, Hunt G, Fielding KL, et al. Resistance to tenofovir-based regimens during treatment failure of subtype C HIV-1 in South Africa. *Antiviral Therapy*. 2013;18(7):915–920. doi:10.3851/IMP2652.
- [97] Hunt GM, Dokubo EK, Takuva S, de Oliveira T, Ledwaba J, Dube N, et al. Rates of virological suppression and drug resistance in adult HIV-1-positive patients attending primary healthcare facilities in KwaZulu-Natal, South Africa. *Journal of Antimicrobial Chemotherapy*. 2017;72(11):3141–3148. doi:10.1093/jac/dkx252.
- [98] Sanne I, Orrell C, Fox MP, Conradie F, Iwe P, Zeinecker J, et al. Nurse versus doctor management of HIV-infected patients receiving antiretroviral therapy (CIPRA-SA): a randomised non-inferiority trial. *Lancet*. 2010;376(9734):33–40. doi:10.1016/S0140-6736(10)60894-X.
- [99] Wester CW, Thomas AM, Bussmann H, Moyo S, Makhema JM, Gaolathe T, et al. Non-nucleoside reverse transcriptase inhibitor outcomes among combination antiretroviral therapy-treated adults in Botswana. *AIDS*. 2010;24(SUPPL. 1):S27–S36. doi:10.1097/01.aids.0000366080.91192.55.
- [100] Bussmann H, Wester CW, Thomas A, Novitsky V, Okezie R, Muzenda T, et al. Response to Zidovudine/Didanosine-Containing Combination Antiretroviral Therapy Among HIV-1 Subtype C-Infected Adults in Botswana: Two-Year Outcomes from a Randomized Clinical Trial. *JAIDS Journal of Acquired Immune Deficiency Syndromes*. 2009;51(1):37–46. doi:10.1097/QAI.0b013e31819ff102.
- [101] Gregson J, Tang M, Ndemi N, Hamers RL, Rhee SY, Marconi VC, et al. Global epidemiology of drug resistance after failure of WHO recommended first-line regimens for adult HIV-1 infection: a multicentre retrospective cohort study. *The Lancet Infectious Diseases*. 2016;16(5):565–575. doi:10.1016/S1473-3099(15)00536-8.
- [102] Aboud M, Kaplan R, Lombaard J, Zhang F, Hidalgo JA, Mamedova E, et al. Dolutegravir versus ritonavir-boosted lopinavir both with dual nucleoside reverse transcriptase inhibitor therapy in adults with HIV-1 infection in whom first-line therapy has failed (DAWNING): an open-label, non-inferiority, phase 3b trial. *The Lancet Infectious Diseases*. 2019;19(3):253–264. doi:10.1016/S1473-3099(19)30036-2.
- [103] Wandeler G, Buzzi M, Anderegg N, Sculier D, Béguelin C, Egger M, et al. Virologic failure and HIV drug resistance on simplified, dolutegravir-based maintenance therapy: Systematic review and meta-analysis. *F1000 Research*. 2019;doi:10.12688/f1000research.15995.1.
- [104] Paton NI, Kityo C, Thompson J, Nankya I, Bagenda L, Hoppe A, et al. Nucleoside reverse-transcriptase inhibitor cross-resistance and outcomes from second-line antiretroviral therapy in the public health approach: an observational analysis within the randomised, open-label, EARNEST trial. *The Lancet HIV*. 2017;4(8):e341–e348. doi:10.1016/S2352-3018(17)30065-6.
- [105] Stockdale AJ, Saunders MJ, Boyd MA, Bonnett LJ, Johnston V, Wandeler G, et al. Effectiveness of Protease Inhibitor/Nucleos(t)ide Reverse Transcriptase Inhibitor-Based Second-line Antiretroviral Therapy for the Treatment of Human Immunodeficiency Virus Type 1 Infection in Sub-Saharan Africa: A Systematic Review and Meta-analysis. *Clinical Infectious Diseases*. 2017;doi:10.1093/cid/cix1108.
- [106] Boyd MA, Moore CL, Molina JM, Wood R, Madero JS, Wolff M, et al. Baseline HIV-1 resistance, virological outcomes, and emergent resistance in the SECOND-LINE trial: an exploratory analysis. *The Lancet HIV*. 2015;2(2):e42–e51. doi:10.1016/S2352-3018(14)00061-7.
- [107] Rhee SY, Liu T, Ravela J, Gonzales MJ, Shafer RW. Distribution of human immunodeficiency virus type 1 protease and reverse transcriptase mutation patterns in 4,183 persons undergoing genotypic resistance testing. *Antimicrobial Agents and Chemotherapy*. 2004;48(8):3122–3126. doi:10.1128/AAC.48.8.3122-3126.2004.
- [108] Ssemwanga D, Lihana RW, Ugoji C, Abimiku A, Nkengasong J, Dakum P, et al. Update on HIV-1 acquired and transmitted drug resistance in Africa. *AIDS reviews*. 2015;17(1):3–20.

- [109] Barth RE, van der Loeff MFS, Schuurman R, Hoepelman AI, Wensing AM. Virological follow-up of adult patients in antiretroviral treatment programmes in sub-Saharan Africa: a systematic review. *The Lancet Infectious Diseases*. 2010;10(3):155–166. doi:10.1016/S1473-3099(09)70328-7.
- [110] Boender TS, Sigaloff KCE, McMahon JH, Kiertiburanakul S, Jordan MR, Barcarolo J, et al. Long-term Virological Outcomes of First-Line Antiretroviral Therapy for HIV-1 in Low- and Middle-Income Countries: A Systematic Review and Meta-analysis. *Clinical Infectious Diseases*. 2015;61(9):1453–1461. doi:10.1093/cid/civ556.
- [111] Gupta RK, Hill A, Sawyer AW, Cozzi-Lepri A, von Wyl V, Yerly S, et al. Virological monitoring and resistance to first-line highly active antiretroviral therapy in adults infected with HIV-1 treated under WHO guidelines: a systematic review and meta-analysis; 2009. Available from: <https://www.sciencedirect.com/science/article/pii/S1473309909701367>.
- [112] Zaniewski E, Dao Ostinelli CH, Chammartin F, Maxwell N, Davies M, Euvrard J, et al. Trends in CD4 and viral load testing 2005 to 2018: multi-cohort study of people living with HIV in Southern Africa. *Journal of the International AIDS Society*. 2020;23(7). doi:10.1002/jia2.25546.
- [113] UNAIDS. South Africa | UNAIDS data;. Available from: <http://www.unaids.org/en/regionscountries/countries/southafrica>.
- [114] Tang MW, Shafer RW. HIV-1 Antiretroviral Resistance. *Drugs*. 2012;72(9):e1–e25. doi:10.2165/11633630-000000000-00000.
- [115] Meintjes G, Moorhouse MA, Carmona S, Davies N, Dlamini S, Van Vuuren C, et al. Adult antiretroviral therapy guidelines 2017. *Southern African Journal of HIV Medicine*. 2017;18.
- [116] Joint United Nations Programme on HIV/AIDS (UNAIDS) . 90-90-90. An ambitious treatment target to help end the AIDS epidemic. Geneva; 2014. Available from: http://www.unaids.org/sites/default/files/media_asset/90-90-90_en_0.pdf.
- [117] Eaton JW, Johnson LF, Salomon JA, Bärnighausen T, Bendavid E, Bershteyn A, et al. HIV Treatment as Prevention: Systematic Comparison of Mathematical Models of the Potential Impact of Antiretroviral Therapy on HIV Incidence in South Africa. *PLoS Medicine*. 2012;9(7):e1001245. doi:10.1371/journal.pmed.1001245.
- [118] Estill J, Egger M, Blaser N, Vizcaya LS, Garone D, Wood R, et al. Cost-effectiveness of point-of-care viral load monitoring of antiretroviral therapy in resource-limited settings: mathematical modelling study. *AIDS (London, England)*. 2013;27(9):1483–92. doi:10.1097/QAD.0b013e328360a4e5.
- [119] Cambiano V, Bertagnolio S, Jordan MR, Pillay D, Perriens JH, Venter F, et al. Predicted levels of HIV drug resistance. *AIDS*. 2014;28:S15–S23. doi:10.1097/QAD.0000000000000082.
- [120] Grenfell BT, Pybus OG, Gog JR, Wood JLN, Daly JM, Mumford JA, et al. Unifying the Epidemiological and Evolutionary Dynamics of Pathogens. *Science*. 2004;303(5656):327–332. doi:10.1126/science.1090727.
- [121] Kouyos RD, Metcalf CJE, Birger R, Klein EY, Abel zur Wiesch P, Ankomah P, et al. The path of least resistance: aggressive or moderate treatment? *Proceedings of the Royal Society B: Biological Sciences*. 2014;281(1794):20140566–20140566. doi:10.1098/rspb.2014.0566.
- [122] Metcalf CJE, Birger RB, Funk S, Kouyos RD, Lloyd-Smith JO, Jansen VAA. Five challenges in evolution and infectious diseases. *Epidemics*. 2015;10:40–44. doi:10.1016/j.epidem.2014.12.003.
- [123] Stanford University. NNRTI Resistance Notes - HIV Drug Resistance Database;. Available from: <https://hivdb.stanford.edu/dr-summary/resistance-notes/NNRTI/#%k103n.s.h.t.r.q.e>.
- [124] Johnson LF, Rehle TM, Jooste S, Bekker LG. Rates of HIV testing and diagnosis in South Africa. *AIDS*. 2015;29(11):1401–1409. doi:10.1097/QAD.0000000000000721.
- [125] Fairlie L, Bernheimer J, Sipambo N, Fick C, Kuhn L. Lamivudine monotherapy in children and adolescents: The devil is in the detail. *South African Medical Journal*. 2017;107(12):1055. doi:10.7196/SAMJ.2017.v107i12.12776.
- [126] Muri L, Gamell A, Ntamatungiro AJ, Glass TR, Luwanda LB, Battegay M, et al. Development of HIV drug resistance and therapeutic failure in children and adolescents in rural Tanzania: an emerging public health concern. 2016;doi:10.1097/QAD.0000000000001273.
- [127] Maduna PH, Dolan M, Kondlo L, Mabuza H, Dlamini JN, Polis M, et al. Morbidity and Mortality According to Latest CD4+ Cell Count among HIV Positive Individuals in South Africa Who Enrolled in Project Phidisa. *PLOS ONE*. 2015;10(4):e0121843. doi:10.1371/journal.pone.0121843.
- [128] Orrell C, Walensky RP, Losina E, Pitt J, Freedberg KA, Wood R. HIV type-1 clade C resistance genotypes in treatment-naïve patients and after first virological failure in a large community antiretroviral therapy programme. *Antiviral therapy*. 2009;14(4):523–31.
- [129] Patel P, Borkowf CB, Brooks JT, Lasry A, Lansky A, Mermin J. Estimating per-act HIV transmission risk. *AIDS*. 2014;28(10):1509–1519. doi:10.1097/QAD.0000000000000298.
- [130] Anova Health Institute. Rapid Assessment of HIV Prevention, Care and Treatment Programming for MSM in South Africa; 2013.
- [131] Brennan AT, Maskew M, Sanne I, Fox MP. The interplay between CD4 cell count, viral load suppression and duration of antiretroviral therapy on mortality in a resource-limited setting. *Tropical medicine & international health* : TM & IH. 2013;18(5):619–31. doi:10.1111/tmi.12079.
- [132] Gupta RK, Gregson J, Parkin N, Haile-Selassie H, Tanuri A, Andrade Forero L, et al. HIV-1 drug resistance before initiation or re-initiation of first-line antiretroviral therapy in low-income and middle-income countries: a systematic review and meta-regression analysis. *The Lancet Infectious diseases*. 2018;18(3):346–355. doi:10.1016/S1473-3099(17)30702-8.
- [133] Mckay MD, Beckman RJ, Conover WJ. A Comparison of Three Methods for Selecting Values of Input Variables in the Analysis of Output from a Computer Code. *Technometrics*. 1979;21(2):239–245.
- [134] Rosenberg MS, Gómez-Olivé FX, Rohr JK, Houle BC, Kabudula CW, Wagner RG, et al. Sexual Behaviors and HIV Status: A Population-Based Study Among Older Adults in Rural South Africa. *Journal of acquired immune deficiency syndromes (1999)*. 2017;74(1):e9–e17. doi:10.1097/QAI.0000000000001173.
- [135] Parboosing R, Naidoo A, Gordon M, Taylor M, Vella V. Resistance to antiretroviral drugs in newly diagnosed, young treatment-naïve HIV-positive pregnant women in the province of KwaZulu-Natal, South Africa. *Journal of Medical Virology*. 2011;83(9):1508–1513. doi:10.1002/jmv.22143.
- [136] Manasa J, Danaviah S, Lessells R, Elshareef M, Tanser F, Wilkinson E, et al. Increasing HIV-1 Drug Resistance Between 2010 and 2012 in Adults Participating in Population-Based HIV Surveillance in Rural KwaZulu-Natal, South Africa. *AIDS research and human retroviruses*. 2016;32(8):763–9.

- doi:10.1089/AID.2015.0225.
- [137] Steegen K, Carmona S, Bronze M, Papathanasopoulos MA, van Zyl G, Goedhals D, et al. Moderate Levels of Pre-Treatment HIV-1 Antiretroviral Drug Resistance Detected in the First South African National Survey. *PLOS ONE*. 2016;11(12):e0166305. doi:10.1371/journal.pone.0166305.
- [138] Yanik EL, Napravnik S, Hurt CB, Dennis A, Quinlivan EB, Sebastian J, et al. Prevalence of transmitted antiretroviral drug resistance differs between acutely and chronically HIV-infected patients. *Journal of acquired immune deficiency syndromes (1999)*. 2012;61(2):258–62. doi:10.1097/QAI.0b013e3182618f05.
- [139] Hamers RL, Wallis CL, Kityo C, Siwale M, Mandaliya K. HIV-1 drug resistance in antiretroviral-naïve individuals in sub-Saharan Africa after rollout of antiretroviral therapy: a multicentre observational study. *Articles Lancet Infect Dis*. 2011;11:750–59. doi:10.1016/S1473.
- [140] National Department of Health SA. FOR THE PREVENTION OF MOTHER-TO-CHILD TRANSMISSION OF HIV (PMTCT) AND THE MANAGEMENT OF HIV IN CHILDREN, ADOLESCENTS AND ADULTS NATIONAL CONSOLIDATED GUIDELINES; 2014. Available from: www.doh.gov.za.
- [141] World Health Organization (WHO). WHO's Response; 2018. Available from: http://www.who.int/medicines/publications/drugalerts/Statement_on_DTC_18May_2018final.pdf.
- [142] Blanco JL, Rojas J, Paredes R, Negredo E, Mallolas J, Casadella M, et al. Dolutegravir-based maintenance monotherapy versus dual therapy with lamivudine: a planned 24 week analysis of the DOLAM randomized clinical trial. *Journal of Antimicrobial Chemotherapy*. 2018;73(7):1965–1971. doi:10.1093/jac/dky093.
- [143] Wijting I, Roxk C, Boucher C, van Kampen J, Pas S, de Vries-Sluijs T, et al. Dolutegravir as maintenance monotherapy for HIV (DOMONO): a phase 2, randomised non-inferiority trial. *The Lancet HIV*. 2017;4(12):e547–e554. doi:10.1016/S2352-3018(17)30152-2.
- [144] Heaton LM, Bouey PD, Fu J, Stover J, Fowler TB, Lyerla R, et al. Estimating the impact of the US President's Emergency Plan for AIDS Relief on HIV treatment and prevention programmes in Africa. *Sexually Transmitted Infections*. 2015;91(8):615–620. doi:10.1136/sextrans-2014-051991.
- [145] Chimukangara B, Lessells RJ, Rhee SY, Giandhari J, Kharsany ABM, Naidoo K, et al. Trends in Pretreatment HIV-1 Drug Resistance in Antiretroviral Therapy-naïve Adults in South Africa, 2000–2016: A Pooled Sequence Analysis. *EClinicalMedicine*. 2019;9:26–34. doi:10.1016/j.eclinm.2019.03.006.
- [146] South Africa National Department of Health. Dolutegravir/TLD Roll Out in South Africa. Johannesburg; 2018. Available from: https://www.sahivsoc2018.co.za/wp-content/uploads/2018/11/17_Steve-Smith_SAHIVCS-Oct-2018-oct-26-draft.pdf.
- [147] Inzaule SC, Jordan MR, Cournil A, Vitoria M, Ravasi G, Cham F, et al. Increasing levels of pretreatment HIV drug resistance and safety concerns for dolutegravir use in women of reproductive age. *AIDS (London, England)*. 2019;33(11):1797–1799. doi:10.1097/QAD.0000000000002277.
- [148] Goh OQ, Colby DJ, Pinyakorn S, Sacdalan C, Kroon E, Chan P, et al. Switch to dolutegravir is well tolerated in Thais with HIV infection. *Journal of the International AIDS Society*. 2019;22(7):e25324. doi:10.1002/jia2.25324.
- [149] Venter WDF, Moorhouse M, Sokhela S, Fairlie L, Mashabane N, Masenya M, et al. Dolutegravir plus Two Different Prodrugs of Tenofovir to Treat HIV. *New England Journal of Medicine*. 2019;381(9):803–815. doi:10.1056/nejmoa1902824.
- [150] Phillips AN, Cambiano V, Nakagawa F, Revill P, Jordan MR, Hallett TB, et al. Cost-effectiveness of public-health policy options in the presence of pretreatment NNRTI drug resistance in sub-Saharan Africa: a modelling study. *The Lancet HIV*. 2018;5(3):e146–e154. doi:10.1016/S2352-3018(17)30190-X.
- [151] WHO. Information on Neural Tube Defects. Statement on DTC – Geneva. 2018;18.
- [152] The NAMSAL ANRS 12313 Study Group. Dolutegravir-Based or Low-Dose Efavirenz-Based Regimen for the Treatment of HIV-1. *New England Journal of Medicine*. 2019;381(9):816–826. doi:10.1056/nejmoa1904340.
- [153] Zash R, Holmes L, Diseko M, Jacobson DL, Brummel S, Mayondi G, et al. Neural-Tube Defects and Antiretroviral Treatment Regimens in Botswana. *New England Journal of Medicine*. 2019; p. NEJMoa1905230. doi:10.1056/NEJMoa1905230.
- [154] The Acting CEO of SAHPRA: South African Health Products Regulatory Authority. Recommendations about the use of the HIV medicine DOLUTEGRAVIR in Pregnancy in response to the Potential Risk of Birth Defects; 2018. Available from: <http://www.mcca.za.com>.
- [155] Dugdale CM, Ciaranello AL, Bekker LG, Stern ME, Myer L, Wood R, et al. Risks and Benefits of Dolutegravir- and Efavirenz-Based Strategies for South African Women With HIV of Child-Bearing Potential. *Annals of Internal Medicine*. 2019;170(9):614. doi:10.7326/M18-3358.
- [156] World Health Organization (WHO). Update of recommendations on first- and second-line antiretroviral regimens. Geneva, Switzerland; 2019. Available from: <http://apps.who.int/bookorders>.
- [157] Inzaule SC, Hamers RL, Doherty M, Shafer RW, Bertagnolio S, Rinke de Wit TF. Curbing the rise of HIV drug resistance in low-income and middle-income countries: the role of dolutegravir-containing regimens; 2019. Available from: <https://pubmed.ncbi.nlm.nih.gov/30902440/>.
- [158] Hauser A, Kusejko K, Johnson LF, Wandeler G, Riou J, Goldstein F, et al. Bridging the gap between HIV epidemiology and antiretroviral resistance evolution: Modelling the spread of resistance in South Africa. *PLOS Computational Biology*. 2019;15(6):e1007083. doi:10.1371/journal.pcbi.1007083.
- [159] World Bank. Contraceptive prevalence, any methods (% of women ages 15-49) | Data; 2015. Available from: <https://data.worldbank.org/indicator/SP.DYN.CONU.ZS?locations=ZA>.
- [160] Seaholm SK, Ackerman E, Wu SC. Latin hypercube sampling and the sensitivity analysis of a Monte Carlo epidemic model. *International journal of bio-medical computing*. 1988;23(1-2):97–112.
- [161] Boyer S, Iwujic C, Gosset A, Protopopescu C, Okesola N, Plazy M, et al. Factors associated with antiretroviral treatment initiation amongst HIV-positive individuals linked to care within a universal test and treat programme: early findings of the ANRS 12249 TasP trial in rural South Africa. *AIDS care*. 2016;28 Suppl 3(Suppl 3):39–51. doi:10.1080/09540121.2016.1164808.
- [162] Yang, Wan-Lin and Kouyos, Roger and Scherrer, Alexandra U and Böni, Jürg and Shah, Cyril and Yerly, Sabine and Klimkait, Thomas and Aubert, Vincent and Furrer, Hansjakob and Battegay, Manuel and Cavassini, Matthias and Bernasconi, Enos and Vernazza, Piet fSHCS. Assessing the Paradox Between Transmitted and Acquired HIV Type 1 Drug Resistance Mutations in the

- Swiss HIV Cohort Study From 1998 to 2012. *Journal of Infectious Diseases*. 2015;212(1):28–38.
- [163] World Health Organization. Guideline on when to start antiretroviral therapy and on pre-exposure prophylaxis for HIV. Geneva: World Health Organization; 2015. Available from: <http://www.who.int/hiv/pub/guidelines/earlyrelease-arv/en/>.
- [164] Lundgren JD, Babiker AG, Gordin F, Emery S, Grund B, Sharma S, et al. Initiation of Antiretroviral Therapy in Early Asymptomatic HIV Infection. *New England Journal of Medicine*. 2015;373(9):795–807. doi:10.1056/NEJMoa1506816.
- [165] Cohen MS, Chen YQ, McCauley M, Gamble T, Hosseinipour MC, Kumarasamy N, et al. Antiretroviral Therapy for the Prevention of HIV-1 Transmission. *New England Journal of Medicine*. 2016;375(9):830–839. doi:10.1056/nejmoa1600693.
- [166] Nachega JB, Uthman OA, Del Rio C, Mugavero MJ, Rees H, Mills EJ. Addressing the achilles' heel in the HIV care continuum for the success of a test-and-treat strategy to achieve an AIDS-free generation. *Clinical Infectious Diseases*. 2014;59(SUPPL.1). doi:10.1093/cid/ciu299.
- [167] Adakun SA, Siedner MJ, Muzoora C, Haberer JE, Tsai AC, Hunt PW, et al. Higher baseline CD4 cell count predicts treatment interruptions and persistent viremia in patients initiating ARVs in rural Uganda. *Journal of Acquired Immune Deficiency Syndromes*. 2013;62(3):317–321. doi:10.1097/QAI.0b013e3182800daf.
- [168] Palumbo PJ, Fogel JM, Hudelson SE, Wilson EA, Hart S, Hovind L, et al. HIV Drug Resistance in Adults Receiving Early vs. Delayed Antiretroviral Therapy: HPTN 052. *Journal of Acquired Immune Deficiency Syndromes*. 2018;77(5):484–491. doi:10.1097/QAI.0000000000001623.
- [169] World Health Organization. Guidelines on the public health response to pretreatment HIV drug resistance. Geneva: World Health Organization; 2017.
- [170] Walmsley S, Baumgarten A, Berenguer J, Felzarta F, Florence E, Khuong-Josses MA, et al. Dolutegravir plus abacavir/lamivudine for the treatment of HIV-1 infection in antiretroviral therapy-naïve patients: Week 96 and week 144 results from the SINGLE randomized clinical trial. *Journal of Acquired Immune Deficiency Syndromes*. 2015;70(5):515–519. doi:10.1097/QAI.0000000000000790.
- [171] Molina JM, Clotet B, van Lunzen J, Lazzarin A, Cavassini M, Henry K, et al. Once-daily dolutegravir versus darunavir plus ritonavir for treatment-naïve adults with HIV-1 infection (FLAMINGO): 96 week results from a randomised, open-label, phase 3b study. *The Lancet HIV*. 2015;2(4):e127–e136. doi:10.1016/S2352-3018(15)00027-2.
- [172] Taiwo BO, Zheng L, Stefanescu A, Nyaku A, Bezins B, Wallis CL, et al. ACTG A5353: A Pilot Study of Dolutegravir Plus Lamivudine for Initial Treatment of Human Immunodeficiency Virus-1 (HIV-1)-infected Participants with HIV-1 RNA <50000 Copies/mL. *Clinical Infectious Diseases*. 2017;66(11):1689–1697. doi:10.1093/cid/cix1083.
- [173] Aboud M, Kaplan R, Lombaard J, Zhang F, Hidalgo J, Mamedova E, et al. Superior Efficacy of Dolutegravir (DTG) Plus 2 Nucleoside Reverse Transcriptase Inhibitors (NRTIs) Compared With Lopinavir/Ritonavir (LPV/RTV) Plus 2 NRTIs in Second-Line Treatment: Interim Data From the DAWNING Study. In: 9th IAS Conference on HIV Science. Paris; 2017. Available from: https://www.natap.org/2017/IAS/IAS_j26.htm.
- [174] Reynes J, Meftah N, Montes B. Dual regimen with dolutegravir and lamivudine maintains virologic suppression even in heavily treatment-experienced HIV-infected patients: 48-week results from a pilot study (DOLULAM). In: *HIV Drug Therapy*. Glasgow; 2016.
- [175] Oliveira M, Ibanescu RI, Pham HT, Brenner B, Mesplede T, Wainberg MA. The M184I/V and K65R nucleoside resistance mutations in HIV-1 prevent the emergence of resistance mutations against dolutegravir. *AIDS*. 2016;30(15):2267–2273. doi:10.1097/QAD.0000000000001191.
- [176] Egger M, Johnson L, Althaus C, Schöni A, Salanti G, Low N, et al. Developing WHO guidelines: Time to formally include evidence from mathematical modelling studies. *F1000Research*. 2017;6:1584. doi:10.12688/f1000research.12367.2.
- [177] Phillips AN, Cambiano V, Miners A, Revill P, Pillay D, Lundgren JD, et al. Effectiveness and cost-effectiveness of potential responses to future high levels of transmitted HIV drug resistance in antiretroviral drug-naïve populations beginning treatment: Modelling study and economic analysis. *The Lancet HIV*. 2014;1(2):e85–e93. doi:10.1016/S2352-3018(14)70021-9.
- [178] Nichols BE, Boucher CAB, van Dijk JH, Thuma PE, Nouwen JL, Baltussen R, et al. Cost-Effectiveness of Pre-Exposure Prophylaxis (PrEP) in Preventing HIV-1 Infections in Rural Zambia: A Modeling Study. *PLoS ONE*. 2013;8(3):e59549. doi:10.1371/journal.pone.0059549.
- [179] Supervie V, Barrett M, Kahn JS, Musuka G, Moeti TL, Busang L, et al. Modeling dynamic interactions between pre-exposure prophylaxis interventions & treatment programs: predicting HIV transmission & resistance. *Scientific reports*. 2011;1:185. doi:10.1038/srep00185.
- [180] Phillips AN, Pillay D, Garnett G, Bennett D, Vitoria M, Cambiano V, et al. Effect on transmission of HIV-1 resistance of timing of implementation of viral load monitoring to determine switches from first to second-line antiretroviral regimens in resource-limited settings. *AIDS*. 2011;25(6):843–850. doi:10.1097/QAD.0b013e328344037a.
- [181] Cambiano V, Bertagnolio S, Jordan MR, Lundgren JD, Phillips A. Transmission of drug resistant HIV and its potential impact on mortality and treatment outcomes in resource-limited settings. *Journal of Infectious Diseases*. 2013;207(SUPPL.2). doi:10.1093/infdis/jit111.
- [182] Supervie V, García-Lerma JC, Heneine W, Blower S. HIV, transmitted drug resistance, and the paradox of preexposure prophylaxis. *Proceedings of the National Academy of Sciences of the United States of America*. 2010;107(27):12381–6. doi:10.1073/pnas.1006061107.
- [183] International epidemiology Databases to Evaluate AIDS. Available from: <https://www.iedea.org/>.
- [184] Vitoria M, Hill A, Ford N, Doherty M, Clayden P, Venter F, et al. The transition to dolutegravir and other new antiretrovirals in low-income and middle-income countries: What are the issues? *AIDS*. 2018;32(12):1551–1561. doi:10.1097/QAD.0000000000001845.
- [185] Venter WF, Kaiser B, Pillay Y, Conradie F, Gomez GB, Clayden P, et al. Cutting the cost of South African antiretroviral therapy using newer, safer drugs. *South African medical journal = Suid-Afrikaanse tydskrif vir geneeskunde*. 2016;107(1):28–30. doi:10.7196/SAMJ.2016.v107.i1.12058.
- [186] Murphy RA, Court R, Maartens G, Sunpath H. Second-Line Antiretroviral Therapy in Sub-Saharan Africa: It Is Time to Mind the Gaps. *AIDS Research and Human Retroviruses*. 2017;33(12):1181–1184. doi:10.1089/aid.2017.0134.
- [187] Sigaloff KCE, Hamers RL, Wallis CL, Kityo C, Siwale M, Iwe P, et al. Unnecessary antiretroviral treatment switches and accumulation of HIV resistance mutations; two arguments for viral load monitoring in Africa.

- Journal of Acquired Immune Deficiency Syndromes. 2011;58(1):23–31. doi:10.1097/QAI.0b013e318227fc34.
- [188] Haas AD, Keiser O, Balestre E, Brown S, Bissagnene E, Chimbete E, et al. Monitoring and switching of first-line antiretroviral therapy in adult treatment cohorts in sub-Saharan Africa: Collaborative analysis. *The Lancet HIV*. 2015;2(7):e271–e278. doi:10.1016/S2352-3018(15)00087-9.
- [189] Barron P, Pillay Y, Doherty T, Sherman C, Jackson D, Bhardwaj S, et al. Eliminating mother-to-child HIV transmission in South Africa. *Bulletin of the World Health Organization*. 2013;91(1):70–74. doi:10.2471/BLT.12.106807.
- [190] de Oliveira T, Kharsany ABM, Gräf T, Cawood C, Khanyile D, Grobler A, et al. Transmission networks and risk of HIV infection in KwaZulu-Natal, South Africa: a community-wide phylogenetic study. *The Lancet HIV*. 2017;4(1):e41–e50. doi:10.1016/S2352-3018(16)30186-2.
- [191] Rhee SY, Grant PM, Tzou PL, Barrow G, Harrigan PR, Ioannidis JPA, et al. A systematic review of the genetic mechanisms of dolutegravir resistance; 2019. Available from: <https://pubmed.ncbi.nlm.nih.gov/pmc/articles/PMC6798839/>.
- [192] Cahn P, Pozniak AL, Mingrone H, Shuldjakov A, Brites C, Andrade-Villanueva JF, et al. Dolutegravir versus raltegravir in antiretroviral-experienced, integrase-inhibitor-naïve adults with HIV: Week 48 results from the randomised, double-blind, non-inferiority SAILING study. *The Lancet*. 2013;382(9893):700–708. doi:10.1016/S0140-6736(13)61221-0.
- [193] Eron JJ, Clotet B, Durant J, Katlama C, Kumar P, Lazzarin A, et al. Safety and efficacy of dolutegravir in treatment-experienced subjects with raltegravir-resistant HIV type 1 infection: 24-Week results of the VIKING study. *Journal of Infectious Diseases*. 2013;207(5):740–748. doi:10.1093/infdis/jis750.
- [194] Castillo-Mancilla JR, Haberer JE. Adherence Measurements in HIV: New Advancements in Pharmacologic Methods and Real-Time Monitoring; 2018. Available from: <https://pubmed.ncbi.nlm.nih.gov/pmc/articles/PMC5876155/>.
- [195] McGee KS, Okeke NL, Hurt CB, McKellar MS. Canary in the coal mine? Transmitted mutations conferring resistance to all integrase strand transfer inhibitors in a treatment-naïve patient. *Open Forum Infectious Diseases*. 2018;5(11). doi:10.1093/ofid/ofy294.
- [196] Olearo F, Nguyen H, Bonnet F, Yerly S, Wandeler G, Stoeckle M, et al. Impact of the M184V/I Mutation on the Efficacy of Abacavir/Lamivudine/Dolutegravir Therapy in HIV Treatment-Experienced Patients. *Open Forum Infectious Diseases*. 2019;6(10). doi:10.1093/ofid/ofz330.
- [197] Dorward J, Lessells R, Drain PK, Naidoo K, de Oliveira T, Pillay Y, et al. Dolutegravir for first-line antiretroviral therapy in low-income and middle-income countries: uncertainties and opportunities for implementation and research; 2018. Available from: <https://pubmed.ncbi.nlm.nih.gov/29884404/>.
- [198] Staszewski S, Morales-Ramirez J, Tashima KT, Rachlis A, Skiest D, Stanford J, et al. Efavirenz plus Zidovudine and Lamivudine, Efavirenz plus Indinavir, and Indinavir plus Zidovudine and Lamivudine in the Treatment of HIV-1 Infection in Adults. *New England Journal of Medicine*. 1999;341(25):1865–1873. doi:10.1056/nejm199912163412501.
- [199] Van Leth F, Phanuphak P, Ruxrungtham K, Baraldi E, Miller S, Gazzard B, et al. Comparison of first-line antiretroviral therapy with regimens including nevirapine, efavirenz, or both drugs, plus stavudine and lamivudine: A randomised open-label trial, the 2NN Study. *Lancet*. 2004;363(9417):1253–1263. doi:10.1016/S0140-6736(04)15997-7.
- [200] Mugavero MJ, Hicks CB. HIV resistance and the effectiveness of combination antiretroviral treatment; 2004.
- [201] Gallant JE, Staszewski S, Pozniak AL, DeJesus E, Suleiman JMAH, Miller MD, et al. Efficacy and safety of tenofovir DF vs stavudine in combination therapy in antiretroviral-naïve patients: A 3-year randomized trial. *Journal of the American Medical Association*. 2004;292(2):191–201. doi:10.1001/jama.292.2.191.
- [202] Clevenger P, Cua E, Dam E, Durant J, Schmit JC, Boulme R, et al. Prevalence of nonnucleoside reverse transcriptase inhibitor (NNRTI) resistance-associated mutations and polymorphisms in NNRTI-naïve HIV-infected patients. *HIV Clinical Trials*. 2002;3(1):36–44. doi:10.1310/SHOR-UDC8-8RR7-XEMJ.
- [203] Martínez E, Arnaiz JA, Podzamczar D, Dalmau D, Ribera E, Domingo P, et al. Three-year follow-up of protease inhibitor-based regimen simplification in HIV-infected patients. *AIDS*. 2007;21(3):367–369. doi:10.1097/QAD.0b013e3280121ab1.
- [204] Pillay D, Taylor S, Richman DD. Incidence and impact of resistance against approved antiretroviral drugs; 2000.
- [205] Harries AD, Nyangulu DS, Hargreaves NJ, Kaluwa O, Salaniponi FM. Preventing antiretroviral anarchy in sub-Saharan Africa; 2001.
- [206] Trachtenberg JD, Sande MA. Emerging resistance to nonnucleoside reverse transcriptase inhibitors: A warning and a challenge; 2002. Available from: <https://jamanetwork.com/journals/jama/fullarticle/195090>.
- [207] Petrella M, Brenner B, Loemba H, Wainberg MA. HIV drug resistance and implications for the introduction of antiretroviral therapy in resource-poor countries. *Drug Resistance Updates*. 2001;4(6):339–346. doi:10.1054/drup.2002.0235.
- [208] Patrick Jackson. BBC NEWS | Health | Can Africa handle Aids drugs?; 2003. Available from: <http://news.bbc.co.uk/2/hi/health/3067345.stm>.
- [209] Maartens G, Meintjes G. Resistance matters in EARNEST; 2017. Available from: <http://dx.doi.org/10.1016/S2352->.
- [210] World Health Organization. Coronavirus disease 2019 (COVID-19) Situation Report 117; 2020. https://www.who.int/docs/default-source/coronavirus/situation-reports/20200516-covid-19-sitrep-117.pdf?sfvrsn=8f562cc_2.
- [211] Wang C, Horby PW, Hayden FG, Gao GF. A novel coronavirus outbreak of global health concern. *The Lancet*. 2020;395(10223):470–473.
- [212] Huang C, Wang Y, Li X, Ren L, Zhao J, Hu Y, et al. Clinical features of patients infected with 2019 novel coronavirus in Wuhan, China. *The Lancet*. 2020;395(10223):497–506.
- [213] Riou J, Althaus CL. Pattern of early human-to-human transmission of Wuhan 2019 novel coronavirus (2019-nCoV), December 2019 to January 2020. *Eurosurveillance*. 2020;25(4).
- [214] World Health Organization. WHO Director-General's opening remarks at the media briefing on COVID-19 - 3 March 2020; 2020. Available from: <https://www.who.int/dg/speeches/detail/who-director-general-s-opening-remarks-at-the-media-briefing-on-covid-19--3-march-2020>.
- [215] Lipsitch M, Donnelly CA, Fraser C, Blake IM, Cori A, Dorigatti I, et al. Potential biases in estimating absolute and relative case-fatality risks during outbreaks. *PLoS neglected tropical diseases*. 2015;9(7).
- [216] Battegay M, Kuehl R, Tschudin-Sutter S, Hirsch

- HH, Widmer AF, Neher RA. 2019-novel Coronavirus (2019-nCoV): estimating the case fatality rate—a word of caution. *Swiss Medical Weekly*. 2020;150(0506).
- [217] World Health Organization-China Joint Mission on Coronavirus Disease 2019 Group. Report of the WHO-China Joint Mission on Coronavirus Disease 2019 (COVID-19); 2020. <https://www.who.int/docs/default-source/coronaviruse/who-china-joint-mission-on-covid-19-final-report.pdf>.
- [218] Zhang J, Klepac P, Read JM, Rosello A, Wang X, Lai S, et al. patterns of human social contact and contact with animals in Shanghai, china. *Scientific reports*. 2019;9(1):1–11.
- [219] The Novel Coronavirus Pneumonia Emergency Response Epidemiology Team. Vital Surveillances: The Epidemiological Characteristics of an Outbreak of 2019 Novel Coronavirus Diseases (COVID-19) — China, 2020. *China CDC Weekly*. 2020;2(8):113–122.
- [220] nCov2019: An R package with real-time data and historical data and Shiny app; 2020. <https://github.com/Guangchuangyu/nCov2019>.
- [221] Bundesministerium für Soziales, Gesundheit, Pflege und Konsumentenschutz. Amtliches Dashboard COVID19;. Available from: <https://info.gesundheitsministerium.at/>.
- [222] Robert Koch Institute. Epidemiological Situation in Germany;. Available from: <https://corona.rki.de>.
- [223] Presidenza del Consiglio dei Ministri - Dipartimento della Protezione Civile. GitHub repository on COVID-19;. <https://github.com/pcm-dpc>.
- [224] Istituto Superiore di Sanita. EPIDEMIA COVID-19, Aggiornamento nazionale (appendice), 28 aprile 2020 – ore 16:00;.
- [225] Ministerio de Sanidad. Actualización nº 89. Enfermedad por el coronavirus (COVID-19). 28.04.2020;.
- [226] Federal office of Public Health. Personal communication from Federal office of Public Healths (FOPH), Switzerland, through SSPHplus website;.
- [227] Mossong J, Hens N, Jit M, Beutels P, Auranen K, Mikolajczyk R, et al. Social Contacts and Mixing Patterns Relevant to the Spread of Infectious Diseases. *PLoS Medicine*. 2008;5(3):e74. doi:10.1371/journal.pmed.0050074.
- [228] Bi Q, Wu Y, Mei S, Ye C, Zou X, Zhang Z, et al. Epidemiology and Transmission of COVID-19 in Shenzhen China: Analysis of 391 cases and 1,286 of their close contacts. *Lancet Inf Dis*. 2020;doi:10.1016/S1473-3099(20)30287-5.
- [229] Buitrago-Garcia DC, Egli-Gany D, Counotte MJ, Hossmann S, Imeri H, Salanti G, et al. The role of asymptomatic SARS-CoV-2 infections: rapid living systematic review and meta-analysis. *medRxiv*. 2020;.
- [230] Counotte MJ. Preliminary updated meta-analyses to <https://www.medrxiv.org/content/10.1101/2020.04.02.20051318v1>. 2020;doi:10.7910/DVN/VA62TK.
- [231] Japanese National Institute of Infectious Diseases. Field Briefing: Diamond Princess COVID-19 Cases; 2020. <https://www.niid.go.jp/niid/en/2019-ncov-e/9407-covid-dp-fe-01.html>.
- [232] Linton NM, Kobayashi T, Yang Y, Hayashi K, Akhmetzhanov AR, Jung Sm, et al. Incubation Period and Other Epidemiological Characteristics of 2019 Novel Coronavirus Infections with Right Truncation: A Statistical Analysis of Publicly Available Case Data. *Journal of Clinical Medicine*. 2020;9(2):538.
- [233] Carpenter B, Gelman A, Hoffman MD, Lee D, Goodrich B, Betancourt M, et al. Stan: A probabilistic programming language. *Journal of statistical software*. 2017;76(1).
- [234] Pellis L, Cauchemez S, Ferguson NM, Fraser C. Systematic selection between age and household structure for models aimed at emerging epidemic predictions. *Nature Communications*. 2020;11(1):1–11.
- [235] Riou J, Poletto C, Boëlle PY. Improving early epidemiological assessment of emerging Aedes-transmitted epidemics using historical data. *PLoS neglected tropical diseases*. 2018;12(6):e0006526.
- [236] Pérez-Trallero E, Piñeiro L, Vicente D, Montes M, Cilla G. Residual immunity in older people against the influenza A (H1N1)—recent experience in northern Spain. *Eurosurveillance*. 2009;14(39):19344.
- [237] Mizumoto K, Kagaya K, Watsuki A, Chowell G. Estimating the asymptomatic proportion of coronavirus disease 2019 (COVID-19) cases on board the Diamond Princess cruise ship, Yokohama, Japan, 2020. *Eurosurveillance*. 2020;25(10). doi:<https://doi.org/10.2807/1560-7917.ES.2020.25.10.2000180>.
- [238] Carrat F, Vergu E, Ferguson NM, Lemaître M, Cauchemez S, Leach S, et al. Time lines of infection and disease in human influenza: a review of volunteer challenge studies. *American journal of epidemiology*. 2008;167(7):775–785.
- [239] Stringhini S, Wisniak A, Piumatti G, Azman AS, Baysson H, De Ridder D, et al. Repeated seroprevalence of anti-SARS-CoV-2 IgG antibodies in a population-based sample from Geneva, Switzerland. *medRxiv*. 2020;doi:10.1101/2020.05.02.20088898.
- [240] Ministerio de Sanidad. ESTUDIO ENE-COVID19: PRIMERA RONDA ESTUDIO NACIONAL DE SERO-EPIDEMIOLOGÍA DE LA INFECCIÓN POR SARS-COV-2 EN ESPAÑA;.
- [241] Modi C, Boehm V, Ferraro S, Stein G, Seljak U. Total COVID-19 Mortality in Italy: Excess Mortality and Age Dependence through Time-Series Analysis. *medRxiv*. 2020;.
- [242] Verity R, Okell LC, Dorigatti I, Winskill P, Whittaker C, Imai N, et al. Estimates of the severity of coronavirus disease 2019: a model-based analysis. *The Lancet Infectious Diseases*. 2020;.
- [243] Wu JT, Leung K, Bushman M, Kishore N, Niehus R, de Salazar PM, et al. Estimating clinical severity of COVID-19 from the transmission dynamics in Wuhan, China. *Nature Medicine*. 2020; p.1–5.
- [244] Wang X, Ma Z, Ning Y, Chen C, Chen R, Chen Q, et al. Estimating the case fatality ratio of the COVID-19 epidemic in China. *medRxiv*. 2020;.
- [245] Jung Sm, Akhmetzhanov AR, Hayashi K, Linton NM, Yang Y, Yuan B, et al. Real-time estimation of the risk of death from novel coronavirus (covid-19) infection: Inference using exported cases. *Journal of clinical medicine*. 2020;9(2):523.
- [246] Dorigatti I, Okell L, Cori A, Imai N, Baguelin M, Bhatia S. Severity of 2019 novel coronavirus (nCoV); 2020. <https://www.imperial.ac.uk/media/imperial-college/medicine/sph/ide/gida-fellowships/Imperial-College-2019-nCoV-severity-10-02-2020.pdf>.
- [247] Riou J, Hauser A, Counotte MJ, Althaus CL. Adjusted age-specific case fatality ratio during the COVID-19 epidemic in Hubei, China, January and February 2020. *medRxiv*. 2020;doi:10.1101/2020.03.04.20031104.
- [248] Hethcote HW. The mathematics of infectious diseases. *SIAM review*. 2000;42(4):599–653.
- [249] Flaxman S, Mishra S, Gandy A, Unwin JT, Coupland H, Mellan TA, et al. Report 13: Estimating the number of infections and the impact of non-pharmaceutical interventions on COVID-19 in 11 European countries;. Available from: <https://doi.org/10.25561/77731>.

Annexes

Annex A: S1 File of Chapter 2

eAppendix Hauser

Search strategies performed in 7 databases:

| | Before deduplication | After deduplication | Date searched |
|-----------------------------|----------------------|---------------------|---------------|
| Medline Ovid | 1794 | 1794 | 15.05.2019 |
| Embase Ovid | 2854 | 1250 | 15.05.2019 |
| Cochrane Library | 433 | 233 | 15.05.2019 |
| African Index Medicus (AIM) | 62 | 62* | 16.05.2019 |
| Web-of-Science | 2108 | 779 | 16.05.2019 |
| Clinical Trials. gov | 119 | 118 | 16.05.2019 |
| Google Scholar | 200 | 154 | 16.05.2019 |
| Total | 7570 | 4323 | |

*not possible to import AIM results in Endnote – please screen separately

4 Blocks:

1) Antiretroviral therapy AND 2) HIV1 AND 3) (Drug) resistance AND 4) Africa South of the Sahara

Search strategies

Database: **Ovid MEDLINE**(R) and Epub Ahead of Print, In-Process & Other Non-Indexed Citations, Daily and Versions(R) <1946 to May 14, 2019>

-
- 1 exp Anti-Retroviral Agents/ or exp Antiretroviral Therapy, Highly Active/ or exp Anti-HIV Agents/ (89260)
 - 2 (anti-hiv or antihiv or (anti-retrovir* or antiretrovir*) or ARV or ART or cART or HAART or (anti and hiv) or (anti and retroviral*) or (anti and acquired immun#deficiency) or (anti and acquired immun#-deficiency) or (anti and acquired immun* and deficiency)).ti,ab,kw. (167334)
 - 3 1 or 2 (210116)
 - 4 exp HIV Infections/ (269917)
 - 5 (hiv or hiv?1 or human immun#deficiency virus or human immun#-deficiency virus or (human immun# adj3 deficiency virus) or acquired immun#deficiency syndrome or acquired immun#-deficiency syndrome or (acquired immun# adj3 deficiency syndrome)).ti,ab,kw. (323922)
 - 6 4 or 5 (384542)
 - 7 exp Drug Resistance, Viral/ (12976)
 - 8 (resistan* and (mutat* or genotyp* or genetic* or drug*)).ti,ab,kw. (289103)
 - 9 7 or 8 (292643)
 - 10 exp Africa South of the Sahara/ (193898)
 - 11 (Africa or (African* not African-American*) or Afrika* or sub-Sahara* or subsahara* or Southern Africa or Western Africa or Eastern Africa or Central Africa or Angola or Benin or Botswana or Burkina Faso or Burundi or Cameroon or Cape Verde or Cabo Verde or Chad or Tchad or Comoros or Congo or Cote d'Ivoire or Ivory Coast or Djibouti or Equatorial Guinea or Eritrea or Ethiopia or Gabon or Gambia or Ghana or Guinea or Guinea-Bissau or Kenya or Lesotho or Liberia or Madagascar or Malawi or Mali or Mauritius or Mauritania or Mozambique or Namibia or Niger or Nigeria or Rwanda or Sao Tome or Senegal or Seychelles or Sierra Leone or Somalia or South Africa or Sudan or South Sudan or Swaziland or Togo or Uganda or Tanzania or Zambia or Zimbabwe).ti,ot,ab,kw,in,jn,ia,cp. (543020)
 - 12 10 or 11 (565920)
 - 13 3 and 6 and 9 and 12 (1794)

- 1 exp antiretrovirus agent/ or exp highly active antiretroviral therapy/ or antiviral agent/ (251078)
- 2 (anti-hiv or antihiv or (anti-retrovir* or antiretrovir*) or ARV or ART or cART or HAART or (anti and hiv) or (anti and retroviral*) or (anti and acquired immun#deficiency) or (anti and acquired immun#-deficiency) or (anti and acquired immun* and deficiency)).ti,ab,kw. (219391)
- 3 1 or 2 (396846)
- 4 exp Human immunodeficiency virus infection/ (361038)
- 5 (hiv or hiv?1 or human immun#deficiency virus or human immun#-deficiency virus or (human immun# adj3 deficiency virus) or acquired immun#deficiency syndrome or acquired immun#-deficiency syndrome or (acquired immun# adj3 deficiency syndrome)).ti,ab,kw. (407459)
- 6 4 or 5 (509145)
- 7 exp antiviral resistance/ (7854)
- 8 (resistan* and (mutat* or genotyp* or genetic* or drug*)).ti,ab,kw. (390742)
- 9 7 or 8 (393257)
- 10 exp "Africa south of the Sahara"/ (222698)
- 11 (Africa or (African* not African-American*) or Afrika* or sub-Sahara* or subsahara* or Southern Africa or Western Africa or Eastern Africa or Central Africa or Angola or Benin or Botswana or Burkina Faso or Burundi or Cameroon or Cape Verde or Cabo Verde or Chad or Tchad or Comoros or Congo or Cote d'Ivoire or Ivory Coast or Djibouti or Equatorial Guinea or Eritrea or Ethiopia or Gabon or Gambia or Ghana or Guinea or Guinea-Bissau or Kenya or Lesotho or Liberia or Madagascar or Malawi or Mali or Mauritius or Mauritania or Mozambique or Namibia or Niger or Nigeria or Rwanda or Sao Tome or Senegal or Seychelles or Sierra Leone or Somalia or South Africa or Sudan or South Sudan or Swaziland or Togo or Uganda or Tanzania or Zambia or Zimbabwe).ti,ab,kw,ot,jn,in,cp,ox,ga,go. (706876)
- 12 10 or 11 (706936)
- 13 3 and 6 and 9 and 12 (2854)

Cochrane Database of Systematic Reviews

Issue 5 of 12, May 2019
141 Cochrane Reviews

Cochrane Central Register of Controlled Trials

Issue 5 of 12, May 2019
280 Trials

| | | | | |
|-------------------------|--------------------------|---------------|-----------------|--------------------------|
| Cochrane Reviews 141 | Cochrane Protocols 12 | Trials 280 | Editorials 2 | Special collections 3 |
|-------------------------|--------------------------|---------------|-----------------|--------------------------|

Date Run: 15/05/2019 17:09:50

ID Search Hits

- #1 (anti-hiv OR antihiv OR anti-retrovir* OR antiretrovir*) OR ARV OR ART OR cART OR HAART OR (anti AND hiv) OR (anti AND retroviral*) OR (anti AND acquired immun?deficiency) OR (anti AND acquired immun? deficiency) OR (anti AND acquired immune* AND deficiency) 21338
- #2 (hiv OR hiv-1* OR hiv1 OR "human immunodeficiency virus" OR "human immunodeficiency virus" OR "human immuno-deficiency virus" OR "human immune-deficiency virus" OR ((human immun*) NEAR/3 (deficiency virus)) OR "acquired immunodeficiency syndrome" OR "acquired immunodeficiency syndrome" OR "acquired immuno-deficiency syndrome" OR "acquired immune-deficiency syndrome" OR ((acquired immun*) NEAR/3 (deficiency syndrome))) 31858
- #3 (resistan* AND (mutat* OR genotyp* OR genetic* OR drug*)) 40744
- #4 (Africa or (African* not African-American*) or Afrika* or sub-Sahara* or subsahara* or Southern Africa or Western Africa or Eastern Africa or Central Africa or Angola or Benin or Botswana or Burkina Faso or Burundi or Cameroon or Cape Verde or Cabo Verde or Chad or Tchad or Comoros or Congo or Cote d'Ivoire or Ivory Coast or Djibouti or Equatorial Guinea or Eritrea or Ethiopia or Gabon or Gambia or Ghana or Guinea or Guinea-Bissau or Kenya or Lesotho or Liberia or Madagascar or Malawi or Mali or Mauritius or Mauritania or Mozambique or Namibia or Niger or Nigeria or Rwanda or Sao Tome or Senegal or Seychelles or Sierra Leone or Somalia or South Africa or Sudan or South Sudan or Swaziland or Togo or Uganda or Tanzania or Zambia or Zimbabwe) 29366
- #5 #1 AND #2 AND #3 AND #4 441

Database: **AIM (African Index Medicus)**

Search history

2) Quick search: term **hiv + (antiretrovir* ART HAART ARV) + resistan*** in **Titles Keywords** for **all material types**

hiv + (antiretrovir* ART HAART ARV) + resistan*

62 records

AIM has an export function to Endnote, but it does not work. For screening you either have to reproduce the search (see above, in <http://indexmedicus.afro.who.int/> or you go through the html version I was able to generate (in the attachment of the mail).

Database: **Web of Science (WoS)**

| Set | Results | Save History / Create Alert Open Saved History |
|-----|-------------------------|---|
| # 5 | 2,108 | #1 AND #2 AND #3 AND #4 <i>Indexes=SCI-EXPANDED, SSCI, A&HCI, CPCI-S, CPCI-SSH, ESCI Timespan=All years</i> |
| # 4 | 854,679 | TS=(Africa or (African* not African-American*) or Afrika* or sub-Sahara* or subsahara* or Southern Africa or Western Africa or Eastern Africa or Central Africa or Angola or Benin or Botswana or Burkina Faso or Burundi or Cameroon or Cape Verde or Cabo Verde or Chad or Tchad or Comoros or Congo or Cote d'Ivoire or Ivory Coast or Djibouti or Equatorial Guinea or Eritrea or Ethiopia or Gabon or Gambia or Ghana or Guinea or Guinea-Bissau or Kenya or Lesotho or Liberia or Madagascar or Malawi or Mali or Mauritius or Mauritania or Mozambique or Namibia or Niger or Nigeria or Rwanda or Sao Tome or Senegal or Seychelles or Sierra Leone or Somalia or South Africa or Sudan or South Sudan or Swaziland or Togo or Uganda or Tanzania or Zambia or Zimbabwe) <i>Indexes=SCI-EXPANDED, SSCI, A&HCI, CPCI-S, CPCI-SSH, ESCI Timespan=All years</i> |
| # 3 | 393,697 | TS=(resistan* AND (mutat* OR genotyp* OR genetic* OR drug*)) <i>Indexes=SCI-EXPANDED, SSCI, A&HCI, CPCI-S, CPCI-SSH, ESCI Timespan=All years</i> |
| # 2 | 387,652 | TS=(hiv OR hiv-1* OR hiv1 OR "human immunodeficiency virus" OR "human immunodeficiency virus" OR "human immuno-deficiency virus" OR "human immune-deficiency virus" OR ((human immun*) NEAR/3 (deficiency virus)) OR "acquired immunodeficiency syndrome" OR "acquired immunodeficiency syndrome" OR "acquired immuno-deficiency syndrome" OR "acquired immune-deficiency syndrome" OR ((acquired immun*) NEAR/3 (deficiency syndrome))) <i>Indexes=SCI-EXPANDED, SSCI, A&HCI, CPCI-S, CPCI-SSH, ESCI Timespan=All years</i> |
| # 1 | 607,962 | TS=((anti-hiv OR antihiv OR anti-retrovir* OR antiretrovir*) OR ARV OR ART OR cART OR HAART OR (anti AND hiv) OR (anti AND retroviral*) OR (anti AND acquired immunodeficiency) OR (anti AND acquired immunodeficiency) OR (anti AND acquired immun* AND deficiency)) <i>Indexes=SCI-EXPANDED, SSCI, A&HCI, CPCI-S, CPCI-SSH, ESCI Timespan=All years</i> |

Database: **Clinical Trials.gov**

119 Studies found for: (Africa OR sub-Sahara OR Subsahara OR Southern Africa OR Western Africa OR Eastern Africa OR Central Africa OR Angola OR Benin OR Botswana OR Burkina Faso OR Burundi OR Cameroon OR Cape Verde OR Cabo Verde OR Chad OR Tchad OR Comoros OR Congo OR Cote d'Ivoire OR Ivory Coast OR Djibouti OR Equatorial Guinea OR Eritrea OR Ethiopia OR Gabon OR Gambia OR Ghana OR Guinea OR Guinea-Bissau OR Kenya OR Lesotho OR Liberia OR Madagascar OR Malawi OR Mali OR Mauritius OR Mauritania OR Mozambique OR Namibia OR Niger OR Nigeria OR Rwanda OR Sao Tome OR Senegal OR Seychelles OR Sierra Leone OR Somalia OR South Africa OR Sudan OR South Sudan OR Swaziland OR Togo OR Uganda OR Tanzania OR Zambia OR Zimbabwe) | HIV Infections OR Acquired Immunodeficiency Syndrome | HAART OR ART OR ARV OR antihiv OR antiretroviral | (drug OR genotype OR genetic OR mutation) AND resistance

Database: **Google Scholar**

antiretroviral|anti hiv|ART|HAART|ARV hiv|"human immunodeficiency virus"|"human immune deficiency virus"|"acquired immune deficiency syndrome"|"acquired immunodeficiency syndrome" (drug|mutation|genotype|genetic resistance) africa

Result set of 200 includes:

The first 100 results of the search without year restriction (relevancy ranking) -> the results' publication years range from 1999-2017. To catch the newer ones, an additional search for publications 2018-19 was performed, from which also the first 100 were taken (relevancy ranking).

Last but not least: We recommend citation tracking (backward and forward) in Google Scholar or Web of Science for included studies.

Please fill in the PRISMA Flow diagram:

<http://prisma-statement.org/prismastatement/flowdiagram.aspx>

Annex B: S2 File of Chapter 2

SUPPLEMENTARY MATERIAL

Acquired HIV drug resistance mutations on first-line anti-retroviral therapy in Southern Africa: Systematic review and Bayesian evidence synthesis

Anthony Hauser¹, Fardo Goldstein¹, Martina L. Reichmuth¹, Roger D. Kouyos^{2,3}, Nicola Low¹, Gilles Wandeler^{1,4}, Matthias Egger^{1,5,6}, and Julien Riou¹

¹Institute of Social and Preventive Medicine, University of Bern, Switzerland

²Division of Infectious Diseases and Hospital Epidemiology, University Hospital Zurich, University of Zurich, Zurich, Switzerland

³Institute of Medical Virology, University of Zurich, Zurich, Switzerland

⁴Department of Infectious Diseases, Bern University Hospital, University of Bern, Bern, Switzerland

⁵Centre for Infectious Disease Epidemiology and Research, University of Cape Town, South Africa

⁶Population Health Sciences, Bristol Medical School, University of Bristol, Bristol, United Kingdom

March 24, 2021

Contents

| | | |
|----------|---|----------|
| 1 | Model description | 2 |
| 1.1 | Modeling the prevalence of NRTI mutations | 2 |
| 1.2 | Estimating the prevalence of any TAM mutation | 3 |
| 1.3 | Likelihood function for the NRTI mutations | 4 |
| 1.4 | Selection of regression variables | 4 |
| 1.5 | Modeling the prevalence of NNRTI mutations | 5 |
| 1.6 | Imputing missing information on ART duration | 6 |
| 2 | Parameter estimates | 7 |
| 2.1 | Prevalence of the NRTI mutations | 7 |
| 2.2 | Prevalence of the NNRTI mutations | 7 |
| 2.3 | Other parameter estimates | 7 |
| 3 | Sensitivity analysis | 9 |
| 3.1 | Risk of bias | 9 |
| 3.2 | Removing studies with missing information on ART duration | 9 |
| 3.3 | No selection of regression variables | 10 |

1 Model description

1.1 Modeling the prevalence of NRTI mutations

Main model

We used a mathematical model to estimate the prevalence $p_{m,x}(t)$ of a given NRTI mutation m after a duration t on a given treatment x . The treatment x consists of the combination of two NRTI drugs. We considered the effect of five different NRTI drugs: didanosine (ddI), emtricitabine/lamivudine (FTC/3TC), tenofovir disoproxil fumarate (TDF), stavudine (d4T) and zidovudine (ZDV). A parameter α_m represents the baseline prevalence (i.e. the prevalence at time $t = 0$) of the mutation m : $p_{m,x}(0) = \alpha_m$. Assuming that the risk of acquiring resistance is constant over time, we used an exponential distribution to represent the time to acquire the mutation m . The prevalence $p_{m,x}(t)$ over time after a given treatment x was described by:

$$p_{m,x}(t) = 1 - (1 - \alpha_m) \cdot \exp(-\lambda_{m,x} \cdot t), \quad (1)$$

where $\lambda_{m,x} = \sum_{j \in x} \beta_m^j$ represents the combined effect of the two NRTI drugs x .

Model accounting for study heterogeneity

The model was fitted to 17 populations collected from 16 studies that reported the prevalence of the eight single NRTI mutations. We defined x_i^j as the proportion of people using the NRTI drug j ($j = 1, \dots, 5$) in study i and t_i the duration of treatment. To represent the heterogeneity observed between studies, we introduced a hierarchical study effect for the parameters β_m^j . It consists of two random effects U and V_m that multiply the parameters β_m^j . The random effect U does not depend on the mutation and therefore affects all the eight NRTI mutations equally. Such effect reflects the different study characteristics, e.g. levels of adherence, which influenced the level of any resistance mutation. The random effect V_m represents the remaining heterogeneity that is specific to the mutation m . To obtain the study-specific parameter $\tilde{\beta}_{i,m}^j$ for study i , we multiplied β_m^j by \tilde{u}_i and $\tilde{v}_{i,m}$, which are the realizations of the two random effects U and V_m , respectively:

$$\tilde{\beta}_{i,m}^j = \beta_m^j \cdot \tilde{u}_i \cdot \tilde{v}_{i,m}. \quad (2)$$

We assumed that U and V_m followed log-normal distributions with free variance parameters τ^2 and σ_m^2 respectively. The mean parameters are fixed to $-\tau^2/2$ for u_i and $-\sigma_m^2/2$ for $v_{i,m}$, so that $\mathbb{E}(U) = 1$ and $\mathbb{E}(V_m) = 1$:

$$U \sim \log\mathcal{N}\left(-\frac{\tau^2}{2}, \tau^2\right), \quad (3)$$

$$V_m \sim \log\mathcal{N}\left(-\frac{\sigma_m^2}{2}, \sigma_m^2\right). \quad (4)$$

If we write $B_m^j := \beta_m^j \cdot U \cdot V_m$ the random variable representing the distribution of β_m^j across the studies, we thus have:

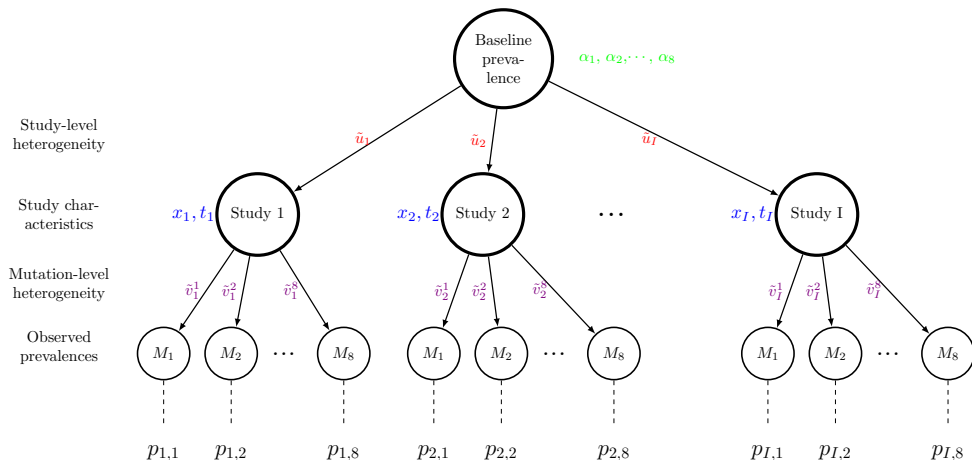
$$B_m^j \sim \log\mathcal{N}\left(-\frac{\tau^2 + \sigma_m^2}{2} + \log(\beta_m^j), \tau^2 + \sigma_m^2\right) \quad \text{and} \quad \mathbb{E}(B_m^j) = \beta_m^j. \quad (5)$$

The prevalence of the mutation m in study i is :

$$p_{i,m} = 1 - (1 - \alpha_m) \cdot \exp\left(-\sum_{j=1}^5 \tilde{\beta}_{i,m}^j x_i^j \cdot t_i\right), \quad (6)$$

where x_i^j represents the proportion of people treated with NRTI drug j in study i .

Fig 1 displays the hierarchical model with the two heterogeneity levels: 1) study-level and 2) mutation-level.



$$p_{i,m} = 1 - (1 - \alpha_m) \cdot \exp\left(-\sum_{j=1}^J \tilde{\beta}_{i,m}^j x_i^j \cdot t_i\right), \text{ where}$$

$$\tilde{\beta}_{i,m}^j = \beta_m^j \cdot \tilde{u}_i \cdot \tilde{v}_{i,m} \quad \tilde{u}_i \sim \log\mathcal{N}\left(-\frac{\tau^2}{2}, \tau^2\right) \quad \tilde{v}_{i,m} \sim \log\mathcal{N}\left(-\frac{\sigma_m^2}{2}, \sigma_m^2\right)$$

Fig 1: Hierarchical model developed to represent the study-specific prevalences of the 8 NRTI mutations.

1.2 Estimating the prevalence of any TAM mutation

We estimated the prevalence of having at least one of the six TAM mutations (M41L, D67E/G/N, K70E/G/R, L210W, T215F/I/N/S/Y, K219Q/E) differently as for the eight single NRTI mutations. Unlike the eight single NRTI mutations, modelling the prevalence of any TAMs is more complex as it depends on the prevalence of six mutations. In addition, only 11 of the 17 study populations reported the prevalence of any TAM. For these reasons, applying the same model to measure the prevalence of any TAM could provide unreliable estimates of the parameters α_m , β_m^j and σ_m . We thus used another model that involved less parameters to estimate this prevalence.

First, we observe:

$$\Pr(\text{any TAM}) = 1 - \Pr(\text{no TAM}). \quad (7)$$

The probability $\Pr(\text{no TAM})$ has two natural boundaries determined by the level of correlation of the six TAM mutations. The lower boundary is reached when the six TAMs are independent. In this case, we have $\Pr(\text{no TAM}) = \prod_{i=1}^6 \Pr(\text{no TAM}_i) = \prod_{i=1}^6 (1 - \Pr(\text{TAM}_i))$. We assumed here that TAMs could only be positively correlated. The higher boundary is reached at $\Pr(\text{no TAM}) = \min(\Pr(\text{no TAM}_i)) = 1 - \max(\Pr(\text{TAM}_i))$, which occurs when the TAMs are highly positively correlated. To formally express the probability $\Pr(\text{no TAM})$ as a function of the correlations between the single TAMs, we used a multivariate Bernoulli distribution. If we write $p_i := \Pr(\text{no TAM}_i)$ and $X_i \sim \text{Bernoulli}(p_i)$, the probability $\Pr(\text{no TAM})$ is fully determined by the correlations between the variables X_1, \dots, X_6 :

$$\begin{aligned} \Pr(\text{no TAM}) &= \Pr(X_1 = 1, \dots, X_6 = 1) \\ &= \sigma_{1,\dots,6} + \sum_{i=1}^6 p_i \cdot \sigma_{\{1,\dots,6\} \setminus i} + \sum_{1 \leq i < j \leq 6} p_i p_j \cdot \sigma_{\{1,\dots,6\} \setminus \{i,j\}} \\ &\quad + \sum_{1 \leq i < j < k \leq 6} p_i p_j p_k \cdot \sigma_{\{1,\dots,6\} \setminus \{i,j,k\}} + \dots + \prod_{i=1}^6 p_i \\ &:= f(p_1, \dots, p_6, \sigma), \end{aligned} \quad (8)$$

where $\sigma_S := \mathbb{E}\left(\prod_{i \in S} (X_i - p_i)\right)$ corresponds to the correlations (second and higher order) between the variables comprised in a subset S of $\{1, \dots, 6\}$ (see [1]).

We wrote σ_{\min} and σ_{\max} the correlation sets that reach the lower and higher bound, respectively: $p_{\min} = f(p_1, \dots, p_6, \sigma_{\min})$ and $p_{\max} = f(p_1, \dots, p_6, \sigma_{\max})$. From Eq 8, we easily see that $\sigma_{\min} = 0$. To estimate the

correlations σ between TAMs observed in the studies, we used a scale parameter γ ($\gamma \in [0, 1]$) that measures the level of correlation between the six TAMs:

$$\Pr(\text{no TAM}) = f(p_1, \dots, p_6, \gamma \cdot \sigma_{\max}). \quad (9)$$

A value $\gamma = 0$ corresponds to the situation where the six TAM mutations are independent (i.e. $\sigma = 0$), while $\gamma = 1$ corresponds to the situation where probability of any TAM reaches the maximum p_{\max} . From Eq 8, we also observed:

$$\Pr(\text{no TAM}) = f(p_1, \dots, p_6, \gamma \cdot \sigma_{\max}) \quad (10)$$

$$= p_{\min} + \gamma \cdot (p_{\max} - p_{\min}). \quad (11)$$

Therefore, the prevalence of any of the six TAMs in study i were:

$$\Pr_i(\text{TAM}) = 1 - (p_i^{\min} + \gamma \cdot (p_i^{\max} - p_i^{\min})), \quad (12)$$

with $p_i^{\min} = \prod_{m=1}^6 (1 - p_{i,m})$ and $p_i^{\max} = 1 - \max(p_{i,m})$.

1.3 Likelihood function for the NRTI mutations

Given the number of participants n_i in study i , we assumed that the number $k_{i,m}$ of them with mutation m and the number $k_{i,\text{TAM}}$ with at least one TAM mutation are binomially distributed:

$$k_{i,m} \sim \text{Bin}(p_{i,m}, n_i), \quad (13)$$

$$k_{i,\text{TAM}} \sim \text{Bin}(\Pr_i(\text{TAM}), n_i). \quad (14)$$

The prevalence $p_{i,m}$ of the mutation m in study i is given by Eq 6. It depends on the baseline prevalence α_m of mutation m , the effect β_m^j of drug j on mutation m , the shared and mutation-specific study-perturbations u_i and $v_{i,m}$, respectively. The prevalence $\Pr_i(\text{TAM})$ of any of the six TAMs in study i is given by Eq 12. It depends on the prevalences of the 6 TAMs in study i (as given by Eq 6) and on the correlation parameter γ .

We simultaneously estimated the parameters α_m , β_m^j , τ , σ_m and γ with the following likelihood function:

$$L(\alpha_m, \beta_m^j, \tau, \sigma_m, \gamma) = \prod_{i=1}^I \prod_{m=1}^N \Pr(k_{i,m} | n_i, p_{i,m}) \cdot \prod_{i \in S_{\text{TAM}}} \Pr(k_{i,\text{TAM}} | n_i, \Pr_i(\text{TAM})) \quad (15)$$

where I is the number of studies (here $I = 17$), N the number of NRTI mutations (here $N = 8$) and S_{TAM} the indices of the eleven studies reporting the prevalence of any TAM. We implemented the model in a Bayesian framework using Stan [2]. The prior distributions used for the different parameters are displayed in Table 1.

Table 1: Summary of parameters for NRTI mutations.

| Symbol | Comment | Support | Prior |
|-------------|---|----------------|------------|
| α_m | Baseline prevalence of mutation m | $[0 - 1]$ | Beta(1, 9) |
| β_m^j | Effect of the NRTI drug j on the prevalence of mutation m | $[0 - \infty[$ | Exp(1) |
| τ | Overall between-study heterogeneity | $[0 - \infty[$ | Exp(1) |
| σ_m | Study-heterogeneity for mutation m | $[0 - \infty[$ | Exp(1) |
| γ | Level of correlation between TAM mutations | $[0 - 1]$ | Beta(1, 1) |

1.4 Selection of regression variables

In the 17 study populations where the use of NRTI drugs was reported, most of the patients were taking either ddI or FTC/3TC, combined with one of the three following NRTIs: TDF, ZDV, d4T. As a result, we observe negative correlations between ddI and FTC/3TC and between any two NRTI drugs among TDF, ZDV and d4T (Fig 2). These correlations between the different covariates can prevent the model from disentangling the effects of the different NRTI drugs on the mutation prevalence. Therefore, we used a simple variable selection method

to select covariates that have an effect on the occurrence of a mutation. We first separated the five NRTI drugs into two groups 1) ddI and FTC/3TC, and 2) TDF, ZDV, d4T. Each group gathers the drugs that show high correlation between each other, as they are used exchangeably. The selection method removed the covariate with the most negative effect (i.e. the lowest estimated β) for each of the two groups and estimated the prevalences with the remaining covariates. The rationale of this method is based on two observations. First, NRTI drugs do not have a negative effect on the occurrence of a mutation. Second, for each NRTI mutation, there is at least one NRTI drug that has minor or no effect on the occurrence of the mutation. The estimated prevalences of the nine NRTI mutations when applying the full model (i.e. without variable selection) are displayed in Section 3.3.

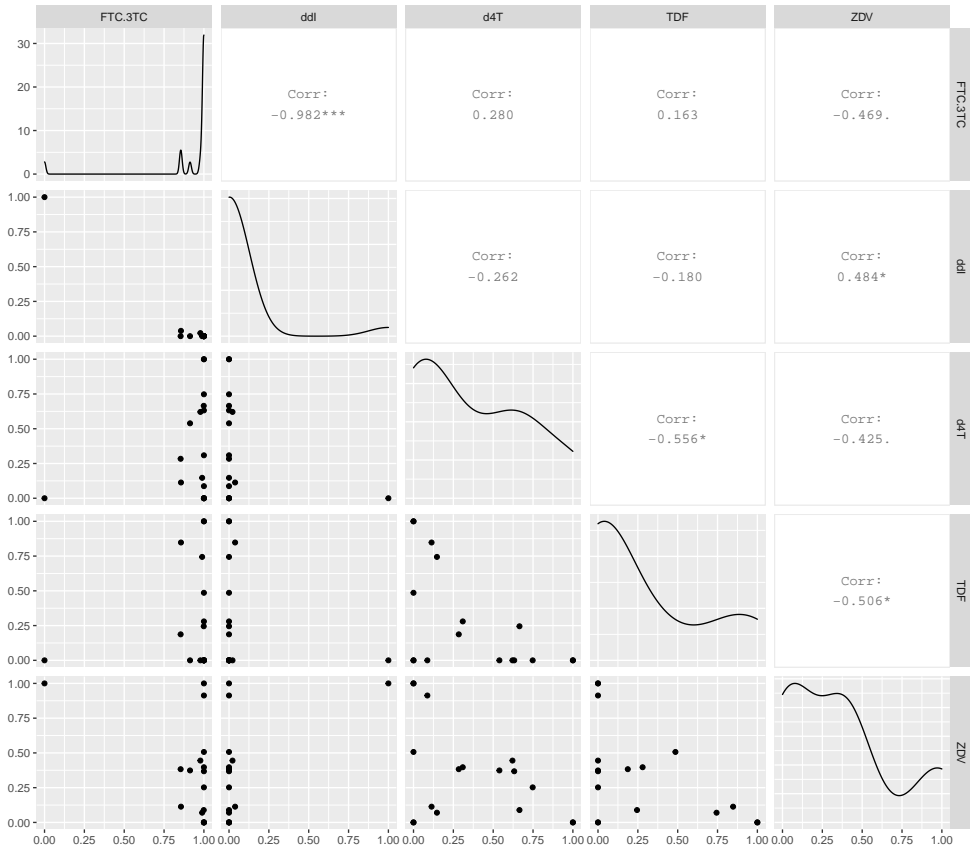


Fig 2: Correlation between the uses of NRTI drugs across studies. Abbreviation: FTC.3TC, emtricitabine; or lamivudine; ddI, didanosine; TDF, tenofovir disoproxil fumarate; d4T, stavudine; ZDV, zidovudine.

1.5 Modeling the prevalence of NNRTI mutations

We used the same mathematical model to estimate the prevalence $p_{m,x}(t)$ of a given NNRTI mutation m after a duration t on a given NNRTI drug x . We considered the effect of two different NNRTI drugs: nevirapine (NVP) and efavirenz (EFV). Using the aforementioned notations, we derive the prevalence $p_{m,x}(t)$ over time after a given treatment x (NVP or EFV):

$$p_{m,x}(t) = 1 - (1 - \alpha_m) \cdot \exp(-\beta_m^x \cdot t). \quad (16)$$

The prevalence of the mutation m in study i is :

$$p_{i,m} = 1 - (1 - \alpha_m) \cdot \exp\left(-\sum_{j=1}^2 \tilde{\beta}_{i,m}^j \cdot x_i^j \cdot t_i\right), \quad (17)$$

where x_i^j represents the proportion of people treated with NNRTI drug j in study i . Again, we assumed that the number $k_{i,m}$ of participants of study i with mutation m is binomially distributed:

$$k_{i,m} \sim \text{Bin}(p_{i,m}, n_i). \quad (18)$$

We simultaneously estimated the parameters $\alpha_m, \beta_m^j, \tau, \sigma_m$ by using the following likelihood function:

$$L(\alpha_m, \beta_m^j, \tau, \sigma_m) = \prod_{i=1}^I \prod_{m=1}^N \Pr(k_{i,m} | n_i, p_{i,m}), \quad (19)$$

where I is the number of studies (here $I = 13$) and N the number of NNRTI mutations (here $N = 7$). Table 2 displays the prior distributions assumed for the different parameters.

Table 2: Summary of parameters for NNRTI mutations.

| Symbol | Comment | Support | Prior |
|-------------|--|----------------|------------|
| α_m | Baseline prevalence of mutation m | $[0 - 1]$ | Beta(1, 9) |
| β_m^j | Effect of the NNRTI drug j on the prevalence of mutation m | $[0 - \infty[$ | Exp(1) |
| τ | Overall between-study heterogeneity | $[0 - \infty[$ | Exp(1) |
| σ_m | Study-heterogeneity for mutation m | $[0 - \infty[$ | Exp(1) |

1.6 Imputing missing information on ART duration

Among the 17 study populations that were used to estimate the prevalence of the NRTI/NNRTI mutations, three of them did not report the ART duration [3, 4, 5]. In order not to lose the information given by the three studies with missing ART duration, we imputed the duration on ART, assuming a gamma distribution with the same mean and standard deviation as found in the 14 study populations with reported ART duration. The mean was 25.6 months and standard deviation 15.7 months. The estimated NRTI/NNRTI prevalences when discarding studies that do not report ART duration are displayed in Section 3.2.

2 Parameter estimates

2.1 Prevalence of the NRTI mutations

Table 3: Prevalences of the nine NRTI mutations at baseline and after 2 and 3 years on either FTC/3TC + TDF or FTC/3TC + ZDV.

| Mutation | Prevalence [95% CrI] | | | | |
|----------|-----------------------|------------------------------|------------------------------|------------------------------|------------------------------|
| | At baseline | After 2 years on FTC/3TC+TDF | After 2 years on FTC/3TC+ZDV | After 3 years on FTC/3TC+TDF | After 3 years on FTC/3TC+ZDV |
| M41 | 2.1% [0.7%,4.3%] | 5.5% [2.4%,19%] | 15.9% [8.8%,29.6%] | 7% [2.8%,26.4%] | 22.1% [11.7%,40.4%] |
| K65 | 1.5% [0.1%,3.2%] | 55.2% [34.3%,79.4%] | 1.5% [0.1%,3.2%] | 69.9% [46.3%,90.6%] | 1.5% [0.1%,3.2%] |
| D67 | 5% [2.4%,8.1%] | 5% [2.4%,8.1%] | 25% [14.8%,39.9%] | 5% [2.4%,8.1%] | 33.3% [19.3%,52.2%] |
| K70 | 4.1% [1.8%,7.1%] | 15.1% [9.5%,25%] | 23.8% [15.8%,36.2%] | 19.9% [12.3%,33.8%] | 32% [20.6%,48.1%] |
| M184 | 15.1% [0.9%,29.9%] | 78.3% [64.7%,90.5%] | 73.5% [57.9%,87.1%] | 89.1% [76.7%,96.9%] | 85.2% [69.8%,95%] |
| L210 | 0.6% [0.1%,1.3%] | 0.6% [0.1%,1.3%] | 5.4% [1.5%,18.3%] | 0.6% [0.1%,1.3%] | 7.8% [2%,25.8%] |
| T215 | 0.9% [0.1%,2.8%] | 0.9% [0.1%,2.8%] | 26% [15.2%,41.1%] | 0.9% [0.1%,2.8%] | 36% [21.5%,54.6%] |
| K219 | 1.2% [0.1%,3.8%] | 12% [7.2%,22%] | 17.2% [10.1%,28.4%] | 16.8% [9.9%,30.6%] | 24.2% [14%,38.9%] |
| TAM | 8.5% [5.7%,11.7%] | 22.9% [16.1%,34.8%] | 45.6% [34%,59.3%] | 29.5% [20.1%,45%] | 49.9% [38.2%,62.6%] |

2.2 Prevalence of the NNRTI mutations

Table 4: Prevalences of the seven NNRTI mutations at baseline and after 2 and 3 years on either EFV or NVP.

| Mutation | Prevalence [95% CrI] | | | | |
|----------|-----------------------|------------------------|------------------------|------------------------|------------------------|
| | At baseline | After 2 years on EFV | After 2 years on NVP | After 3 years on EFV | After 3 years on NVP |
| K101 | 2.1% [1.2%,3.4%] | 7.5% [2.3%,24.1%] | 18.7% [5.7%,45.1%] | 10.1% [2.5%,33.1%] | 25.8% [7.3%,58.9%] |
| K103 | 16.8% [8.2%,30.6%] | 59.8% [42.8%,78.8%] | 39.3% [22%,66%] | 71.9% [51.5%,89.3%] | 47.8% [25.6%,78.4%] |
| V106 | 9.5% [5.5%,14.3%] | 44.6% [32.5%,62.6%] | 13% [7.4%,27.8%] | 56.7% [41.2%,75.8%] | 14.4% [7.8%,35%] |
| V108 | 5.1% [3.1%,7.6%] | 8.9% [4.8%,21.4%] | 15.3% [6.3%,35%] | 10.7% [5.2%,28.6%] | 19.9% [7%,46.3%] |
| Y181 | 5.5% [3.1%,8.4%] | 9.5% [4.7%,22.7%] | 41.9% [23.5%,63.1%] | 11.2% [5.1%,30%] | 54.4% [31%,77%] |
| Y188 | 5.5% [3.1%,8.4%] | 13.3% [8.8%,27.1%] | 8.1% [4.5%,21.5%] | 16.9% [10%,36.3%] | 9.1% [4.8%,28.5%] |
| G190 | 8.3% [4.9%,11.9%] | 15.4% [9.5%,25.2%] | 35.8% [22.4%,54.1%] | 18.7% [10.3%,32.6%] | 46.2% [28.8%,67.7%] |

2.3 Other parameter estimates

Table 5: Estimates of other parameters

| (a) NRTI mutations | | (b) NNRTI mutations | |
|--------------------------------|---------------------|--------------------------------|---------------------|
| Parameters | Median [95% CrI] | Parameters | Median [95% CrI] |
| τ^2 | 0.5 [0.2,1.25] | τ^2 | 0.67 [0.25,1.57] |
| σ_1^2 | 0.32 [0,2.07] | σ_1^2 | 1.74 [0.62,3.41] |
| σ_2^2 | 0.96 [0.3,2.42] | σ_2^2 | 0.42 [0.06,1.38] |
| σ_3^2 | 0.13 [0,0.85] | σ_3^2 | 0.21 [0,1.33] |
| σ_4^2 | 0.05 [0,0.52] | σ_4^2 | 0.86 [0.01,2.86] |
| σ_5^2 | 0.19 [0.03,0.65] | σ_5^2 | 0.25 [0,1.56] |
| σ_6^2 | 1.61 [0.15,3.56] | σ_6^2 | 0.66 [0,2.86] |
| σ_7^2 | 0.08 [0,0.73] | σ_7^2 | 0.03 [0,0.59] |
| σ_8^2 | 0.03 [0,0.36] | $\tau^2/(\tau^2 + \sigma_1^2)$ | 28% [10.1%,59.7%] |
| $\tau^2/(\tau^2 + \sigma_1^2)$ | 61.6% [14.8%,99.8%] | $\tau^2/(\tau^2 + \sigma_2^2)$ | 61.2% [28.2%,92.2%] |
| $\tau^2/(\tau^2 + \sigma_2^2)$ | 34.5% [12.2%,70.5%] | $\tau^2/(\tau^2 + \sigma_3^2)$ | 76.7% [23.7%,99.9%] |
| $\tau^2/(\tau^2 + \sigma_3^2)$ | 80.1% [30.3%,99.8%] | $\tau^2/(\tau^2 + \sigma_4^2)$ | 44.7% [13.7%,98.8%] |
| $\tau^2/(\tau^2 + \sigma_4^2)$ | 92.1% [42.2%,100%] | $\tau^2/(\tau^2 + \sigma_5^2)$ | 73% [24.8%,99.6%] |
| $\tau^2/(\tau^2 + \sigma_5^2)$ | 72.8% [39%,95.9%] | $\tau^2/(\tau^2 + \sigma_6^2)$ | 50.8% [13.2%,99.5%] |
| $\tau^2/(\tau^2 + \sigma_6^2)$ | 25% [8.1%,79.2%] | $\tau^2/(\tau^2 + \sigma_7^2)$ | 95.3% [45.4%,100%] |
| $\tau^2/(\tau^2 + \sigma_7^2)$ | 86.6% [36.6%,99.9%] | | |
| $\tau^2/(\tau^2 + \sigma_8^2)$ | 94.8% [55.4%,100%] | | |
| γ | 63.2% [54.4%,71.7%] | | |

3 Sensitivity analysis

3.1 Risk of bias

Fig 3 displays the estimated prevalences of the NRTI (Panel A) and NNRTI (Panel B) DRMs after having removed the studies with high risk of bias.

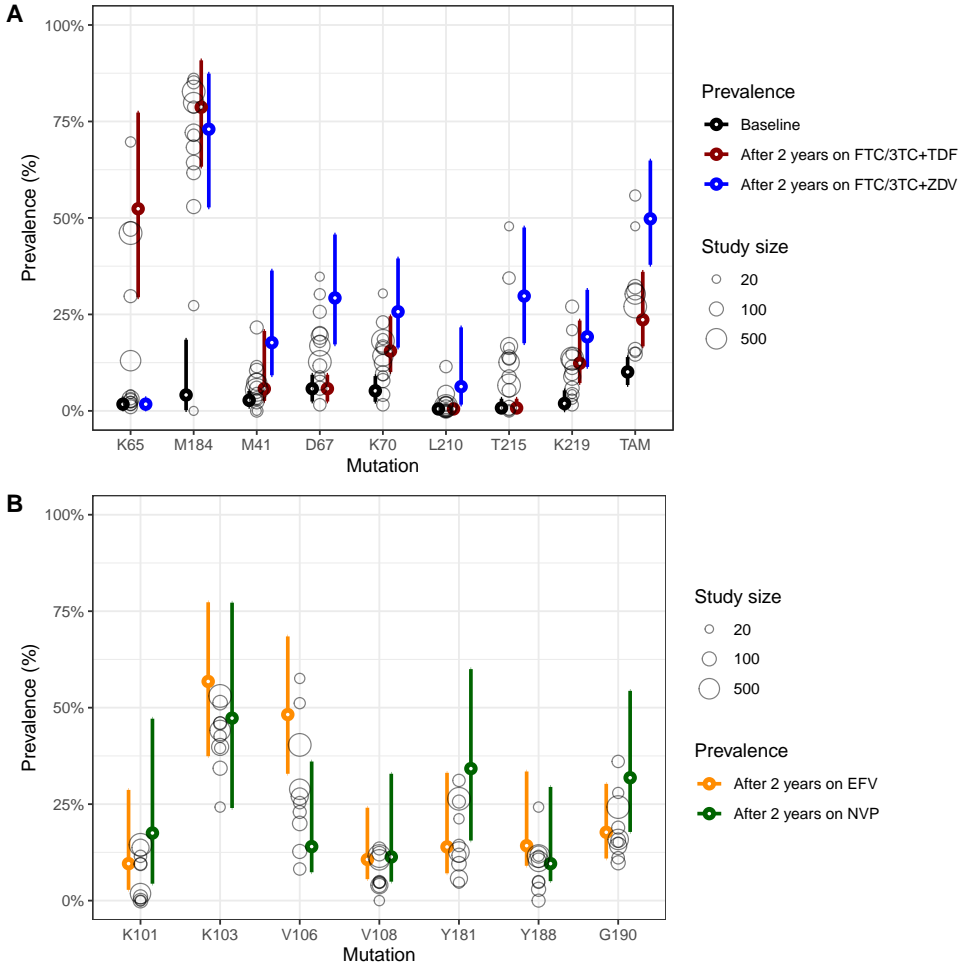


Fig 3: Panel A: prevalence of the nine NRTI drug resistance mutations by first-line regimen. Points and vertical lines: median and 95% credibility intervals of baseline prevalence (black), prevalence after 2 years on 3TC/FTC + TDF (red) or 3TC/FTC + ZDV (blue). Panel B: prevalence of seven NNRTI drug resistance mutations by first-line regimen. Points and vertical lines: median and 95% credibility intervals of prevalence after 2 years on EFV (orange) or NVP (green).

3.2 Removing studies with missing information on ART duration

Fig 4 displays the estimated prevalences of the NRTI (Panel A) and NNRTI (Panel B) DRMs after having removed the studies with missing information on ART duration.

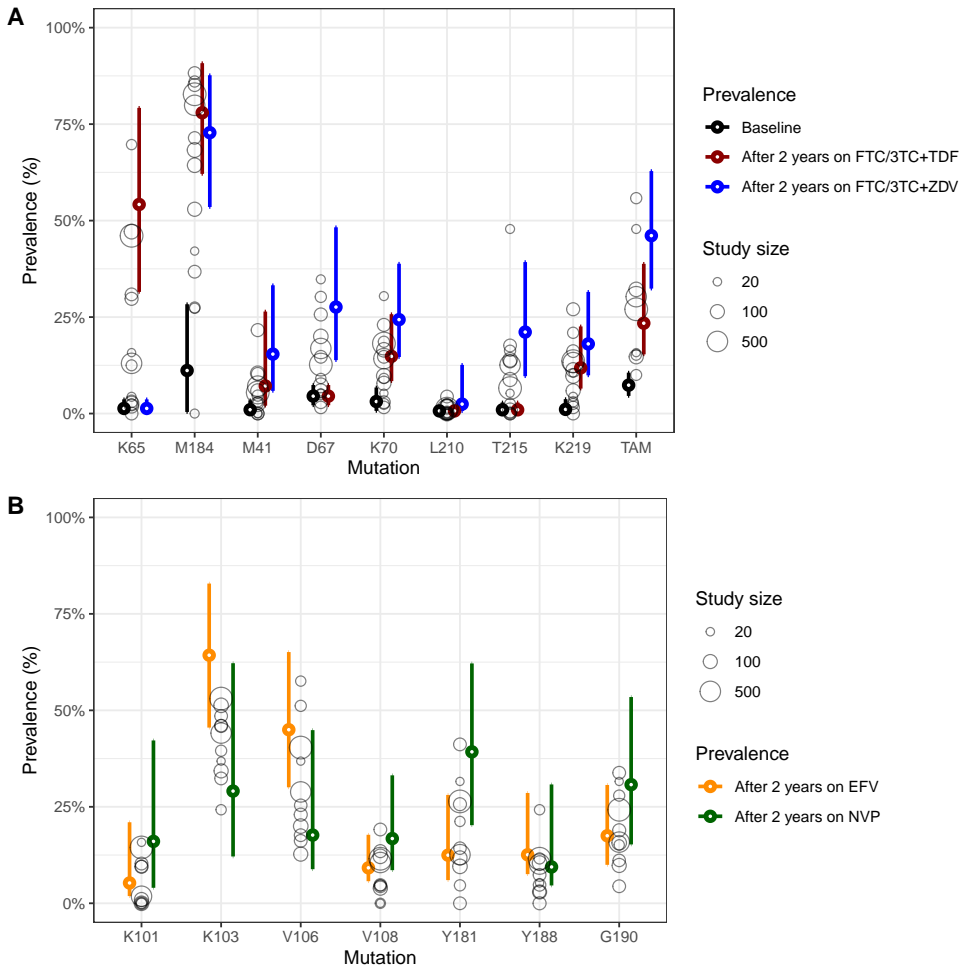


Fig 4: Panel A: prevalence of the nine NRTI drug resistance mutations by first-line regimen. Points and vertical lines: median and 95% credibility intervals of baseline prevalence (black), prevalence after 2 years on 3TC/FTC + TDF (red) or 3TC/FTC + ZDV (blue). Panel B: prevalence of seven NNRTI drug resistance mutations by first-line regimen. Points and vertical lines: median and 95% credibility intervals of prevalence after 2 years on EFV (orange) or NVP (green).

3.3 No selection of regression variables

Fig 5 displays the estimated prevalences of the NRTI DRMs when we used the five NRTI drugs as regression variables (i.e. we did not apply the selection step).

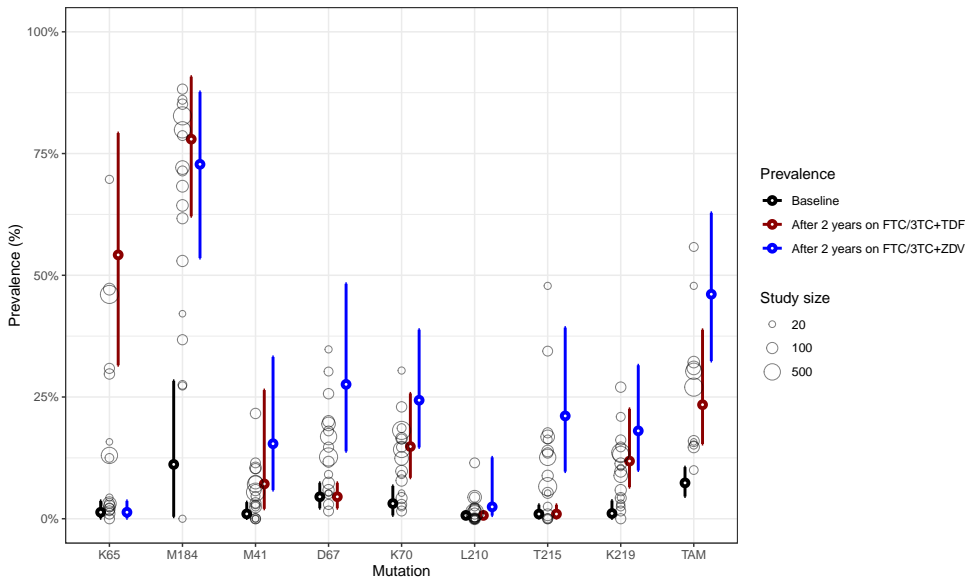


Fig 5: Prevalence of the nine NRTI drug resistance mutations by first-line regimen. Points and vertical lines: median and 95% credibility intervals of baseline prevalence (black), prevalence after 2 years on 3TC/FTC + TDF (red) or 3TC/FTC + ZDV (blue).

References

- [1] Teugels JL. Some representations of the multivariate Bernoulli and binomial distributions. *Journal of Multivariate Analysis*. 1990 feb;32(2):256–268.
- [2] Carpenter B, Gelman A, Hoffman MD, Lee D, Goodrich B, Betancourt M, et al. Stan: A probabilistic programming language. *Journal of statistical software*. 2017;76(1).
- [3] El-Khatib Z, Ekstrom AM, Ledwaba J, Mohapi L, Laher F, Karstaedt A, et al. Viremia and drug resistance among HIV-1 patients on antiretroviral treatment: a cross-sectional study in Soweto, South Africa. *Wolters Kluwer Health | Lippincott Williams & Wilkins AIDS Wolters Kluwer Health*. 2010;24:1679–1687. Available from: <https://insights.ovid.com/crossref?an=00002030-201007170-00008>.
- [4] Rupérez M, Pou C, Maculuve S, Cedeño S, Luis L, Rodríguez J, et al. Determinants of virological failure and antiretroviral drug resistance in Mozambique. *Journal of Antimicrobial Chemotherapy*. 2015 sep;70(9):2639–2647. Available from: <https://academic.oup.com/jac/article-lookup/doi/10.1093/jac/dkv143>.
- [5] Wallis CL, Mellors JW, Venter WDF, Sanne I, Stevens W. Varied Patterns of HIV-1 Drug Resistance on Failing First-Line Antiretroviral Therapy in South Africa. *JAIDS Journal of Acquired Immune Deficiency Syndromes*. 2010 apr;53(4):480–484. Available from: <http://journals.lww.com/00126334-201004010-00007>.

Annex C: S1 File of Chapter 3

SUPPLEMENTARY MATERIAL

Bridging the gap between HIV epidemiology and antiretroviral resistance evolution: Modelling the spread of resistance in South Africa

Anthony HAUSER & al.

March 24, 2021

Contents

| | | |
|----------|--|-----------|
| 1 | Model structure | 1 |
| 1.1 | Modelling HIV transmission | 2 |
| 1.2 | Modelling mortality | 2 |
| 1.3 | Modelling diagnosis and treatment rate | 3 |
| 1.4 | Modelling resistance | 4 |
| 1.5 | Modelling demographic changes | 5 |
| 2 | Model equations | 5 |
| 2.1 | Notations | 5 |
| 2.2 | ODEs | 8 |
| 2.3 | Starting values | 8 |
| 3 | Calibration and model simulation | 9 |
| 3.1 | Survival analysis | 9 |
| 3.2 | Likelihood maximisation | 10 |
| 4 | Results | 12 |
| 4.1 | Best fits | 12 |
| 4.2 | Sensitivity analysis | 13 |
| 5 | References | 14 |

1 Model structure

The model is split in 4 dimensions: 1) care stages (8 levels), 2) disease progression, characterised by the CD4 counts (4 levels), 3) NNRTI resistance, and 4) gender. The eight care stages are "infected but not diagnosed" (I), "diagnosed but not treated" (D), "started treatment" (T_1 and T_2 , respectively for first and second-line treatment), "suppressed" (S_1 and S_2) and "failed" (F_1 and F_2). An individual is considered as having "started treatment" (T_1 or T_2) if he initiated treatment less than 3 months ago. Afterwards, he/she is considered either as suppressed if VL < 1000 cp/ml, or as failed otherwise.

The four different CD4 strata are represented by the letter i in the equations and are respectively: $CD4 > 500\text{cells}/\mu\text{l}$ ($i = 1$), $350 < CD4 < 500\text{c}/\mu\text{l}$ ($i = 2$), $200 < CD4 < 350\text{c}/\mu\text{l}$ ($i = 3$) and $CD4 < 200\text{c}/\mu\text{l}$ ($i = 4$). NNRTI resistance is represented by j , and its value is 0 if an individual is susceptible to NNRTI and 1 otherwise. The gender dimension, represented by k , takes 0 for male and 1 for female. The indices i , j and k are used in equations in order to specify a particular layer of each dimension. When an index is missing, it means that we have summed over all the layers that the dimension contains (e.g. $I^k(t) := \sum_{i,j} I^{i,j,k}(t)$).

1.1 Modelling HIV transmission

The number of newly infected individuals per time step (1 month) is split in three parts, characterising the three different transmission routes: from men to men (men who have sex with men - MSM), from men to women and from women to men (heterosexual transmission - HET). Let k and k' respectively be the gender of a susceptible (HIV-negative) and an infected individual. Assuming a density-dependent transmission and different risk behaviours between infected individuals knowing or not their status, the number of individuals of gender k that have been newly infected by individuals of gender k' is:

$$\Delta_{k,k'} = \beta_u \nu_{k,k'} \frac{I^{k',k}}{N^{k',k}} Susc^{k,k'} + \beta_d \nu_{k,k'} \frac{D^{k',k} + T_1^{k',k} + F_1^{k',k} + T_2^{k',k} + F_2^{k',k}}{N^{k',k}} Susc^{k,k'}, \quad (1)$$

where $I^{k,k'}$, $Susc^{k,k'}$ and $N^{k,k'}$ represent respectively the number of infected people, the number of susceptible people and the total number of people of gender k that have unprotected intercourse with the gender k' , β_d and β_u the frequency of unprotected intercourse per month, respectively for infected people knowing their status (diagnosed) and for those who do not (undiagnosed) and $\nu_{k,k'}$ the probability that an unprotected intercourse leads to a new infection between an infected individual of gender k' and a susceptible individual of gender k .

As HET and MSM populations were not formally split in the model, we approximated $\frac{I^{k',k}}{N^{k',k}}$ by $\frac{I^{k'}}{N^{k'}}$ (where $I^{k'} := \sum_k I^{k',k}$ and $N^{k'} := \sum_k N^{k',k}$), assuming a similar HIV prevalence in MSM as in the overall male population. We also replaced $Susc^{k,k'}$ by $\rho_{k,k'} Susc^k$, where $\rho_{k,k'}$ represents the proportion of people having sexual intercourse with gender k' among sexually active people of gender k and where $Susc^k = Susc^{k,0} + Susc^{k,1}$. We assumed that $\nu_{1,1} = 0$ as there is no risk of infection during a sexual intercourse between two women. The proportion of MSM among men $\rho_{0,0}$ is 0.05, as reported by Anova Health Foundation [1]. Similarly, we set the proportion of sexually active women that have a sexual intercourse with men $\rho_{1,0}$ to 0.95. Using Eq 1, the number of newly infected individuals of gender k per time step is:

$$\begin{aligned} \Delta_k &= \Delta_{k,0} + \Delta_{k,1} \\ &= \beta_u \nu_{k,0} \rho_{k,0} \frac{I^{k'=0}}{N^{k'=0}} Susc^k + \beta_d \nu_{k,0} \rho_{k,0} \frac{D^{k'=0} + T_1^{k'=0} + F_1^{k'=0} + T_2^{k'=0} + F_2^{k'=0}}{N^{k'=0}} Susc^k \\ &\quad + \beta_u \nu_{k,1} \rho_{k,1} \frac{I^{k'=1}}{N^{k'=1}} Susc^k + \beta_d \nu_{k,1} \rho_{k,1} \frac{D^{k'=1} + T_1^{k'=1} + F_1^{k'=1} + T_2^{k'=1} + F_2^{k'=1}}{N^{k'=1}} Susc^k. \end{aligned} \quad (2)$$

We assumed that all newly infected individuals arrive at the first CD4 stratum ($i = 1$). See Eq 18 for more details.

1.2 Modelling mortality

Mortality rates differ according to CD4 counts and care stages. We combined the results of two studies in order to estimate the relative risks for each group [2, 3]. The group of suppressed individuals with $CD4 > 500\text{c}/\mu\text{l}$ is defined as the reference as they have the lowest risk. To convert the relative risks into rates, we used a free parameter μ , which corresponds to the mortality rate of the reference group (see Table 5).

As [2] observed a high heterogeneity in mortality risk among people with $CD4 < 200\text{c}/\mu\text{l}$ depending on CD4 counts, mortality was modelled differently for this class, based on what has already been done in Thembisa model [4]. Instead of assuming a fixed risk as for the other classes, we allowed the mortality

rate of the last CD4 stratum ($CD4 < 200c/\mu l$) to vary within a range, according to its proportion of people with very low CD4 counts. The upper level of the range corresponds to the relative risk in the scenario where all individuals have $CD4 < 50c/\mu l$, while the lower level corresponds to the scenario where all individuals have $CD4 > 50c/\mu l$. As we do not have any accurate information over time about this proportion, we used rate of ART initiation as a proxy. We assumed that average treatment rate of the 3 previous years determines the proportion of individuals with $CD4 > 50c/\mu l$, as shown in Eq 3. This average corresponds to the increase in treatment rate relative to 2005. We assumed an exponential decrease of the proportion of people with $CD4 < 50c/\mu l$ when the treatment rate is increasing, in line with structure of the compartmental model assuming exponential distribution of the rates.

$$\begin{aligned} p_{CD4>50}(t) &= p_{CD4>50}(2005) \cdot \exp\left(q \cdot \text{"diff. in 3-year Average"}(\gamma_{D \rightarrow T_1}^4(t))\right) \\ &= p_{CD4>50}(2005) \cdot \exp\left(q \cdot \left(\sum_{s=1}^{36} \gamma_{D \rightarrow T_1}^4\left(t - \frac{s}{12}\right) - \sum_{s=1}^{36} \gamma_{D \rightarrow T_1}^4\left(2005 - \frac{s}{12}\right)\right)\right), \end{aligned} \quad (3)$$

where $p_{CD4>50}(0) := 27\%$ is the proportion of people with $CD4 > 50c/\mu l$ [5]. Therefore, the relative mortality risk for people with $CD4 < 200c/\mu l$ is

$$\mu_{CD4<200}(t) = p_{CD4>50}(t) \cdot \mu_{50<CD4<200}(t) + (1 - p_{CD4>50}(t)) \cdot \mu_{CD4<50}(t),$$

where $\mu_{50<CD4<200}(t)$ and $\mu_{CD4<50}(t)$ are relative mortality risks and represent respectively the lower and upper bounds of $\mu_{CD4<200}(t)$ (see Table 4).

1.3 Modelling diagnosis and treatment rate

Diagnosis rate

To model the diagnosis rate, we needed to distinguish three different types of testing: 1) testing asymptomatic individuals γ_{diag1}^k , 2) testing symptomatic (opportunistic infection - OI) γ_{diag2}^i and 3) testing pregnant women $\gamma_{diag3}^{i,k}$. The overall diagnosis rate for a given CD4 stratum i and gender k is thus: $\gamma_{I \rightarrow D}^{i,k} = \gamma_{diag1}^k + \gamma_{diag2}^i + \gamma_{diag3}^{i,k}$ [6].

The diagnosis rate γ_{diag1}^k has increased over the years, as a consequence of the augmentation in the number of HIV-tests performed (in the asymptomatic population). To model the increase over time, two free parameters are included into the diagnosis rate: one representing the diagnosis rate in 2005 for men, and one representing its increase between 2005 and 2015. We assumed similar diagnosis rates for the four CD4 strata. As reported in [6], diagnosis rate varies across gender, being higher for women. The diagnosis for women is thus: $\gamma_{diag1}^{k=1} = \gamma_{diag1}^{k=0}/p_{I \rightarrow D}$, where $p_{I \rightarrow D}$ is a fixed parameter [6].

The rate of diagnosis due to OI γ_{diag2}^i depends on CD4 counts as OI is more likely to occur with low CD4 counts. Following what has been done by Thembisa [4], we set γ_{diag2}^i as: $\gamma_{diag2}^i = inc_{OI}^i \cdot \gamma_{test2}(t)$, where inc_{OI}^i represents the OI incidence and is set as 0.05/(1000person·year) for ind. with $CD4 > 500c/\mu l$, 0.12/(1000py) for ind. with $350 < CD4 < 500c/\mu l$, 0.27/(1000py) for ind. with $200 < CD4 < 350c/\mu l$, 0.9/(1000py) for ind. with $CD4 < 200c/\mu l$. $\gamma_{test2}(t)$ represents the monthly testing rate for individuals having an OI. To model its increase over time, we used a sigmoid function increasing from 2% in 2005 to 8% in 2015 [4].

$\gamma_{diag3}^{i,k}$ model the increased diagnosis rate due to pregnancy. It is set as 0 for men and decreases with CD4 counts, as fertility rate is lower for women with low CD4 counts. This rate is: $\gamma_{diag3}^{i,k}(t) = \theta_{birth}^i \cdot \theta_{birth}^k \cdot \gamma_{test3}^k(t)$, where $\theta_{birth}^i = 23/(1000py)$ is the birth rate in the overall South African population, θ_{birth}^k the decreased in birth rate according to CD4 counts and $\gamma_{test3}^k(t)$ the monthly testing rate for pregnant women [4]. θ_{birth}^k is 1 for women with $CD4 > 500c/\mu l$, 0.96 for women with $350 < CD4 < 500c/\mu l$, 0.87 for women with $200 < CD4 < 350c/\mu l$, 0.74 for women with $CD4 < 200c/\mu l$. We used a sigmoid function to model to model the monthly testing rate for pregnant women. This increases from 4% in 2005 to 8% in 2010 [4].

Treatment rate

We allowed treatment rate to vary over time and CD4 classes. The treatment rate for the CD4 class i at time t is :

$$\gamma_{D \rightarrow T_1}^i(t) = \gamma_{2005}^{CD4 < 200} \cdot r_i^{elig}(t) \cdot r_i^{CD4} \cdot r^{time}(t), \quad (4)$$

where $\gamma_{2005}^{CD4 < 200}$ is a free parameter representing the treatment rate for an eligible individual in 2005 with $CD4 < 200c/\mu l$, $r_i^{elig}(t)$ the proportion of individuals assumed to be eligible within CD4 class i at time t , $r_i^{CD4}(t)$ the relative treatment rate for CD4 class i relative to that in $CD4 < 200c/\mu l$ class ($i = 4$), $r^{time}(t)$ the relative treatment rate at time t relative to that in 2005.

Aside from the free parameter $\gamma_{2005}^{CD4 < 200}$, the values of all other parameters from Eq 4 are taken from the Thembisa model [4]. We set r_i^{CD4} to 0.4 for the $CD4 > 500c/\mu l$ class ($i = 1$), 0.5 for the $500 > CD4 > 350c/\mu l$ class ($i = 2$), 0.7 for the $350 > CD4 > 200c/\mu l$ class ($i = 3$) and 1 (reference group) for the $CD4 < 200c/\mu l$ class ($i = 4$). The parameter $r_i^{elig}(t)$ models the broadening of eligibility criteria over time as well as the delay between guideline change and change in practice. The product $r_i^{elig}(t) \cdot r_i^{CD4}(t)$ is displayed in Figure 1. We used a sigmoid function in order to model the gradual increase of the treatment rate over time, represented by $r^{time}(t)$ in the equation. Based on Thembisa data [4, p.28], the function $r^{time}(t)$ implies a 17-fold increase between 2002 and 2012. Initiation of

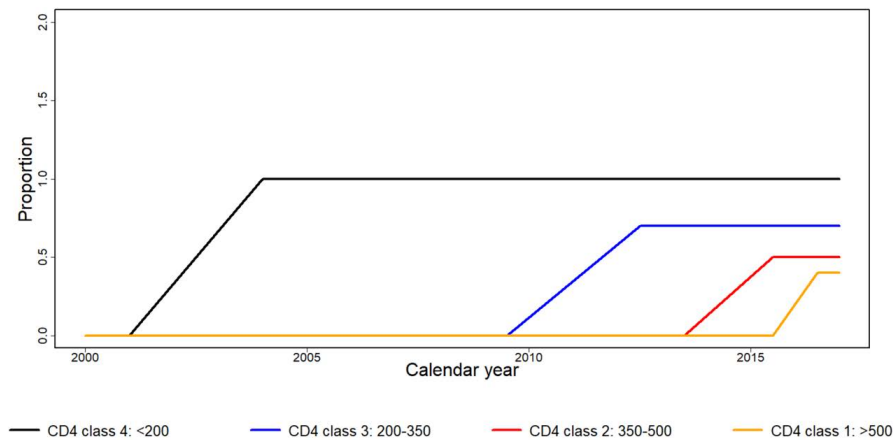


Figure 1: Proportion of eligible individuals across CD4 classes over time multiplied by relative treatment rates (relative to the $CD4 < 200$ class): $r_i^{elig}(t) \cdot r_i^{CD4}$.

PI-based treatment as a first-line regimen is represented by the rates $\gamma_{D \rightarrow T_2}^i$. These rates has been estimated using IeDEA-SA data (see section 3.1).

1.4 Modelling resistance

The resistance dimension consists of two layers: "being NNRTI-susceptible" and "being NNRTI-resistant". Individuals can enter the resistant layer in two different ways: either by acquiring drug resistance or by being infected by a resistant strain. Acquisition of NNRTI resistance at a rate σ_{res} is only possible when failing the first-line treatment. Alternatively, there is a risk to be directly infected by a resistant virus, this risk being proportional to the percentage of infectious individuals that are resistant. Resistant individuals can also revert back to the susceptible layer at a rate σ_{rev} when no more drug pressure is exerted. As time to virological failure is lower for resistant individuals [7], we added a fixed parameter α in order to express this difference. It represents the hazard ratio of the time to virological suppression (susceptible vs resistant) and has been collected from literature [7]. Similar differences have been observed in time to viral failure between susceptible and resistant individuals. For the sake of simplicity, we decided to use the same parameter α to model both differences, as estimates found in the literature were within the same range.

1.5 Modelling demographic changes

Susceptible people

As the model only describes the HIV-infected population, the susceptible population $Susc^k(t)$ is not part of the model. However, as $Susc_k(t)$ is needed in order to model infections, it is estimated as follows: $Susc^k(t) = N^k(t) - Inf_k(t)$, where $N^k(t)$ is the total number of adults of gender k in South Africa estimated by the World Health Organisation (WHO) [8] and $Inf^k(t)$ is the total number of infected adults of gender k calculated by the model (sum over all compartments). We used demographic data and interpolated them in order to obtain a function $N^k(t)$ that is continuous over time.

Children reaching adulthood

The inflow of children reaching adulthood (≥ 15 years old) was calculated using [4], [9] and [10]. Thembisa model provides yearly estimates of the number of 15-year olds that are 1) HIV-infected, 2) diagnosed and 3) on ART, stratified by gender. NNRTI resistance prevalence in 15-year olds on ART were estimated by only considering acquisition of NNRTI-resistance during ART. Transmission of resistance due to the prevention of mother to child transmission (PMTCT) treatment was not considered, as the national PMTCT programme only started in 2002 in South Africa, and thus does not have any effect on 15-year olds before 2017. Moreover, we did not consider transmission of resistance from mother to child, as level of resistance was very low in 2002. We considered that 20% of 15-year olds were on a failing ART [9]. Among them, we considered that 90% were resistant to NNRTI [10]. We interpolated these yearly estimates into continuous monthly estimates.

2 Model equations

2.1 Notations

Eq 6-9 model the difference in treatment failure/success rates depending on the absence or presence of NNRTI-resistance. Table 1 shows the different compartments of the model and model outcomes (see also Eq 10-17).

$$\delta(j) = \begin{cases} -1 & \text{if } j = 0 \\ 1 & \text{if } j = 1 \end{cases} \quad (5)$$

Impact of resistance on clinical outcome

$$\gamma_{T_1 \rightarrow S_1}^{i,j=1}(t) = 1/\alpha \cdot \gamma_{T_1 \rightarrow S_1}^{i,j=0}(t) \quad (6)$$

$$\gamma_{T_1 \rightarrow F_1}^{i,j=1}(t) = \alpha \cdot \gamma_{T_1 \rightarrow F_1}^{i,j=0}(t) \quad (7)$$

$$\gamma_{F_1 \rightarrow S_1}^{i,j=1}(t) = 1/\alpha \cdot \gamma_{F_1 \rightarrow S_1}^{i,j=0}(t) \quad (8)$$

$$\gamma_{S_1 \rightarrow F_1}^{i,j=1}(t) = \alpha \cdot \gamma_{S_1 \rightarrow F_1}^{i,j=0}(t) \quad (9)$$

Number of newly infections between time $s - 1$ and s (see Eq.2)

$$\begin{aligned} \Delta Inf(s) = & \int_{s-1}^s \left(\beta_u \sum_{k=0}^1 \left(\rho_{k,1-k} \nu_{k,1-k} \frac{Inf_u^{1-k}}{N^k} Susc^k + \rho_{k,k} \nu_{k,k} \frac{Inf_u^k}{N^k} Susc^k \right) \right. \\ & \left. + \beta_d \sum_{k=0}^1 \left(\rho_{k,1-k} \nu_{k,1-k} \frac{Inf_d^{1-k}}{N^k} Susc^k + \rho_{k,k} \nu_{k,k} \frac{Inf_d^k}{N^k} Susc^k \right) \right) dt \end{aligned} \quad (10)$$

| Notation | Description | Definition |
|--------------------------------|---|--|
| <i>Dimensions/Compartments</i> | | |
| i | index for the 2nd dimension (CD4 counts) | $i = 1, 2, 3, 4$ (4 CD4 strata) |
| j | index for the 3rd dimension (resistance) | $j = 0$: NNRTI-susceptible $j = 1$: NNRTI-resistant |
| k | index for the 4th dimension (gender) | $k = 0$: men, $k = 1$: women |
| $I^{ijk}(t)$ | number of infected (not diagnosed) indiv. | |
| $D^{ijk}(t)$ | number of diagnosed (not treated) indiv. | |
| $T_1^{ijk}(t)$ | number of indiv. that have started 1st line treatment for less than 3 months | |
| $S_1^{ijk}(t)$ | number of suppressed indiv. on 1st-line treatment | |
| $F_1^{ijk}(t)$ | number of indiv. failing 1st-line treatment | |
| $T_2^{ijk}(t)$ | number of indiv. that have started 2nd line treatment for less than 3 months | |
| $S_2^{ijk}(t)$ | number of suppressed indiv. on 2nd-line treatment | |
| $F_2^{ijk}(t)$ | number of indiv. failing 2nd-line treatment | |
| $N^k(t)$ | number of adults of gender k | [8] |
| $Susc^k$ | number of susceptible indiv. of gender k | by definition: $Susc^k := N^k(t) - I^k(t)$. |
| $Inf_u^{jk}(t)$ | number of undiagnosed indiv. | $Inf_u^{jk}(t) := I^{jk}(t)$ |
| $Inf_d^{jk}(t)$ | number of infectious diagnosed indiv. | see Eq 14 |
| <i>Model outcomes</i> | | |
| $\Delta Inf(t)$ | number of newly infected indiv. between times t and $t + \Delta t$ ($\Delta(t)$ is the time step: 1 month) | see equation 10 |
| $Diag(t)$ | number of indiv. diagnosed | see Eq 11 |
| $Mort(t)$ | number of AIDS-related deaths | see Eq 12 |
| $Treat(t)$ | number of indiv. treated | see Eq 13 |
| $ADR(t)$ | level of ADR (among failed indiv.) | see Eq 15 |
| $TDR(t)$ | level of TDR (among newly diagnosed indiv.) | see Eq 16 |

Table 1: Description of the compartments and dimensions of the model.

Number of diagnosed HIV-infected individuals at time t

$$Diag(t) = D(t) + T_1(t) + S_1(t) + F_1(t) + T_2(t) + S_2(t) + F_2(t) \quad (11)$$

Number of AIDS-related deaths between time $s - 1$ and s

$$Mort(s) = \int_{s-1}^s \left(\mu_I^{i=4} \cdot I^{i=4} + \mu_D^{i=4} \cdot D^{i=4} + \mu_{T_1}^{i=4} \cdot T_1^{i=4} + \dots + \mu_{F_2}^{i=4} \cdot F_2^{i=4} \right) (t) dt \quad (12)$$

Number of individuals on ART at time t

$$Treat(t) = T_1(t) + S_1(t) + \dots + F_2(t) \quad (13)$$

Number of infectious and diagnosed individuals

$$Inf_d^{jk}(t) = D^{jk}(t) + T_1^{jk}(t) + F_1^{jk}(t) + T_2^{jk}(t) + F_2^{jk}(t) \quad (14)$$

Acquired NNRTI resistance (in failing patients)

$$ADR(t) = \frac{F_1^{j=1}(t)}{\sum_{j=0}^1 F_1^j(t)} \quad (15)$$

Transmitted NNRTI (in newly diagnosed individuals)

$$TDR(t) = \frac{\Delta D^{j=1}(t)}{\sum_{j=0}^1 \Delta D^j(t)} \quad (16)$$

where $\Delta D^j(t)$ represent the inflow of individuals going from I^j to D^j at each time step (newly diagnosed individuals).

Contribution of TDR to ADR between times $s - 1$ and s (see Discussion section in the manuscript)

$$\rho_{TDR \rightarrow ADR}(s) = \frac{\sum_{i=1}^4 \int_{s-1}^s \left(\gamma_{S_1 \rightarrow F_1}^{i,j=1} \cdot S_1^{i,j=1}(t) + \gamma_{T_1 \rightarrow F_1}^{i,j=1} \cdot T_1^{i,j=1}(t) \right) dt}{\sum_{i=1}^4 \int_{s-1}^s \left(\gamma_{S_1 \rightarrow F_1}^{i,j=1} \cdot S_1^{i,j=1}(t) + \gamma_{T_1 \rightarrow F_1}^{i,j=1} \cdot T_1^{i,j=1}(t) + \sigma_{res} \cdot F_1^{i,j=0}(t) \right) dt} \quad (17)$$

2.2 ODEs

$$\begin{aligned}
 \dot{I}^{ijk}(t) &= -\nu_{CD4}^{I,i} \cdot I^{ijk}(t) \mathbf{1}_{i \leq 3} + \nu_{CD4}^{I,i-1} \cdot I^{(i-1)jk}(t) \mathbf{1}_{i \geq 2} \\
 &+ \beta_u \left(\rho_{k,1-k} \nu_{k,1-k} \frac{Inf_u^{ij(1-k)}}{N^k} Susc^k + \rho_{k,k} \nu_{k,k} \frac{Inf_u^{ijk}}{N^k} Susc^k \right) \mathbf{1}_{i=1} \\
 &+ \beta_d \left(\rho_{k,1-k} \nu_{k,1-k} \frac{Inf_d^{ij(1-k)}}{N^k} Susc^k + \rho_{k,k} \nu_{k,k} \frac{Inf_d^{ijk}}{N^k} Susc^k \right) \mathbf{1}_{i=1} \\
 &- \gamma_{I \rightarrow D}^{ik}(t) \cdot I^{ijk}(t) - \delta(j) \cdot \sigma_{rev} \cdot I^{ik}(t) - \mu_I^i \cdot I^{ijk}(t) + \Delta Inf_{15years}^{I,ijk}(t), \\
 \dot{D}^{ijk}(t) &= -\nu_{CD4}^{D,i} \cdot D^{ijk}(t) \mathbf{1}_{i \leq 3} + \nu_{CD4}^{D,i-1} \cdot D^{(i-1)jk}(t) \mathbf{1}_{i \geq 2} - (\gamma_{D \rightarrow T_1}^{ik}(t) + \gamma_{D \rightarrow T_2}^i(t)) \cdot D^{ijk}(t) \\
 &+ \gamma_{T_1 \rightarrow D}^i \cdot T_1^{ijk}(t) + \gamma_{S_1 \rightarrow D}^i \cdot S_1^{ijk}(t) + \gamma_{F_1 \rightarrow D}^i \cdot F_1^{ijk}(t) + \gamma_{I \rightarrow D}^{ik}(t) \cdot I^{ijk}(t) \\
 &- \delta(j) \cdot \sigma_{rev} \cdot D^{ik}(t) - \mu_D^i \cdot D^{ijk}(t) + \Delta Inf_{15years}^{D,ijk}(t), \\
 \dot{T}_1^{ijk}(t) &= \left(\nu_{CD4}^{T_1,i-1} \cdot T_1^{(i-1)jk}(t) - \tilde{\nu}_{CD4}^{T_1,i-1} \cdot T_1^{ijk}(t) \right) \mathbf{1}_{i \geq 2} + \left(\tilde{\nu}_{CD4}^{T_1,i} \cdot T_1^{(i+1)jk}(t) - \nu_{CD4}^{T_1,i} \cdot T_1^{ijk}(t) \right) \mathbf{1}_{i \leq 3} \\
 &- (\gamma_{T_1 \rightarrow S_1}^{ij} + \gamma_{T_1 \rightarrow F_1}^{ij} + \gamma_{T_1 \rightarrow D}^{ij}) \cdot T_1^{ijk}(t) + \gamma_{D \rightarrow T_1}^{ik}(t) \cdot D^{ijk}(t) - \mu_{T_1}^i \cdot T_1^{ijk}(t) + \Delta Inf_{15years}^{T_1,ijk}(t), \\
 \dot{S}_1^{ijk}(t) &= -\tilde{\nu}_{CD4}^{S_1,i-1} \cdot S_1^{ijk}(t) \mathbf{1}_{i \geq 2} + \tilde{\nu}_{CD4}^{S_1,i} \cdot S_1^{(i+1)jk}(t) \mathbf{1}_{i \leq 3} \\
 &- (\gamma_{S_1 \rightarrow F_1}^{ij} + \gamma_{S_1 \rightarrow D}^{ij}) \cdot S_1^{ijk}(t) + \gamma_{T_1 \rightarrow S_1}^{ij} \cdot T_1^{ijk}(t) + \gamma_{F_1 \rightarrow S_1}^{ij} \cdot S_1^{ijk}(t) - \mu_{S_1}^i \cdot S_1^{ijk}(t), \\
 \dot{F}_1^{ijk}(t) &= \nu_{CD4}^{F_1,i-1} \cdot F_1^{(i-1)jk}(t) \mathbf{1}_{i \geq 2} - \nu_{CD4}^{F_1,i} \cdot F_1^{ijk}(t) \mathbf{1}_{i \leq 3} + \delta(j) \cdot \sigma_{res} \cdot F_1^{0k}(t) \\
 &- (\gamma_{F_1 \rightarrow S_1}^{ij} + \gamma_{F_1 \rightarrow T_2}^{ik} + \gamma_{F_1 \rightarrow D}^{ij}) \cdot F_1^{ijk}(t) + \gamma_{S_1 \rightarrow F_1}^{ij} \cdot S_1^{ijk}(t) + \gamma_{T_1 \rightarrow F_1}^{ij} \cdot T_1^{ijk}(t) \\
 &- \mu_{F_1}^i \cdot F_1^{ijk}(t), \\
 \dot{T}_2^{ijk}(t) &= \left(\nu_{CD4}^{T_2,i-1} \cdot T_2^{(i-1)jk}(t) - \tilde{\nu}_{CD4}^{T_2,i-1} \cdot T_2^{ijk}(t) \right) \mathbf{1}_{i \geq 2} + \left(\tilde{\nu}_{CD4}^{T_2,i} \cdot T_2^{(i+1)jk}(t) - \nu_{CD4}^{T_2,i} \cdot T_2^{ijk}(t) \right) \mathbf{1}_{i \leq 3} \\
 &- (\gamma_{T_2 \rightarrow S_2}^{ij} + \gamma_{T_2 \rightarrow F_2}^{ij}) \cdot T_2^{ijk}(t) + \gamma_{F_1 \rightarrow T_2}^{ik}(t) \cdot F_1^{ijk}(t) + \gamma_{D \rightarrow T_2}^i \cdot D^{ijk}(t) - \mu_{T_2}^i \cdot T_2^{ijk}(t), \\
 \dot{S}_2^{ijk}(t) &= -\tilde{\nu}_{CD4}^{S_2,i-1} \cdot S_2^{ijk}(t) \mathbf{1}_{i \geq 2} + \tilde{\nu}_{CD4}^{S_2,i} \cdot S_2^{(i+1)jk}(t) \mathbf{1}_{i \leq 3} \\
 &- \gamma_{S_2 \rightarrow F_2}^{ij} \cdot S_2^{ijk}(t) + \gamma_{T_2 \rightarrow S_2}^{ij} \cdot T_2^{ijk}(t) + \gamma_{F_2 \rightarrow S_2}^{ij} \cdot F_2^{ijk}(t) - \mu_{S_2}^i \cdot S_2^{ijk}(t), \\
 \dot{F}_2^{ijk}(t) &= \nu_{CD4}^{F_2,i-1} \cdot F_2^{(i-1)jk}(t) \mathbf{1}_{i \geq 2} - \nu_{CD4}^{F_2,i} \cdot F_2^{ijk}(t) \mathbf{1}_{i \leq 3} \\
 &- \gamma_{F_2 \rightarrow S_2}^{ij} \cdot F_2^{ijk}(t) + \gamma_{S_2 \rightarrow F_2}^{ij} \cdot S_2^{ijk}(t) + \gamma_{T_2 \rightarrow F_2}^{ij} \cdot T_2^{ijk}(t) - \mu_{F_2}^i \cdot F_2^{ijk}(t).
 \end{aligned} \tag{18}$$

2.3 Starting values

Model simulation started in 2005. The distribution of the infected individuals over the 128 compartments at the start of the simulation were chosen as follows. As reported by Thembisa, there were 4.4 million adult people living with HIV in 2005 in South Africa, 1.7 million of them were men. These individuals were distributed across 3 of the 8 care stages: infected (I), diagnosed (D) and treated with first-line (T_1). 72% were in I , 26% in D and 2% in T_1 . The distribution of individuals across the four

CD4 classes has been determined by running with different distributions across CD4 classes and by keeping the one with the best fit. For infected I individuals, we chose a homogeneous distribution, i.e. the same number of individuals in the four CD4 classes. For diagnosed and treated individuals (D and T_1), the fourth CD4 class ($CD4 < 200c/\mu l$) has the most individuals. It has twice as many individuals as in the third CD4 class, which has twice as many as in the second CD4 class, which has twice as many as in the first one. Finally, we assumed that 1% of infected individuals were resistant to NNRTI. For sake of simplicity, this percentage did not depend on CD4 counts or on care stages.

3 Calibration and model simulation

We calibrated the model in two successive steps. First, IeDEA data were used to estimate the majority of the rates with survival analysis. Second, we fitted our model to Thembisa data using a maximum likelihood approach. A few parameters, mainly the ones related to resistance, were collected from literature. For more details, see Table 4.

3.1 Survival analysis

To estimate the majority of the rates that are related to continuum of care or disease progression, we used data from IeDEA-SA, a network collecting individual information about HIV-infected patients from several cohorts in Southern Africa. After having selected only adults from the 5 South African cohorts and discarded patients with erroneous information, we ended up with information about 54'016 patients. This includes 1) start/end of drug regimen, 2) VL measurements, 3) CD4 counts measurements and 4) outcome (i.e. death).

Let A and B be two compartments of the model and $r_{A \rightarrow B}$ the rate corresponding to the movement from A to B . When a linear interaction ($\frac{dB}{dt} = r_{A \rightarrow B} \cdot A$) is chosen, the compartmental model assumes that the *time* $T_{A \rightarrow B}$ *spent in* A *before switching to* B is exponentially distributed with mean $r_{A \rightarrow B}^{-1}$: $T_{A \rightarrow B} \sim \text{Exp}(r_{A \rightarrow B})$. Therefore, we estimated the different rates summarised in the section below by using survival analysis and assuming an exponentially distributed times.

Rates related to movement between CD4 classes

All the rates that are related to the progression of the disease (switch to another CD4 class) within the same care stage are estimated with IeDEA data. As the time spent on one care stage before switching to another stage is generally long, the interval censoring approach provided accurate estimates of almost all rates. As no reliable data exist about untreated individuals (I and D), the progression in CD4 counts for I and D was estimated from literature [11].

Rates related to movement between care stages

Rates that model HIV-transmission, diagnosis and treatment initiation were not estimated with IeDEA data and have already been described in Section 1. For all the other rates that are related to continuum of care, we adapted the survival analysis method to handle the sparsity of IeDEA data. First, as few VL measurements are reported per individuals, some steps are missing in the IeDEA data, e.g. some individuals passing directly from "diagnosed" (D) to "suppressed" (S_1), which implies that treatment start is missing in the database. In this case, we aimed to reconstruct the history of care of these patients based on the sparse information we had from IeDEA. In this example, as no rate exists between D and S_1 , we should assume that the individual stayed at T_1 before going to S_1 . Therefore, the information provided by IeDEA data could here help us to estimate two rates: $\gamma_{D \rightarrow T_1}$ and $\gamma_{T_1 \rightarrow S_1}$. Second, we also modified the method in order to take into account the risk of bias caused by the sparsity of the CD4 measurements. As an example, let's suppose that we want to estimate the suppression rate $\gamma_{T_1 \rightarrow S_1}^1$ for individuals with $CD4 > 500c/\mu l$. If the CD4 counts fell below $500c/\mu l$ between the last time he has been reported at T_1 and the first time he was at S_1 , it is impossible to know whether the patient got suppressed when his CD4 counts was below or above $500c/\mu l$. Therefore, information about this patient cannot be used to inform any of the two rates $\gamma_{T_1 \rightarrow S_1}^1$ or $\gamma_{T_1 \rightarrow S_1}^2$. Although the quality of the estimates remains good for most of them due to the high number of individuals, rejecting those patients could introduce a bias. We tried to correct for this bias by adapting the standard method.

Let's consider the rate $\gamma_{T_1 \rightarrow S_1}^1$. First, we estimated this rate without CD4 stratification: $\hat{\gamma}_{T_1 \rightarrow S_1}$. Next, we compared the weighted average of the rate stratified by CD4 with its estimate without CD4 stratification, by taking the ratio:

$$c := \frac{\hat{\gamma}_{T_1 \rightarrow S_1}}{\left(\sum_{i=1}^4 \omega_i \cdot \hat{\gamma}_{T_1 \rightarrow S_1}^i\right) / \sum \omega_i}. \quad (19)$$

This constant c represents the bias made when estimating $\hat{\gamma}_{T_1 \rightarrow S_1}$ by CD4 stratification. To correct for this bias, we therefore multiplied the previously estimated rates $\hat{\gamma}_{T_1 \rightarrow S_1}^i$ by c : $c \cdot \hat{\gamma}_{T_1 \rightarrow S_1}^i$. Table 2 shows estimates of the rates that are related to the progression of the disease and Table 3 estimates of the rates that are related to the continuum of care.

| Parameter | Description | Values | | |
|-----------------------------|---|-----------|-------|-------|
| | | CD4 class | | |
| | | 1 → 2 | 2 → 3 | 3 → 4 |
| $1/\nu_{CD4}^I$ | Time before leaving one CD4 class to another one (estimated from [11]) | 60 | 36 | 42 |
| $1/\nu_{CD4}^D$ | idem (estimated from [11]) | 60 | 36 | 42 |
| $1/\nu_{CD4}^{T_1}$ | idem | 28 | 18 | 45 |
| $1/\nu_{CD4}^{F_1}$ | idem | 17 | 11 | 16 |
| $1/\nu_{CD4}^{T_2}$ | idem | 28 | 18 | 45 |
| $1/\nu_{CD4}^{F_2}$ | idem | 15 | 14 | 11 |
| | | 1 ← 2 | 2 ← 3 | 3 ← 4 |
| $1/\tilde{\nu}_{CD4}^{T_1}$ | idem | 13 | 22 | 115 |
| $1/\tilde{\nu}_{CD4}^{S_1}$ | idem | 15 | 13 | 10 |
| $1/\tilde{\nu}_{CD4}^{T_2}$ | idem (set as $1/\tilde{\nu}_{CD4}^{T_1}$) | 13 | 22 | 115 |
| $1/\tilde{\nu}_{CD4}^{S_2}$ | idem | 14 | 13 | 8 |

Table 2: Inverse of the rates (in month) related to disease progression estimated with survival analysis and IeDEA data. Because no or too little data were available to measure them accurately, two rates ($1/\nu_{CD4}^I$ and $1/\nu_{CD4}^{T_2}$) were approximation by other similar rates.

3.2 Likelihood maximisation

Four different rates - transmission rate, diagnosis rate, ART initiation rate and mortality rate - were estimated during the second phase. These four rates were modelled with 7 parameters (see Table 5). Estimates from the first phase (Table 2 and 3) and from literature (Table 4) were used to run the model. We used an maximum likelihood approach to fit four model outcomes to outcomes from Thembisa model (see Eq 20). The four model outcomes are: the number of yearly new infection ΔInf , the number of undiagnosed individuals $Diag$, the number of treated individuals $Treat$ and the number of AIDS-related deaths $Mort$.

We used the `optim` function in **R** together with the **L-BFGS-B** method. This method allowed us to provide lower and upper bounds for each parameters. These bounds were chosen in order to include all reasonable values. As optimisation of the likelihood function might give different results depending on the starting values of the parameters, different starting values were randomly chosen within the range defined by the lower and upper bounds. We selected the set of parameters that maximized the likelihood over the simulations that converged. Calculations were performed on UBELIX

| Parameter | Description | Values | | | |
|----------------------------------|---|-----------|------|------|-----|
| | | CD4 class | | | |
| | | 1 | 2 | 3 | 4 |
| $1/\gamma_{T_1 \rightarrow S_1}$ | Time from T_1 to S_1 | 6 | 9 | 9 | 14 |
| $1/\gamma_{T_1 \rightarrow F_1}$ | Time from T_1 to F_1 | 23 | 22 | 15 | 13 |
| $1/\gamma_{S_1 \rightarrow F_1}$ | Time from S_1 to F_1 | 621 | 460 | 225 | 87 |
| $1/\gamma_{F_1 \rightarrow S_1}$ | Time from F_1 to S_1 | 28 | 46 | 48 | 53 |
| $1/\gamma_{F_1 \rightarrow T_2}$ | Time from F_1 to T_2 | 94 | 161 | 65 | 35 |
| $1/\gamma_{T_2 \rightarrow S_2}$ | Time from T_2 to S_2 | 5 | 8 | 4 | 4 |
| $1/\gamma_{T_2 \rightarrow F_2}$ | Time from T_2 to F_2 | 20 | 24 | 12 | 8 |
| $1/\gamma_{S_2 \rightarrow F_2}$ | Time from S_2 to F_2 | 59 | 43 | 40 | 21 |
| $1/\gamma_{F_2 \rightarrow S_2}$ | Time from F_2 to S_2 | 2 | 10 | 6 | 12 |
| $1/\gamma_{T_1 \rightarrow D}$ | Time from T_1 to D (stop treatment) | 414 | 322 | 172 | 156 |
| $1/\gamma_{S_1 \rightarrow D}$ | Time from S_1 to D (stop treat.) | 2069 | 1241 | 759 | 368 |
| $1/\gamma_{F_1 \rightarrow D}$ | Time from F_1 to D (stop treat.) | 621 | 478 | 285 | 129 |
| $1/\gamma_{T_2 \rightarrow D}$ | Time from T_2 to D (stop treatment) | 414 | 322 | 172 | 156 |
| $1/\gamma_{S_2 \rightarrow D}$ | Time from S_2 to D (stop treat.) | 2069 | 1241 | 759 | 368 |
| $1/\gamma_{F_2 \rightarrow D}$ | Time from F_2 to D (stop treat.) | 621 | 478 | 285 | 129 |
| $1/\gamma_{D \rightarrow T_2}$ | Time from D to T_2 | 1149 | 2759 | 2989 | 425 |

Table 3: Inverse of the rates (in month) related to continuum of care estimated with survival analysis and IeDEA data.

(<http://www.id.unibe.ch/hpc>), the HPC cluster at the University of Bern.

$$\begin{aligned}
 \log L = & \sum_{i=2005}^{2015} \log \text{Poisson}(\Delta Inf_{data}(t), \lambda = \Delta Inf(t)) \\
 & + \sum_{i=2005}^{2015} \log \text{Poisson}(Diag_{data}(t), \lambda = Diag(t)) \\
 & + \sum_{i=2005}^{2015} \log \text{Poisson}(Mort_{data}(t), \lambda = Mort(t)) \\
 & + \sum_{i=2005}^{2015} \log \text{Poisson}(Treat_{data}(t), \lambda = Treat(t))
 \end{aligned} \tag{20}$$

| Parameter | Description | Values | Ref |
|------------------------------|--|-----------|----------------------|
| <i>Resistance parameters</i> | | | |
| $1/\sigma_{res}$ | Time to acquire resistance (in month) | 5 | [12, 13, 14, 15, 16] |
| $1/\sigma_{rev}$ | Time to revert back to "drug-susceptible" (in month) | 120 | [17] |
| α | Hazard ratio of "being suppressed" between drug-susceptible and drug-resistant individuals | 2 | [7] |
| <i>Other parameters</i> | | | |
| $p_{I \rightarrow D}$ | ratio of diagnosis rate between asymptomatic men and women | 0.8 | |
| $\nu_{0,0}$ | probability that a male infects a male (per act) | 0.8% | [18] |
| $\nu_{0,1}$ | probability that a male infects a female (per act) | 0.3% | [18] |
| $\nu_{1,0}$ | probability that a female infects a male (per act) | 0.3% | [18] |
| $\rho_{0,0}$ | percentage of MSM | 5% | [1] |
| μ^i | relative mortality risk (Ref: suppressed indiv. with $CD4 > 500$) | | [2] [3] |
| | | CD4 class | |
| | | 1 | 2 |
| | | 3 | 4 |
| | $\mu_{I/D}^i$: not treated (I and D) | 1.6 | 2 |
| | μ_{T_1/T_2}^i : started treatment (T_1 and T_2) | 2.5 | 2.6 |
| | μ_{S_1/S_2}^i : suppressed (S_1 and S_2) | 1 | 1.3 |
| | μ_{F_1/F_2}^i : failed (F_1 and F_2) | 3.9 | 3.9 |
| | | 4.6 | 40.9-134.4 |
| | | 3.1 | 10-50.7 |
| | | 2 | 8.3-41.7 |
| | | 4.3 | 11.8-59.7 |

Table 4: Parameters collected from literature.

| Parameter | Description | Values |
|---|--|--------------------|
| β_u | number of unprotected sexual acts per month (for undiagnosed individual) | 3.3 |
| β_d | number of unprotected sexual acts per month (for diagnosed individual) | 1.8 |
| $\gamma_{I \rightarrow D}(2016)/\gamma_{I \rightarrow D}(2005)$ | Ratio of diagnosis rates between 2005 and 2016 | 7.7 |
| $1/(12 \cdot \gamma_{I \rightarrow D}(2005))$ | time to diagnosis in 2005 in asymptotic HIV-infected men (in year) | 22.8 |
| $1/(12 \cdot \gamma_{D \rightarrow T_1}(2005))$ | time to ART initiation in 2005 (in year) | 7.8 |
| q | parameter linking the increase of treatment rate with the decrease of the prop. of ind. with $CD4 < 50$ cell/ μl | 0.05 (see Eq 3) |
| μ_0 | Mortality risk (in (month \cdot 1000 people) $^{-1}$) for a suppressed individual with $CD4 > 500$ cell/ μl | 0.16 |

 Table 5: Parameters estimated during the second-phase calibration (likelihood maximisation). Rates are in month $^{-1}$.

4 Results

4.1 Best fits

Figure 2A-D shows the 10 best fits among those that converged. Figure 2E-F shows ADR and TDR levels over time as estimated by the model using the formulas 15 and 16 respectively. The table 6 shows some characteristics of the studies that are used in Figure 2E-F.

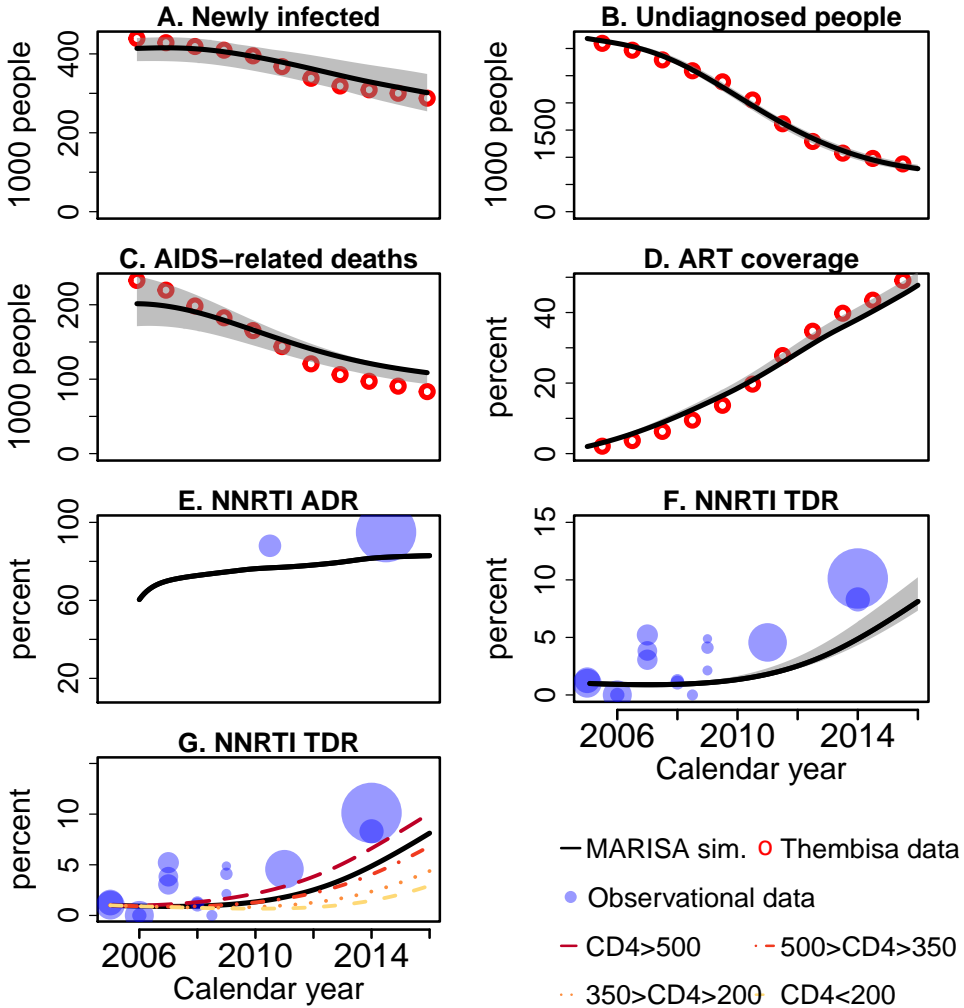


Figure 2: The plots A, B, C and D correspond to the four indicators used during the fitting procedure: A. the number of newly infected per year, B. the number of undiagnosed individuals, C. the number of AIDS-related deaths per year and D. the percentage of infected individuals that are on ART. ADR and TDR levels are displayed in Figure E. and F. respectively. Note, however, that these two latter indicators are not used during the fitting procedure. The lines correspond to the best model fit while the grey area is delimited by the lower and upper bounds of the 10 best fits, whose variation is due to different starting points (see Section 3.2).

4.2 Sensitivity analysis

In the sensitivity analysis, we perturbed 200 times seven parameters using a Latin Hypercube Sampling method (see Table 7). As varying the transmission-related parameters may modify the overall transmission rate, an adjustment is made to have a transmission rate similar to the baseline model. Sensitivity analysis were run for the baseline model as well as for each counterfactual scenario (10 different scenarios in total). 100% sensitivity ranges are displayed in Figures 2 and 3 and Table 1 of the main paper.

| Where | Level | CI (95%) | sample size | Year | Reference |
|---|------------|---------------|----------------------------|-----------|-----------|
| ADR levels | | | | | |
| Cape Town | 88% | 80.3% – 93.3% | 110 | 2002-2007 | [12] |
| 8 over the 9 South African provinces (no data from Northern Cape province) | 95.4% | 93.7% – 96.7% | 788 | 2013-2014 | [19] |
| TDR levels | | | | | |
| South Africa (meta-analysis) | 0% – 10.1% | not given | 41 – 1719 (total: 5064) | 2005-2014 | [20] |

Table 6: Cross-sectional studies used to compare resistance outcomes of the model (levels of ADR and TDR over time).

| Parameters | Value | Lower Bound | Upper bound |
|--|--------------------------------|-------------|------------------|
| <i>Resistance-related parameters</i> | | | |
| $1/\sigma_{res}$ | 5 | 3 | 9 |
| $1/\sigma_{rev}$ | 125 | 36 | 200 |
| α | 2 | 1 | 5 |
| $\gamma_{T_1 \rightarrow D}, \gamma_{S_1 \rightarrow D}, \gamma_{F_1 \rightarrow D}$ | rate γ (see Table 3) | γ | $2 \cdot \gamma$ |
| <i>Transmission-related parameters</i> | | | |
| $\rho_{0,0}$ | 5% | 1% | 10% |
| $\nu_{0,0}/\nu_{0,1}$ | 2.7 | 1 | 5 |
| Ratio between HIV prevalence in MSM and in HET | 1 | 1 | 3 |

Table 7: Parameter ranges used in sensitivity analysis.

5 References

- [1] Anova Health Institute. Rapid Assessment of HIV Prevention, Care and Treatment Programming for MSM in South Africa; 2013.
- [2] Maduna PH, Dolan M, Kondlo L, Mabuza H, Dlamini JN, Polis M, et al. Morbidity and Mortality According to Latest CD4+ Cell Count among HIV Positive Individuals in South Africa Who Enrolled in Project Phidisa. PLOS ONE. 2015 apr;10(4):e0121843. Available from: <http://www.ncbi.nlm.nih.gov/pubmed/25856495><http://www.pubmedcentral.nih.gov/articlerender.fcgi?artid=PMC4391777><http://dx.plos.org/10.1371/journal.pone.0121843>.
- [3] Brennan AT, Maskew M, Sanne I, Fox MP. The interplay between CD4 cell count, viral load suppression and duration of antiretroviral therapy on mortality in a resource-limited setting. Tropical medicine & international health : TM & IH. 2013 may;18(5):619–31. Available from: <http://www.ncbi.nlm.nih.gov/pubmed/23419157><http://www.pubmedcentral.nih.gov/articlerender.fcgi?artid=PMC3625450>.
- [4] Johnson LF, Dorrington RE. Thembisa version 4.1: A model for evaluating the impact of HIV/AIDS in South Africa; 2018.
- [5] Boule A, Bock P, Osler M, Cohen K, Channing L, Hilderbrand K, et al. Antiretroviral therapy and early mortality in South Africa. Bulletin of the World Health Organization. 2008 sep;86(9):678–87. Available from: <http://www.ncbi.nlm.nih.gov/pubmed/18797643><http://www.pubmedcentral.nih.gov/articlerender.fcgi?artid=PMC2649489>.

- [6] Johnson LF, Rehle TM, Jooste S, Bekker LG. Rates of HIV testing and diagnosis in South Africa. *AIDS*. 2015 jul;29(11):1401–1409. Available from: <http://www.ncbi.nlm.nih.gov/pubmed/26091299><http://content.wkhealth.com/linkback/openurl?sid=WKPPLP:landingpage{&}an=00002030-201507170-00015>.
- [7] Wittkop L, Günthard HF, de Wolf F, Dunn D, Cozzi-Lepri A, de Luca A, et al. Effect of transmitted drug resistance on virological and immunological response to initial combination antiretroviral therapy for HIV (EuroCoord-CHAIN joint project): a European multicohort study. *The Lancet Infectious Diseases*. 2011 may;11(5):363–371. Available from: <http://www.ncbi.nlm.nih.gov/pubmed/21354861><http://linkinghub.elsevier.com/retrieve/pii/S1473309911700329>.
- [8] (WHO) WHO. WHO | South Africa; 2018. Available from: <http://www.who.int/countries/zaf/en/>.
- [9] Fairlie L, Bernheimer J, Sipambo N, Fick C, Kuhn L. Lamivudine monotherapy in children and adolescents: The devil is in the detail. *South African Medical Journal*. 2017 nov;107(12):1055. Available from: <http://www.samj.org.za/index.php/samj/article/view/12151>.
- [10] Muri L, Gamell A, Ntamatungiro AJ, Glass TR, Luwanda LB, Bategay M, et al. Development of HIV drug resistance and therapeutic failure in children and adolescents in rural Tanzania: an emerging public health concern. *AIDS*. 2016. Available from: <https://www.ncbi.nlm.nih.gov/pmc/articles/PMC5131685/pdf/aids-31-061.pdf>.
- [11] Mangal TD, UNAIDS Working Group on CD4 Progression and Mortality Amongst HIV Seroconverters including the CASCADE Collaboration in EuroCoord. Joint estimation of CD4+ cell progression and survival in untreated individuals with HIV-1 infection. *AIDS*. 2017 may;31(8):1073–1082. Available from: <http://www.ncbi.nlm.nih.gov/pubmed/28301424><http://www.pubmedcentral.nih.gov/articlerender.fcgi?artid=PMC5414573><http://insights.ovid.com/crossref?an=00002030-201705150-00003>.
- [12] Orrell C, Walensky RP, Losina E, Pitt J, Freedberg KA, Wood R. HIV type-1 clade C resistance genotypes in treatment-naïve patients and after first virological failure in a large community antiretroviral therapy programme. *Antiviral therapy*. 2009;14(4):523–31. Available from: <http://www.ncbi.nlm.nih.gov/pubmed/19578237><http://www.pubmedcentral.nih.gov/articlerender.fcgi?artid=PMC3211093>.
- [13] Sigaloff KCE, Ramatsebe T, Viana R, de Wit TFR, Wallis CL, Stevens WS. Accumulation of HIV Drug Resistance Mutations in Patients Failing First-Line Antiretroviral Treatment in South Africa. *AIDS Research and Human Retroviruses*. 2012 feb;28(2):171–175. Available from: <http://www.liebertpub.com/doi/10.1089/aid.2011.0136>.
- [14] Wallis CL, Mellors JW, Venter WDF, Sanne I, Stevens W. Varied Patterns of HIV-1 Drug Resistance on Failing First-Line Antiretroviral Therapy in South Africa. *JAIDS Journal of Acquired Immune Deficiency Syndromes*. 2010 apr;53(4):480–484. Available from: <https://insights.ovid.com/crossref?an=00126334-201004010-00007>.
- [15] Manasa J, Lessells RJ, Skingsley A, Naidu KK, Newell ML, McGrath N, et al. High-Levels of Acquired Drug Resistance in Adult Patients Failing First-Line Antiretroviral Therapy in a Rural HIV Treatment Programme in KwaZulu-Natal, South Africa. *PLoS ONE*. 2013 aug;8(8):e72152. Available from: <https://dx.plos.org/10.1371/journal.pone.0072152>.
- [16] van Zyl GU, van der Merwe L, Claassen M, Zeier M, Preiser W. Antiretroviral resistance patterns and factors associated with resistance in adult patients failing NNRTI-based regimens in the western cape, South Africa. *Journal of Medical Virology*. 2011 oct;83(10):1764–1769. Available from: <http://doi.wiley.com/10.1002/jmv.22189>.

- [17] Yang WL, Kouyos RD, Böni J, Yerly S, Klimkait T, Aubert V, et al. Persistence of Transmitted HIV-1 Drug Resistance Mutations Associated with Fitness Costs and Viral Genetic Backgrounds. *PLOS Pathogens*. 2015 mar;11(3):e1004722. Available from: <http://dx.plos.org/10.1371/journal.ppat.1004722>.
- [18] Patel P, Borkowf CB, Brooks JT, Lasry A, Lansky A, Mermin J. Estimating per-act HIV transmission risk. *AIDS*. 2014 jun;28(10):1509–1519. Available from: <http://www.ncbi.nlm.nih.gov/pubmed/24809629><http://content.wkhealth.com/linkback/openurl?sid=WKPTLP:landingpage&an=00002030-201406190-00014>.
- [19] Steegen K, Bronze M, Papathanasopoulos MA, van Zyl G, Goedhals D, Variava E, et al. HIV-1 antiretroviral drug resistance patterns in patients failing NNRTI-based treatment: results from a national survey in South Africa. *Journal of Antimicrobial Chemotherapy*. 2017 jan;72(1):210–219. Available from: <http://www.ncbi.nlm.nih.gov/pubmed/27659733><https://academic.oup.com/jac/article-lookup/doi/10.1093/jac/dkw358>.
- [20] Gupta RK, Gregson J, Parkin N, Haile-Selassie H, Tanuri A, Andrade Forero L, et al. HIV-1 drug resistance before initiation or re-initiation of first-line antiretroviral therapy in low-income and middle-income countries: a systematic review and meta-regression analysis. *The Lancet Infectious diseases*. 2018 mar;18(3):346–355. Available from: <http://www.ncbi.nlm.nih.gov/pubmed/29198909><http://www.pubmedcentral.nih.gov/articlerender.fcgi?artid=PMC5835664>.

Annex D: S1 Text of Chapter 4

SUPPLEMENTARY MATERIAL

Impact of scaling up dolutegravir on antiretroviral resistance in South Africa: A modeling study

Anthony Hauser¹, Katharina Kusejko², Leigh Johnson³, Huldrych Günthard^{2,4}, Julien Riou¹, Gilles Wandeler^{1,5}, Matthias Egger^{1,3,6,*}, and Roger Kouyos^{2,4,*}

¹Institute of Social and Preventive Medicine, University of Bern, Switzerland

²Division of Infectious Diseases and Hospital Epidemiology, University Hospital Zurich, University of Zurich, Zurich, Switzerland

³Centre for Infectious Disease Epidemiology and Research, University of Cape Town, South Africa

⁴Institute of Medical Virology, University of Zurich, Zurich, Switzerland

⁵Department of Infectious Diseases, Bern University Hospital, University of Bern, Bern, Switzerland

⁶Population Health Sciences, Bristol Medical School, University of Bristol, Bristol, United Kingdom

*Corresponding authors (matthias.egger@ispm.unibe.ch, roger.kouyos@uzh.ch)

March 24, 2021

Contents

| | | |
|----------|--|-----------|
| 1 | Adapted MARISA model | 2 |
| 1.1 | MARISA model | 2 |
| 1.2 | Adapted MARISA model | 2 |
| 2 | Parameters and rates of the adapted MARISA model | 3 |
| 2.1 | Rates related to continuum of care and disease progression | 3 |
| 2.2 | Diagnosis, treatment initiation and switching rates | 4 |
| 2.3 | Resistance rates | 5 |
| 2.4 | Impact of NNRTI-resistance on NNRTI | 6 |
| 2.5 | DTG-efficacy and impact of NRTI-resistance on DTG | 7 |
| 2.6 | Other parameters: HIV transmission and mortality | 8 |
| 3 | Model simulation | 9 |
| 3.1 | Prospective scenarios | 9 |
| 3.2 | Sensitivity analysis | 9 |
| 4 | Model ODEs | 10 |
| 4.1 | Description of the compartments | 10 |
| 4.2 | Model ODEs | 11 |
| 5 | Sensitivity analysis and additional results | 13 |
| 5.1 | Effect of no Treat-All policy | 15 |
| 5.2 | Effect of treatment interruption | 17 |
| 5.3 | Effect of NRTI-resistance and higher efficacy of DTG | 18 |

1 Adapted MARISA model

1.1 MARISA model

MARISA is a mechanistic, compartmental model developed to capture the dynamics of HIV NNRTI resistance among adults in South Africa over the years 2005-2016. It models the continuum of care - including NNRTI-based first-line and PI-based second-line regimens -, the disease progression, acquisition and transmission of NNRTI-resistance, and its impact on the efficacy of NNRTI-based regimen. The model was calibrated using different sources of data: 1) cohort data about more than 30,000 people living with HIV from IeDEA collaboration [1], 2) data from literature, and 3) general HIV estimates at the country scale produced by the Thembisa model. The Thembisa model is a compartmental model providing UNAIDS with estimates on the South African HIV epidemic [2].

We adapted this model to investigate the impact of the introduction of DTG-based regimens in South Africa from 2020. The changes include 1) incorporating DTG-based regimen into the continuum of care, 2) distinguishing between DTG-eligible and -ineligible individuals, and 3) adding a NRTI-resistance dimension.

1.2 Adapted MARISA model

The adapted MARISA model is split in 5 dimensions: 1) care stages (15 levels), 2) disease progression, characterised by the CD4 counts (4 levels), 3) sex (2 levels), 4) NNRTI resistance (2 levels) and 5) NRTI resistance (2 levels).

The first dimension of the model accounts for the whole continuum of care (see Fig A). The first three compartments model respectively HIV-infection of susceptible individuals and diagnosis (with a distinction between DTG-eligible and -ineligible women). We then considered the three different regimens - NNRTI-based, PI-based and DTG-based -, again with a distinction by DTG-eligibility for individuals on a NNRTI-based regimen. For each of the three regimens, three compartments are used to model treatment initiation ("Treat init.") with subsequent virological suppression ("Supp") or failure ("Fail"). "Treat init." compartments represent individuals who initiated treatment less than 3 months ago. Before 2020, all individuals receive a NNRTI-based first-line regimen and switch to the second-line PI-based regimen in case of prolonged failure. From 2020, the DTG-based regimen is used as a first-line regimen for all DTG-eligible individuals. From this time, DTG-eligible individuals who are currently on NNRTI-based regimen can transition to DTG-based regimen. PI-based regimen is still used as a second-line regimen, either for DTG-ineligible patients failing NNRTI-based ART, or for patients failing DTG-based ART.

The second dimension splits individuals in 4 classes according to CD4 counts: 1) $CD4 > 500$ cells/ μL , 2) $350 < CD4 < 500$ cells/ μL , 3) $200 < CD4 < 350$ cells/ μL and 4) $CD4 < 200$ cells/ μL . The third dimension makes the distinction between male and female. The fourth and fifth dimensions respectively model NNRTI- and NRTI-resistance. They each have two layers that distinguish between NNRTI-/NRTI-susceptible and -resistant individuals. We used the following indices to indicate a layer of a dimension: j for the second dimension ($j = 1, 2, 3, 4$), k for the third dimension ($k = 1, 2$), l for the fourth dimension ($l = 1, 2$) and m for the fifth dimension ($m = 1, 2$).

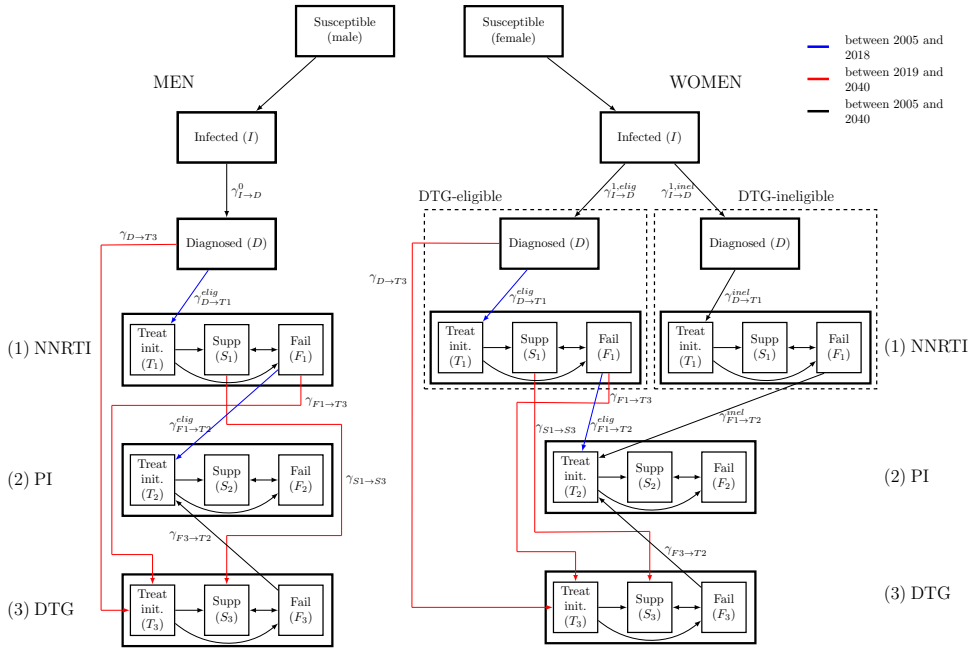


Fig A: Adapted MARISA model. Only the first (continuum of care) and the third (sex) dimensions are represented.

2 Parameters and rates of the adapted MARISA model

2.1 Rates related to continuum of care and disease progression

Rates related to disease progression ν_{CD4} and $\bar{\nu}_{CD4}$ as well as rates related to continuum of care γ , which respectively model transition from one to another CD4 class and transition from one to another care stage, were estimated using observational cohort data from IeDEA-SA collaboration. Survival analyses were performed using information of more than 30'000 patients from South Africa. Mean estimates and 95% confidence intervals (95%CI) are reported in Table A and B.

Table A: Rates related to disease progression. Rates are in month⁻¹.

| Parameter | Description | Values [95% CI] | | |
|--|---|-----------------|------------|------------|
| <i>Parameters related to disease progression</i> | | | | |
| | | 1 → 2 | CD4 class | |
| | | | 2 → 3 | 3 → 4 |
| $1/\nu_{CD4}^I$ | Average time to progress from one to another CD4 class, at I (taken from [3]) | 60 | 36 | 42 |
| $1/\nu_{CD4}^D$ | Average time to progress from one to another CD4 class, at D (taken from [3]) | 60 | 36 | 42 |
| $1/\nu_{CD4}^{T_1}$ | Average time to progress from one to another CD4 class, at T_1 | 47 [42,54] | 30 [28,34] | 60 [55,66] |
| $1/\nu_{CD4}^{F_1}$ | Average time to progress from one to another CD4 class, at F_1 | 18 [16,20] | 15 [14,16] | 22 [21,24] |
| $1/\nu_{CD4}^{T_2}$ | Average time to progress from one to another CD4 class, at T_2 | 32 [14,72] | 22 [12,43] | 33 [17,64] |
| $1/\nu_{CD4}^{F_2}$ | Average time to progress from one to another CD4 class, at F_2 | 14 [8,26] | 15 [8,27] | 16 [10,25] |
| | | 1 ← 2 | 2 ← 3 | 3 ← 4 |
| $1/\bar{\nu}_{CD4}^{T_1}$ | Average time to progress from one to another CD4 class, at T_1 | 16 [15,17] | 16 [15,17] | 18 [17,19] |
| $1/\bar{\nu}_{CD4}^{S_1}$ | Average time to progress from one to another CD4 class, at S_1 | 17 [16,17] | 14 [14,14] | 9 [9,10] |
| $1/\bar{\nu}_{CD4}^{T_2}$ | Average time to progress from one to another CD4 class, at T_2 | 16 [9,27] | 19 [11,31] | 41 [23,73] |
| $1/\bar{\nu}_{CD4}^{S_2}$ | Average time to progress from one to another CD4 class, at S_2 | 17 [13,21] | 14 [11,17] | 7 [6,10] |

Table B: Rates related to transition between care stages. Rates are in month⁻¹.

| Parameter | Description | Values [95% CI] | | | |
|--|--------------------------|----------------------|------------------------|------------------------|---------------------|
| <i>Parameters related to care stages</i> | | | | | |
| | | CD4 class | | | |
| | | 1 | 2 | 3 | 4 |
| $1/\gamma_{T_1 \rightarrow S_1}$ | Time from T_1 to S_1 | 3.4 [3.3,3.6] | 3.5 [3.3,3.7] | 3.6 [3.4,3.7] | 3.9 [3.8,4.1] |
| $1/\gamma_{T_1 \rightarrow F_1}$ | Time from T_1 to F_1 | 23.4 [20.1,27.3] | 22.8 [19.6,26.4] | 18.9 [17.5,20.4] | 12.9 [12.3,13.5] |
| $1/\gamma_{S_1 \rightarrow F_1}$ | Time from S_1 to F_1 | 176.3 [157,197.9] | 133.8 [118.6,150.8] | 62.1 [57,67.6] | 22.1 [20.2,23.9] |
| $1/\gamma_{F_1 \rightarrow S_1}$ | Time from F_1 to S_1 | 6.4 [5.5,7.4] | 12.9 [11,14.9] | 14.3 [12.9,15.9] | 18.2 [16.3,20.2] |
| $1/\gamma_{F_1 \rightarrow T_2}$ | Time from F_1 to T_2 | 467.5 [243,898.9] | 376 [240.4,589.9] | 258.9 [200.7,334.6] | 166.4 [140,199] |
| $1/\gamma_{T_2 \rightarrow S_2}$ | Time from T_2 to S_2 | 3.8 [2.7,5.2] | 3.8 [2.6,5.5] | 4 [3.5,3] | 5 [4,6.4] |
| $1/\gamma_{T_2 \rightarrow F_2}$ | Time from T_2 to F_2 | 14.3 [7.8,26.8] | 14 [7.3,27] | 11.8 [7.8,18] | 7.6 [5.9,9.9] |
| $1/\gamma_{S_2 \rightarrow F_2}$ | Time from S_2 to F_2 | 61.4 [30.8,122.8] | 40.9 [21.4,78.9] | 40 [21.4,74.3] | 19.1 [9,40] |
| $1/\gamma_{F_2 \rightarrow S_2}$ | Time from F_2 to S_2 | 2.3 [1.1,4.1] | 12.9 [3.2,51.3] | 5.5 [2.8,11.3] | 11.7 [4.8,28] |

2.2 Diagnosis, treatment initiation and switching rates

Diagnosis rates depend on sex and CD4 class and treatment initiation rates depend on CD4 class. They have been described in details in [4], S1 File, Section 1.3. In the adapted MARISA model, we assumed that diagnosis rates are constant from 2016, while the treatment initiation rate has been adapted in order to model the impact of the Treat-All policy. We increased treatment initiation rates for the first three CD4 count classes from 2017 to 2022 in order to have identical rates from 2022, irrespective of CD4 counts (see Fig B). To ensure a proportion p_1 of DTG-eligible women, two diagnosis rates are used $\gamma_{I \rightarrow D}^{k,elig} := p_1 \cdot \gamma_{I \rightarrow D}^k$, $\gamma_{I \rightarrow D}^{k,incl} := (1 - p_1) \cdot \gamma_{I \rightarrow D}^k$, in order

to distribute women into the two DTG-eligibility classes.

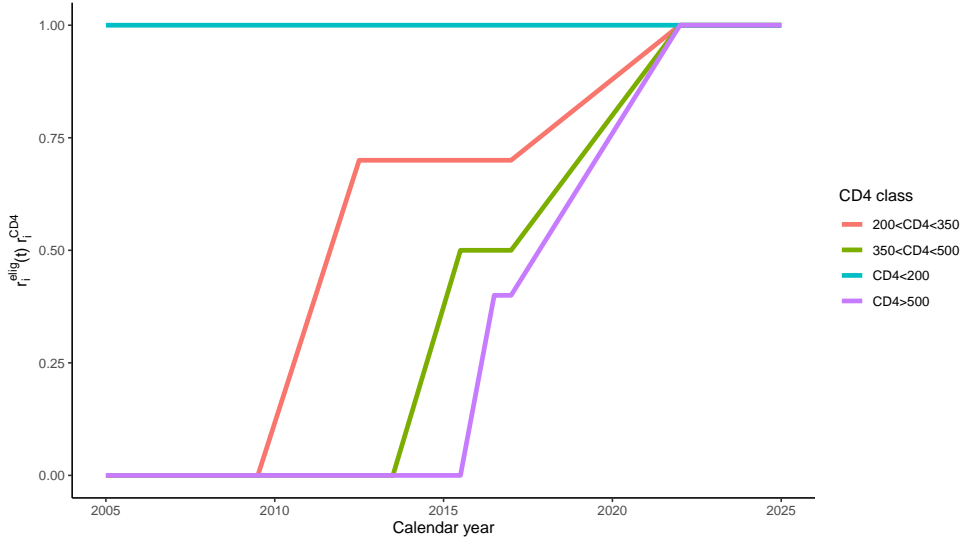


Fig B: $r_i^{elig}(t) \cdot r_i^{CD4}$ represents the level of treatment eligibility $r_i^{elig}(t)$ multiplied by r_i^{CD4} , representing the lower treatment initiation rate of CD4 class i relative to the CD4 class $i = 4$. These two components are parts of the overall treatment initiation rate $\gamma_{D \rightarrow T_1}^i(t) = \gamma_{2005}^{CD4 < 200} \cdot r_i^{elig}(t) \cdot r_i^{CD4} \cdot r^{time}(t)$.

We rescaled the switching rates from unsuppressed NNRTI-based regimen to PI-based regimen $\gamma_{F_1 \rightarrow T_2}^{k,elig/inel}$ in order to reflect PI-coverage in South Africa ($\sim 4\%$ in 2016 according to [5]). The new rates $\gamma_{F_1 \rightarrow T_2}^{k,elig/inel}$ can be found in Table B.

2.3 Resistance rates

Two rates model the flow between the two NNRTI-resistance layers: the reversion rate σ_{rev} and the rate of acquiring NNRTI-resistance σ_{res}^{NNRTI} . Reversion to wild-type occurs when no more drug pressure is exerted, i.e. in the "Infected" and "Diagnosed" compartments. An individual can acquire NNRTI-resistance when failing first-line regimen. Both parameters σ_{rev} and σ_{res}^{NNRTI} were collected from literature and can be found in Table C.

Table C: Parameters collected from literature. As mortality estimates in the fourth CD4 class vary according to the proportion of people with $CD4 < 50$ cells/ μL , lower and upper bounds are given (see [4] S1 File Section 1.2 for more details). The mortality risk μ_X^j in CD4 class j ($i = 1, \dots, 4$) and care stage X ($X = I, D, T_1, \dots$) is given by: $\mu_X^j = \mu_0 \cdot \tilde{\mu}_X^j$.

| Parameter | Description | Values | Ref | | |
|------------------------------|---|-----------|------------------|-----|------------|
| <i>Resistance parameters</i> | | | | | |
| $1/\sigma_{res}^{NNRTI}$ | Time to acquire NNRTI-resistance (in month) | 5 | [6, 7, 8, 9, 10] | | |
| $1/\sigma_{res}^{NRTI}$ | Time to acquire NRTI-resistance (in month) | 40 | [11] | | |
| $1/\sigma_{rev}$ | Time to revert back to wild-type (in month) | 125 | [12] | | |
| α_1 | Impact of NNRTI-resistance on NNRTI-based ART | 1.97 | [13, 14] | | |
| α_2 | Impact of NNRTI-resistance on NNRTI-based ART | 3.24 | [13, 14] | | |
| α_3 | Impact of NRTI-resistance on DTG-based ART | 1 | [15, 16, 17] | | |
| α_4 | Scaling factor for the efficacy NNRTI-based regimen (see Section 2.4) | 1.62 | [1] | | |
| α_5 | Scaling factor for the efficacy DTG-based regimen (see Section 2.5) | 0.85 | [18] | | |
| <i>Other parameters</i> | | | | | |
| $\nu_{0,0}$ | probability that a male infects a male (per act) | 0.8% | [19] | | |
| $\nu_{0,1}$ | probability that a male infects a female (per act) | 0.3% | [19] | | |
| $\nu_{1,0}$ | probability that a female infects a male (per act) | 0.3% | [19] | | |
| $\rho_{0,0}$ | percentage of MSM | 5% | [20] | | |
| $\tilde{\mu}^i$ | relative mortality risk (Ref: suppressed indiv. with $CD4 > 500$) | | [21] [22] | | |
| | | CD4 class | | | |
| | | 1 | 2 | 3 | 4 |
| | $\tilde{\mu}_{I/D}^i$: not treated (I and D) | 1.6 | 2 | 4.6 | 40.9-134.4 |
| | $\tilde{\mu}_{T_1/T_2}^i$: started treatment (T_1 and T_2) | 2.5 | 2.6 | 3.1 | 10-50.7 |
| | $\tilde{\mu}_{S_1/S_2}^i$: suppressed (S_1 and S_2) | 1 | 1.3 | 2 | 8.3-41.7 |
| | $\tilde{\mu}_{F_1/F_2}^i$: failed (F_1 and F_2) | 3.9 | 3.9 | 4.3 | 11.8-59.7 |

For the sake of simplicity and in view of the scarcity of evidence on the impact of NRTI-resistance on DTG-based regimen, the dimension modelling NRTI-resistance has only two layers that distinguish between NRTI-resistant and NRTI-susceptible individuals. NRTI resistance is defined as having both the K65R and the M184V mutations, which confers high level of resistance to tenofovir (TDF) and lamivudine/emtricitabine (3TC/FTC), respectively. In view of the low level of NRTI pre-treatment drug resistance (PDR) [12, 23], we assume that NRTI resistance is not transmitted. The rate σ_{res}^{NRTI} models the process of acquiring NRTI-resistance, which occurs when individuals are failing first-line NNRTI-based regimen. We calibrated σ_{res}^{NRTI} using results from a meta-analysis that estimates the prevalence of NRTI resistance mutation after 3 years on a failing NNRTI-based first-line regimen [11]. This meta-analysis found that 75% of them had the K65R mutation and 73% the M184V mutation. Assuming no association between the two mutations as suggested by [24], we inferred σ_{res}^{NRTI} so that 54.8% (i.e. 75% · 73%) of individuals failing NNRTI-based regimen were resistant to NRTI after 3 years of ART. We found $\sigma_{res}^{NRTI} = 1/40$ months⁻¹ (see Table C).

2.4 Impact of NNRTI-resistance on NNRTI

Unlike the previous MARISA model, the adapted MARISA used two parameters α_1 and α_2 to model the impact of NNRTI resistance on NNRTI treatment response. Both parameters increase the previously estimated rates of failure $\gamma_{T_1 \rightarrow F_1}$, $\gamma_{S_1 \rightarrow F_1}$ and decrease the suppression rates $\gamma_{T_1 \rightarrow S_1}$ and $\gamma_{F_1 \rightarrow S_1}$ for NNRTI-resistant individuals, but at different treatment stages. While α_1 represents the impact of NNRTI resistance among individuals having just started treatment (less than 3 months), α_2 models this impact at the later stage of treatment. In order that the MARISA model achieves the same suppression level with these modified rates as estimated from IeDEA-SA cohort data, we used a third scaling parameter α_4 which increases the overall suppression rates and decreases the failing rates. The different failing and suppression rates according to CD4 class j and NNRTI-resistance status l are given in Eq 1-8. The rates $\gamma_{T_1 \rightarrow F_1}$, $\gamma_{T_1 \rightarrow S_1}$, $\gamma_{S_1 \rightarrow F_1}$ and $\gamma_{F_1 \rightarrow S_1}$ represent the overall suppression and failure rate for NNRTI-based ART, as estimated with IeDEA cohort data (see Tables A and B).

$$\gamma_{T_1 \rightarrow F_1}^{j,l=0} = 1/\alpha_4 \cdot \gamma_{T_1 \rightarrow F_1} \quad (1)$$

$$\gamma_{T_1 \rightarrow F_1}^{j,l=1} = \alpha_1/\alpha_4 \cdot \gamma_{T_1 \rightarrow F_1} \quad (2)$$

$$\gamma_{T_1 \rightarrow S_1}^{j,l=0} := 1/3 - \gamma_{T_1 \rightarrow F_1}^{j,l=0} \quad (3)$$

$$\gamma_{T_1 \rightarrow S_1}^{j,l=1} := 1/3 - \gamma_{T_1 \rightarrow F_1}^{j,l=1} \quad (4)$$

$$\gamma_{F_1 \rightarrow S_1}^{j,l=0} = \alpha_4 \cdot \gamma_{F_1 \rightarrow S_1} \quad (5)$$

$$\gamma_{F_1 \rightarrow S_1}^{j,l=1} = \alpha_4/\alpha_2 \cdot \gamma_{F_1 \rightarrow S_1} \quad (6)$$

$$\gamma_{S_1 \rightarrow F_1}^{j,l=0} = 1/\alpha_4 \cdot \gamma_{S_1 \rightarrow F_1} \quad (7)$$

$$\gamma_{S_1 \rightarrow F_1}^{j,l=1} = \alpha_2/\alpha_4 \cdot \gamma_{S_1 \rightarrow F_1} \quad (8)$$

The three parameters α_1 , α_2 and α_3 were simultaneously calibrated using two different kinds of data. To identify α_1 and α_2 , we used estimates from two studies that compared level of NNRTI failure between NNRTI-susceptible and NNRTI-resistant individuals. Both studies reported a hazard ratio (HR) of ART failure between NNRTI-resistant and NNRTI-susceptible people of 3.13. To identify α_4 , we used the overall suppression level of 88% for NNRTI-based regimen, as estimated from IeDEA cohort data. The values of the three parameter estimates are given in Table C. The higher estimated value of α_2 compared with α_1 ($\alpha_1 = 1.97$, $\alpha_2 = 3.24$) reflects the long-term impact of NNRTI-resistance on the NNRTI-treatment response.

2.5 DTG-efficacy and impact of NRTI-resistance on DTG

In this updated MARISA model, we also model the potential impact of NRTI-resistance on DTG-based regimen. We used the same suppression and failure rates for DTG-based regimen as for NNRTI-based one, but replace the scaling factor α_4 by α_5 , to take into account the difference in treatment efficacy between NNRTI and DTG. The scaling factor α_5 was calibrated to reflect results of the NAMSAL study [18], which observed a crude odds ratio (OR) of failure of 1.46 between NNRTI- and DTG-based regimens, after 48 weeks of treatment. To do so, we fitted the OR calculated by the MARISA model to the OR observed in NAMSAL studies, taking into account the different baseline characteristics (distribution of CD4 counts and level of baseline NNRTI-resistance) of the NNRTI- and DTG-groups. After these adjustments, we found an OR of 1.02 between the two groups, assuming that they are both susceptible to their respective ART regimen (i.e. no NNRTI-resistance). This decrease in OR after adjustment is due to the fact that the NNRTI-group in the NAMSAL had lower baseline CD4 counts and that part of them had baseline NNRTI-resistance. Other efficacies of DTG-based regimens, corresponding to ORs of 2 and 5, were investigated in the sensitivity analysis (see Section 5).

As a simplifying assumption, all individuals that transitions to DTG-based regimen are considered to have received a NNRTI-drug combined with TDF and 3TC/FTC and to keep this NRTI-backbones combination after transitioning to DTG-based regimen. This assumption is motivated by the expected reluctance of clinicians to prescribe zidovudine (AZT) for TDF-experienced individuals transitioning to DTG due to its side effects. In the case where NRTI backbones would be adapted when transitioning to DTG, the model might overestimate the impact of NRTI resistance on DTG-based regimen. We applied the same approach to model the impact of NRTI resistance on DTG-based regimen as we did to model the impact of NNRTI resistance on NNRTI-based regimen. The suppression and failure rates for NRTI-resistant individual starting a DTG-based regimen are respectively divided and multiplied by a factor α_3 . The different failing and suppression rates according to CD4 class j and NRTI-resistance status m are given in Eq 9-16.

$$\gamma_{T_3 \rightarrow F_3}^{j,m=0} = 1/\alpha_5 \cdot \gamma_{T_1 \rightarrow F_1} \quad (9)$$

$$\gamma_{T_3 \rightarrow F_3}^{j,m=1} = \alpha_3/\alpha_5 \cdot \gamma_{T_1 \rightarrow F_1} \quad (10)$$

$$\gamma_{T_3 \rightarrow S_3}^{j,m=0} := 1/3 - \gamma_{T_1 \rightarrow F_1}^{j,l=0} \quad (11)$$

$$\gamma_{T_3 \rightarrow S_3}^{j,m=1} := 1/3 - \gamma_{T_1 \rightarrow F_1}^{j,l=1} \quad (12)$$

$$\gamma_{F_3 \rightarrow S_3}^{j,m=0} = \alpha_5 \cdot \gamma_{F_1 \rightarrow S_1} \quad (13)$$

$$\gamma_{F_3 \rightarrow S_3}^{j,m=1} = \alpha_5/\alpha_3 \cdot \gamma_{F_1 \rightarrow S_1} \quad (14)$$

$$\gamma_{S_3 \rightarrow F_3}^{j,m=0} = 1/\alpha_5 \cdot \gamma_{S_1 \rightarrow F_1} \quad (15)$$

$$\gamma_{S_3 \rightarrow F_3}^{j,m=1} = \alpha_3 / \alpha_5 \cdot \gamma_{S_1 \rightarrow F_1} \quad (16)$$

In the main analysis, we calibrated α_3 so that the odds ratio (OR) of DTG-failure between NRTI-susceptible and -resistant individuals takes two particular values : OR=1, OR=2. Higher impact of NRTI-resistance on DTG-based regimen (OR=5) is investigated in the sensitivity analysis, together with different DTG-efficacies (see Section 5).

2.6 Other parameters: HIV transmission and mortality

The MARISA model accounts for both heterosexual and homosexual HIV-transmission, with different risks of transmission per intercourse. We also assumed that undiagnosed individuals have a more risky behaviour. Parameters related to HIV-transmission were either collected from literature (see Table C) or estimated using results from Thembisa model (see Table D). We assumed that mortality depends on both the CD4 counts and the treatment stage. Relative mortality estimates were collected from literature (see Table C) and a scaling parameter, representing the mortality risk among suppressed individual with $CD4 > 500$ copies/ml, was fitted to HIV-mortality estimate provided by the Thembisa model. More information about HIV-transmission and mortality can be found in S1 Text of [4].

Table D: Parameters estimated from outputs of the Thembisa model.

| Parameter | Description | Values |
|---|--|--------|
| β_u | Number of unprotected sexual acts per month (for undiagnosed individual) | 3.1 |
| β_d | Number of unprotected sexual acts per month (for diagnosed individual) | 1.24 |
| $\gamma_{I \rightarrow D}(2016) / \gamma_{I \rightarrow D}(2005)$ | Ratio of diagnosis rates between 2005 and 2016 | 4.4 |
| $1 / \gamma_{I \rightarrow D}(2005)$ | Time to diagnosis in 2005 (in month) | 26 |
| $1 / \gamma_{D \rightarrow T_1}(2005)$ | Time to ART initiation in 2005 (in month) | 60 |
| μ_0 | Mortality risk (in $(\text{month} \cdot 1000 \text{ people})^{-1}$) for a suppressed individual with $CD4 > 500$ cells/ μL | 0.08 |

3 Model simulation

3.1 Prospective scenarios

We simulated 2 different scenarios:

1. DTG only used in first-line regimen of ART-initiators and, as second-line, in patients failing NNRTI-based ART ($\gamma_{D \rightarrow T3}$ and $\gamma_{F1 \rightarrow T3}$ in Fig A),
2. DTG used as initial first-line regimen (for ART-initiators), with all patients on NNRTI-based regimens being switched to a DTG-based regimen (all the red arrows).

Within these 2 scenarios, 4 sub-scenarios investigated the impact of different percentages p_1 of DTG-prescription for women: a) no women (0%), b) women outside reproductive age (17.5%), c) women outside reproductive age or using contraception (63%), and d) all women (100%). Percentage in b) is calculated with the help of IeDEA-SA cohorts [1] which estimated that 17.5% of adult women under ART were older than 49. Percentage in c) is calculated with the help of both IeDEA-SA estimate and World Bank [25], which estimated that 54.6% of women aged 15-49 in South Africa were using any contraception method in 2015:

$$\begin{aligned}
 p_1 &:= \text{P}(\text{women eligible for DTG}) \\
 &= 1 - \text{P}(15 \leq \text{age} \leq 49 \ \& \ \text{no contraception} | \text{women on ART}) \\
 &= 1 - \text{P}(15 \leq \text{age} \leq 49 | \text{women on ART}) \cdot \text{P}(\text{no contraception} | 15 \leq \text{age} \leq 49 \ \& \ \text{on ART}) \\
 &= 1 - (1 - 0.175) \cdot (1 - 0.546) = 63\%.
 \end{aligned} \tag{17}$$

As no information about contraceptive prevalence in South African adult women on ART have been found, we approximated it by the contraceptive prevalence in the general South African adult women population (see 17). By definition, the percentage p_0 of DTG-eligible men is 100%.

3.2 Sensitivity analysis

In the sensitivity analysis, we perturbed eight parameters 200 times using a Latin Hypercube Sampling method (see Table E). Table E displays the main values of the eight parameters, which were informed from literature and lower and upper bounds, chosen to reflect plausible values of the parameters. As varying the transmission-related parameters may modify the overall transmission rate, an adjustment is made to have a transmission rate similar to the baseline model. We ran the sensitivity analysis for each prospective scenario (13 different scenarios in total).

Table E: Parameter ranges used in sensitivity analysis. Lower and upper bounds for α_1 and α_2 were determined in order to have an OR of ART failure between NNRTI-susceptible and -resistant individuals of 1 and 5, respectively. For α_5 , lower and upper bounds were determined in order to have an OR between NNRTI- and DTG-failure of 1 and 2, respectively.

| Parameter | Definition | Value | Lower bound | Upper bound |
|--|--|-------|-------------|-------------|
| <i>Resistance-related parameters</i> | | | | |
| $1/\sigma_{res}^{NNRTI}$ | Time to acquisition of NNRTI resistance (months) | 5 | 3 | 9 |
| $1/\sigma_{rev}$ | Time to reversion to wild-type virus (months) | 125 | 36 | 200 |
| α_1 | Impact of NNRTI resistance on NNRTI-based ART | 1.97 | 1 (OR=1) | 3.1 (OR=5) |
| α_2 | Impact of NNRTI resistance on NNRTI-based ART (see Eq 1-8) | 3.24 | 1 (OR=1) | 5.1 (OR=5) |
| α_5 | Scaling factor for the efficacy DTG-based ART | 0.85 | 0.84 (OR=1) | 1.25 (OR=2) |
| <i>Transmission-related parameters</i> | | | | |
| $\rho_{0,0}$ | Percentage of MSM | 5% | 1% | 10% |
| $\nu_{0,0}/\nu_{0,1}$ | Increase in risk of transmission in MSM (see Table C) | 2.7 | 1 | 5 |
| - | Ratio between HIV prevalence in MSM and in HET | 1 | 1 | 3 |

4 Model ODEs

4.1 Description of the compartments

Table F describes the compartments used in the model, while model ODEs are given in Equations 19.

Table F: Description of the compartments used in the model.

| Notation | Description | Definition |
|--------------------------------|---|--|
| <i>Dimensions/Compartments</i> | | |
| j | index for the 2nd dimension (CD4 counts) | $j = 1, 2, 3, 4$ (4 CD4 strata) |
| k | index for the 3rd dimension (sex) | $k = 0$: men, $k = 1$: women |
| l | index for the 4th dimension (NNRTI-resistance) | $l = 0$: NNRTI-susceptible $l = 1$: NNRTI-resistant |
| m | index for the 5th dimension (NRTI-resistance) | $m = 0$: NRTI-susceptible $m = 1$: NRTI-resistant |
| $I^{jklm}(t)$ | number of infected (not diagnosed) indiv. | |
| $D_{elig}^{jklm}(t)$ | number of diagnosed (not treated) indiv. | |
| $D_{inel}^{jklm}(t)$ | for resp. DTG-eligible and -ineligible ind. (by def. $D_{inel}^{j0lm}(t) = 0$) | |
| <i>NNRTI-based treatment</i> | | |
| $T_{1,elig}^{jklm}(t)$ | number of indiv. that have started NNRTI-based treatment for less than 3 months | |
| $T_{1,inel}^{jklm}(t)$ | for resp. DTG-eligible and -ineligible ind. (by def. $T_{1,inel}^{j0lm}(t) = 0$) | |
| $S_{1,elig}^{jklm}(t)$ | number of suppressed indiv. on NNRTI-based treatment | |
| $S_{1,inel}^{jklm}(t)$ | for resp. DTG-eligible and -ineligible ind. (by def. $S_{1,inel}^{j0lm}(t) = 0$) | |
| $F_{1,elig}^{jklm}(t)$ | number of indiv. failing NNRTI-based treatment | |
| $F_{1,inel}^{jklm}(t)$ | for resp. DTG-eligible and -ineligible ind. (by def. $F_{1,inel}^{j0lm}(t) = 0$) | |
| <i>PI-based treatment</i> | | |
| $T_2^{jklm}(t)$ | number of indiv. that have started PI-based treatment for less than 3 months | |
| $S_2^{jklm}(t)$ | number of suppressed indiv. on PI-based treatment | |
| $F_2^{jklm}(t)$ | number of indiv. failing PI-based treatment | |
| <i>DTG-based treatment</i> | | |
| $T_3^{jklm}(t)$ | number of indiv. that have started DTG-based treatment for less than 3 months | |
| $S_3^{jklm}(t)$ | number of suppressed indiv. on DTG-based treatment | |
| $F_3^{jklm}(t)$ | number of indiv. failing DTG-based treatment | |
| <i>Aggregated compartments</i> | | |
| $Susc^k$ | number of susceptible indiv. of sex k | |
| $Inf_u^{kl}(t)$ | number of undiagnosed indiv. | $Inf_u^{kl}(t) := I^{kl}(t)$ |
| $Inf_d^{kl}(t)$ | number of infectious diagnosed indiv. | |

4.2 Model ODEs

The rates γ represent the transition between care stages, ν_{CD4} the transition between CD4 stages and μ_{ij} the mortality. The rate σ_{rev} represents reversion of NNRTI-resistance when no more drug pressure is exerted, while σ_{res}^{NNRTI} and σ_{res}^{NRTI} represents the rates of acquiring NNRTI resistance and NRTI resistance, respectively, when an individual is failing NNRTI-based treatment. To model new infections, we used β_u and β_d the respective monthly number of sexual contacts among undiagnosed and diagnosed individuals, $\rho_{k,k}$ the assumed proportion of heterosexual individuals within men and women and $\nu_{k,k'}$ the probability of HIV transmission per sexual act. Finally, we also used a function $\delta(x)$, which is given by :

$$\delta(x) = \begin{cases} -1 & \text{if } x = 0, \\ 1 & \text{if } x = 1. \end{cases} \quad (18)$$

$$\begin{aligned} \dot{I}^{jklm}(t) &= -\nu_{CD4}^{I,j} \cdot I^{jklm}(t) \mathbb{1}_{j \leq 3} + \nu_{CD4}^{I,j-1} \cdot I^{(j-1)klm}(t) \mathbb{1}_{j \geq 2} \\ &+ \beta_u \left(\rho_{1-k,k} \nu_{1-k,k} \frac{Susc_k}{N_k} Inf_u^{(1-k)l} + \rho_{k,k} \nu_{k,k} \frac{Susc_k}{N_k} Inf_u^{kl} \right) \mathbb{1}_{j=1} \\ &+ \beta_d \left(\rho_{1-k,k} \nu_{1-k,k} \frac{Susc_k}{N_k} Inf_d^{(1-k)l} + \rho_{k,k} \nu_{k,k} \frac{Susc_k}{N_k} Inf_d^{kl} \right) \mathbb{1}_{j=1} \\ &- \gamma_{I \rightarrow D}^{jk} \cdot I^{jklm}(t) - \delta(l) \cdot \sigma_{rev} \cdot I^{jk1m}(t) - \mu_I^j \cdot I^{jklm}(t), \\ \dot{D}_{elig}^{jklm}(t) &= -\nu_{CD4}^{D,j} \cdot D_{elig}^{jklm}(t) \mathbb{1}_{j \leq 3} + \nu_{CD4}^{D,j} \cdot D_{elig}^{(j-1)klm}(t) \mathbb{1}_{j \geq 2} \\ &- (\gamma_{D \rightarrow T_1}^{j,elig}(t) + \gamma_{D \rightarrow T_2}^{jk}(t) + \gamma_{D \rightarrow T_3}^{jk}(t)) \cdot D_{elig}^{jklm}(t) \\ &+ p_k \gamma_{I \rightarrow D}^{jk} \cdot I^{jklm}(t) - \delta(l) \cdot \sigma_{rev} \cdot D_{elig}^{jk1m}(t) - \mu_D^j \cdot D_{elig}^{jklm}(t), \\ \dot{D}_{inel}^{jklm}(t) &= -\nu_{CD4}^{D,j} \cdot D_{inel}^{jklm}(t) \mathbb{1}_{j \leq 3} + \nu_{CD4}^{D,j} \cdot D_{inel}^{(j-1)klm}(t) \mathbb{1}_{j \geq 2} \\ &- \gamma_{D \rightarrow T_1}^{j,inel}(t) \cdot D_{inel}^{jklm}(t) \\ &+ (1 - p_k) \gamma_{I \rightarrow D}^{jk} \cdot I^{jklm}(t) - \delta(l) \cdot \sigma_{rev} \cdot D_{inel}^{jk1m}(t) - \mu_D^j \cdot D_{inel}^{jklm}(t), \\ \dot{T}_{1,elig}^{jklm}(t) &= \left(\nu_{CD4}^{T_1,j-1} \cdot T_{1,elig}^{(j-1)klm}(t) - \tilde{\nu}_{CD4}^{T_1,j-1} \cdot T_{1,elig}^{jklm}(t) \right) \mathbb{1}_{j \geq 2} \\ &+ \left(\tilde{\nu}_{CD4}^{T_1,j} \cdot T_{1,elig}^{(j+1)klm}(t) - \nu_{CD4}^{T_1,j} \cdot T_{1,elig}^{jklm}(t) \right) \mathbb{1}_{j \leq 3} \\ &- (\gamma_{T_1 \rightarrow S_1}^{jl} + \gamma_{T_1 \rightarrow F_1}^{jl}) \cdot T_{1,elig}^{jklm}(t) + \gamma_{D \rightarrow T_1}^{jk} \cdot D_{elig}^{jklm}(t) - \mu_{T_1}^j \cdot T_{1,elig}^{jklm}(t) \\ \dot{S}_{1,elig}^{jklm}(t) &= -\tilde{\nu}_{CD4}^{S_1,j-1} \cdot S_{1,elig}^{jklm}(t) \mathbb{1}_{j \geq 2} + \tilde{\nu}_{CD4}^{S_1,j} \cdot S_{1,elig}^{(j+1)klm}(t) \mathbb{1}_{j \leq 3} \\ &- \gamma_{S_1 \rightarrow F_1}^{jl} \cdot S_{1,elig}^{jklm}(t) + \gamma_{T_1 \rightarrow S_1}^{jl} \cdot T_{1,elig}^{jklm}(t) + \gamma_{F_1 \rightarrow S_1}^{jl} \cdot F_{1,elig}^{jklm}(t) - \mu_{S_1}^j \cdot S_{1,elig}^{jklm}(t) \\ &- \gamma_{S_1 \rightarrow S_3}(t) \cdot S_{1,elig}^{jklm}(t), \\ \dot{F}_{1,elig}^{jklm}(t) &= \nu_{CD4}^{F_1,j-1} \cdot F_{1,elig}^{(j-1)klm}(t) \mathbb{1}_{j \geq 2} - \nu_{CD4}^{F_1,j} \cdot F_{1,elig}^{jklm}(t) \mathbb{1}_{j \leq 3} \\ &+ \delta(l) \cdot \sigma_{res}^{NNRTI} \cdot F_{1,elig}^{jk0m}(t) + \delta(m) \cdot \sigma_{res}^{NRTI} \cdot F_{1,elig}^{jkl0}(t) \\ &- (\gamma_{F_1 \rightarrow S_1}^{jl} + \gamma_{F_1 \rightarrow T_2}^{j,elig}(t)) \cdot F_{1,elig}^{jklm}(t) + \gamma_{S_1 \rightarrow F_1}^{jl} \cdot S_{1,elig}^{jklm}(t) + \gamma_{T_1 \rightarrow F_1}^{jl} \cdot T_{1,elig}^{jklm}(t) \\ &- \mu_{F_1}^j \cdot F_{1,elig}^{jklm}(t) - \gamma_{F_1 \rightarrow T_3}^j(t) \cdot F_{1,elig}^{jklm}(t), \\ \dot{T}_{1,inel}^{jklm}(t) &= \left(\nu_{CD4}^{T_1,j-1} \cdot T_{1,inel}^{(j-1)klm}(t) - \tilde{\nu}_{CD4}^{T_1,j-1} \cdot T_{1,inel}^{jklm}(t) \right) \mathbb{1}_{j \geq 2} \\ &+ \left(\tilde{\nu}_{CD4}^{T_1,j} \cdot T_{1,inel}^{(j+1)klm}(t) - \nu_{CD4}^{T_1,j} \cdot T_{1,inel}^{jklm}(t) \right) \mathbb{1}_{j \leq 3} \\ &- (\gamma_{T_1 \rightarrow S_1}^{jl} + \gamma_{T_1 \rightarrow F_1}^{jl}) \cdot T_{1,inel}^{jklm}(t) + \gamma_{D \rightarrow T_1}^{jk} \cdot D_{inel}^{jk1m}(t) - \mu_{T_1}^j \cdot T_{1,inel}^{jklm}(t), \end{aligned}$$

$$\begin{aligned}
\dot{S}_{1,inel}^{jklm}(t) &= -\tilde{\nu}_{CD4}^{S_1,j-1} \cdot S_{1,inel}^{jklm}(t) \mathbb{1}_{j \geq 2} + \tilde{\nu}_{CD4}^{S_1,j} \cdot S_{1,inel}^{(j+1)klm}(t) \mathbb{1}_{j \leq 3} \\
&\quad - \gamma_{S_1 \rightarrow F_1}^{jl} \cdot S_{1,inel}^{jklm}(t) + \gamma_{T_1 \rightarrow S_1}^{jl} \cdot T_{1,inel}^{jklm}(t) + \gamma_{F_1 \rightarrow S_1}^{jl} \cdot F_{1,inel}^{jklm}(t) - \mu_{S_1}^j \cdot S_{1,inel}^{jklm}(t), \\
\dot{F}_{1,inel}^{jklm}(t) &= \nu_{CD4}^{F_1,j-1} \cdot F_{1,inel}^{(j-1)klm}(t) \mathbb{1}_{j \geq 2} - \nu_{CD4}^{F_1,j} \cdot F_{1,inel}^{jklm}(t) \mathbb{1}_{j \leq 3} \\
&\quad + \delta(l) \cdot \sigma_{res}^{NNRTI} \cdot F_{1,inel}^{jk0m}(t) + \delta(m) \cdot \sigma_{res}^{NRTI} \cdot F_{1,inel}^{jk0l}(t) \\
&\quad - (\gamma_{F_1 \rightarrow S_1}^{jl} + \gamma_{F_1 \rightarrow T_2}^{j,inel}) \cdot F_{1,inel}^{jklm}(t) + \gamma_{S_1 \rightarrow F_1}^{jl} \cdot S_{1,inel}^{jklm}(t) + \gamma_{T_1 \rightarrow F_1}^{jl} \cdot T_{1,inel}^{jklm}(t) \\
&\quad - \mu_{F_1}^j \cdot F_{1,inel}^{jklm}(t), \\
\dot{T}_2^{jklm}(t) &= \left(\nu_{CD4}^{T_2,j-1} \cdot T_2^{(j-1)klm}(t) - \tilde{\nu}_{CD4}^{T_2,j-1} \cdot T_2^{jklm}(t) \right) \mathbb{1}_{j \geq 2} + \\
&\quad \left(\tilde{\nu}_{CD4}^{T_2,j} \cdot T_2^{(j+1)klm}(t) - \nu_{CD4}^{T_2,j} \cdot T_2^{jklm}(t) \right) \mathbb{1}_{j \leq 3} \\
&\quad - (\gamma_{T_2 \rightarrow S_2}^j + \gamma_{T_2 \rightarrow F_2}^j) \cdot T_2^{jklm}(t) + \gamma_{F_1 \rightarrow T_2}^{j,elig} \cdot F_{1,elig}^{jklm}(t) + \gamma_{F_1 \rightarrow T_2}^{j,inel} \cdot F_{1,inel}^{jklm}(t) \\
&\quad - \mu_{T_2}^j \cdot T_2^{jklm}(t), \\
\dot{S}_2^{jklm}(t) &= -\tilde{\nu}_{CD4}^{S_2,j-1} \cdot S_2^{jklm}(t) \mathbb{1}_{j \geq 2} + \tilde{\nu}_{CD4}^{S_2,j} \cdot S_2^{(j+1)klm}(t) \mathbb{1}_{j \leq 3} \\
&\quad - \gamma_{S_2 \rightarrow F_2}^j \cdot S_2^{jklm}(t) + \gamma_{T_2 \rightarrow S_2}^j \cdot T_2^{jklm}(t) + \gamma_{F_2 \rightarrow S_2}^j \cdot F_2^{jklm}(t) - \mu_{S_2}^j \cdot S_2^{jklm}(t), \\
\dot{F}_2^{jklm}(t) &= \nu_{CD4}^{F_2,j-1} \cdot F_2^{(j-1)klm}(t) \mathbb{1}_{j \geq 2} - \nu_{CD4}^{F_2,j} \cdot F_2^{jklm}(t) \mathbb{1}_{j \leq 3} \\
&\quad - \gamma_{F_2 \rightarrow S_2}^j \cdot F_2^{jklm}(t) + \gamma_{S_2 \rightarrow F_2}^j \cdot S_2^{jklm}(t) + \gamma_{T_2 \rightarrow F_2}^j \cdot T_2^{jklm}(t) - \mu_{F_2}^j \cdot F_2^{jklm}(t), \\
\dot{T}_3^{jklm}(t) &= \left(\nu_{CD4}^{T_3,j-1} \cdot T_3^{(j-1)klm}(t) - \tilde{\nu}_{CD4}^{T_3,j-1} \cdot T_3^{jklm}(t) \right) \mathbb{1}_{j \geq 2} \\
&\quad + \left(\tilde{\nu}_{CD4}^{T_3,j} \cdot T_3^{(j+1)klm}(t) - \nu_{CD4}^{T_3,j} \cdot T_3^{jklm}(t) \right) \mathbb{1}_{j \leq 3} \\
&\quad - (\gamma_{T_3 \rightarrow S_3}^{j0} + \gamma_{T_3 \rightarrow F_3}^{j0}) \cdot T_3^{jklm}(t) + \gamma_{D \rightarrow T_3}^{jk} \cdot D_{elig}^{jklm}(t) - \mu_{T_3}^j \cdot T_3^{jklm}(t) \\
&\quad + \gamma_{F_1 \rightarrow T_3}^j \cdot F_{1,elig}^{jklm}(t), \\
\dot{S}_3^{jklm}(t) &= -\tilde{\nu}_{CD4}^{S_3,j-1} \cdot S_3^{jklm}(t) \mathbb{1}_{j \geq 2} + \tilde{\nu}_{CD4}^{S_3,j} \cdot S_3^{(j+1)klm}(t) \mathbb{1}_{j \leq 3} \\
&\quad - \gamma_{S_3 \rightarrow F_3}^{j0} \cdot S_3^{jklm}(t) + \gamma_{T_3 \rightarrow S_3}^{j0} \cdot T_3^{jklm}(t) + \gamma_{F_3 \rightarrow S_3}^{j0} \cdot F_3^{jklm}(t) - \mu_{S_3}^j \cdot S_3^{jklm}(t) \\
&\quad + \gamma_{S_1 \rightarrow S_3}(t) \cdot S_{1,elig}^{jklm}(t), \\
\dot{F}_3^{jklm}(t) &= \nu_{CD4}^{F_3,j-1} \cdot F_3^{(j-1)klm}(t) \mathbb{1}_{j \geq 2} - \nu_{CD4}^{F_3,j} \cdot F_3^{jklm}(t) \mathbb{1}_{j \leq 3} \\
&\quad - (\gamma_{F_3 \rightarrow S_3}^{jm} + \gamma_{F_1 \rightarrow T_2}^j) \cdot F_3^{jklm}(t) + \gamma_{S_3 \rightarrow F_3}^{jm} \cdot S_3^{jklm}(t) + \gamma_{T_3 \rightarrow F_3}^{jm} \cdot T_3^{jklm}(t) \\
&\quad - \mu_{F_3}^j \cdot F_3^{jklm}(t).
\end{aligned} \tag{19}$$

5 Sensitivity analysis and additional results

The main sensitivity analysis reflects the uncertainty about eight parameters related to resistance and HIV-transmission. The 95% sensitivity ranges in 2040 for each scenario are shown in Fig 3 of the main manuscript. The evolution of uncertainty over time is represented in Fig C, which displays the 95% sensitivity ranges from 2005 to 2040 for each scenario. The difference in NNRTI TDR levels over time between the different scenarios of DTG-introduction and the scenario where DTG is not introduced is displayed in Fig D with the 95% sensitivity ranges. Fig E displays the predicted percentage of women failing NNRTI-based ART after 1 and 2 years of ART in 2025 and 2035, depending on the scenario of the rollout of DTG-based ART. Finally, we simulated three sensitivity analyses in order to investigate 1) the impact of the Treat-All policy, 2) the impact of treatment interruption, and 3) the impact of NRTI-resistance and higher efficacy of DTG.

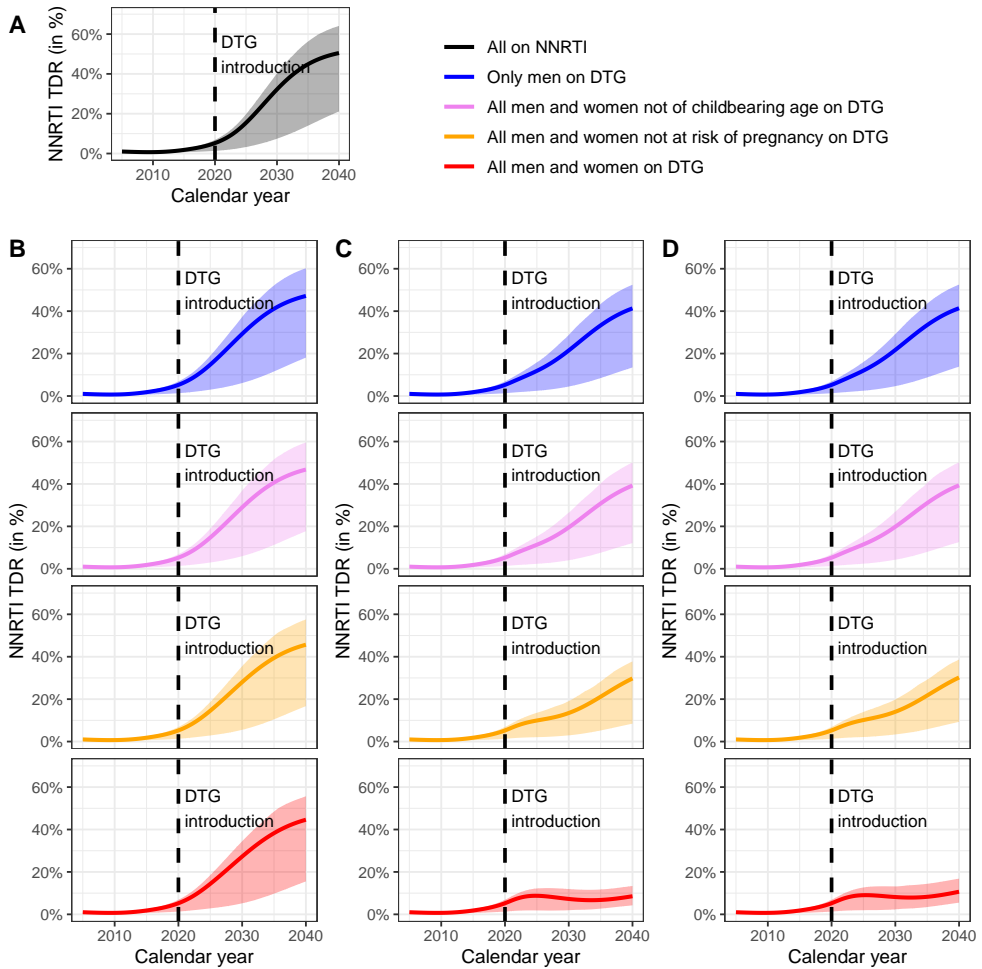


Fig C: Level of NNRTI PDR according to different levels of DTG-eligible women (colors), and different strategies of DTG-introduction. Panel A: no DTG-introduction; panel B: DTG used as a first-line regimen; panel C: DTG used for all patients; panel D: DTG used for all patients, assuming an OR of failure of 2 when having NRTI-resistance. The solid lines correspond to the simulations with the fixed parameter values and the shaded areas represent the 95% sensitivity ranges.

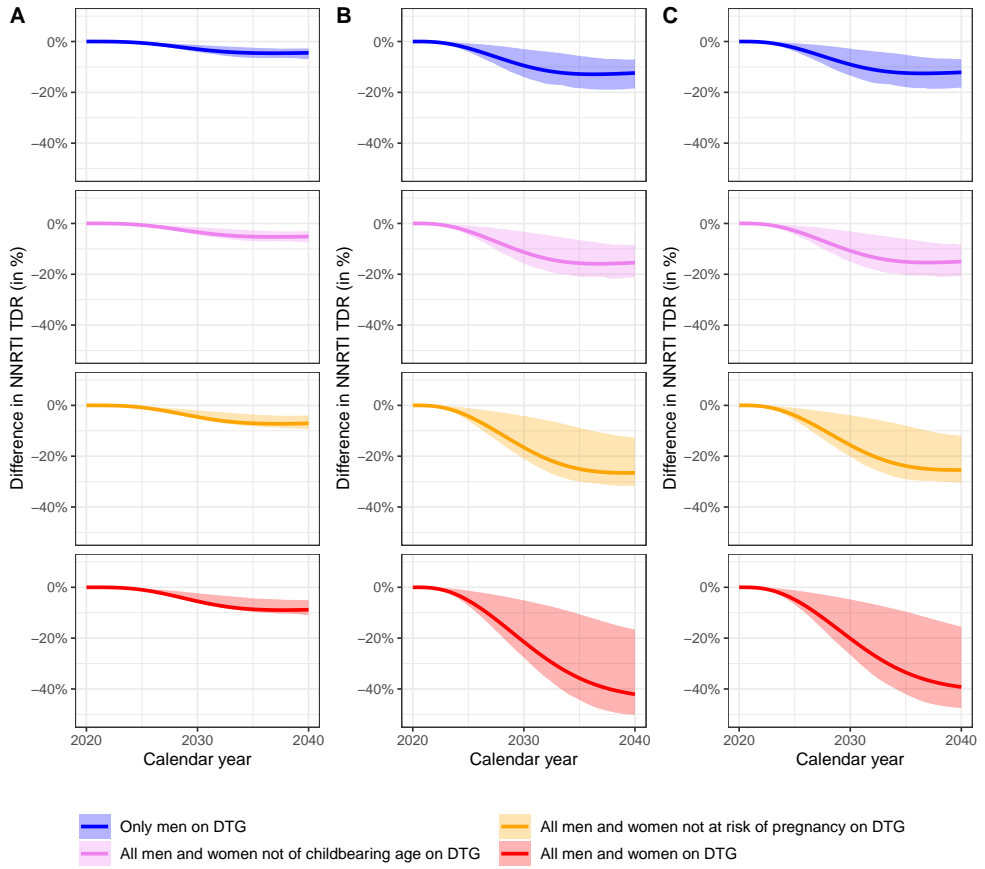


Fig D: Difference in level of NNRTI PDR from 2020 to 2040 between the different strategies of DTG-introduction and the scenario where DTG is not introduced. Panel A: DTG used as a first-line regimen; panel B: DTG used for all patients; panel C: DTG used for all patients, assuming an OR of DTG-failure of 2 when having NRTI-resistance. The solid lines correspond to the simulations with the fixed parameter values and the shaded areas represent the 95% sensitivity ranges.

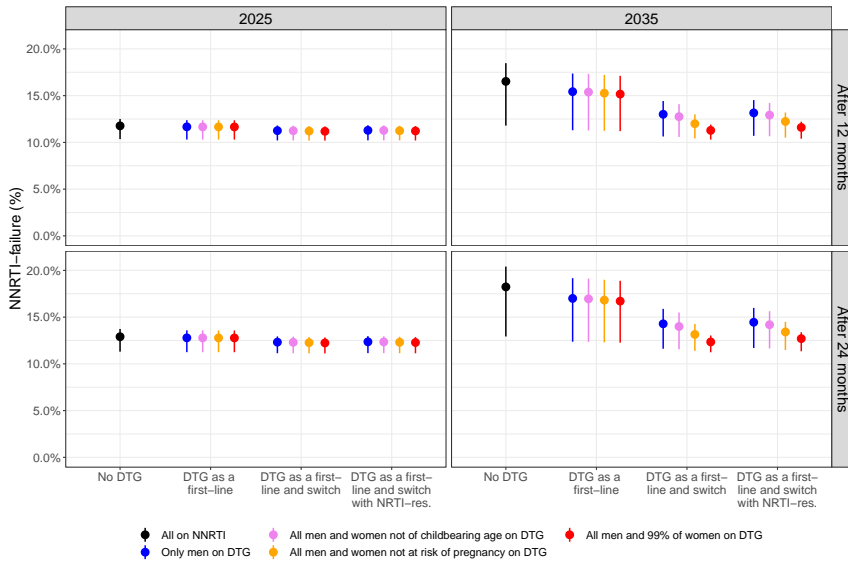


Fig E: Predicted percentage of women failing NNRTI-based ART after 1 and 2 years of ART in 2025 and 2035, depending on the scenario of the rollout of DTG based-ART.

5.1 Effect of no Treat-All policy

We previously assumed that the Treat-All policy increased the treatment initiation rates for people with $CD4 > 200$ cells/ μL from 2017 to 2022. Here, we investigated the scenario where the Treat-All policy does not have any impact on the treatment initiation rates (which is equivalent to assuming no Treat-All policy, see FigF). Globally, assuming a Treat-All policy increases the levels of NNRTI PDR for each scenario, but does not change our conclusion (see FigG).

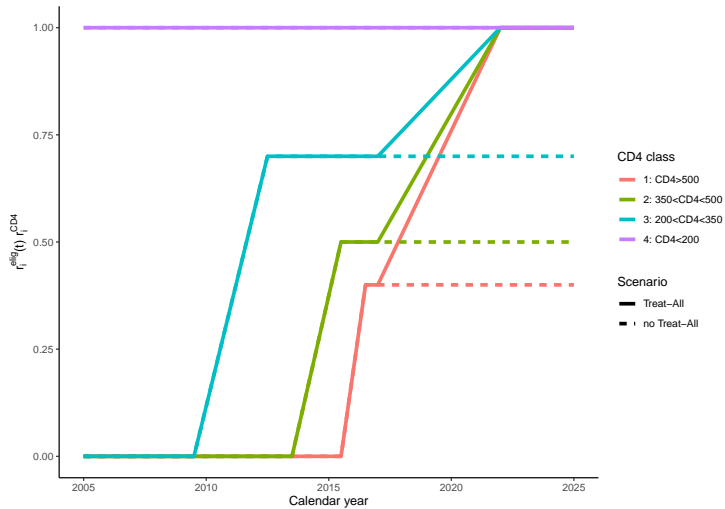


Fig F: $r_i^{elig}(t) \cdot r_i^{CD4}$ represents the level of treatment eligibility $r_i^{elig}(t)$ multiplied by r_i^{CD4} , representing the decrease in treatment initiation rate in CD4 class i relative to the fourth CD4 class ($CD4 < 200$ cells/ μL). In the scenario where we assumed no impact of the Treat-All policy on the treatment initiation rates, the rates remain unchanged from 2016.

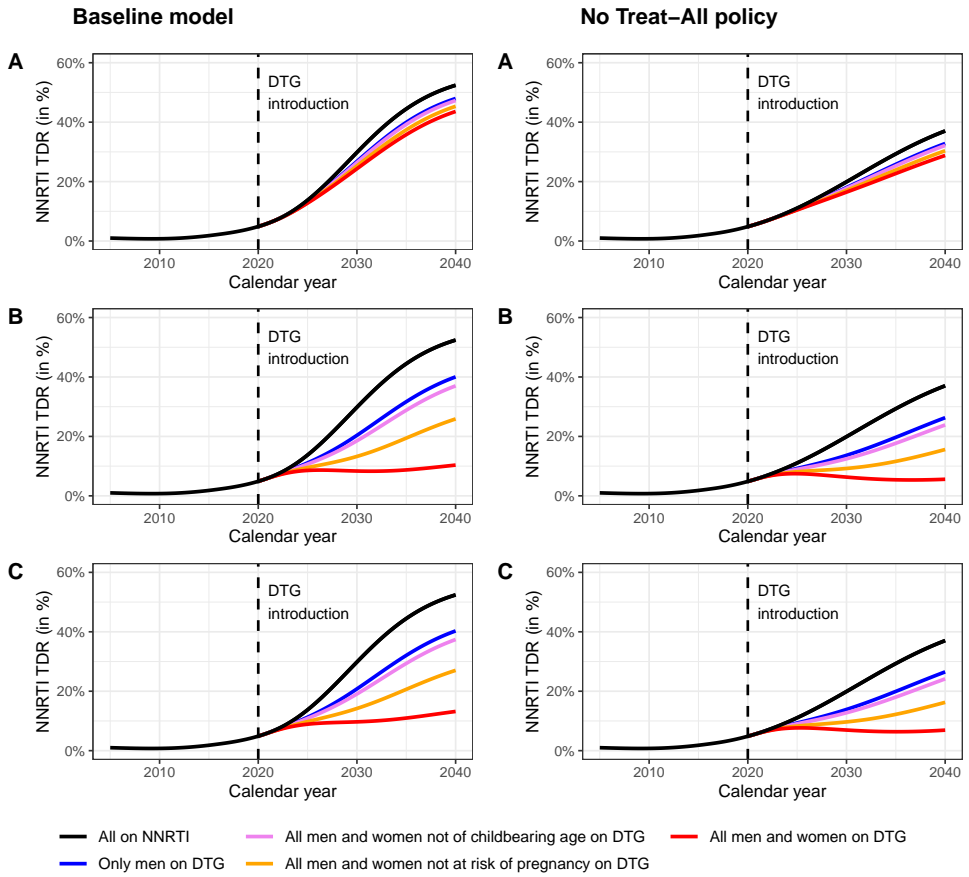


Fig G: Levels of NNRTI resistance when assuming increase in treatment initiation rates due to the Treat-All policy ("Baseline Model") and when assuming identical treatment initiation rates from 2017 ("No Treat-All policy"). Dolutegravir is introduced in 2020 under three scenarios: DTG as first-line regimen for ART-initiators (panel A), DTG for all patients (panel B), DTG for all patients, assuming an OR of failure of 2 when having NNRTI-resistance (panel C), and with different eligibility criteria for women (colors).

5.2 Effect of treatment interruption

We introduced treatment interruption rates for the three ART regimens. Table G shows these rates estimated from IeDEA-SA data [1]. The introduction of treatment interruption did not substantially change the results (see Fig H).

Table G: Treatment interruption rates. Rates are in month⁻¹

| Parameter | Description | CD4 class | | | |
|------------------------------|--------------------------------|-----------|------|-----|-----|
| | | 1 | 2 | 3 | 4 |
| $1/\gamma_{T \rightarrow D}$ | Time from $T_1/T_2/T_3$ to D | 414 | 322 | 172 | 156 |
| $1/\gamma_{S \rightarrow D}$ | Time from $S_1/S_2/S_3$ to D | 2069 | 1241 | 759 | 368 |
| $1/\gamma_{F \rightarrow D}$ | Time from $F_1/F_2/F_3$ to D | 621 | 478 | 285 | 129 |

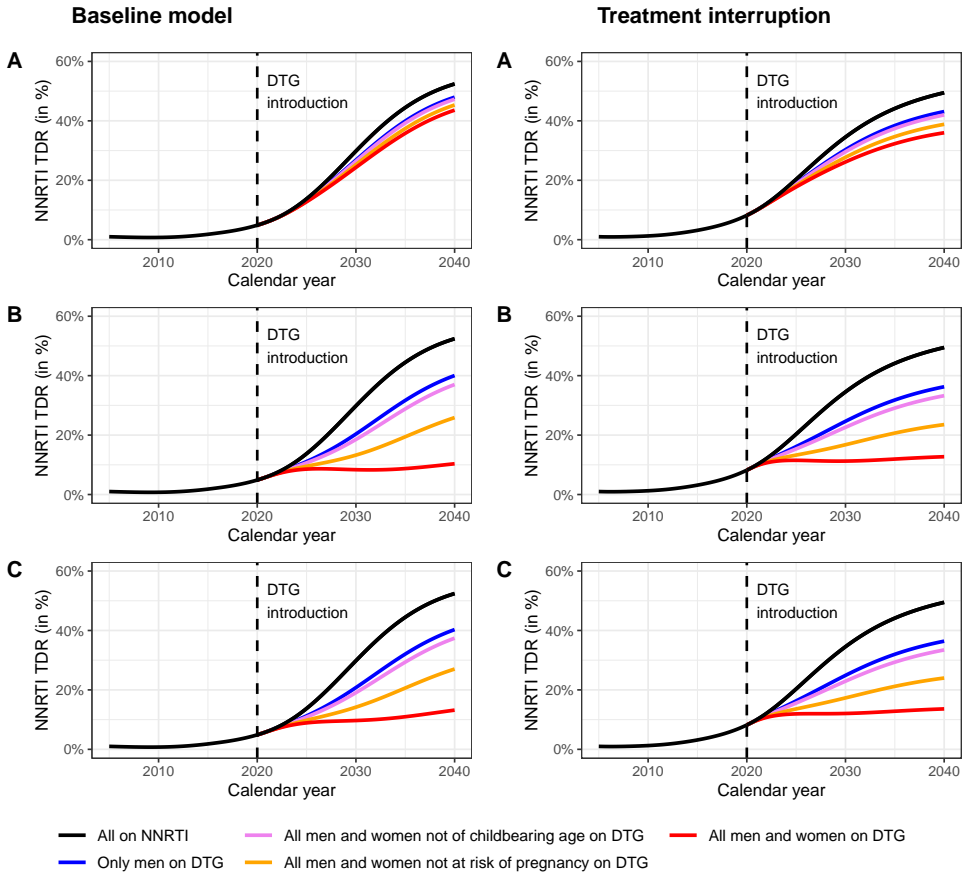


Fig H: Levels of NNRTI resistance using the baseline model ("Baseline Model") and when including treatment interruption ("Treatment interruption"). Dolutegravir is introduced in 2020 under three scenarios: DTG as first-line regimen for ART-initiators (panel A) or DTG for all patients (panel B), DTG for all patients, assuming an OR of failure of 2 when having NRTI-resistance (panel C), and with different eligibility criteria for women (colors).

5.3 Effect of NRTI-resistance and higher efficacy of DTG

We assessed the impact of NRTI resistance and higher efficacy of DTG-based regimen on the level of NNRTI PDR. We investigated three different scenarios regarding the impact of NRTI-resistance: 1) no impact (i.e OR of failure between NRTI-resistant and NRTI-susceptible individuals equals 1), 2) OR=2, and 3) OR=5. A meta-analysis comparing DTG-monotherapy with DTG-dual therapy found an odds ratio of failure of 13.9 after 48 weeks (8.9% vs 0.7% of failure, respectively) [17]. However, we expect lower difference between NRTI-resistant and -susceptible individuals, as some activity of the NRTI-backbones are observed even in resistant individuals [15]. Another study comparing DTG-efficacy according to the presence of specific NRTI-mutations found a HR of 3.23 (95%CI: 0.27-38.40) when having the K65R mutation and a HR of 0.99 (95%CI: 0.19-5.21) when having the M184V, suggesting low impact of NRTI-resistance on DTG-failure [16].

We also investigated three different scenarios regarding the efficacy of DTG compared with NNRTI: 1) OR of failure between NNRTI- and DTG-based regimen of 1.02, 2) OR=2, and 3) OR=5. The first scenario refers to the results of the NAMSAL study after the adjusting for CD4 counts (see Section 2.5). The two other scenarios were investigated in view of the higher efficacy of DTG compared with NNRTI found in some studies [26].

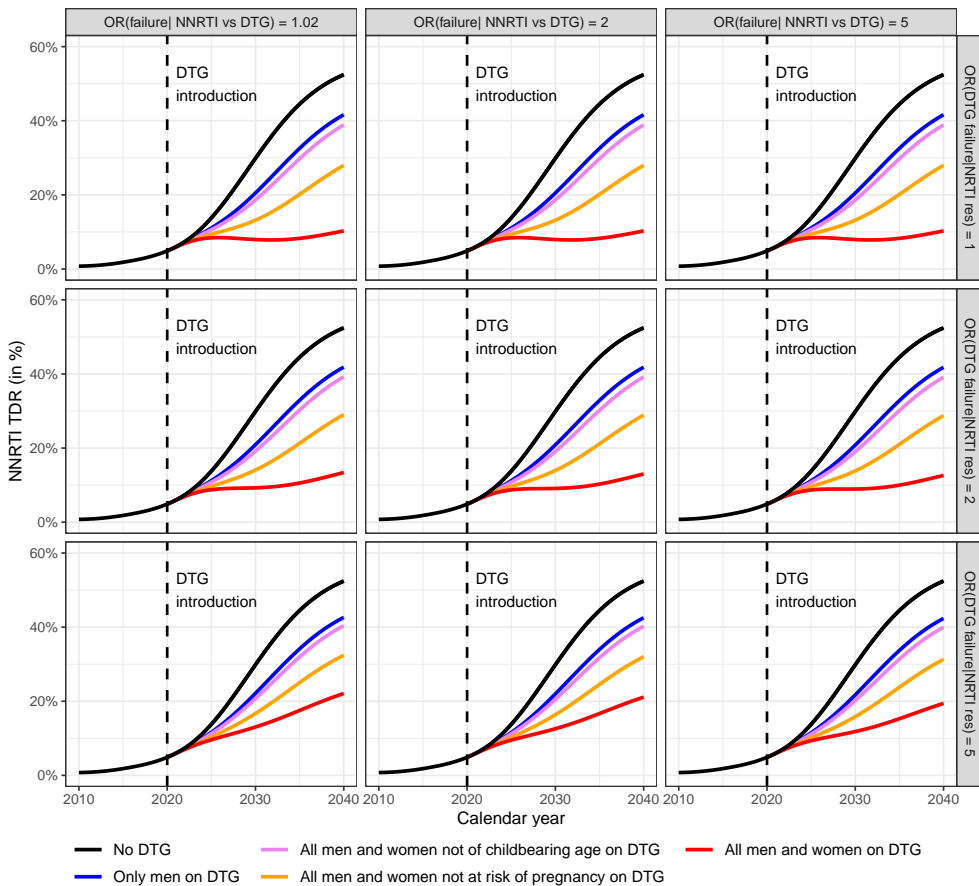


Fig I: Levels of NNRTI TDR from 2010 to 2040, when assuming that DTG is used both as first-line and switch regimens. Different impacts of NRTI-resistance on DTG-failure (horizontally) and different DTG-efficacies (vertically) are investigated.

References

- [1] Egger M, Ekouevi DK, Williams C, Lyamuya RE, Mukumbi H, Braitstein P, et al. Cohort Profile: The international epidemiological databases to evaluate AIDS (IeDEA) in sub-Saharan Africa. *International Journal of Epidemiology*. 2012 oct;41(5):1256–1264. Available from: <http://www.ncbi.nlm.nih.gov/pubmed/21593078><http://www.pubmedcentral.nih.gov/articlerender.fcgi?artid=PMC3465765><https://academic.oup.com/ije/article-lookup/doi/10.1093/ije/dyr080>.
- [2] Johnson LF, Dorrington RE. Thembisa version 4.1: A model for evaluating the impact of HIV/AIDS in South Africa; 2018. Available from: <https://www.thembisa.org/publications>.
- [3] Mangal TD, UNAIDS Working Group on CD4 Progression and Mortality Amongst HIV Seroconverters including the CASCADE Collaboration in EuroCoord. Joint estimation of CD4+ cell progression and survival in untreated individuals with HIV-1 infection. *AIDS*. 2017 may;31(8):1073–1082. Available from: <http://www.ncbi.nlm.nih.gov/pubmed/28301424><http://www.pubmedcentral.nih.gov/articlerender.fcgi?artid=PMC5414573><https://insights.ovid.com/crossref?an=00002030-201705150-00003>.
- [4] Hauser A, Kusejko K, Johnson LF, Wandeler G, Riou J, Goldstein F, et al. Bridging the gap between HIV epidemiology and antiretroviral resistance evolution: Modelling the spread of resistance in South Africa. *PLOS Computational Biology*. 2019 jun;15(6):e1007083. Available from: <http://dx.plos.org/10.1371/journal.pcbi.1007083>.
- [5] Moorhouse M, Maartens G, Venter WDF, Moosa MY, Steegen K, Jamaloodien K, et al. Third-Line Antiretroviral Therapy Program in the South African Public Sector: Cohort Description and Virological Outcomes. *Journal of acquired immune deficiency syndromes (1999)*. 2019 jan;80(1):73–78. Available from: <http://www.ncbi.nlm.nih.gov/pubmed/30334876><http://www.pubmedcentral.nih.gov/articlerender.fcgi?artid=PMC6319697>.
- [6] Orrell C, Walensky RP, Losina E, Pitt J, Freedberg KA, Wood R. HIV type-1 clade C resistance genotypes in treatment-naïve patients and after first virological failure in a large community antiretroviral therapy programme. *Antiviral therapy*. 2009;14(4):523–31. Available from: <http://www.ncbi.nlm.nih.gov/pubmed/19578237><http://www.pubmedcentral.nih.gov/articlerender.fcgi?artid=PMC3211093>.
- [7] Sigaloff KCE, Ramatsebe T, Viana R, de Wit TFR, Wallis CL, Stevens WS. Accumulation of HIV Drug Resistance Mutations in Patients Failing First-Line Antiretroviral Treatment in South Africa. *AIDS Research and Human Retroviruses*. 2012 feb;28(2):171–175. Available from: <http://www.liebertpub.com/doi/10.1089/aid.2011.0136>.
- [8] Wallis CL, Mellors JW, Venter WDF, Sanne I, Stevens W. Varied Patterns of HIV-1 Drug Resistance on Failing First-Line Antiretroviral Therapy in South Africa. *JAIDS Journal of Acquired Immune Deficiency Syndromes*. 2010 apr;53(4):480–484. Available from: <https://insights.ovid.com/crossref?an=00126334-201004010-00007>.
- [9] Manasa J, Lessells RJ, Skingsley A, Naidu KK, Newell ML, McGrath N, et al. High-Levels of Acquired Drug Resistance in Adult Patients Failing First-Line Antiretroviral Therapy in a Rural HIV Treatment Programme in KwaZulu-Natal, South Africa. *PLoS ONE*. 2013 aug;8(8):e72152. Available from: <https://dx.plos.org/10.1371/journal.pone.0072152>.
- [10] van Zyl GU, van der Merwe L, Claassen M, Zeier M, Preiser W. Antiretroviral resistance patterns and factors associated with resistance in adult patients failing NNRTI-based regimens in the western cape, South Africa. *Journal of Medical Virology*. 2011 oct;83(10):1764–1769. Available from: <http://doi.wiley.com/10.1002/jmv.22189>.
- [11] Hauser A. Acquired HIV drug resistance mutations on first-line antiretroviral therapy in Southern Africa: Bayesian evidence synthesis. Available from: <https://github.com/anthonyhauser/ADR-meta-analysis>.
- [12] Yang WL, Kouyos RD, Böni J, Yerly S, Klimkait T, Aubert V, et al. Persistence of Transmitted HIV-1 Drug Resistance Mutations Associated with Fitness Costs and Viral Genetic Backgrounds. *PLOS Pathogens*. 2015 mar;11(3):e1004722. Available from: <http://dx.plos.org/10.1371/journal.ppat.1004722>.
- [13] Wittkop L, Günthard HF, de Wolf F, Dunn D, Cozzi-Lepri A, de Luca A, et al. Effect of transmitted drug resistance on virological and immunological response to initial combination antiretroviral therapy for HIV (EuroCoord-CHAIN joint project): a European multicohort study. *The Lancet Infectious Diseases*. 2011 may;11(5):363–371. Available from: <http://www.ncbi.nlm.nih.gov/pubmed/21354861><http://linkinghub.elsevier.com/retrieve/pii/S1473309911700329>.

- [14] Kuritzkes DR, Lalama CM, Ribaldo HJ, Marcial M, Meyer III WA, Shikuma C, et al. Preexisting Resistance to Nucleoside Reverse-Transcriptase Inhibitors Predicts Virologic Failure of an Efavirenz-Based Regimen in Treatment-Naïve HIV-1-Infected Subjects. *The Journal of Infectious Diseases*. 2008 mar;197(6):867–870. Available from: <https://academic.oup.com/jid/article-lookup/doi/10.1086/528802>.
- [15] Hakim JG, Thompson J, Kityo C, Hoppe A, Kambugu A, van Oosterhout JJ, et al. Lopinavir plus nucleoside reverse-transcriptase inhibitors, lopinavir plus raltegravir, or lopinavir monotherapy for second-line treatment of HIV (EARNEST): 144-week follow-up results from a randomised controlled trial. *The Lancet Infectious Diseases*. 2018 jan;18(1):47–57. Available from: <http://www.thelancet.com/article/S1473309917306308/fulltext><http://www.thelancet.com/article/S1473309917306308/abstract>[https://www.thelancet.com/journals/laninf/article/PIIS1473-3099\(17\)30630-8/abstract](https://www.thelancet.com/journals/laninf/article/PIIS1473-3099(17)30630-8/abstract).
- [16] Giacomelli A, Lai A, Franzetti M, Maggiolo F, Di Giambenedetto S, Borghi V, et al. No impact of previous NRTIs resistance in HIV positive patients switched to DTG+2NRTIs under virological control: Time of viral suppression makes the difference. *Antiviral Research*. 2019 dec;172. Available from: <https://pubmed.ncbi.nlm.nih.gov/31629714/>.
- [17] Wandeler G, Buzzi M, Anderegg N, Sculier D, Béguelin C, Egger M, et al. Open Peer Review Virologic failure and HIV drug resistance on simplified, dolutegravir-based maintenance therapy: Systematic review and meta-analysis [version 2; peer review: 3 approved]. *F1000 Research*. 2019. Available from: <https://doi.org/10.12688/f1000research.15995.1>.
- [18] Group TNAS. Dolutegravir-Based or Low-Dose Efavirenz-Based Regimen for the Treatment of HIV-1. *New England Journal of Medicine*. 2019 aug;381(9):816–826. Available from: <http://www.nejm.org/doi/10.1056/NEJMoa1904340>.
- [19] Patel P, Borkowf CB, Brooks JT, Lasry A, Lansky A, Mermin J. Estimating per-act HIV transmission risk. *AIDS*. 2014 jun;28(10):1509–1519. Available from: <http://www.ncbi.nlm.nih.gov/pubmed/24809629><http://content.wkhealth.com/linkback/openurl?sid=WKPTLP:landingpage{&}an=00002030-201406190-00014>.
- [20] Anova Health Institute. Rapid Assessment of HIV Prevention, Care and Treatment Programming for MSM in South Africa; 2013.
- [21] Maduna PH, Dolan M, Kondlo L, Mabuza H, Dlamini JN, Polis M, et al. Morbidity and Mortality According to Latest CD4+ Cell Count among HIV Positive Individuals in South Africa Who Enrolled in Project Phidisa. *PLOS ONE*. 2015 apr;10(4):e0121843. Available from: <http://www.ncbi.nlm.nih.gov/pubmed/25856495><http://www.pubmedcentral.nih.gov/articlerender.fcgi?artid=PMC4391777><https://dx.plos.org/10.1371/journal.pone.0121843>.
- [22] Brennan AT, Maskew M, Sanne I, Fox MP. The interplay between CD4 cell count, viral load suppression and duration of antiretroviral therapy on mortality in a resource-limited setting. *Tropical medicine & international health : TM & IH*. 2013 may;18(5):619–31. Available from: <http://www.ncbi.nlm.nih.gov/pubmed/23419157><http://www.pubmedcentral.nih.gov/articlerender.fcgi?artid=PMC3625450>.
- [23] Kühnert D, Kouyos R, Shirreff G, Pečerska J, Scherrer AU, Böni J, et al. Quantifying the fitness cost of HIV-1 drug resistance mutations through phylodynamics. *PLOS Pathogens*. 2018 feb;14(2):e1006895. Available from: <http://dx.plos.org/10.1371/journal.ppat.1006895>.
- [24] Rhee SY, Varghese V, Holmes SP, Van Zyl GU, Steegen K, Boyd MA, et al. Mutational Correlates of Virological Failure in Individuals Receiving a WHO-Recommended Tenofovir-Containing First-Line Regimen: An International Collaboration. *EBioMedicine*. 2017 apr;18:225–235. Available from: <https://pubmed.ncbi.nlm.nih.gov/28365230/>.
- [25] World Bank. Contraceptive prevalence, any methods (% of women ages 15-49) | Data; 2015. Available from: <https://data.worldbank.org/indicator/SP.DYN.CONU.ZS?locations=ZA>.
- [26] Snedecor SJ, Radford M, Kratochvil D, Grove R, Punekar YS. Comparative efficacy and safety of dolutegravir relative to common core agents in treatment-naïve patients infected with HIV-1: A systematic review and network meta-analysis. *BMC Infectious Diseases*. 2019 may;19(1). Available from: [/pmc/articles/PMC6543679/?report=abstract](https://pubmed.ncbi.nlm.nih.gov/31629714/)<https://www.ncbi.nlm.nih.gov/pmc/articles/PMC6543679/>.

Curriculum vitae & list of publications

Anthony HAUSER

Moulin 20 – 2740 Moutier

☎ +41 77 410 08 92 • ✉ anthony.hauser@ispm.unibe.ch

📄 orcid.org/0000-0002-7221-1929

Age : 28 (6.7.1992) ▪ Nationality : Swiss

Research interests

Mathematics, statistics, Bayesian inference, infectious disease modelling, epidemiology

Education

| | |
|--|-----------------------------------|
| ISPM, Institute of Social and Preventive Medicine <i>PhD at the University of Bern</i> Modelling the dynamic of HIV drug resistance in South Africa | Bern 2.2017–Present |
| EPFL, Ecole polytechnique fédérale de Lausanne <i>Master in Ingénierie Mathématique with honours (average mark of 5.37)</i> | Lausanne 9.2014–7.2016 |
| UNINE, Université de Neuchâtel <i>Bachelor in Mathématiques with honours (average mark of 5.33),</i> | Neuchâtel 9.2011–7.2014 |
| Gymnase français de Bienne <i>Maturité gymnasiale (Baccalaureate) of Science (average note 5.70),</i> | Bienne 8.2008–6.2011 |

PhD thesis

Title: Modelling HIV drug resistance in South Africa

Supervisors: Prof. Matthias Egger, Prof. Roger Kouyos

Description: In my PhD project, I explored the past and future dynamics of HIV drug resistance in Southern Africa, using mathematical models.

Previous work experience

| | |
|--|--------------------------------|
| Novartis Consumer Health, a GSK venture <i>Internship in biostatistics</i> Development of a mathematical model to predict topical products skin permeation behaviour from physico-chemical data | Nyon 8.2015–12.2015 |
| Gymnase Français de Bienne <i>Dr Maxime Zuber's substitute mathematics teacher</i> | Bienne 8.2011–7.2015 |

Highlighted courses

09–12.2019: Biological Principles of Human Medicine (University of Bern)

07.2019: Applied Bayesian Statistics in Medical Research (ISPM, Bern)

01.2019: Network meta-analysis (Wengen Winterschool, organized by the Swiss School of Public

Health)

07.2017: Model fitting and inference for infectious disease dynamics (London School of Hygiene and Tropical Medicine)

05–12.2017: Book Club: Epidemiology (ISPM, Bern)

Conferences

COVID-19 Dynamics and Evolution

Poster presentation

Virtual conference

10.2020

GCB graduate school symposium

Poster flash session

Bern, Switzerland

01.2020

GCB: Graduate School for Cellular and Biomedical Sciences

3rd leDEA All Africa Meeting

Oral presentation

Johannesburg, South Africa

10.2019

leDEA: International epidemiology Database to Evaluate AIDS

CROI 2019

Poster presentation

Seattle, USA

03.2019

CROI: Conference on Retroviruses and Opportunistic Infections

International Workshop on HIV Drug Resistance

Oral presentation (Roger Kouyos)

Johannesburg, South Africa

10.2018

22nd IWHOD

Oral presentation

Fuengirola, Spain

03.2018

IWHOD: International Workshop on HIV and Hepatitis Observational Databases

Previous projects and academic works

Master project in Statistics

Supervised by Prof. Stephan Morgenthaler and passed with note 6

EPFL, Lausanne

2.2016–7.2016

Representation of the dependence structure of a distribution with the help of a graphical model

Semester project in Biostatistics

Supervised by Prof. Stephan Morgenthaler and passed with note 6

EPFL, Lausanne

2.2015–7.2015

Survival analysis and random process

IT skills

Advanced level: R, STAN, MATLAB, \LaTeX

Basic knowledge: STATA, C++, JAVA, Bash, MS Office

Languages

English: C1

German: B1

French: mother tongue

Interests

Sport: Tennis, football, cycling, hiking

Publications

René de Waal, Richard Lessells, Anthony Hauser, Roger Kouyos, Mary-Ann Davies, Matthias Egger, and Gilles Wandeler. HIV drug resistance in sub-Saharan Africa: public health questions and the potential role of real-world data and mathematical modelling. *Journal of virus eradication*, 4(Suppl 2):55–58, nov 2018.

Anthony Hauser, Michel J. Counotte, Charles C. Margossian, Garyfallos Konstantinoudis, Nicola Low, Christian L. Althaus, and Julien Riou. Estimation of SARS-CoV-2 mortality during the early stages of an epidemic: A modeling study in Hubei, China, and six regions in Europe. *PLOS Medicine*, 17(7):e1003189, jul 2020.

Anthony Hauser, Katharina Kusejko, Leigh F. Johnson, Huldrych F. Günthard, Julien Riou, Gilles Wandeler, Matthias Egger, and Roger D. Kouyos. Impact of scaling up dolutegravir on antiretroviral resistance in South Africa: A modeling study. *PLOS Medicine*, 17(12):e1003397, dec 2020.

Anthony Hauser, Katharina Kusejko, Leigh F. Johnson, Gilles Wandeler, Julien Riou, Fardo Goldstein, Matthias Egger, and Roger D. Kouyos. Bridging the gap between HIV epidemiology and antiretroviral resistance evolution: Modelling the spread of resistance in South Africa. *PLOS Computational Biology*, 15(6):e1007083, jun 2019.

Acknowledgements

I would like to thank Matthias Egger and Roger Kouyos for their co-supervision and for offering me their different but very complementary expertise. In particular, I would like to thank Matthias for always bringing his public-health perspective to the table and for introducing me to the world of HIV research and Roger for his constant availability to solve the technical issues I encountered and for always coming up with new modelling ideas. I am also thankful to the leDEA group, who helps me to progressively acquire knowledge on different aspects of HIV. The Friday visits to the Roger Kouyos' research group in Zurich were also a great opportunity to exchange in a real student-oriented atmosphere.

I would also like to thank Nicola Low and Christian Althaus for including me in their research groups, which was essential for receiving regular feedback on my work. Spending almost four year would not have possible without the great working atmosphere that prevails at ISPM. Thanks to my colleagues Diana, Julien, Michel, Martina, Hira, Maurane, Fardo, Million, Joost and Dominique. A special thanks to Julien, who introduces me to the world of Bayesian statistics and Stan modelling, which has been a new source of excitement in the middle of my PhD. Thanks also to Carole, Astrid and Julien for still maintaining some real social contact during the SARS-CoV-2 crisis.

On a more personal note, I would like to thank my brother Sylvain, my sister Lauriane, my parents Nicole and Jean-Jacques and my grandparents Heidi and Willy, who brought me motivation throughout this PhD by showing constant interest in my research.

Declaration of originality

Last name, first name: Hauser, Anthony

Matriculation number: 11-508-843

I hereby declare that this thesis represents my original work and that I have used no other sources except as noted by citations.

All data, tables, figures and text citations which have been reproduced from any other source, including the internet, have been explicitly acknowledged as such.

I am aware that in case of non-compliance, the Senate is entitled to withdraw the doctorate degree awarded to me on the basis of the present thesis, in accordance with the "Statut der Universität Bern (Universitätsstatut; UniSt)", Art. 69, of 7 June 2011.

Place, date

Bern, 12.12.2020

Signature

A handwritten signature in blue ink that reads "A Hauser". The signature is written in a cursive style with a large initial 'A' and a long horizontal stroke extending to the right.

